ZooKeys 1025: 1–19 (2021)
doi: 10.3897/zookeys.1025.56780
https://zookeys.pensoft.net

RESEARCH ARTICLE

A peer-reviewed open-access journal
ZooKeys
Launched to accelerate biodiversity research

A new species of the genus *Arria* Stål, 1877 (Mantodea, Haaniidae) from China with notes on the tribe Arriini Giglio-Tos, 1919

Ying-jian Wang[1,2,3], Lin Yang[1,2,3], Fei Ye[4], Xiang-sheng Chen[1,2,3]

1 *Institute of Entomology, Guizhou University, Guiyang, Guizhou, 550025, China* **2** *The Provincial Special Key Laboratory for Development and Utilization of Insect Resources of Guizhou, Guizhou University, Guiyang, Guizhou, 550025, China* **3** *Guizhou Key Laboratory for Plant Pest Management of Mountainous Region, Guizhou University, Guiyang, Guizhou, 550025, China* **4** *School of life sciences, Sun Yat-sen University, Guangzhou, Guangdong, 510275, China*

Corresponding author: Xiang-Sheng Chen (chenxs3218@163.com)

Academic editor: Fred Legendre | Received 21 July 2020 | Accepted 12 February 2021 | Published 18 March 2021

http://zoobank.org/0E2D3978-11A1-43F6-8D42-20BA15C44DC1

Citation: Wang Y-j, Yang L, Ye F, Chen X-s (2021) A new species of the genus *Arria* Stål, 1877 (Mantodea, Haaniidae) from China with notes on the tribe Arriini Giglio-Tos, 1919. ZooKeys 1025: 1–19. https://doi.org/10.3897/zookeys.1025.56780

Abstract

A new species of the praying mantis genus *Arria* Stål, *Arria pura* **sp. nov.** from southwest China is described and illustrated. An overview, comparison, and distribution data of this tribe are given. A new synonym is created: *Sinomiopteryx yunnanensis* Xu, 2007 is a junior synonym of *Arria pallida* (Zhang, 1987). One new combination *Arria brevifrons* (Wang, 1991) **comb. nov.** (from *Sinomiopteryx* Tinkham), is proposed.

Keywords

Arriini, Cernomantodea, genitalia, Oriental Region, praying mantis, taxonomy

Introduction

The tribe Arriini Giglio-Tos, 1919 (Mantodea, Haaniidae) comprises two genera, *Arria* Stål, 1877 and *Sinomiopteryx* Tinkham, 1937 (Schwarz and Roy 2019). The genus *Arria* was established by Stål (1877) based on the type species *A. cinctipes* Stål, 1877 from India. The other genus *Sinomiopteryx* was established by Tinkham (1937) based on the type species *S. grahami* Tinkham, 1937 from China. Recently, Schwarz and

Roy (2018) proposed that *Palaeothespis* Tinkham, 1937 and *Pseudothespis* Mukherjee, 1995 are junior synonyms of *Arria*. So far, the number of species in the genus *Arria* and *Sinomiopteryx* has changed from six to eight and four to two, respectively, including the new species, new synonym and new combination (Xu 2007; Schwarz and Roy 2018; Otte et al. 2020).

The species of Arriini are quite similar in appearance and there are few previous descriptions and illustrations of male genitalia. In this paper, during a study of the external morphology and male genitalia of Arriini, we found that *Arria* and *Sinomiopteryx* can be easily distinguished by male genitalia and other valuable appearance features, which are also provided to help distinguish the two genera.

Material and methods

Specimens were collected by sweeping net. The tip of the abdomen was separated and macerated in 10% water solution of KOH for about 12 hours, then washed in water and absolute ethanol. The terminalia were isolated into supra-anal and subgenital parts, the phallomeres were separated into left phallomere, ventral phallomere and right phallomere without overlapping, then all parts were preserved in glycerine in a microvial pinned with the specimen. Some wings were removed and mounted on a slide provided with the data of the specimen. External morphology and male genitalia were observed using a Leica M125 stereomicroscope. Photographs of phallomeres, terminalia and wings were taken with Nikon SMZ25, and photographs of the mounted specimens were taken with Canon EOS-70D digital camera with a Canon 100 mm Macro EF Lens or a Laowa 60 mm Macro Lens. Photo stacks were created using Helicon focus 6.0.18. Figures were processed with Adobe Photoshop CS6. Measurements were collected with the Keyence VHX-1000 system using the live measurement mode. Numeric patterns of the discoidal spines: The numbers (from left to right) represent the position (proximal to distal). Their value is representative of their respective length relation to the other spines with 1 being the shortest and 4 being the longest spine. Identical values represent equally long spines (Wieland 2013). L/W ratio of forewing means length to max width ratio of forewing. The classification system follows Schwarz and Roy (2019). Terminology and abbreviations follow Brannoch et al. (2017), for genitalia, we follow Schwarz and Roy (2019). Measurements follow Brannoch et al. (2017), but head length includes the labrum, foretibia length was from the base to the apex of the tibial spur, for apterous females the total length was from the vertex of the head to the posterior tip of the abdomen. The distribution map was created in SimpleMappr (Shorthouse 2010). Examined specimens were deposited in the following collections:

NFU Nanjing Forestry University, Nanjing, China;
SEM Shanghai Entomological Museum, CAS, Shanghai, China.

The type specimens of *Arria pura* sp. nov. are deposited in the Institute of Entomology, Guizhou University, Guiyang, Guizhou Province, China (IEGU).

Abbreviations

afa phalloid apophysis;
AvS anteroventral spine;
CuA anterior Cubitus;
DS discoidal spine;
fda main posterior lobe of right phallomere;
HT holotype;
L1 sclerite L1 of left phallomere;
L2 sclerite L2 of left phallomere;
L4 sclerite extending over most of the dorsal and ventral walls of left phallic;
L4A ventral sclerite of L4;
L4B dorsal sclerite of L4;
loa membranous lobe of left phallomere;
paa apical process of left phallomere;
pda primary distal process;
pia a process arising from the midlength to posterior right ventral wall of right phallomere, posterolateral to process pva;
pva a process arising from the midlength of the ventral wall of right phallomere, anteromesal to process pia;
PvS posteroventral spine;
PT paratype;
R1A dorsal sclerite of fda;
R1B sclerite on process pia and pva;
R3 anteriorly extending sclerite of right phallomere;
sdp secondary distal process;
sdpm median secondary distal process;
tl terminal lobe of ventral phallomere in *Arria*.

Checklist and distributions of species of Arriini

A. brevifrons (Wang, 1991), China (Zhejiang), comb. nov.
A. cinctipes Stål, 1877, India (Manipur).
A. leigongshanensis, (Ge & Chen, 2008), China (Guizhou, Yunnan).
A. meghalayensis, (Mukherjee, 1995), India (Meghalaya).
A. oreophila, (Tinkham, 1937), China (Sichuan).
A. pallida, (Zhang, 1987), China (Yunnan), *S. yunnanensis*, Xu 2007 is a junior synonym of *A. pallida.*
A. pura Wang & Chen, sp. nov., China (Guizhou).
A. sticta (Zhou & Shen, 1992), China (Guizhou, Hunan, Zhejiang).
S. grahami Tinkham, 1937, China (Sichuan).
S. guangxiensis Wang & Bi, 1991, China (Guangxi).

Taxonomy

Arriini Giglio-Tos, 1919

Arriini Giglio-Tos, 1919: 65; Schwarz and Roy 2019: 141.

Type genus. *Arria* Stål, 1877.
Distribution. China, India (Fig. 11).

Arria Stål, 1877

Arria Stål, 1877: 46; Tinkham 1937: 497; Zhang 1987: 239; Zhou and Shen 1992: 62; Wang and Bi 1991: 125; Wang 1993: 114; Mukherjee and Ghosh 1995: 251; Ehrmann 2002: 72, 259, 298; Xu 2007: 244; Ge and Chen 2008: 53; Schwarz and Roy 2018: 456; Schwarz and Roy 2019: 141.

Type species. *Arria cinctipes* Stål, 1877, original designation.

Diagnosis. Body medium and slender (Fig. 7), female stronger than male. Head narrowly transverse with juxtaocular bulges; compound eyes broadly oval, prominent; ocelli large in male (Fig. 8), minute in female. Lower frons transverse, 3.3–4.2 times as wide as high. Antennae filiform, long in male, much shorter in female. Forefemur slender, with 4 discoidal, 10–13 anteroventral and 4 posteroventral spines; foretibia with 7–9 anteroventral and 4–7 posteroventral spines. Pronotum short with supracoxal dilatation well marked, lateral margins with small denticles in male and strongly tuberculate in female. Forewing narrow with narrowly rounded apex, CuA branches no less than 5, L/W ratio is 4.3–5.5; fore margin with widely spaced cilia, hindwing with pointed apex, vein M with brunet band near the tip; both pairs of wings fully developed and exceeding the end of abdomen in male (Fig. 9); female apterous. Sclerite L4A approximately rhomboidal, males with terminal lobe (tl) of ventral phallomere fused to vla, protruding as a truncate lobe, close to sdpm ventrad; sdpm short; right phallomere with large pia and ear-shaped pva. Styli close to each other (Fig. 4).

Arria brevifrons (Wang & Bi, 1991), comb. nov.

Fig. 10A–D

Sinomiopteryx brevifrons Wang & Bi, 1991: 125; Wang 1993: 114.

Material examined. ***Holotype***, 1♂, China: Zhejiang Prov., Qingyuan County, Baishanzu, 1100 m, 14.X.1963, Gen-tao Jin leg., ID: 0800123 (SEM).

Remarks. This species was described and illustrated by Wang and Bi in 1991 based on one male specimen from Zhejiang. The ocelli are not closely grouped as in the males of *Sinomiopteryx*; forewings are narrow, L/W ratio is 4.8 with CuA_5, hindwings with pointed apex and brunet band of near apex of vein M. All features fall into the range of *Arria*. The specimen has had the abdomen removed, but we did not find the genitalia. According to the spots on the forelegs, *A. brevifrons* can be distinguished from *A. pallida* and *A. sticta*.

Arria cinctipes Stål, 1877

Arria cinctipes Stål, 1877: 46; Schwarz and Roy 2018: 456.

***Arria leigongshanensis* (Ge & Chen, 2008)**
Figs 4D–F, 9A, 10E–H

Palaeothespis leigongshanensis Ge & Chen, 2008: 53–58.

Material examined. ***Holotype***, 1♂, China: Guizhou Prov., Leigong Mountain National Natural Reserve, 13.IX.2005, Qiong-Zhang Song leg.; ***Paratype***, 1♀, same locality as for holotype, 14.IX.2005, Zhi-Jie Wang leg. (IEGU).

***Arria meghalayensis* (Mukherjee, 1995)**

Pseudothespis meghalayensis Mukherjee, 1995: 60; Schwarz and Roy 2018: 456.

***Arria oreophila* (Tinkham, 1937)**

Palaeothespis oreophila Tinkham, 1937: 497–499; Svenson 2014: 55–56.

Remarks. *Arria oreophila* was described and illustrated by Tinkham based on 1 male and 1 female from Sichuan, China. In Tinkham (1937), the foretibial consists of 13 anteroventral spines in males and 11 in females. But according to Svenson (2014), the anteroventral spines of the foretibia is R9/L8 in the male and 8 in the female. It falls into the range described for other species of *Arria*. *Arria oreophila* differs from others in both fore- and hindwings brownish, veins RP and M with two forks.

***Arria pallida* (Zhang, 1987)**
Figs 4G–I, 10I–L

Palaeothespis pallida Zhang, 1987: 239
Sinomiopteryx yunnanensis Xu, 2007: 244 syn. nov.

Material examined. ***Holotype***, 1♂, China: Yunnan Prov., Lushui County, 10.X.1980, Guo-zhong Zhang leg. (NFU); 2♂♂, Yunnan Prov., Fenshuiling National Natural Reserve, 19.V.2015, Yun-fei Wu and Jia-jia Wang leg. (IEGU).

Remarks. Xu (2007) described this species in *Sinomiopteryx* from Yunnan, China. The descriptions and illustrations for both external morphology and genitalia of *Sinomiopteryx yunnanensis* Xu, 2007 fall into the range presented for *Arria pallida* (Zhang, 1987), especially the significant differences of male genitalia between *Arria* and *Sinomiopteryx* (Figs 4A–L, 5A–F). Therefore, we consider *S. yunnanensis* Xu, 2007 as a junior synonym of *A. pallida* Zhang, 1987.

Figure 1. *Arria pura* sp. nov., dorsal habitus **A** male holotype **B** female paratype **C** posteroventral genicular spines of male forefemur (not to scale). Scale bar: 10 mm.

***Arria pura* Wang & Chen, sp. nov.**
http://zoobank.org/12C0F813-0717-4B2D-81C7-1E713062E2AE
Figs 1–3, 4A–C, 6

Type material. ***Holotype*:** ♂, China: Guizhou Province, Weining County, Jinzhong Town (26°42.34'N, 104°37.29'E), 2550 m, 17.VIII.2017, Ying-Jian Wang; ***Paratypes*:** 1♀, same data and locality as holotype (IEGU), PT1; 1♀, Guizhou Province, Weining County, Xueshan Town (27°04.04'N, 104°06.68'E), 2450 m, 2.IX.2019, Feng-E Li, PT2.

Description. Measurements are provided in Table 1.

Male. Small, slender (Figs 1A, 3).

Head (Fig. 2A). Triangular, about 1.4 times as wide as long. Vertex with pair of paramedian depressions, otherwise flat. Compound eyes oval and large, conspicuously projecting outside profile of head. Juxtaocular bulges present, extending to the dorsal edge of vertex. Ocelli large and elliptic, lateral paired ocelli larger. Antennae filiform, ciliated. Scapus cylinder-shaped, slightly depressed in the middle, approximate as length as width. Pedicellus almost as long as scapus yet narrower, goblet-space. Third antennomere about as long as pedicel. Fourth antennomere less than half of third length.

Table 1. *Arria pura* sp. nov., measurements of type specimens, in mm.

Measured structure	HT (male)	PT1(female) #1	PT2(female)
Head width	2.6	3.2	3.1
Head length	1.8	2.5	2.3
Lower frons width	1.0	1.2	1.2
Lower frons length	0.4	0.5	0.4
Body length	26.3	23.0	21.9
Pronotum length	5.3	6.1	5.7
Prozone length	2.1	2.4	2.3
Metazone length	3.2	3.7	3.4
Pronotum max. width	1.7	2.1	2.0
Forewing length	21.6	–	–
Forewing max. width	4.0	–	–
Forecoxa length	4.3	4.7	4.5
Forefemur length	5.3	5.6	5.3
Forefemur max. width	0.7	1.0	1.0
Foretibia length	2.8	3.2	3.1
Foretarsus length	4.0	3.0	2.8
Mesocoxa length	1.5	1.6	1.8
Mesofemur length	4.4	4.0	3.8
Mesotibia length	3.2	3.0	2.9
Mesotarsus length	2.9	2.4	2.2
Metacoxa length	1.8	1.8	1.8
Metafemur length	5.2	4.7	4.5
Metatibia length	5.6	4.8	4.4
Metatarsus length	4.3	3.5	3.1
Subgenital plate length	1.7	1.9	1.6
Subgenital plate width	1.4	3.5	3.2

Lower frons transverse, 4.2 times as wide as high, flat medially, with dorsal and lateral margins bordered by protruding ridge, ventral margin inconspicuous, dorsal margin obtuse-angled. Clypeus smooth, above of ventral margin with a transverse groove.

Prothorax (Fig. 2B). Short, 3.2 times as long as wide, metazone 1.5 times as long as prozone, lateral margins with small and few setiferous denticulations, middle carina present but feeble in prozone, behind supracoxal sulcus with pair of depressions, posterior margin with pair of paramedian bulges. Prosternum with middle carina posteriad supracoxal sulcus.

Cervix. No ventral cervical sclerite. Intercervical sclerite merged at middle, without torus intercervicalis. Postcervical plate and furcasternite flat.

Metathorax. With cyclopean ear of DK type.

Forelegs. Forecoxa longer than metazone with anterior lobes diverging, dorsal edge and ventral edge with 3–4 and 9–11 tubercules respectively, all tubercules with small seta (Fig. 2D); anterior and posterior surface of forecoxa mostly smooth. Forefemur (Fig. 2E) slender, with four posteroventral spines, almost as long as each other; four discoidal spines, numeric patterns: 1231, the fourth discoidal spines inclined toward apex strongly; eleven anteroventral spines, the resulting arrangement of the holotype being iIiIiIiIiiI; posteroventral genicular lobe with two spines arranged in a row and the small one near apex (Fig. 1C); anteroventral genicular lobe with a single spine; F = 4DS/11AvS/4PvS. Foretibia armament: six posteroventral spines, the apical two

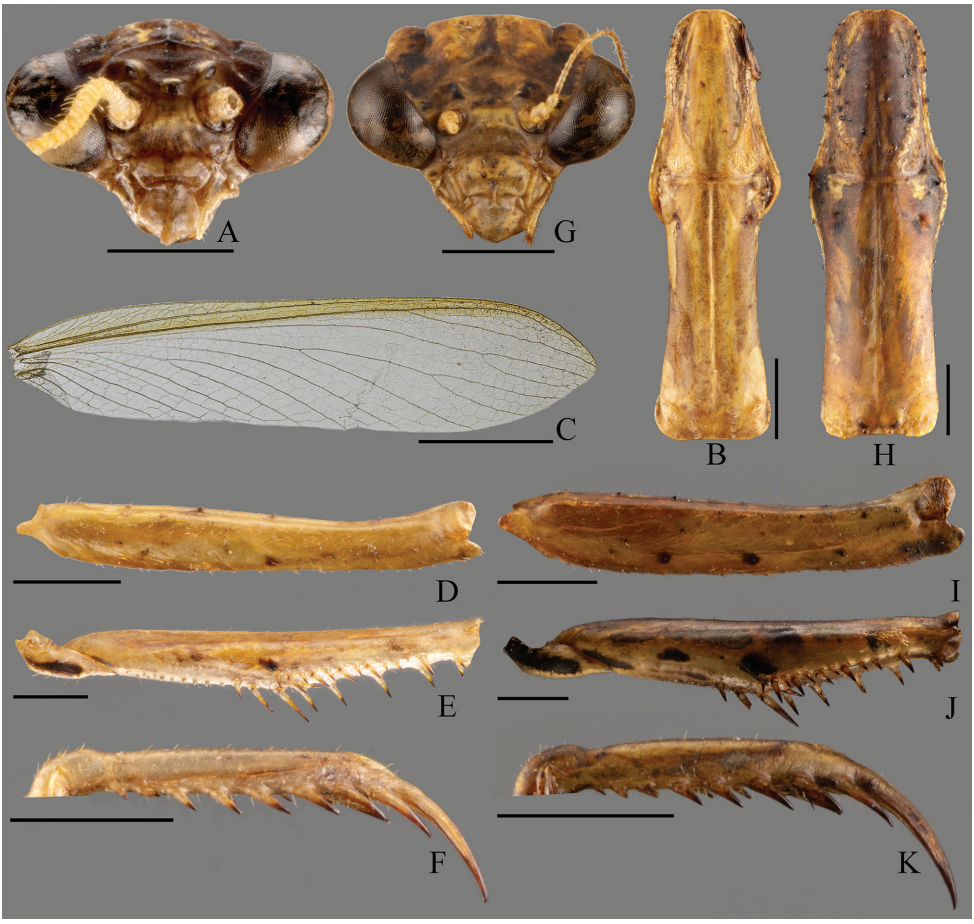

Figure 2. *Arria pura* sp. nov., details of morphology **A–F** male **G–K** female **A, G** head, frontal view **B, H** pronotum, dorsal view **C** forewing, dorsal view **D, I** forecoxa, ventral view **E, J** fore- trochanter and femur, ventral view **F, K** foretibia, ventral view. Scale bars: 5 mm (**C**); 1 mm (**A, B, D–K**).

closes to each other; eight anteroventral spines, elongating distally; T = 8AvS/6PvS. Metatarsus 1.5 times as long as remaining tarsomeres combined.

Middle and hind legs. Long, cursorial. Meso- and metafemur apically without genicular spine. Meso- and metatibia apically with two spines. Middle 2 to 5 tarsomeres combined 1.6 times as long as middle metatarsus. Hind metatarsus slightly longer than remaining tarsomeres combined.

Wings (Fig. 2C). Fully developed, surpassing the end of abdomen. Forewing hyaline without spots, 5.4 times as long as width. Costal field reaches 4/5 of the forewing's length. Stigma elongated, inconspicuous.

Abdomen. Depressed dorsoventrally, coxosternite 9 (subgenital plate) (Fig. 4C) longer than wide, covered ventrally and laterally by numerous setae. Tergite 10 (supra-anal plate) (Fig. 4B) triangular. Cerci with approximate 12 cercomeres, difficult to distinguish from each other near the base, distal-most cercomere elongate.

Figure 3. Male last instar nymph of *A. pura* sp. nov. holotype, life habitus **A** dorsal view **B** lateral view. Photograph by Ying-Jian Wang.

Male genitalia (Fig. 4A). Sclerite L4A approximately rhomboidal, with strongly transverse terminal lobe (tl) on right side of distal process in ventral view. Distal process inclined dorsolaterally, at an angle of 100° relative to the plane of L4A. Sclerite L4B winebottle-shaped, slightly curved near base. Sclerite L2 with apical process paa strongly curved, almost parallel to L4B dorsally. Sclerite L1 elongated, afa sclerotized, covered by numerous small granules apically. Fda of right phallomere sclerotized by sclerite R1A densely covered by long setae. Sclerite R1A more or less triangular. Sclerite R3 drumstick-shaped; sclerotized processes very developed. Sclerite R1B with pia well sclerotized, process pva large, ear-shaped.

Coloration. General color brown. Vertex brown; juxtaocular bulges fuscous. Ocelli hyaline. Foretrochanter black ventrally, base anteroventral of forefemur black as well as base of tibial spur groove (Fig. 2E). All spines arising from forefemoral, foretibial and tibial spur fuscous apically. Meso- and metatibia light brown. Fore- and hindwings hyaline, light brown, apex and costal area of forewings brownish (Fig. 2C).

Female. Apterous (Fig. 1B).

Head (Fig. 2G). Triangular, about 1.3 times as wide as long. Compound eyes oval and large, obviously projecting outside profile of head. Juxtaocular bulges slightly exceeding dorsal margin of vertex. Ocelli smaller than male. Antennae much shorter than male. Lower front transverse 3.9 times as wide as long, dorsal and lateral margins depressed.

Prothorax (Fig. 2H). 3 times as long as wide, metazone 1.5 times as long as prozone. Lateral margin with more and stronger denticulations. Several tubercules present

Figure 4. Male genitalia (ventral view) and terminalia (dorsal view) of *Arria* spp. **A–C** *A. pura* sp. nov., holotype **D–F** *A. leigongshanensis* (Ge & Chen, 2008), holotype **G–I** *A. pallida* (Zhang, 1987) (IEGU: HAAP1) **J–L** *A.* sp.2 (IEGU: HAASP2-1). Scale bars: 1 mm.

Figure 5. Male genitalia (ventral view) and terminalia (dorsal view) of *Sinomiopteryx* spp. **A–C** *S. guangxiensis* Wang & Bi, 1991 (IEGU: HASG1) **D–F** *S.* sp.1 (IEGU: HASSP1-1) **G–I** *S.* sp.2 (IEGU: HASSP2-1). Scale bars: 1 mm.

on pronotum, especially prozone. The paramedian bulges near posterior margin more prominent. Carina on prosternum short.

Cervix. As in the male.

Metathorax. With cyclopean ear of DNK type.

Forelegs. Forecoxa longer than metazone with anterior lobes diverging, dorsal margin with 5–6 small tubercules, ventral edge with 13–15 smaller tubercules, all tubercules with small seta, anterior and posterior of forecoxa mostly smooth (Fig. 2I). Forfemur stronger than male; forefemoral armament with four posteroventral spines; four discoidal spines, numeric patterns: 1231, the fourth discoidal spine strongly inclined toward apex; anteroventral spines with the resulting arrange-

Figure 6. Ootheca of *Arria pura* sp. nov. **A** lateral view **B** dorsal view. Scale bar: 1 mm.

Figure 7. Comparition of Arriini spp., dorsal habitus **A** *A.* sp.1 (IEGU: HAASP1-1) **B** *S.* sp.1 (IEGU: HASSP1-1). Scale bar: 10 mm.

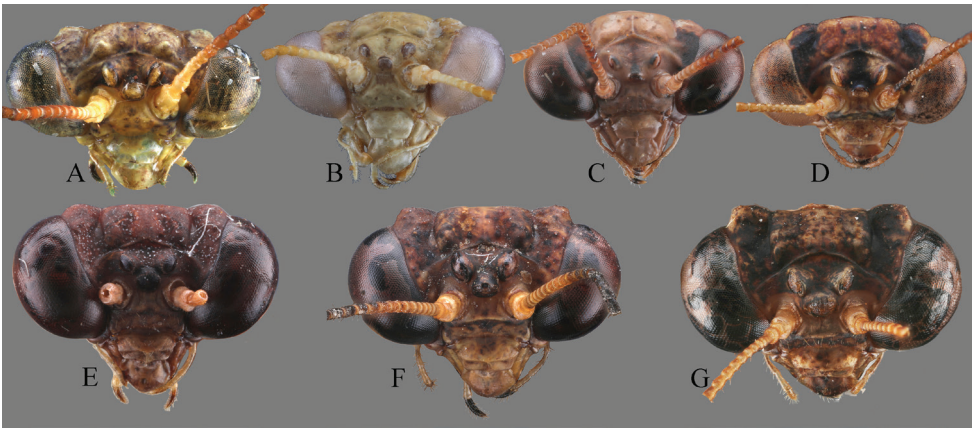

Figure 8. Comparison of Arriini spp., head, frontal view **A** *A. leigongshanensis*, holotype **B** *A. pallida* (IEGU: HAAP1) **C** *A.* sp.1 (IEGU: HAASP1-1) **D** *A.* sp.2 (IEGU: HAASP2-1) **E** *S. guangxiensis* (IEGU: HASG1) **F** *S.* sp. 1 ((IEGU: HASSP1-1) **G** *S.* sp. 2 (HASSP2-1). Not to scale.

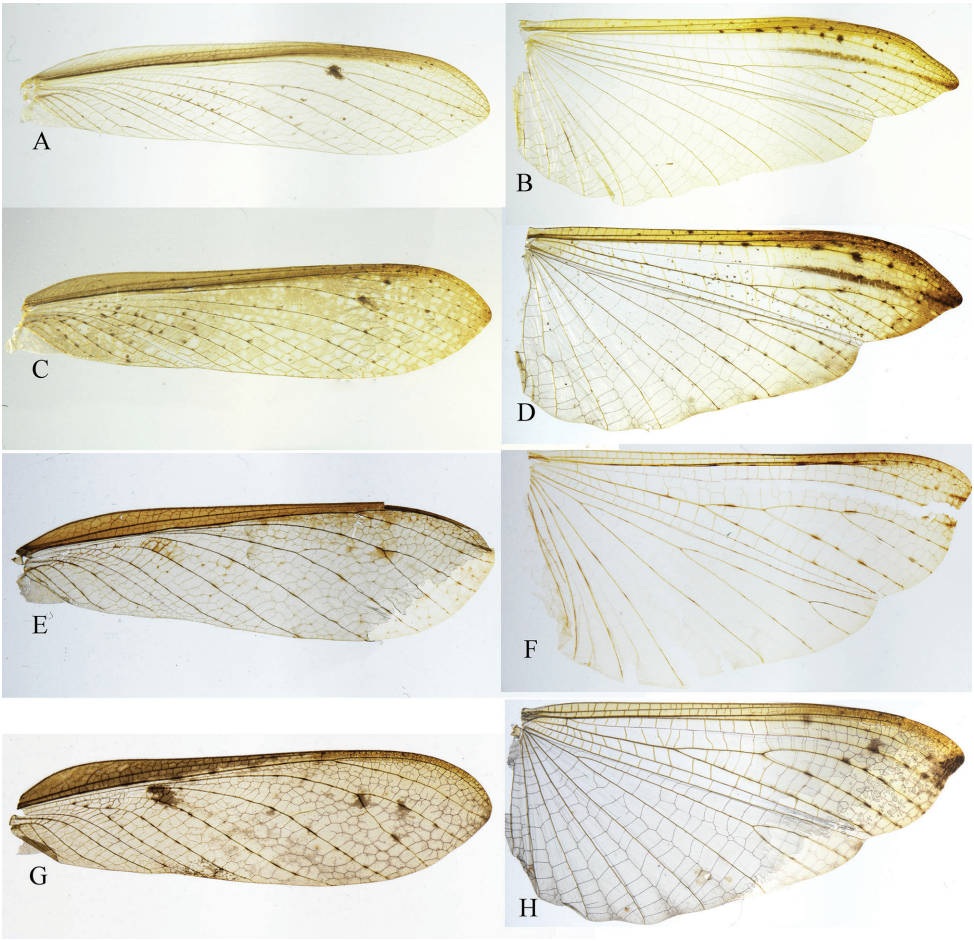

Figure 9. Comparison of Arriini spp., right fore- and hindwings, dorsal view **A, C, E, G** forewings **B, D–F** hindwings **A, B** *A.* sp.1 (IEGU: HAASP1-1) **C, D** *A.* sp.2 (IEGU: HAASP2-1) **E, F** *A.* sp.2 (IEGU: HAASP2-1) **G, H** *S.* sp.2 (HASSP2-1). Not to scale.

ment: iIiIiIiIiiI; F = 4DS/11AvS/4PvS; both genicular lobes with only one spine. Foretibial armament consisting of 5 posteroventral and 7–8 anteroventral spines; T = 7–8AvS/5PvS.

Middle and hind legs. As in the male.

Wings. Apterous, wing pads fused to meso- and metathorax (Fig 1B).

Abdomen. Much wider than male, fusiform. Posterior margin of 1–9 tergites and 2–6 coxosternites with several small tubercles. The lobes on the middle of tergites inconspicuous. Tergite 10 trapezoidal, longer than wide. Cerci short, slightly surpassing tergite 10.

Coloration. General color brown (Fig. 1B). Vertex and juxtaocular bulge yellowish-brown (Fig. 2G). Ocelli hyaline. Clypeus with several dark spots. Tubercules on pronotum dark brown as well as denticulations on lateral margin of pronotum

(Fig. 2H). Anterior surface of forecoxa with 3–4 black spots near ventral margin (Fig. 2I). Foretrochanter black ventrally. Anteroventral base of forefemur, base of tibial spur groove and the middle of them black; anteroventral base of forefemur and base of tibial spur groove black, with another irregular black spots near one-fourth basal of anteroventral margin (Fig. 2J). All spines arsing from forefemoral, foretibial and tibial spur fuscous apically. Meso- and metatibia light brown. The tubercles on abdomen fuscous (Fig. 1B).

Ootheca (Fig. 6). Small, rectangular, mostly trapezoid in cross-section. Residual process long, aciculiform. External wall generally russet brown, with many bubble-like structures embedded, without external coating. Ventral surface attached to complanate substrates, such as surface of leaves. Emergence area raised, openings inconspicuous. Measurements (in mm): length (without residual process), 6.1; length of residual process, 3.1; width, 3.8; thickest girth, 25.3; length of emergence area, 5.7; width of emergence area, 1.8.

Distribution. China (Guizhou) (Fig. 11).

Etymology. The specific name is derived from the Latin words "*pura*" (meaning pure) which refers to the forewing without any spots.

Remarks. The new male species is much smaller than all other known species of *Arria*. Additionally, it can be distinguished from *A. brevifrons*, *A. cinctipes*, *A. leigongshanensis*, *A. pallida* and *A. sticta* by tegmina without any spots. *Arria pura* also differs from *A. oreophila* in having less forked RP and M.

Arria sp. 1

Material examined. China: 3♂♂1♀, Guizhou Prov., Dashahe National Natural Reserve, 26.V.2004, Xiang-Sheng Chen and De-Yan Ge leg. (IEGU); 3♂♂, Hunan Prov., Xiaoxi National Natural Reserve, 15–21.VIII.2016, Ying-jian Wang leg. (IEGU); 5♂♂3♀♀, Guizhou Prov., Leigongshan National Natural Reserve, 17–20.VIII.2019, Ying-jian Wang leg. (IEGU).

Arria sticta (Zhou & Shen, 1992)

Palaeothespis sticta Zhou & Shen, 1992: 62–63.

Remarks. The holotype is probably lost, as we did not find it in the Zhejiang Museum of Natural History where the author used to work. *Arria sticta* is similar to *A. pallida* but differs from the latter in that a dark stripe is located along the anteroventral base to the first discoidal spine of forefemur; with three dark spots on the ventral surface of forefemur.

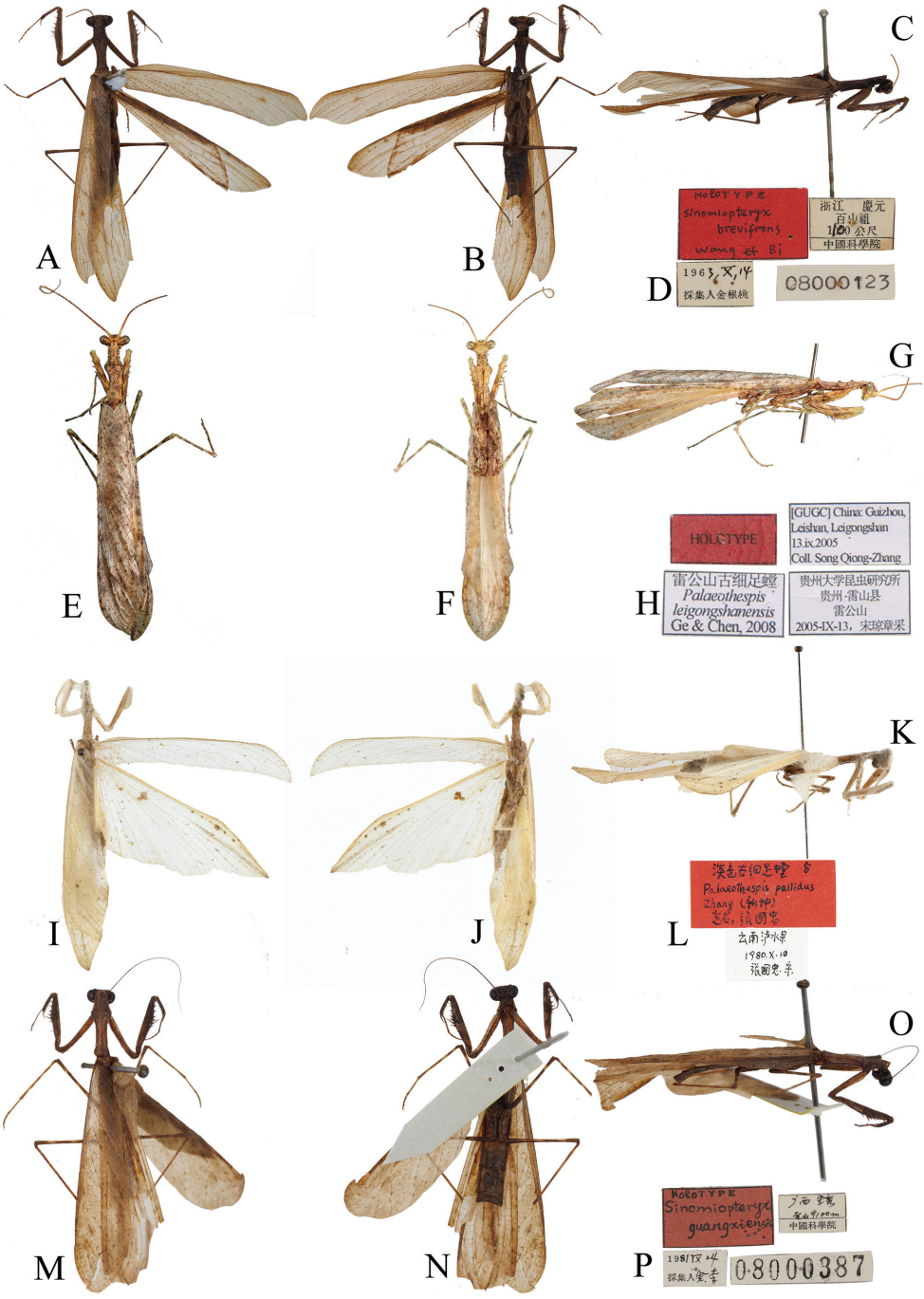

Figure 10. Holotypes of Arriini spp. **A, E, I, M** dorsal habitus **B, F, J, N** ventral habitus **C, G, K, O** lateral habitus **D, H, L, P** labels **A–D** *A. brevifrons* comb. nov. (SEM) **E–H** *A. leigongshanensis* (IEGU) **I–L** *A. pallida* (NFU) M-P *S. guangxiensis* (SEM). Not to scale.

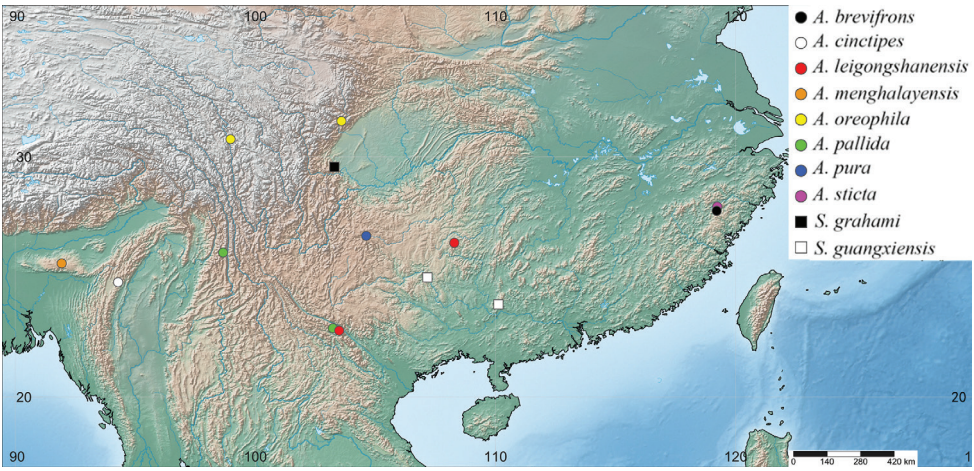

Figure 11. Arriini Giglio-Tos, 1919, distribution map.

Sinomiopteryx Tikham, 1937

Sinomiopteryx Tikham, 1937: 495; Wang and Bi 1991: 126; Wang 1993: 111; Ehrmann 2002: 319.

Type species. *Sinomiopteryx grahami* Tinkham, 1937, original designation.

Diagnosis. Body medium and slender (Fig. 7). Head narrowly transverse with prominent juxtaocular bulges; compound eyes broadly oval, prominent; Ocelli very large closely grouped in the male (Fig. 8E–G), minute in the female. Lower frons narrowly transverse. Antennae filiform, long in male, much shorter in female. Forefemur of males wider than in *Arria*, with 4 discoidal, 11–13 anteroventral and 4 posteroventral spines; foretibia with 8–10 anteroventral and 5–6 posteroventral spines. Pronotum short with supracoxal dilatation well marked, sparsely granulate, lateral margins with sparsely and strongly denticulate. Forewing broader than *Arria*, with rounded apex, CuA branches no more than 4, L/W ratio is 3.3–3.7, fore margin clothed with dense cilia; hindwing with truncate apex; both pairs of wings fully developed and exceeding the end of abdomen in male (Fig. 9E–H); female apterous. Sclerite L4A approximately rhomboidal, sdp thick with tip granulated, no terminal lobe (tl), right phallomere with large pia and pva. Styli far apart from each other.

Sinomiopteryx grahami Tinkham, 1937

Sinomiopteryx grahami Tinkham, 1937: 495; Wang and Bi 1991: 126; Wang 1993: 112; Ehrmann 2002: 319; Svenson 2014: 70.

Remarks. Tinkham (1937) erected *Sinomiopteryx* with this male species, collected from Szechwan, Mt. Omei, Baian-Kara-Ula Range (China, Sichuan Prov., Mountain

Emei), illustrated both male and female lateral habitus, and left tegmen in dorsal view. Wang and Bi (1991) and Wang (1993) illustrated the genitalia for *S. graham,* but it may have been mistaken.

***Sinomiopteryx guangxiensis* Wang & Bi, 1991**

Sinomiopteryx guangxiensis Wang & Bi, 1991: 126; Wang 1993: 112; Ehrmann 2002: 319.

Material examined. ***Holotype***, 1♂, China: Guangxi Prov., Jinxiu county, Laoshan, 24.IX.1981, Gen-tao Jin & Fu-liang Li leg. ID: 08000387 (SEM); 1♂, Guangxi Prov., Tian'e County, Longtan Nature Reserve, 18.VII.2015, Ying-jian Wang leg. (IEGU).

Remarks. This species was described and illustrated by Wang and Bi in 1991 based on one male specimen from Guangxi, the holotype has had the abdomen removed, but we did not find the genitalia. Fortunately, we collected a male from Guangxi, and it perfectly fits with *S. guangxiensis*, and can be used as accurate comparative material.

***Sinomiopteryx* sp. 1**

Material examined. China: 2♂, Guizhou Prov., Ziyun County, Xiaochuandong, 15.XI.2015, Ying-jian Wang leg. (IEGU); 1♂, Guizhou Prov., Ziyun County, Xiaochuandong, 15.IX.2016, Ying-jian Wang leg. (IEGU); 1♂, Guizhou Prov., Ziyun County, Xiaochuandong, 21.X.2019, Ying-jian Wang leg. (IEGU); 1♂, Guizhou prov., Duyun city, Doupengshan, 22.IX.2016, Ying-jian Wang leg. (IEGU); Hunan Prov., Xiaoxi National Natural Reserve, 20.VIII.2016, Ying-jian Wang leg. (IEGU).

***Sinomiopteryx* sp. 2**

Material examined. China: 1♂, Yunnan Prov., Maguan County, Gulinqing town, 23.VIII.2020, Xiang-jin Liu leg. (IEGU).

Discussion

Arria is superficially similar to *Sinomiopteryx*, but differs substantively in details. *Arria* can be distinguished from the latter by the following characters: (1) ventral phallomere with terminal lobe (tl) (*Sinomiopteryx* without pl); (2) styli close to each other (styli further apart in *Sinomiopteryx*) (Figs 4–5); (3) forewings narrower, L/W ratio is 4.3–5.5, CuA with five branches or more (forewings wide, L/W ratio is 3.3–3.7, CuA with four branches or less in *Sinomiopteryx*) (Fig. 9). The ocelli characters seem unstable in *Arria*, especially in *A. leigongshanensis*, they look as in *Sinomiopteryx*, but

they are very large and grouped in *Sinomiopteryx* (Fig. 8). Nevertheless, identification of species may be difficult because original species descriptions are inadequate in that many features are not evaluated and included, especially the male genitalia. Besides, most females of Arriini are undescribed and difficult to distinguish from each other, unless both male and female are collected at the same time or DNA barcoding is performed. Further fieldwork is needed to uncover specimens of the rare tribe, finally allowing for its better characterization.

Acknowledgements

We are indebted to Christian J. Schwarz (Ruhr University Bochum, Germany) for providing important literature and suggestions on earlier drafts of this manuscript. We are grateful to Cuiqing Gao (Nanjing Forestry University), Liwei Liu (Zhejiang Museum of Natural History), Weibing Zhu (Shanghai Entomological Museum), Floyd W. Shockley (National Museum of Natural History, Smithsonian Institution), Gavin Svenson (Cleveland Museum of Natural History) for helping us check the types. This work was supported by the Science and technology support program of Guizhou Province (No. 20201Y129), the Program of Excellent Innovation Talents, Guizhou Province (No. 20154021) and the Program of Science and Technology Innovation Talents Team, Guizhou Province (No. 20144001).

References

Brannoch SK, Wieland F, Rivera J, Klass KD, Béthoux O, Svenson GJ (2017) Manual of praying mantis morphology, nomenclature, and practices (Insecta, Mantodea). ZooKeys 696(3): 1–100. https://doi.org/10.3897/zookeys.696.12542

Ehrmann R (2002) Mantodea. Gottesanbeterinnen der Welt. Münster, Natur und Tier-Verlag Gmb H, 72, 259, 298.

Ge DY, Chen XS (2008) Review of the genus *Palaeothespis* Tinkham, 1937 (Mantodea: Thespidae), with description of one new species. Zootaxa 1716: 53–58. https://doi.org/10.11646/zootaxa.1716.1.5

Giglio-Tos E (1919) Saggio di una nuova classificazione dei Mantidi. Bullettino della Società Entomologica Italiana 49: 50–87.

Mukherjee TK, Hazra AK, Ghosh AK (1995) The mantid fauna of India (Insecta: Mantodea). Oriental Insects 29: 185–358. https://doi.org/10.1080/00305316.1995.10433744

Otte D, Lauren S, Martin BD (2020) Mantodea Species File Online. Version 5.0/5.0. http://Mantodea.SpeciesFile.org [Accessed 10 Jun 2020]

Schwarz CJ, Roy R (2018) Some taxonomic and nomenclatural changes in Mantodea (Insecta: Dictyoptera). Bulletin de la Société entomologique de France 123(4): 456–456. https://doi.org/10.32475/bsef_1990

Schwarz CJ, Roy R (2019) The systematics of Mantodea revisited: an updated classification incorporating multiple data sources (Insecta: Dictyoptera). Annales de la Société entomologique de France (N.S.) 55(2): 141–141. https://doi.org/10.1080/00379271.2018.1556567

Shorthouse DP (2010) SimpleMappr, an online tool to produce publication-quality point maps. Accessed 23 November 2019. http://www.simplemappr.net

Stål C (1877) Systema Mantodeorum. Essai d'une systématisation nouvelle des Mantodées. Bihang till Kongliga Svenska Vetenskaps Akademiens Handlingar 4(10): 1–91.

Svenson GJ (2014) The type material of Mantodea (praying mantises) deposited in the National Museum of Natural History, Smithsonian Institution, USA. Zookeys 433: 31–75. https://doi.org/10.3897/zookeys.433.7054

Tinkham ER (1937) Studies in Chinese Mantidae (Orthoptera). Lingnan Science Journal 16(3): 495–499.

Wang TQ (1993) Synopsis on the classification of Mantodea from China. Shanghai: Science and Technology publication of Shanghai, 110–116.

Wang TQ, Bi DY (1991) Two new species of *Sinomiopteryx* Tinkham, 1937 (Mantodea: Mantidae). Contributions from Shanghai Institute of Entomology Vol. 10: 125–128.

Wieland F (2013) The phylogenetic system of Mantodea (Insecta: Dictyoptera) Species, Phylogeny and Evolution. Universitätsverlag Göttingen (SPE) 3(1): 3–222. https://doi.org/10.17875/gup2013-711

Xu JS (2007) A new species of the genus *Sinomiopteryx* Tinkham, 1937(Mantodea: Mantidae) from Yunnan. Entomotaxonomia 29(4): 244–246.

Zhang GZ (1987) A new species of the genus *Palaeothespis* Tinkham from China. Entomotaxonomia 9(3): 239–241.

Zhou WB, Shen SG (1992) Study of Mantodea fauna in Zhejiang and Yunnan provinces and two new species. Journal of Shanghai Teachers University (Natural Science) 21(1): 62–68.

Zhu XY, Wu C, Yuan Q (2012) Mantodea in China. Xiyuan Publishing House, Beijing, 331 pp.

ZooKeys 1025: 21–34 (2021)
doi: 10.3897/zookeys.1025.59920
https://zookeys.pensoft.net

RESEARCH ARTICLE

A peer-reviewed open-access journal
ZooKeys
Launched to accelerate biodiversity research

The genus *Dasyproctus* (Hymenoptera, Apoidea, Crabronidae) in China, with description of two new species

Dan Yue[1], Li Ma[1], Qiang Li[1]

1 *Department of Entomology, College of Plant Protection, Yunnan Agricultural University, Kunming, Yunnan, 650201, China*

Corresponding authors: Li Ma (maliwasps@aliyun.com); Qiang Li (liqiangkm@126.com)

Academic editor: M.S. Engel | Received 22 October 2020 | Accepted 15 February 2021 | Published 18 March 2021

http://zoobank.org/32E89FDA-E372-4EB4-B352-5116450D4941

Citation: Yue D, Ma L, Li Q (2021) The genus *Dasyproctus* (Hymenoptera, Apoidea, Crabronidae) in China, with description of two new species. ZooKeys 1025: 21–34. https://doi.org/10.3897/zookeys.1025.59920

Abstract

Two new species of the genus *Dasyproctus* Lepeletier de Saint Fargeau & Brullé (Crabronidae, Crabroninae, Crabronini) from China are described and illustrated, namely *D. amplicarinalis* Yue & Ma, **sp. nov.** from Yunnan, and *D. hainanensis* Yue & Li, **sp. nov.** from Hainan. In addition, *D. cevirus* Leclercq and *D. vaporus* Leclercq are recorded for the first time from China. A key to the species of *Dasyproctus* from China is provided.

Keywords

Crabroninae, taxonomy, key, new species, new records

Introduction

The genus *Dasyproctus* Lepeletier de Saint Fargeau & Brullé, 1834 belongs to the subtribe Crabronina, tribe Crabronini, subfamily Crabroninae (Hymenoptera, Crabronidae). At present, *Dasyproctus* includes 79 species with 21 subspecies of small- to medium-sized predatory solitary wasps worldwide, of which 25 species and two subspecies occur in the Oriental Region, 37 species and 16 subspecies in the Afrotropical Region, 12 species in the Australasian Region, one species and one subspecies in both

the Palearctic and Oriental Regions, two species in both the Palearctic and Afrotropical Regions, one species and two subspecies in both the Oriental and Afrotropical Regions, one species in both the Oriental and Australasian Regions, and one species in the Palearctic, Oriental, and Australasian Regions (Pulawski 2020; Binoy et al. 2021). In China, three species and one subspecies have been recorded from Foo Chow, Guangzhou, Szechwan, and Taiwan (Smith 1858; Cameron 1889, 1890; Turner 1912a, b; T. Ma 1936; Leclercq 1954, 1956, 1972, 1982, 2015; Tsuneki 1959, 1966, 1968, 1971, 1977, 1982; Haneda 1971, 1972; Murota 1973; Porter et al. 1999; Hua 2006).

In the present study of the *Dasyproctus* of China, two new species are described and two species are reported from China for the first time. A key to the Chinese species of the genus is provided.

Materials and methods

The specimens examined during this study are deposited in the Insect Collection of Yunnan Agricultural University, Kunming, China (**YNAU**).

All specimens were observed and illustrated with the aid of an Olympus stereomicroscope (SZ Series) with an ocular micrometer. The photographs were taken with a Keyence VHX-5000. The final illustrations were improved for contrast and brightness using Adobe Photoshop CS5.

Terminology follows Bohart and Menke (1976). The abbreviations used in the text are as follows: **HL**, head length in dorsal view (distance from frons to occipital carina in the middle); **HW**, head width (dorsal view, maximum); **POD**, postocellar distance (distance between inner margins of hind ocelli); **OOD**, ocellocular distance (distance between outer margin of hind ocellus and nearest inner orbit). Size of punctures: small or fine, puncture diameters less than 0.1× posterior ocellar diameter; midsize, 0.1–0.2× posterior ocellar diameter.

Systematics

Dasyproctus Lepeletier de Saint Fargeau & Brullé, 1834

Dasyproctus Lepeletier de Saint Fargeau & Brullé, 1834: 801. Type species: *Dasyproctus bipunctatus* Lepeletier de Saint Fargeau & Brullé, 1834, by monotypy.

Megapodium Dahlbom, 1844: 295. Type species: *Megapodium westermanni* Dahlbom, 1844, designated by Pate (1937: 37).

Bishamonis Tsuneki, 1983: 17, as subgenus of *Dasyproctus*. Type species: *Dasyproctus guadalensis* Tsuneki, 1983, by original designation and monotypy.

Diagnosis. Body opaque or dull; scapal basin concave, simple or delimited dorsally by a carina; orbital fovea distinct to evanescent; antennal sockets contiguous with each

other and with inner orbits; scape bicarinate; male flagellum simple or modified, most species without ventral setal fringe (except *D. araboides*); mandible bidentate apically in male, tridentate in female; pronotal collar with anterior carina reaching pronotal lobe in males and most females; postspiracular carina, omaulus, and acetabular carina present, contiguous; verticaulus elongate, sometimes inconspicuous; propodeum moderately sculptured, dorsal face micro-ridged, rugose, or areolate, enclosure not or inconspicuously defined, lateral propodeal carina well developed; legs simple or with hind femur modified; recurrent vein joining submarginal cell beyond its middle; jugal lobe shorter than submedian cell; gaster with first segment elongate-pedunculate; male without pygidial plate, female pygidial plate markedly narrowed, concave (Bohart and Menke 1976; Leclercq 2015).

***Dasyproctus amplicarinalis* Yue & Ma, sp. nov.**
http://zoobank.org/F046D4FA-88E6-48F9-B299-3E03CABC4518
Figure 1a–g

Material examined. ***Holotype.*** ♀, China: Yunnan: Dehong: Yingjiang: Yunyan Mountain, 24°69'N, 97°93'E, 2005.VIII.15, coll. Li Ma (YNAU); ***Paratypes.*** 1♀, same place and date as holotype, coll. Kai Wu (YNAU); 1♀, China: Yunnan: Nujiang: Lushui, 25°97'N, 98°82'E, 2006.VII.19, coll. Li Ma (YNAU).

Diagnosis. The new species clearly differs from the Oriental *D. buddha* (Cameron) by the following combination of characters: frontal area dorsally with a high, lamellar, transverse carina at upper margin of scapal basin, carina interrupted by a broad and deep depression medially, and markedly high on each side of depression (Fig. 1c); antennal scape (except above with two black spots medially) yellow, pedicel brown (Fig. 1b); fore femur with one yellow spot; spots of tergum II larger than those of scutellum and tergum V (Fig. 1e, g). In *D. buddha*: frontal area dorsally with a lamellar, transverse carina at upper margin of scapal basin, carina interrupted by a narrow and shallow depression medially, and slightly higher on each side of depression; scape and pedicel yellow; fore femur with two separated yellow spots; spots of tergum II smaller than those of scutellum and tergum V.

The new species and *D. buddha* can be distinguished from the other species of the genus by the following combination of characters: free margin of clypeus truncate, slightly emarginated medially, lateral area with a blunt tooth on each side; frontal area dorsally with a lamellar, transverse carina at upper margin of scapal basin, carina interrupted by depression medially; anterior carina of pronotal collar laterally not curving toward pronotal lobe; length of petiole more than 2× maximum width.

Description. Female (Fig. 1a). ***Body*** length 9.5–11.0 mm. Black; mandible largely pale yellowish (Fig. 1b); yellow are: scape (except above with two black spots) (Fig. 1b), pronotal collar (except black depression medially), pronotal lobe, anterior corner of scutellum, axilla (Fig. 1e), spot on ventral surface of fore femur subbasally, widely L-shaped band on mid femur ventrally (spot divided into two parts in some specimens),

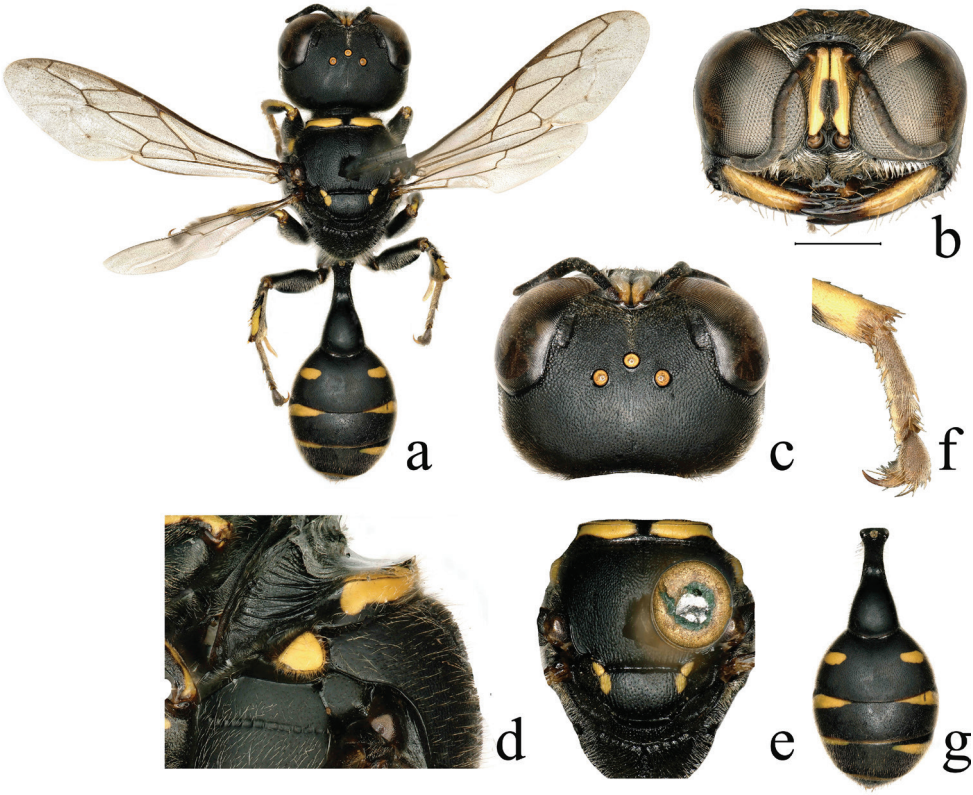

Figure 1. *Dasyproctus amplicarinalis* Yue & Ma, sp. nov., ♀. **a** habitus, dorsal view **b** head, frontal view **c** head, dorsal view **d** collar, lateral view **e** mesosoma, dorsal view **f** fore tarsomere I, dorsal view **g** metasoma, dorsal view. Scale bars: 0.43 mm (**e**); 0.49 mm (**a**); 0.57 mm (**g**); 1 mm (**b, c**); 1.31 mm (**f**); 1.48 mm (**d**).

fore and mid tibiae ventrally and subapical 2/3 of hind tibia ventrally, spots on gastral terga II–V (Fig. 1g). Integument mostly with sparse, silvery setae; upper frons mostly and vertex entirely with sparse, golden setae; upper frons near transverse carina and frontal line with denser, golden setae; gena with short, dense, silvery appressed setae; scapal basin (except frontal line) with short, dense, golden setae; clypeus with dense, appressed, silvery setae; scape with white setae apically; lateral surface of mesosoma with dense, golden setae; gastral terga I–V with sparse, brown setae; sternum II with silvery setae and a nearly round setal spot laterally; posterior margin of sterna II–V with long, sparse, brown setae; tergum V laterally and pygidial plate basally and laterally with long, brown setae.

Head. Mandible tridentate apically, inner side of mandible produced subapically; free margin of clypeus truncate, slightly emarginated medially, lateral area with a blunt tooth on each side (Fig. 1b); relative lengths of scape:pedicel:flagellum I:flagellum II:flagellum III = 100:18:29:22:20; frontal area dorsally with a high, lamellar, trans-

verse carina at upper margin of scapal basin, carina interrupted by a broad and deep depression medially, and markedly high on each side of depression (Fig. 1c); orbital fovea shiny, oval, distinct, and large, length ca. 3× width, widest area slightly broader than hind ocellus diameter (Fig. 1c); upper frons with line formed by punctures (Fig. 1c), and with dense, small punctures 0.0–0.5× diameters apart; vertex with dense, small punctures ca. 1.5–2.0× diameters apart; gena with small punctures ca. 2–5× diameters apart; vertex to anterior ocellus with extremely fine midline (Fig. 1c). HL:HW:POD:OOD = 40:67:11:13.

Mesosoma. Anterior carina of pronotal collar curving backwards in middle, laterally not curving toward pronotal lobe, nearly parallel to anterior margin of scutum, extending to insertion of fore coxa (Fig. 1d); pronotal collar with mid furrow (Fig. 1e); scutum with dense, midsize punctures ca. 1.0–1.5× diameters apart, and short, longitudinal rugae posteriorly; scutellum with dense, shallow, midsize punctures ca. 3–4× diameters apart and short, oblique longitudinal rugae posteriorly; mesopleuron with dense, shallow, midsize punctures ca. 1–4× diameters apart; metanotum with longitudinal rugae mixed with dense, midsize punctures ca. 0.8–1.0× diameters apart; metapleuron with coarse, oblique rugae; propodeal enclosure with oblique rugae and mid furrow; posterior surface with oblique rugae and mid furrow; lateral surface with dense, oblique rugae; outer margin of fore tarsomere I with three spines subbasally.

Metasoma. Length of petiole 2.27× maximum width (Fig. 1g), and ca. half of hind femur, its surface with dense, midsize punctures ca. 1.5–2.0× diameters apart; terga with dense, fine punctures; sternum II with dense, small punctures; sterna III–VI posteriorly with dense, small to midsize punctures; terga II–V with yellow spot on each side, spots on terga III–IV larger than those of terga II and V, and spots on tergum II larger than those of tergum V (Fig. 1g); spots on tergum II larger than those of scutellum, but shorter than half of those of tergum III (Fig. 1e, g). Pygidial plate concave and narrow, with sparse, small to midsize punctures anteriorly, and with contiguous, midsize punctures and longitudinal rugae posteriorly.

Male. Unknown.

Distribution. China (Yunnan).

Etymology. The species' name, *amplicarinalis*, is derived from the Latin stem *ampl-* (= large, spacious, roomy) and the Latin word *carinalis*, referring to the high, lamellar, transverse carina at the upper margin of the scapal basin, which is one of the main diagnostic characters of this species.

***Dasyproctus hainanensis* Yue & Li, sp. nov.**
http://zoobank.org/62B586B8-1FF3-45AB-9F4C-860816D317BA
Figure 2a–g

Material examined. ***Holotype.*** ♀, China: Hainan, 18°10'–20°10'N, 108°37'–111°05'E, 1934.VIII.2, coll. Qi He (YNAU).

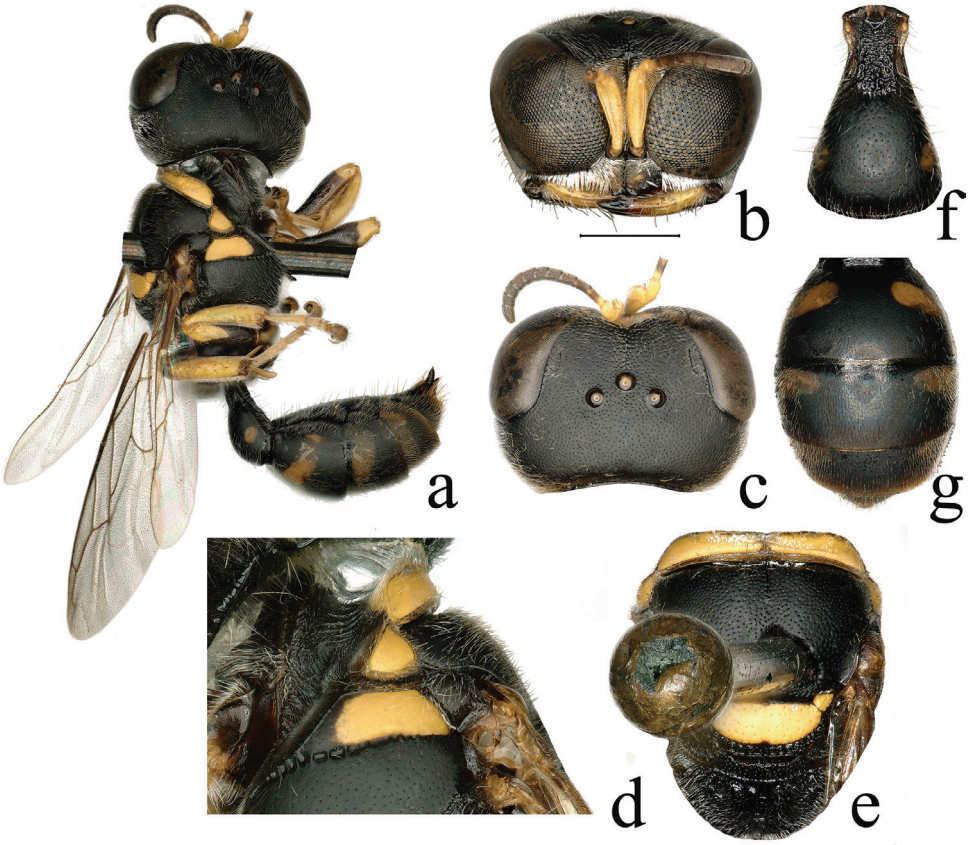

Figure 2. *Dasyproctus hainanensis* Yue & Li, sp. nov., ♀ **a** habitus, lateral view **b** head, frontal view **c** head, dorsal view **d** collar, lateral view **e** mesosoma, dorsal view **f** petiole, gastral tergum I, dorsal view **g** gastral terga II–V, dorsal view. Scale bars: 0.68 mm (**a**); 0.89 mm (**e, g**); 0.99 mm (**c**); 1 mm (**b**); 1.31 mm (**f**); 1.65 mm (**d**).

Diagnosis. The new species clearly differs from the Oriental *D. pentheri* Leclercq by the following combination of characters: free margin of clypeus with a deep, triangular emargination medially, laterally with an angular tooth on each side (Fig. 2b); propodeal enclosure with sparse, sturdy, longitudinal rugae; tibiae largely yellow (inner surface brown). In *D. pentheri*, the free margin of the clypeus has a deep semicircular emargination medially, the lateral area has a round tooth on each side; the propodeal enclosure has irregular, slender rugae; the tibiae are largely black.

The new species and *D. pentheri* can be distinguished from the other species of the genus by the following combination of characters: free margin of clypeus with a deep emargination medially, lateral area with a tooth on each side; anterior carina of pronotal collar laterally curving toward pronotal lobe; length of petiole no more than 2× maximum width (Fig. 2f).

Description. Female (Fig. 2a). ***Body*** length 7.8 mm. Black; yellow are: mandible (largely), two spots on clypeus medially, scape, pedicel, and flagellomere I subbasally, pronotal collar, pronotal lobe, prepectus (largely), scutellum, axilla, outer and inner sides of fore femur apically, apical half of mid femur, fore and mid tibiae, outer surface of hind tibia; fore coxa apically, inner sides of fore and mid trochanters, and tarsus pale yellowish; spots on gastral terga I–II laterally yellowish-brown, spots on terga III–IV laterally ferruginous, bands on tergum V and posterior margin of terga IV–V ferruginous (Fig. 2f, g). Integument mostly with sparse, silvery setae; clypeus with dense appressed silvery setae; scapal basin (except frontal line) with short, dense, appressed, silvery setae; upper frons and vertex with sparse, pale brown setae; gena with short, somewhat dense, silvery setae; gastral terga largely with sparse, brown setae; gastral sterna II–V with long, somewhat sparse, brown setae; setae on sternum II irregular, setae on sterna III–V in nearly linear arrangement, sternum II laterally with oval setal spot; pygidial plate anterolaterally with long, brown setae.

Head. Mandible tridentate apically; median lobe of clypeus with mid carina, free margin with deep, triangular emargination medially, lateral area with an angular tooth on each side (Fig. 2b); relative lengths of scape:pedicel:flagellum I:flagellum II:flagellum III = 35:7:8:9:6; frontal area dorsally with an inconspicuous, transverse carina at upper margin of scapal basin (Fig. 2c); orbital fovea shiny, distinct, large, oval, length ca. 3× width, widest area slightly narrower than hind ocellus diameter (Fig. 2c); upper frons with line formed by punctures, and with somewhat dense, small to midsize punctures ca. 0.0–1.5× diameters apart; gena with dense, fine punctures ca. 1–2× diameters apart; vertex with somewhat dense, small punctures ca. 2× diameters apart; vertex to anterior ocellus with extremely fine midline (Fig. 2c). HL:HW:POD:OOD = 8:6:2:3.

Mesosoma. Anterior carina of pronotal collar laterally curving toward pronotal lobe (Fig. 2d), pronotal collar with mid furrow (Fig. 2e); scutum with somewhat dense, small punctures ca. 1–3× diameters apart, posterior margin with sparse, small punctures ca. 2–5× diameters apart and short, oblique rugae; axilla with sparse, shallow, midsize punctures ca. 0.0–1.5× diameters apart; scutellum (middle area impunctate) with sparse, shallow, midsize punctures ca. 4.5–5.5× diameters apart and short, longitudinal rugae posteriorly; posterior area shiny, alutaceous, and with dense, midsize punctures, precoxal sulcus with sparse, small punctures anteriorly, metanotum with coarse, longitudinal carinae mixed with sparse, coarse punctures; metapleuron with coarse, oblique rugae; propodeal enclosure with sparse, coarse, longitudinal rugae and mid furrow, lateral area with sparse, oblique rugae; posterior surface with dense, transverse rugae, and narrow, deep mid furrow; lateral surface with dense, fine, oblique rugae.

Metasoma. Length of petiole 1.22× maximum width (Fig. 2f), and half of hind femur, its surface rough, with contiguous large punctures; gastral terga I–IV with a yellowish-brown or ferruginous spot on each side, tergum V with a band, spots on

tergum I slightest of all (Fig. 2g); gastral terga with dense, fine punctures, gastral sterna with sparse, small to midsize punctures; pygidial plate concave and narrow, posteriorly with contiguous, small to midsize punctures and longitudinal rugae.

Male. Unknown.

Distribution. China (Hainan).

Etymology. The new species is named after the Hainan Province of China, where the holotype was collected.

Dasyproctus cevirus Leclercq, 1963, first record from China

Figure 3a–g

Dasyproctus cevirus Leclercq, 1963: 16.

Material examined. 1♀, China: Hainan: Baisha, 2008.IV.29, coll. Chengjin Yan; 1♀, China: Hainan: Bangxi Polu Nature Reserve, 2008.V.3, coll. Chengjin Yan; 1♀, China: Hainan: Lanyang Park, 2002.VII.18, coll. Zaifu Xu; 1♀, China: Hainan: Songtao Reservoir, 2002.VII.17, coll. Zaifu Xu; 1♀, China: Yunnan: Anning, 2006.VII.7, coll. Ming Luo; 2♀, China: Yunnan: Baoshan: Longyang District, 2006.VII.18, coll. Rui Zhang; 2♀, China: Yunnan: Baoshan: Longyang: Lu Jiang Ba Thermal Institute, 2006.VII.20, coll. Rui Zhang; 5♀4♂, China: Yunnan: Dehong: Luanchuan, 2005.VIII.13, coll. Chunju Liu (3♀2♂), Tingjing Li (1♀), Kai Wu (1♀2♂); 4♀2♂, China: Yunnan: Dehong: Luxi, 2005.VIII.9–10, coll. Li Ma (2♀2♂), Tingjing Li (1♀), Xiaoli Li (1♀); 1♀2♂, China: Yunnan: Dehong: Ruili, 2005.VIII.12, coll. Tingjing Li (1♂), Li Ma (1♀1♂); 9♀2♂, China: Yunnan: Dehong: Yingjiang, 2005.VIII.15–16, coll. Kai Wu (1♀1♂), Chunju Liu (1♀), Tingjing Li (4♀), Li Ma (3♀1♂); 2♀, China: Yunnan: Hekou, 2003.VII.21, coll. Zhenshan Geng (1♀), Qiang Li (1♀); 1♀, China: Yunnan: Kunming: Songhua dam, 2006.VII.29, coll. Wenliang Li; 2♂, China: Yunnan: Lincang: Linxiang, 2004.X.5, coll. Li Ma (1♂), Chunju Liu (1♂); 1♀, China: Yunnan: Lijiang: Ninglang, 2005.VIII.25, coll. Tingjing Li; 2♂, China: Yunnan: Mengla: Wangtianshu Forest Park, 2005.V.2, coll. Peng Wang; 3♀1♂, China: Yunnan: Mengla, 2005.V.8, coll. Peng Wang; 2♀, China: Yunnan: Mengla, 2005.V.20–21, coll. Peng Wang; 3♀, China: Yunnan: Nujiang: Fugong, 2003.VIII.24, coll. Peng Wang; 3♀, China: Yunnan: Nujiang: Lishui, 2006.VII.19, coll. Li Ma (1♀), Rui Zhang (2♀); 6♀3♂, China: Yunnan: Simao: Jingdong, 2005.IV.28–V.1, coll. Chunju Liu (2♂), Baoxin Dong (3♀), Kai Wu (1♀1♂), Hesheng Wang (2♀); 13♀4♂, China: Yunnan: Simao: Jinggu, 2004.X.4, coll. Baoxin Dong (2♀), Chunju Liu (1♀), Kai Wu (1♀1♂), Li Ma (7♀2♂), Hesheng Wang (1♀1♂), Haiyan Zhang (1♀); 1♀, China: Yunnan: Kunming: Yunnan Agricultural University, 2007.VIII.15, coll. Peng Wang; 1♀, China: Yunnan: Xishuangbanna: Jinghong: Daluo Forest Park, 2004.X.2, coll. Kai Wu; 1♀, China: Yunnan: Jinghong, 2004.X.3, coll. Baoxin Dong (all YNAU).

Distribution. China (Hainan, Yunnan); Philippines; Thailand; Indonesia; Papua New Guinea.

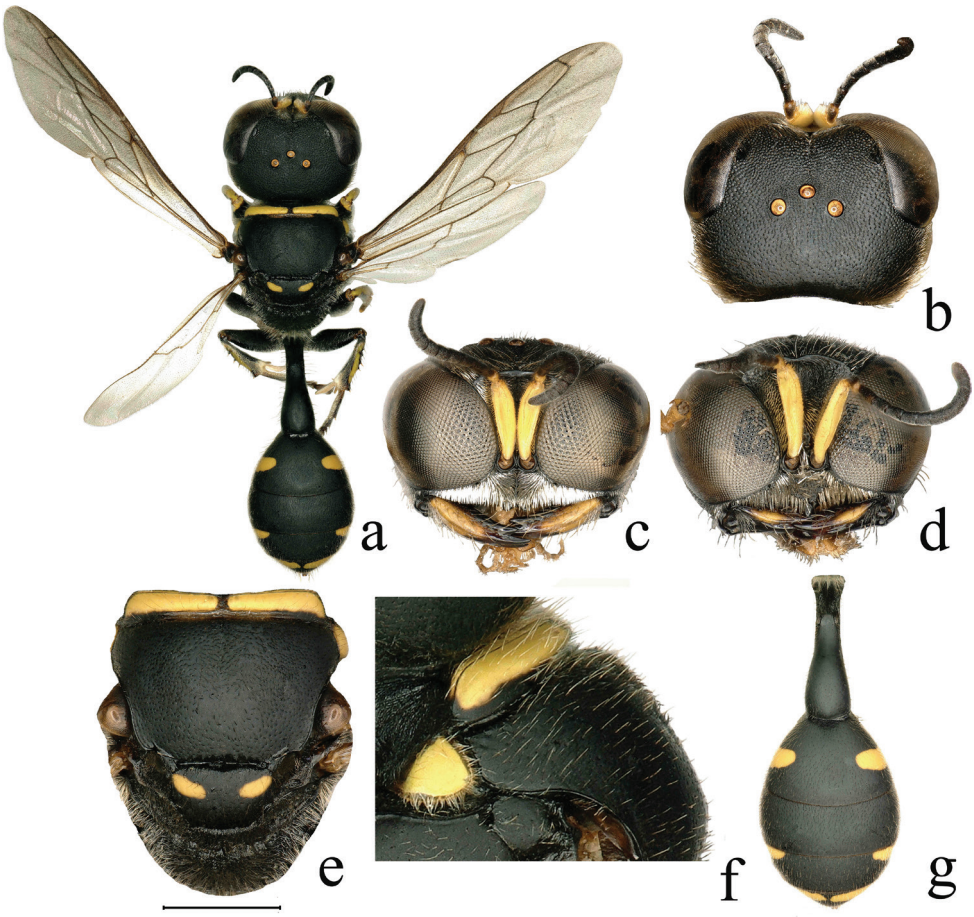

Figure 3. *Dasyproctus cevirus* Leclercq **a** ♀. habitus, dorsal view **b** ♀. head, dorsal view **c** ♀. head, frontal view **d** ♂. head, frontal view **e** ♀. mesosoma, dorsal view **f** ♀. collar, lateral view **g** ♀. metasoma, dorsal view. Scale bars: 0.47 mm (**a**); 0.62 mm (**g**); 0.81 mm (**b**); 0.85 mm (**c**); 1 mm (**e**); 1.09 mm (**d**); 1.79 mm (**f**).

Dasyproctus vaporus Leclercq, 1963, first record from China

Figure 4a–f

Dasyproctus vaporus Leclercq, 1963: 22.
Dasyproctus sculpturatus Tsuneki, 1976: 113, synonymized with *Dasyproctus vaporus* by Tsuneki (1984: 16).

Material examined. 1♂, China: Yunnan: Dehong: Luxi, 2005.VIII.10, coll. Tingjing Li; 5♂, China: Yunnan: Dehong: Yingjiang: Yunyan Mountain, 2005.VIII.15, coll. Li Ma (2♂), Haiyan Zhang (2♂), Tingjing Li (1♂); 1♂, China: Yunnan: Dehong: Yingjiang, 2005.VIII.15, coll. Kai Wu; 1♂, China: Yunnan: Dehong: Yingjiang: Taiping Township, 2005.VIII.15, coll. Xiaoli Li (all YNAU).

Distribution. China (Yunnan); Philippines.

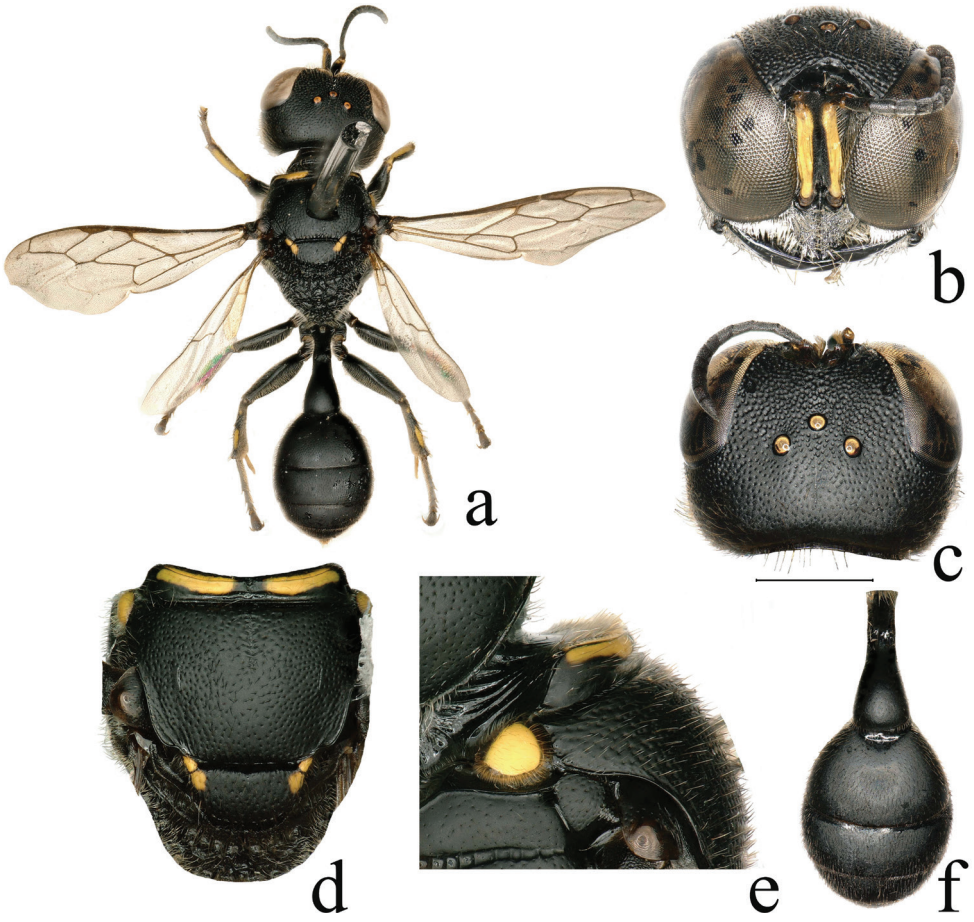

Figure 4. *Dasyproctus vaporus* Leclercq, ♂ **a** habitus, dorsal view **b** head, frontal view **c** head, dorsal view **d** mesosoma, dorsal view **e** collar, lateral view **f** metasoma, dorsal view. Scale bars: 0.46 mm (**a**); 0.67 mm (**f**); 1 mm (**b, c**); 1.07 mm (**d**); 1.64 mm (**e**).

Key to the species of *Dasyproctus* from China

Females

1 Anterior carina of pronotal collar laterally not curving toward pronotal lobe (Fig. 1d) **2**

– Anterior carina of pronotal collar laterally curving toward pronotal lobe (Figs 2d, 3f) **4**

2 Gastral tergum II with basal depression; free margin of clypeus with broad triangular concavity ..... ***D. jungi* T. Ma**

– Gastral tergum II without basal depression; free margin of clypeus nearly truncate, slightly emarginated medially **3**

3 Frontal area dorsally with a high, lamellar, transverse carina at upper margin of scapal basin, carina interrupted by a broad and deep depression medially, and markedly high on each side of depression (Fig. 1c); scape yellow (except above with two black spots medially), pedicel brown; outer margin of fore femur with one yellow spot ..... ***D. amplicarinalis* sp. nov.**

– Frontal area dorsally with a lamellar, transverse carina at upper margin of scapal basin, carina interrupted by a narrow and shallow depression medially, and slightly higher on each side of depression; scape and pedicel yellow; fore femur with two yellow spots..... ***D. buddha* (Cameron)**

4 Petiole broad and short, length not exceeding twice its maximum width, and about half of hind femur (Fig. 2f) ..... ***D. hainanensis* sp. nov.**

– Petiole longer, length of petiole more than twice its maximum width, and longer than hind femur..... **5**

5 Free margin of clypeus with deeply semicircular, median emargination (Fig. 3c); carina at anterior margin of pronotal collar more or less minutely produced near middle of each half (Fig. 3e); hind basitarsus apically brown .... ***D. cevirus* Leclercq**

– Free margin of clypeus with deeply triangular or semicircular emargination medially; carina at anterior margin of pronotal collar not produced anteriorly, either straight or gently incurved and sinuate; hind basitarsus largely brown **6**

6 Clypeus with golden pubescence; metapleuron with fine, transverse striation..... ***D. agilis orientalis* (Cameron)**

– Clypeus with silvery pubescence; metapleuron with conspicuous, close, oblique striation basally, remainder with fine, close, longitudinal striation..... ***D. agilis agilis* (F. Smith)**

Males

1 Gastral tergum II with basal depression; gastral terga without yellow spots (rarely present) or bands..... ***D. jungi* T. Ma**

– Gastral tergum II without basal depression; gastral terga with yellow spots or bands **2**

2 Free margin of clypeus with angular projection medially..... **3**

– Free margin of clypeus without angular projection, variable medially..... **4**

3 Free margin of clypeus more sharply pointed medially (Fig. 3d); outer surface of hind tibia black..... ***D. cevirus* Leclercq**

– Free margin of clypeus broad and blunt medially; outer surface of hind tibia mostly yellow..... ***D. agilis agilis* (F. Smith)**

4 Free margin of clypeus slightly emarginated medially, lateral area without a tooth on each side; gastral terga II and IV with a yellow spot on each side (rarely missing), tergum III without a spot, tergum V or terga V–VI with a broad yellow band ..... ***D. agilis orientalis* (Cameron)**

– Free margin of clypeus truncate or slightly emarginated medially, lateral area with a tooth on each side; gastral terga II and IV with a yellow spot on each side or a

yellow band, tergum III with a spot on each side, terga V and VI with a yellow band, or rarely with a small spot on each side.....**5**

5 Free margin of clypeus truncated medially, lateral teeth at acute angle to middle lobe; scutum with fine punctures, usually smaller than punctures on vertex; gastral tergum III with a pair of spots, spots distinctly larger than those on tergum IV (rarely missing) and tergum II (rarely present), terga V and VI rarely with a small spot on each side.....***D. buddha*** **(Cameron)**

– Free margin of clypeus slightly emarginated medially, lateral teeth at 90° to middle lobe (Fig. 4b); scutum with relatively large punctures, similar to punctures on vertex; gastral terga II–III with a spot on each side (missing in some specimens), terga IV–VI with a broad yellow band (missing in some specimens) (Fig. 4f) ..... ***D. vaporus*** **Leclercq**

Acknowledgements

This study was funded by the National Natural Science Foundation of China (31750002, 31760641). We are grateful to Dr. Wojciech J. Pulawski for valuable literature. Special thanks to Mr. Du Shijie (Yunnan Agricultural University, Kunming) for helping us to take and process some photographs.

References

Binoy C, Girish Kumar P, Santhosh S (2021) A new species of square-headed wasp *Dasyproctus* Lepeletier & Brullé (Hymenoptera: Crabronidae: Crabronini) from India, with notes on its biology. Zootaxa 4920(2): 223–234. https://doi.org/10.11646/zootaxa.4920.2.4

Bohart RM, Menke AS (1976) Sphecid Wasps of the World, a Generic Revision. University of California Press, Berkeley, Los Angeles, London, 695 pp. http://books.google.ru/books?id=FExMjuRhjpIC&pg=PA612&lpg=PA612&dq=Beitr%C3%A4ge+zur+Biologie+der+Hymenoptera.+I.&source=bl&ots=bDmE_eOtKG&sig=Eu5IuEsIwwVxelC9LYNP3th-fSs&hl=ru&ei=wbyiTZj3I4voObX15TQ&sa=X&oi=book_result&ct=result&resnum=2&ved=0CBkQ6AEwATgK#v=thumbnail&q&f=false

Cameron P (1889) A decade of new Hymenoptera. Memoirs and Proceedings of the Manchester Literary & Philosophical Society (Series 4) 2: 11–19.

Cameron P (1890) Hymenoptera Orientalis [sic], or contributions to a knowledge of the Hymenoptera of the Oriental Zoological Region. Part II. Memoirs and Proceedings of the Manchester Literary & Philosophical Society (Series 4) 3: 239–284. [pls. IX–X.]

Cameron P (1898) Hymenoptera Orientalia, or contributions to a knowledge of the Hymenoptera of the Oriental Zoological Region. Part VII. Memoirs and Proceedings of the Manchester Literary & Philosophical Society 42(11): 1–84. [pl. 4.]

Dahlbom AG (1844) Hymenoptera Europaea praecipue borealia; formis typicis nonnullis Specierum Generumve Exoticorum aut Extraneorum propter nexum systematicus associatis;

per Familias, Genera, Species et Varietates disposita atque descripta. Tomus: *Sphex* in sensu Linneano. Officina Lundbergiana, Lund, 528 pp. https://www.biodiversitylibrary.org/page/15796153

Haneda Y (1971) Sphecidae collected in Formosa in 1970. The Life Study (Fukui) 15: 29–33.

Haneda Y (1972) Sphecidae collected in Formosa in 1971. The Life Study (Fukui) 16: 1–7.

Hua LZ (2006) Superfamily Apoidea (Sphecoidea). In: Hua L (Ed.) List of Chinese Insects (Vol. IV). SunYat-sen University Press, Guangzhou, 274–299.

Leclercq J (1954) Monographie Systématique, Phylogénétique et Zoogéographique des Hyménoptères Crabroniens. Les Presses de Lejeunia, Liège, 371 pp.

Leclercq J (1956) Les *Dasyproctus* (Lepeletier de St-Fargeau et Brullé 1834) du Sud-Est Asiatique et de l'Océanie (Hym. Sphecidae Crabroninae). Bulletin & Annales de la Société Royale d'Entomologie de Belgique 92: 139–167.

Leclercq J (1957) Contribution nouvelle à l'étude des *Dasyproctus* de l'Archipel Malais (Hymenoptera Sphecidae Crabroninae). Bulletin de la Société Royale des Sciences de Liège 26(1): 53–58.

Leclercq J (1958) Hymenoptera Sphecoidea (Sphecidae II. Subfam. Crabroninae) in Exploration du Parc National de l'Upemba. I. Mission G.F. de Witte en collaboration avec W. Adam, A. Janssens, L. van Meel et R. Verheyen (1946–1949), Fascicule 45: 1–114.

Leclercq J (1963) Crabroniens d'Asie et des Philippines (Hymenoptera Sphecidae). Bulletin & Annales de la Société Royale d'Entomologie de Belgique 99: 1–82.

Leclercq J (1972) Crabroniens du genre *Dasyproctus* trouvés en Asie et en Océanie (Hymenoptera Sphecidae Crabroninae). Bulletin de la Société Royale des Sciences de Liège 41: 101–122.

Leclercq J (1982) Hyménoptères Crabroniens de Chine et de régions voisines de l'Himalaya. Entomotaxonomia 4: 145–157. http://www.cnki.com.cn/Article/CJFDTotal-KCFL198203000.htm

Leclercq J (2015) Hyménoptères Crabroniens d'Afrique, d'Asie et d'Océanie du genre *Dasyproctus* Lepeletier & Brullé 1835 (Hymenoptera: Crabronidae: Crabroninae). Entomologie Faunistique 68: 41–89. https://popups.uliege.be/2030-6318/index.php?id=3120&file=1&pid=3108

Lepeletier de Saint Fargeau ALM, Brullé A (1834) Monographie du genre *Crabro*, de la famille des Hyménoptères Fouisseurs. Annales de la Société Entomologique de France 3: 683–810.

Ma TC (1936) Notes on some Aculeata from Szechwan, West China. Kun Chong Yu Zhi Bing [= Entomology and Phytopathology] 4: 466–471.

Murota T (1973) Sphecidae, Mutillidae, Scoliidae and Chrysididae collected in Formosa in 1972. The Life Study (Fukui) 17: 115–119.

Pate VSL (1937) The generic names of the sphecoid wasps and their type species (Hymenoptera: Aculeata). Memoirs of the American Entomological Society 9: 1–103. https://www.biodiversitylibrary.org/page/38416580#page/11/mode/1up

Porter CHC, Stange LA, Wang HY (1999) Checklist of the Sphecidae of Taiwan with a key to genera (Hymenoptera: Sphecidae). Journal of the National Taiwan Museum 52: 1–26. http://dx.doi.org/10.6532/JNTMA.199912_52(2).0001

Pulawski WJ (2020) Catalog of Sphecidae. http://researcharchive.calacademy.org/research/entomology/entomology_resources/hymenoptera/sphecidae/genera/*Dasyproctus*.pdf [accessed 25 March 2020]

Smith F (1858) Catalogue of hymenopterous insects collected at Celebes by Mr. A. R. Wallace. Journal of the Proceedings of the Linnean Society, Zoology 3: 4–27. https://doi.org/10.1111/j.1096-3642.1858.tb02506.x

Tsuneki K (1959) On some crabronids from Formosa (Hymenoptera, Sphecidae). Insecta Matsumurana 22: 96–99. http://eprints.lib.hokudai.ac.jp/dspace/bitstream/2115/9642/1/22

Tsuneki K (1966) Contribution to the knowledge of Crabroninae fauna of Formosa and the Ryukyus (Hymenoptera, Sphecidae). Etizenia 15: 1–21.

Tsuneki K (1968) Studies on the Formosan Sphecidae (V). The subfamily Crabroninae (Hymenoptera) with a key to the species of Crabronini occurring in Formosa and the Ryukyus. Etizenia 30: 1–34. [9 pls.]

Tsuneki K (1971) Studies on the Formosan Sphecidae (VIII). A supplement to the subfamily Crabroninae (Hymenoptera). Etizenia 51: 1–29.

Tsuneki K (1976) Sphecoidea taken by the Noona Dan expedition in the Philippine Islands (Insecta, Hymenoptera). Steenstrupia 4: 33–120.

Tsuneki K (1977) H. Sauter's Sphecidae from Formosa in the Hungarian Natural History Museum (Hymenoptera). Annales Historico-Naturales Musei Nationalis Hungarici (= A Természettudományi Múzeum Évkönyve) 69: 261–296. https://agris.fao.org/agris-search/search.do?recordID=US201301287221

Tsuneki K (1982) Sphecidae of the Sauter's Formosa collection preserved in the Ueberseemuseum at Bremen, with taxonomic notes on some species (Hymenoptera). Special Publications of the Japan Hymenopterists Association 23: 6–14.

Tsuneki K (1983) Crabronids from New Guinea and the Solomon Islands. Special Publications of the Japan Hymenopterists Association 27: 2–28.

Tsuneki K (1984) Studies of the Philippine Crabroninae, revision and addition, with an annotated key to the species (Hymenoptera Sphecidae). Special Publications of the Japan Hymenopterists Association 29: 1–50.

Turner RE (1912a) Notes on fossorial Hymenoptera. – IX. On some new species from the Australian and Austro-Malayan Regions. The Annals and Magazine of Natural History (Series 8) 10: 48–63. https://doi.org/10.1080/00222931208693197

Turner RE (1912b) Notes on fossorial Hymenoptera. – X. On new species from the Oriental and Ethiopian Regions. The Annals and Magazine of Natural History (Series 8) 10: 361–377. http://bionames.org/references/aeb3453b30d7c6c5542c4b7deffe4c7d

ZooKeys 1025: 35–71 (2021)
doi: 10.3897/zookeys.1025.62305
https://zookeys.pensoft.net

RESEARCH ARTICLE

A peer-reviewed open-access journal
ZooKeys
Launched to accelerate biodiversity research

Multiple lines of evidence reveal a new species of Krait (Squamata, Elapidae, *Bungarus*) from Southwestern China and Northern Myanmar

Ze-Ning Chen[1,2*], Sheng-Chao Shi[1,3*], Gernot Vogel[4], Li Ding[1], Jing-Song Shi[5]

1 *Chengdu Institute of Biology, Chinese Academy of Sciences, Chengdu, Sichuan 610041, China* **2** *Guangxi Key Laboratory of Rare and Endangered Animal Ecology, Guangxi Normal University, Guilin, Guangxi 541001, China* **3** *University of Chinese Academy of Sciences, Beijing 100049, China* **4** *Society for Southeast Asian Herpetology, Im Sand 3, Heidelberg D-69115, Germany* **5** *Key Laboratory of Vertebrate Evolution and Human Origins of Chinese Academy of Sciences, Institute of Vertebrate Paleontology and Paleoanthropology, Chinese Academy of Sciences, Beijing 100044, China*

Corresponding authors: Li Ding (dingli@cib.ac.cn); Jing-Song Shi (shijingsong@ivpp.ac.cn)

Academic editor: R. Jadin | Received 21 December 2020 | Accepted 21 February 2021 | Published 18 March 2021

http://zoobank.org/1AB94895-532E-4998-9D63-BDD5DAC8F321

Citation: Chen Z-N, Shi S-C, Vogel G, Ding L, Shi J-S (2021) Multiple lines of evidence reveal a new species of Krait (Squamata, Elapidae, *Bungarus*) from Southwestern China and Northern Myanmar. ZooKeys 1025: 35–71. https://doi.org/10.3897/zookeys.1025.62305

Abstract

Kraits of the genus *Bungarus* Daudin 1803 are widely known venomous snakes distributed from Iran to China and Indonesia. Here, we use a combination of mitochondrial DNA sequence data and morphological data to describe a new species from Yingjiang County, Yunnan Province, China: *Bungarus suzhenae* **sp. nov**. Phylogenetically, this species forms a monophyletic lineage sister to the *Bungarus candidus*/*multicinctus*/*wanghaotingi* complex based on cyt *b* and ND4 genes but forms a sister species pair with the species *B. magnimaculatus* Wall & Evans, 1901 based on COI gene fragments. Morphologically, *B. suzhenae* **sp. nov**. is similar to the *B. candidus*/*multicinctus*/*wanghaotingi* complex but differs from these taxa by a combination of dental morphology, squamation, coloration pattern, as well as hemipenial morphology. A detailed description of the cranial osteology of the new species is given based on micro-CT tomography images. We revised the morphological characters of *B. candidus*/*multicinctus*/*wanghaotingi* complex and verified the validity of three species in this complex. The distribution of these species was revised; the records of *B. candidus* in China should be attributed to *B. wanghaotingi*. We also provide an updated key to species of *Bungarus*.

* Contributed equally as the first authors.

Keywords
Bungarus suzhenae sp. nov., cranial osteology, hemipenial morphology, micro-computed tomography, phylogeny, taxonomy

Introduction

Sound taxonomy of lethal snakes provides an essential foundation for venom research, antivenin development and proper snakebite treatment (Fry et al. 2003; Williams et al. 2011). *Bungarus* Daudin 1803 (commonly referred to as 'Kraits') is one of the most medically significant groups of elapid snakes in Asia, and is widely distributed from Iran and Pakistan, eastwards to China and Indonesia (Slowinski 1994; Kuch et al. 2005; Abtin et al. 2014; Ahsan and Rahman 2017; Uetz et al. 2020). Within the fourteen species currently described, *Bungarus* with black-and-white crossbands have been the most taxonomically problematic members of the genus and are difficult to identify in the field due to overlapping characteristics in morphology (Wall 1907; Slowinski 1994; Kuch 2007; Abtin et al. 2014). Most of these black-and-white *Bungarus* species are traditionally identified by the number of the dorsal crossbands on the body and tail (Slowinski 1994; Leviton et al. 2003; Zhao 2006). However, both characters within these species overlap (see: Table 1) and may lead to misidentifications.

Five taxa of *Bungarus* are reported from China, including *B. fasciatus* (Schneider, 1801), *B. bungaroides* (Cantor, 1839), *B. multicinctus multicinctus* Blyth, 1860, *B. m. wanghaotingi* Pope, 1928 and *B. candidus* (Linnaeus, 1758) (Pope 1928; Zhao and Yang 1997; Rao and Zhao 2004; Zhao 2006; Kuch 2007; Yang and Rao 2008; Xie et al. 2018). The former two species *B. fasciatus* and *B. bungaroides* are easily distinguished from their congeners by having divided subcaudal scales, as well as their unique coloration patterns (Kuch et al. 2005; Zhao 2006; Kuch 2007; Yang and Rao 2008). However, *B. m. multicinctus*, *B. m. wanghaotingi* and *B. candidus* are relatively difficult to identify and are differentiated from each other by the number of the white crossbands on the body and the number of ventral scales (Pope 1928; Slowinski 1994; Leviton et al. 2003; Rao and Zhao 2004; Zhao 2006). Leviton et al. (2003) proposed to raise *B. m. wanghaotingi* to species level based on lesser light crossbands on body and tail and geographically distant from *B. m. multicinctus*. However, Kuch (2007) considered *B. candidus* and *B. multicinctus* (including *B. m. multicinctus* and *B. m. wanghaotingi*) as a species complex based on mtDNA sequence data and similar morphology. Considering paraphyly of this complex shown in Kuch (2007), we use the term *B. candidus*/*multicinctus*/*wanghaotingi* complex. In addition, Kuch (2007) tentatively identified a specimen CAS 221526 from northern Myanmar as *Bungarus* cf. *multicinctus*, which is phylogenetically closer to *B. niger* Wall, 1908 than to all other specimens of *B. multicinctus* from China and Vietnam (fig. 20 in Kuch 2007). Since Kuch's (2007) unpublished dissertation, authors have used the species and subspecies categories interchangeably to describe the three names in the

B. candidus/*multicinctus*/*wanghaotingi* complex, and the boundaries between species in this group are still subject to controversy (Nguyen et al. 2017; Xie et al. 2018).

During herpetological surveys in Yunnan Province, China, between 2016 and 2019, a series of *Bungarus* specimens were collected from Yingjiang County. These specimens resembled members of the *B. candidus*/*multicinctus*/*wanghaotingi* complex based on morphology, but nested phylogenetically in the same lineage as the specimen CAS 221526 reported by Kuch (2007). Based on multiple evidence including phylogenetical analysis based on three mitochondrial genes, micro-CT scanning, hemipenial morphology, and other morphological data, we evaluated the taxonomic status of these specimens and compared them to all members of the *B. candidus*/*multicinctus*/*wanghaotingi* complex. The results showed that the specimens from Yingjiang County can be distinguished from these taxa, along with all other congeners. We therefore describe these specimens, along with the CAS 221526 specimen from Myanmar, as a new species in this paper.

Materials and methods

Sampling

Four individuals of the *Bungarus* were collected from Yingjiang, western Yunnan Province, China. Before preservation, we euthanized these specimens and fixed them in 80% ethanol and then deposited in the Herpetology Museum of Chengdu Institute of Biology, Chinese Academy of Sciences, Chengdu City, Sichuan Province, China (CIB). For comparisons of taxa in *B. candidus*/*multicinctus*/*wanghaotingi* complex, fourteen specimens of *B. m. wanghaotingi* were collected from southern and eastern Yunnan Province and southwestern Guangxi Province, China. Two specimens collected from Saigon, Vietnam, two specimens of *B. m. multicinctus* from Fujian Province and Zhejiang Province were also collected. Additional specimens of the *B. candidus*/*multicinctus*/*wanghaotingi* complex were examined in museum collections for morphological comparisons. A full list of specimens examined can be found in Appendix I. Comparative morphological information on other species was obtained from examined specimens and the literature sources listed in Table 1. Museum acronyms follow Leviton et al. (1985) except for collections that are not included in their list. Chengdu Institute of Biology (**CIB**), Shenyang Normal University (**SYNU**), Naturhistorisches Museum Wien, Vienna, Austria (**NMW**), Muséum National d'Histoire Naturelle, Paris, France (**MNHN**), Rijksmuseum van Natuurlijke Historie, Leiden, the Netherlands (**RMNH**).

To ensure the taxonomic relationships within the *B. candidus*/*multicinctus*/*wanghaotingi* complex, we included specimens of *B. m. multicinctus* near type locality, *B. m. wanghaotingi* near type locality, and monophyletic specimens of *B. candidus* in multiple localities from West Java, Indonesia to Binh Phuoc, Vietnam. Muscle or liver tissues were extracted from specimens before specimens were fixed, preserved in 95% ethanol, and stored at –20 °C.

Table 1. Comparison of main morphological characters in the *Bungarus* species.

Species	DSR	VEN	NSC	SC	Loreal	Dorsal body pattern	BB	Reference
B. candidus	15	209–224	41–50	undivided	absent	white bands	18–26	This study
		(215.2 ± 3.8 n = 18)	(46.2 ± 2.1 n = 17)				(21.4 ± 1.8 n = 19)	
B. wanghaotingi	15	209–259	32–64	undivided	absent	white bands	18–33	This study (n = 16); Yang and Rao 2008 (n = 10); Pope 1928 (n = 1)
		(230.4 ± 12.3 n = 23)	(51.1 ± 6.4 n = 22)				(25.1 ± 3.2 n = 27)	
B. multicinctus	15	196–236	38–58	undivided	absent	white bands	31–50	This study
		(214.1 ± 8.9 n = 24)	(47.1 ± 4.9 n = 23)				(39.3 ± 4.7 n = 24)	
***B. suzhenae* sp. nov.**	15	220–229	51–54	undivided	absent	white bands	26–38	This study
		(223 ± 4.1 n = 4)	(53 ± 1.5 n = 3)				(39.3 ± 4.7 n = 4)	
B. magnimaculatus	15	214–235 (n = ?)	40–48	undivided	absent	broad, white bands	11–14	Leviton et al. 2003
B. niger	15	216–231 (n = ?)	47–57	undivided	absent	body black	/	Wall 1908
B. caeruleus	15	200–217 (n > 20)	33–54	undivided	absent	white bands (in pairs)	29–65	Biswas and Sanyal 1978 (n = ?); Slowinski 1994 (n = 11); Whitaker and Captain 2004 (n = ?); This study (n = 9)
B. ceylonicus	15	219–235 (n = ?)	33–40	undivided	absent	narrow white rings	15–20	Boulenger 1890; Wall 1908; this study
B. lividus	15	212–225 (n = ?)	37–56	undivided	absent	black or blackish blue	/	Smits 1943
B. andamanensis	15	193–197 (n = ?)	45–47	undivided	absent	yellow band	39–47	Biswas and Sanyal 1978
B. persicus	17	236–238 (n = 2)	50–53	undivided	present	white crossbars	25	Abtin et al. 2014
B. sindanus	17	220–237 (n = ?)	45–53	undivided	absent	white bands	/	Khan 2002
B. walli	17	196–208 (n = ?)	50–55	undivided	absent	white spots	/	Wall 1907
B. fasciatus	15	217–237 (n > 11)	33–41	undivided	absent	yellow band	19–29	Yang and Rao 2008; Levition et al. 2003; and this study
B. slowinskii	15	225–230 (n = 7)	33–41	divided	absent	narrow white rings	27–33	Kuch et al. 2005 (n = 3); Kharin et al. 2011 (n = 3); Smits and Hauser 2019 (n =1)
B. bungaroides	15	220–237 (n = ?)	44–51	divided	absent	white rings	46–60	Kuch et al. 2005; Kharin et al. 2011; Smits and Hauser 2019
B. flaviceps	13	193–236 (n = ?)	42–52	undivided	absent	head red or orange, body not black and white banded	/	Wall 1908; Kuch 2007

Abbreviations. – See in Material and methods.

Note: In the *B. candidus*/*multicinctus* complex, the values in parentheses represent the mean and standard deviation, and some specimens are incomplete; we only count complete specimens for certain characteristics.

Molecular phylogenetic analysis

Genomic DNA was extracted from muscle or liver tissues using QIAamp DNA Mini Kit (QIAGEN, Hilden, Germany). We sequenced three mitochondrial genes: *cytochrome b* (cyt *b*) (Burbrink et al. 2000), *NADH dehydrogenase subunit 4* (ND4) (Arevalo et al. 1994) and *cytochrome C oxidase 1* (COI) (Che et al. 2012). PCR amplifications were performed in 25 μl reactions (12.5 μl I-5 2×High-Fidelity Master Mix, 10 μl ddH_2O, 1 μl F-primers, 1 μl R-primers, 0.5 μl DNA template) under the following cycling conditions: initial denaturation for 2 min at 95 °C, 35 cycles with denaturation at 94 °C for 40 s, annealing at different temperatures (48.5 °C for cyt *b* and COI, 56 °C for ND4) for 25 s, extension at 72 °C for 15 s, and final extension for 2 min at 72 °C. PCR products were sequenced by Beijing Qingke New Industry Biotechnology Co., Ltd. Raw trace files for sequences were edited in Geneious 7 (Biomatters Limited, New Zealand) before constructing alignments using MEGA 7 (Kumar et al. 2016). Due to differences in taxon sampling for each gene, we reconstructed separate alignments for phylogenetic analysis. The first was based on a concatenated sequence alignment using cyt *b* and ND4, while the other was based solely on COI. Sequences were uploaded to GenBank under the following accession numbers: MN165132–MN165173. Comparative sequences of available species were downloaded from GenBank (Suppl. material 1: Table S1). Distribution of sequences localities were present in Fig. 1.

Optimal models of sequence evolution of nucleotide substitution were identified by BIC using Partition finder 2.1.1 (Lanfear et al. 2012). We performed maximum likelihood (ML) analysis using RaxML v8 (Stamatakis et al. 2014) and IQ-TREE (Nguyen, et al. 2015) respectively. The first ML analysis was implemented in RaxML v8 (Stamatakis et al. 2014) following GTRGAMMA model with 1000 fast bootstrap replicates to assess node support. We consider bootstrap proportions of 70% or greater as strong support for existence of a clade following Hillis and Bull (1993). The second ML analysis was implemented in IQ-TREE (Nguyen et al. 2015), with Ultrafast Bootstrap Approximation (UFB; Hoang et al. 2017) using 5000 bootstrap replicates to assess node support. Nodes with UFB values of 95 and above were considered significantly supported (Hoang et al. 2017). The best evolution models were shown in supplementary materials (Suppl. material 1: Table S2). Bayesian inference phylogenetic trees were inferred using MrBayes 3.2 (Ronquist et al. 2012). We used a random starting tree and four independent runs with a maximum of 20 million generations each, sampled every 1000. Runs were stopped when the average standard deviation of split frequencies had reached 0.001. The first 25% of each run were discarded as burn-in. Nodes with Bayesian posterior probabilities (BPP) of 0.95 and above were considered well supported (Huelsenbeck et al. 2001).

Morphological analysis

Measurements of head and head scales were taken with a digital caliper and rounded to the nearest 0.1 mm; snout–vent length and tail length were taken with a measuring tape and rounded to the nearest 1 mm. Terminology and descriptions follow Slowinski

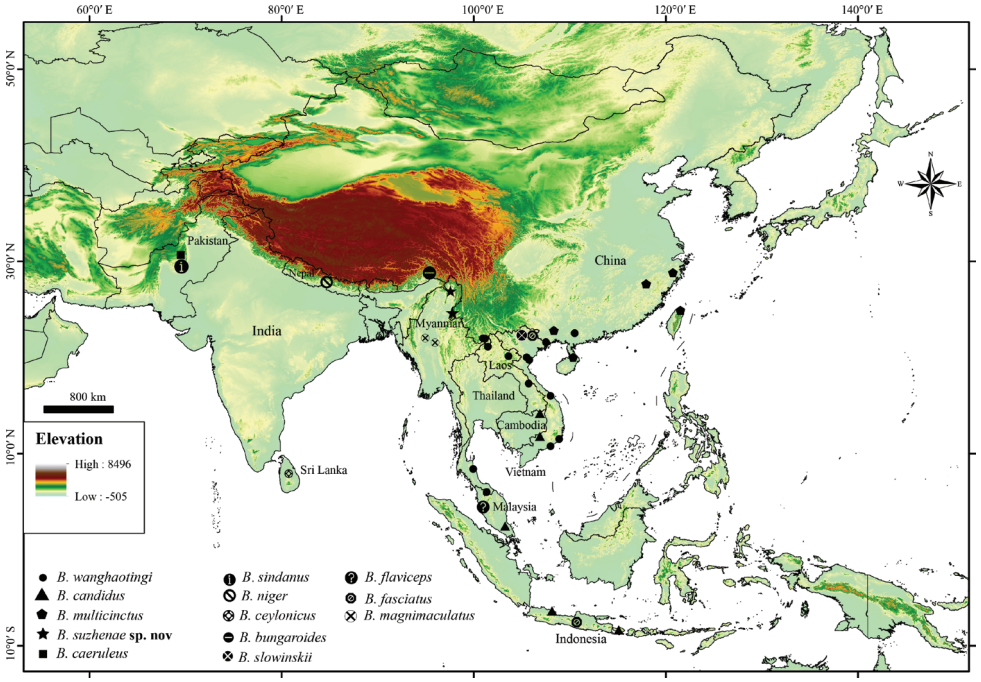

Figure 1. Distribution map of molecular samples localities of *Bungarus* in this study.

(1994), Vogel et al. (2004), and Kuch et al. (2005). Morphometric and meristic characters are abbreviated as follows: total length (TL), from the tip of snout to the tip of tail; snout-vent length (SVL), from the tip of snout to anterior margin of cloaca; tail length (TaL), from posterior margin of cloaca to the tip of tail; ratio of tail length to total length (TaL/TL); head length (HL), from the snout tip to the posterior margin of the mandible; head width (HW) was measured at the widest part of the head on posterior side; head height (HH), at the maximal highest part of the head; the eye horizontal diameter (ED); the eye vertical diameter (VED); distance lower eye margin–edge of the lip (DEL) was measured from the ventral margin of the middle of the eye to the ventral margin of the upper labial below it; the distance from the eye to the nostril (DEN) was measured from the anterior margin of the eye to the posterior margin of the nostril; the dorsal scale rows (DSR) were counted at one head length behind the head, at midbody, and at one head length before the vent; ventral scales (VEN) were counted according to Dowling (1951); half ventrals were counted as one. The enlarged shield(s) anterior to the first ventral were regarded as preventral(s); for subcaudals (SC), first scale under the tail meeting its opposite was regarded as the first subcaudal scale, and the unpaired terminal scute was not included in the number of subcaudals; paired scales on head were counted on both sides of the head and presented in left/right order; supralabials (SL); infralabials (IL) were considered scales and shields that are completely below a supralabial and border the gap between lips. For the number of white bands on the body (BB) and white bands on the tail (TB), incomplete white rings were counted as one. Sex was determined by making a small incision below the vent

to visually inspect for the existence of hemipenes. Descriptions of the hemipenes were based on one population of the new species and three populations of the *B. candidus*/*multicinctus*/*wanghaotingi* complex. Hemipenis terminology follows Dowling (1951) and the organs were prepared based on Jiang (2010).

For obtaining information on skeletal morphology, micro-CT scans of skulls were carried out using a 225-kV micro-computerized tomography, developed by the Institute of High Energy Physics (IHEP), Chinese Academy of Sciences (CAS). A total of 720 transmission images were reconstructed into a 2048 × 2048 matrix of 1536 slices using two-dimensional reconstruction software developed by IHEP, CAS. The final CT reconstructed skull images were exported with a minimum resolution of 14.1 (Holotype) and 29.0 (paratype) μm. The dataset of the 3D models included in this study has been uploaded to the online publicly accessible repository ADMorph at http://www.admorph.org/ (Hou et al. 2020).

Results

Phylogenetic analysis

The concatenated alignment for cyt *b* and ND4 was 1934 bp in length (1069 + 865 bp, respectively) and contained a total of twelve *Bungarus* species. The COI alignment was 613 bp and contained a total of five taxa. Our results show that the most well-supported cyt *b*-ND4 and COI phylogenetic trees were achieved by using Bayesian Inference (BI), followed by Maximum likelihood RaxML (ML) and IQ-TREE (UFB), respectively.

The topological structures of the combined cyt *b* and ND4 sequences (Fig. 2) concur with an earlier study by Kuch (2007). The new species forms a monophyletic lineage with strong support (BI 1.00/ML 100/UFB 100) sister to the *B. candidus*/*multicinctus*/*wanghaotingi* complex. Within the complex, three strongly supported (BI 0.92/ML 87/UFB 88) monophyletic lineages are identified. The first is *B. wanghaotingi* including specimens from localities near type locality and other specimens from Southern China, Southwestern China, Vietnam, Laos and Southern Thailand; the second is *B. candidus*, including specimens from Java and Bali Island, Peninsular Malaysia; the third is *B. multicinctus*, including specimens near type locality and from other localities in Eastern and Southern China. The two lineages *B. wanghaotingi* and *B. candidus* consist of a clade sister to *B. multicinctus*. The uncorrected *p*-distances of available cyt *b* sequences between the *Bungarus* species are shown in the supplementary material (Suppl. material 1: Table S3). The distances between the new species and its closest congeners in the *B. candidus*/*multicinctus*/*wanghaotingi* complex range from (9.7%–11.6%), similar to the distance between *B. niger* and the *B. candidus*/*multicinctus*/*wanghaotingi* complex (11.0%–12.4%). The genetic distances between the three lineages of the *B. candidus*/*multicinctus*/*wanghaotingi* complex were relatively small, ranging from 1.6% to 3.3%.

In the phylogenetic analyses for the COI alignment (Fig. 3), the new species forms a lineage sister to *B. magnimaculatus* instead of the *B. candidus*/*multicinctus*/*wanghaotingi* complex. The specimens of *B. magnimaculatus* from three localities of Myanmar were formed by two lineages with short branches similar to an earlier study (Nguyen et al.

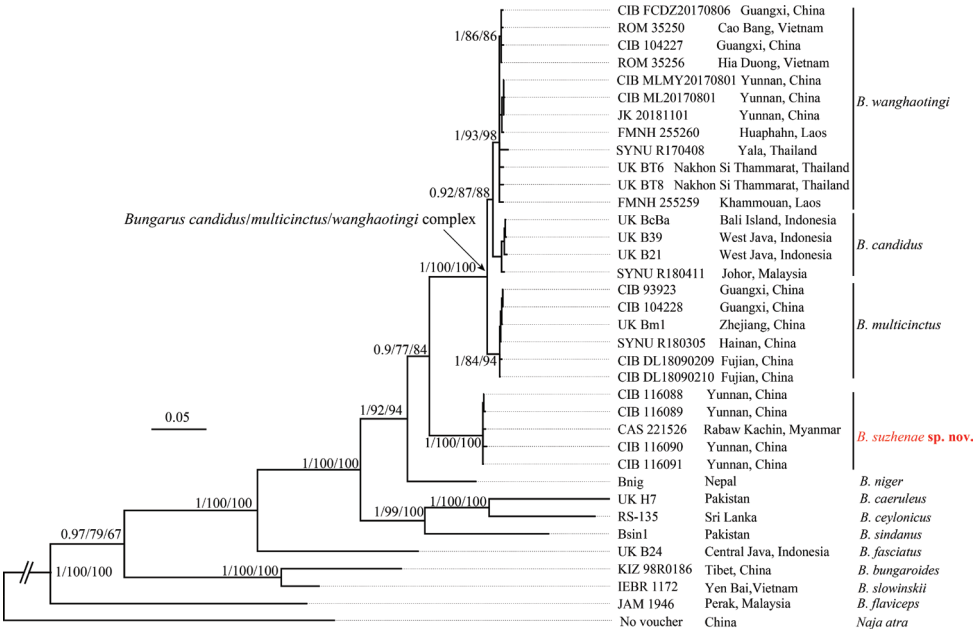

Figure 2. Bayesian inferred tree of the genus *Bungarus* based on combined cyt *b* and ND4 genes fragments. The major clade genetic events BI/ML/IQ posterior probabilities, bootstrap and UFB values were presented (the ones lower than 50 are displayed as "-").

2017). We regard the two lineages of *B. magnimaculatus* as a species complex. The distinct pairwise genetic distance between these two lineages (2.4%–3.1% for COI) indicates that the species diversity of this species may be underestimated. The topology of the *B. candidus*/*multicinctus*/*wanghaotingi* complex agrees with the concatenated cyt *b*-ND4 gene trees and can be considered to constitute three strongly supported lineages (BI 1.00/ML 95/UFB 85) with very short branch lengths. The uncorrected *p*-distances of COI between the species groups are shown in the supplementary material (Suppl. material 1: Table S4). The new species is separated from the *B. candidus*/*multicinctus*/*wanghaotingi* complex by a distinct distance of 4.4%–5.0%, equivalent to the distance between *B. magnimaculatus* and the *B. candidus*/*multicinctus*/*wanghaotingi* complex (4.4%–6.5%). The high pairwise distances between the new species and its congeners support its recognition as a distinct, independently evolutionary lineage that is not conspecific with any other congeners.

Morphological analysis

Morphologically, the three taxa of *B. candidus*/*multicinctus*/*wanghaotingi* complex are different from each other in hemipenial morphology, and coloration patterns (morphology of white bands, ventral coloration, and coloration on temporal and lateral neck regions) (Tables 1, 2, Figs 4–9). Thus, we confirm these three monophyletic taxa of *B. candidus*/*multicinctus*/*wanghaotingi* complex as three distinct species: *B. candidus* (Linnaeus, 1758), *B. multicinctus* Blyth, 1860, and *B. wanghaotingi* Pope, 1928.

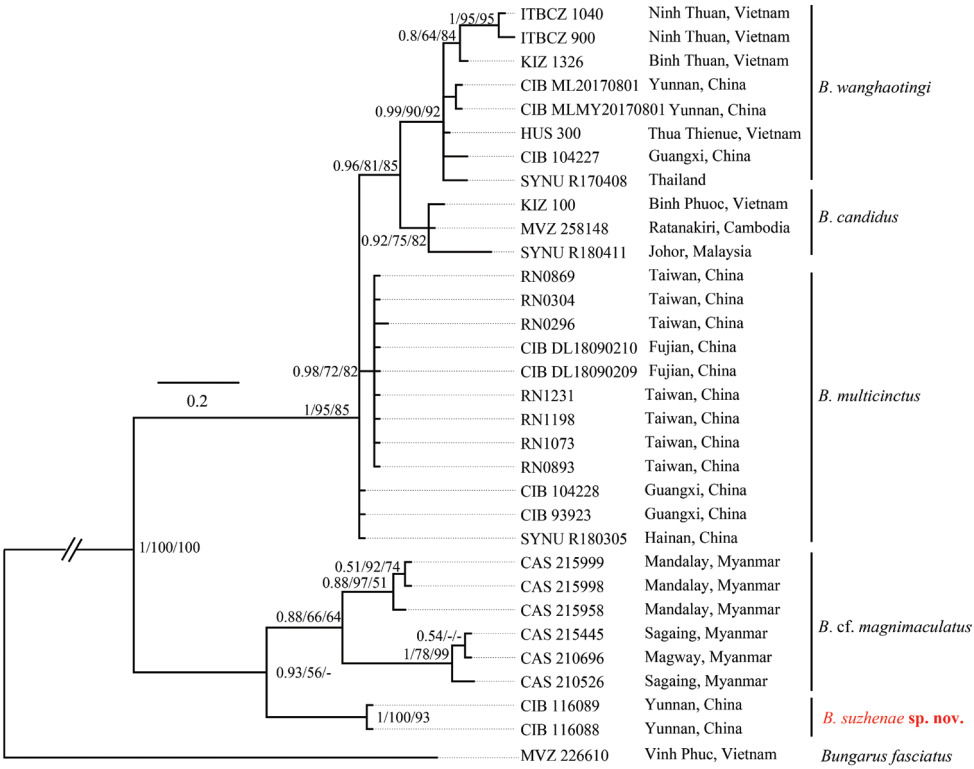

Figure 3. Bayesian inferred tree of the genus *Bungarus* base on COI genes fragments. The major clade genetic events BI /ML/IQ posterior probabilities, bootstrap and UFB values were presented (the ones lower than 50 are displayed as "-").

The specimens from Yingjiang (Yunnan Province) and Myanmar differ from other species of *Bungarus* in crossbands shape, tail pattern (Figs 4, 5, Table 2), head pattern (Fig. 6), mid-body pattern (Fig. 7), the maxilla teeth (Fig. 8 and Table 3) and hemipenial morphology (Fig. 9, Table 2). Therefore, combining morphological and molecular evidence, we identify those specimens from Yingjiang, Yunnan Province, and Myanmar as a new species.

Taxonomy

Bungarus candidus/multicinctus/wanghaotingi complex

Bungarus candidus (Linnaeus, 1758)

Figs 4C, D, 5C, D, 6C, D, 7C, D, 9D–F
[English name: Blue Krait]
[Chinese name: 马来环蛇]

Coluber candidus Linnaeus 1758: 223.
Bungarus candidus – Cantor 1847

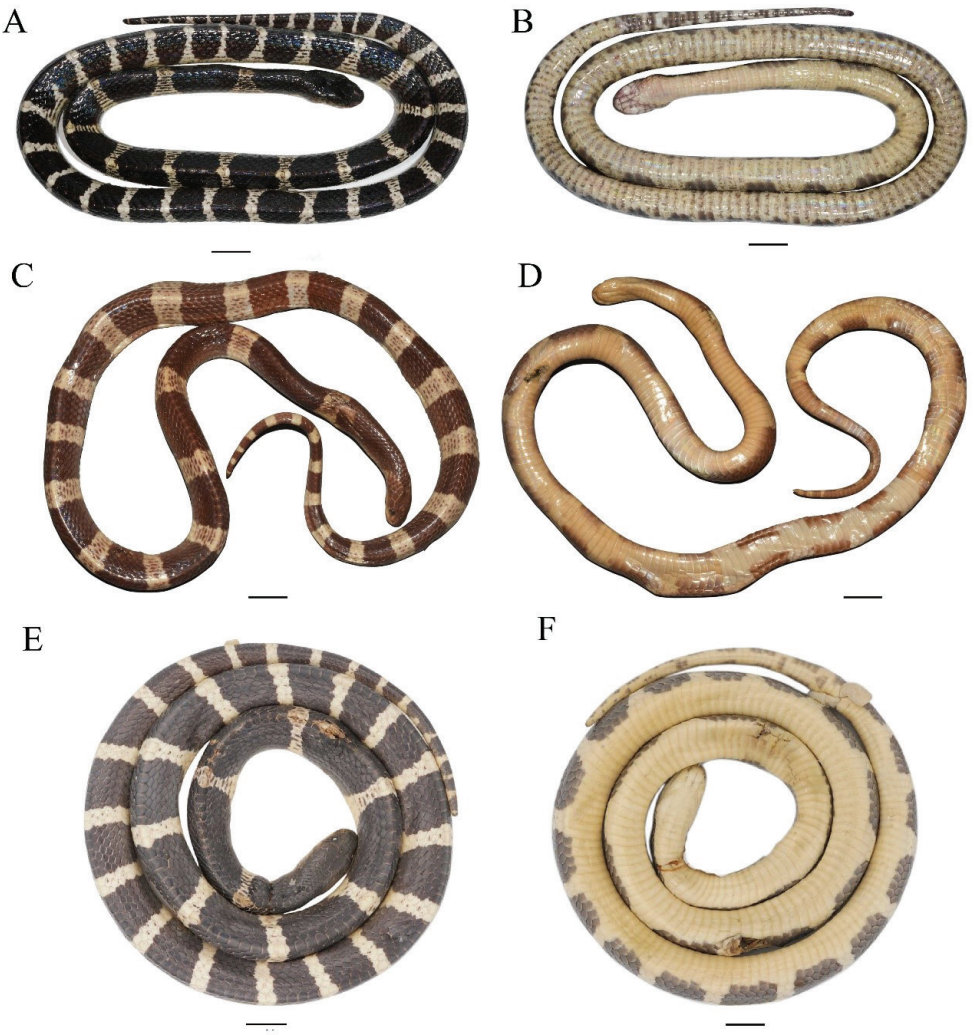

Figure 4. Dorsal (left) and ventral (right) view of adults of the *Bungarus candidus*/*multicinctus*/*wanghaotingi* complex **A, B** *Bungarus multicinctus*, adult male, CIB DL2019051701 from Lishui, Zhejiang, China **C, D** *B. candidus*, female, NMW 9486:1 from Pelambang, Java **E, F** *B. wanghaotingi*, male, CIB MLML20170801 from Mengla, Yunnan, China. Scale bars: 20 mm.

Bungarus semifasciatus Boie 1827
Aspidoclonion semifasciatum – Wagler1828
Bungarus candidus var. *semifasciata* – Werner 1900
Bungarus javanicus Kopstein 1932 (*fide* Slowinski 1994)
Bungarus candidus – Smith 1943: 416

Type locality. "Indiis" (in error). ***Holotype*:** NRM 37 (formerly ZIUS 89).

Typical *B. candidus* possesses following morphological characters based on the examination of 19 specimens from Sumatra and Java, Indonesia; Peninsular Malaysia

(Appendix 1): (1) Dorsum of most specimens with 21.4 ± 1.8, (18–26) broad white crossbands, with each band covers 3.8 ± 0.6, (3.0–5.0) vertebral scales on midbody, (Figs 4C, D, 5C, D), uniform black in some populations (Kuch 2007); (2) ventral body immaculate white, without brown pigments (Figs 4C, D, 5C, D); (3) scales on temporal area and lateral neck stained white, contrast with neighbor scales on neck in adults, creamy white in juveniles (Fig. 6C, D); (4) black bands on body large, covering 3–5 vertebral scales on middle body, intruding to white ventral body, ventrals with narrow black edges 1–2 times of outer dorsal scales (Fig. 7C, D); (5) ventral tail with broad dark crossbands (Figs 4D, 5D); (6) posterior maxilla teeth four (n = 9), slightly curved behind, (Table 3); (7) prefrontal suture 1.4–2.4 (n = 17) times the length of internasals suture; (8) VEN = 209–224 (n = 18), NSC = 41–50 (n = 17).

The hemipenes of *B. candidus* is described based on photos of a male (Fig. 9D–F, collecting No. RH06153, total length 120 cm) from Phong Nha-Ke Bang National Park Administration, Quang Binh Province, Vietnam, by Ralf Hendrix. This specimen was tentatively identified as *B. candidus* by the presence of (1, 2, 4–8) characters in the former morphological description. The hemipenis was partially everted, with large spines present on the medial portion of the organ at the position of the first subcaudal scale; smaller spinous calyces present near the base and another spinous zone present posterior from the row of larger spines. Spinous calyces along organ all elongated, robust at bases and gradually tapering to a tip without distinct bordering. Tips of spines strongly keratinized, semitransparent when fresh, bent towards the base of hemipenes. Sulcus not shown in the photos.

Distribution. This species is known from following localities based on specimens examined and/or DNA sequences data: Java and Sumatra Island, Indonesia; Peninsular Malaysia; Cambodia; Central and Southern Vietnam.

***Bungarus multicinctus* Blyth, 1860**
Figs 4A, B, 5A, B, 6A, B, 7A, B, 8E, 9A–C
[English name: Many-banded Krait]
[Chinese name: 银环蛇]

Bungarus multicinctus BLYTH 1860: 98.
Bungarus semifasciatus Günther 1858: 221 (not of Boie)
Bungarus candidus var. *multicinctus* – Boulenger 1896: 369

Type locality. Likely Amoy (now Xiamen, Fujian Province, China), possibly Formosa (Taiwan, China). ***Holotype*:** lost (*fide* Smith 1943; Nguyen et al. 2009)

This species was described based on one specimen from Amoy (Blyth 1860). The following description is based on 24 examined specimens from Southern China (Appendix 1): (1) narrow white dorsal crossbands 39.3 ± 4.7 (31–50), with each 1.4 ± 0.4 (1.0–2.0) vertebral scales long at midbody (Tables 1, 2, Figs 4A, B, 5A, B); (2) ventral body white scattered with dense brown pigment on adults (n = 19) (Fig. 3B), indistinct on some juveniles (Fig. 5B); (3) scales on neck and head of adults uniform black, scales

Table 2. Comparison of pattern features and hemipenis morphology in of the *B. candidus*/*multicinctus* complex.

Species	Coloration and patterns					Hemipenis morphology		
	Vertebral scales covered by white bands on middle body	Heads and necks of adults	Heads and necks of juveniles	Ventral surface of body	Ventral surface of tail	SLS	LK	Shape of tips
B. multicinctus **n = 24**	1.4 ± 0.4, (1.0–2.0)	uniform black	scales on lateral neck dim white edged	white, with dense with brown pigments	dense black bands and patches	papilla-like	weak	rod like, with a distinct boundary with large spines
B. candidus **n = 18**	3.8 ± 0.6, (3.0–5.0)	temporal area and lateral neck stained white	temporal area and lateral neck creamily white	immaculate white	broad dark crossbands	in shape of fangs	strong	cone, no clear boundary with large spines
B. wanghaotingi **n = 23**	2.2 ± 0.4, (1.5–2.5) n = 7	uniform black	light brown	immaculate white	a row of small light brown dots on middle	thick, relatively short, most pointy,	weak	larger at the bases, no clear boundary with large spines
B. suzhenae **sp. nov n = 4**	1.5 ± 0.4, (1.0–2.0)	uniform black	uniform black	immaculate white	immaculate or with small brown dots	in shape of fangs	strong	cone, no clear boundary with large spines

Abbreviations. – SLS (Shape of large spine); LK (Level of keratinization on tips).

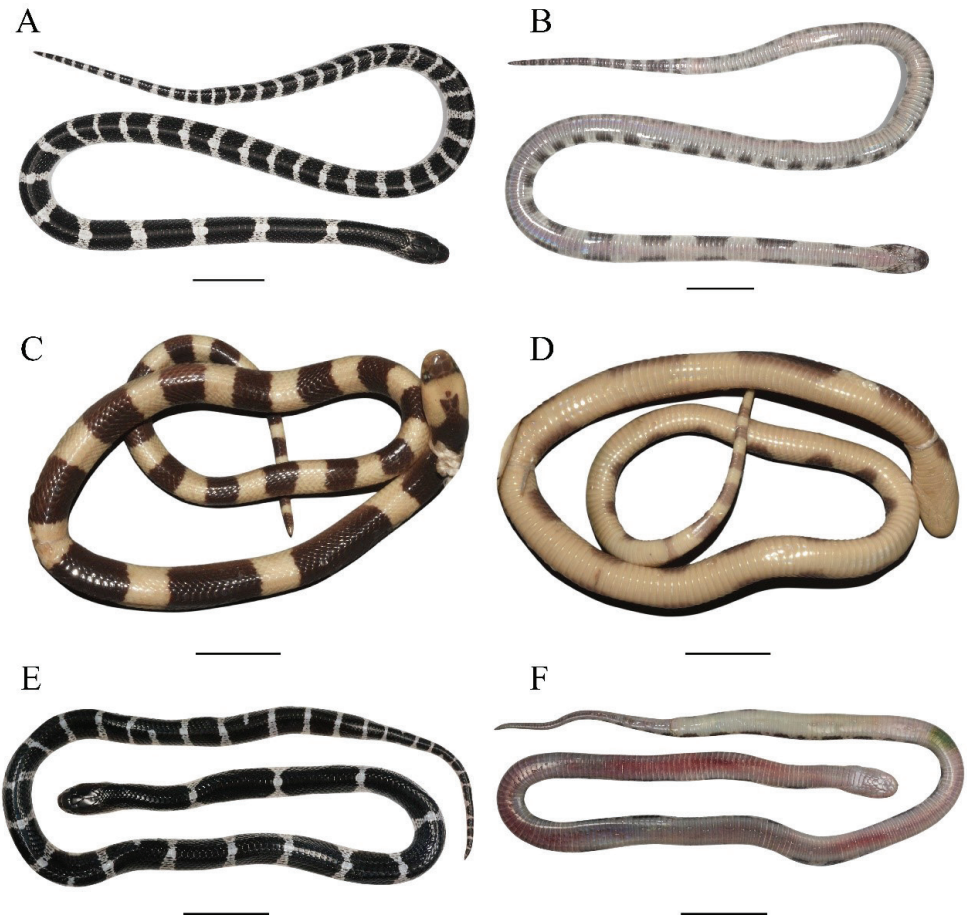

Figure 5. Dorsal (left) and ventral (right) view of juveniles of the *Bungarus candidus*/*multicinctus*/*wanghaotingi* complex **A, B** *B. multicinctus*, female, CIB DL18090209 from Fujian, China **C, D** *B. candidus*, female, NMW 27730:4 from Tasikmalaya, Java **E, F** *B.wanghaotingi*, unknown sex, CIB JCR36 from Jiangcheng, Yunnan, China. Scale bars: 20 mm.

on lateral neck behind parietals for immatures indistinctly edged with white (Fig. 6A); (4) moderately wide black bands on body (3–4 vertebral scales wide) intruding to ventrals for 1.2 to 2 times the width of outer dorsal scales (Fig. 7A); (5) ventral surface of tail with dense black bands and patches (Figs 4B, 5B); (6) posterior maxilla teeth four, distinctly curved backwards (Fig. 8E and Table 3); (7) fangs distinctly curved posteriorly (Fig. 8E); (8) prefrontal suture 1.5–2.5 (n = 17) times length of the internasal suture; (9) VEN 196–236 (n = 24), NSC 38–58 (n = 23).

Hemipenes description based on a sequenced male (Fig. 9A–C, CIB DL2019051701, SVL 993 mm) from Lishui, Zhejiang, China. Hemipenes reaches 9th subcaudal, bilobed near apex. Base of the organ covered with tiny soft basal hooks, medial portion spinous and apex fully calyculate, with the area between the calyculate

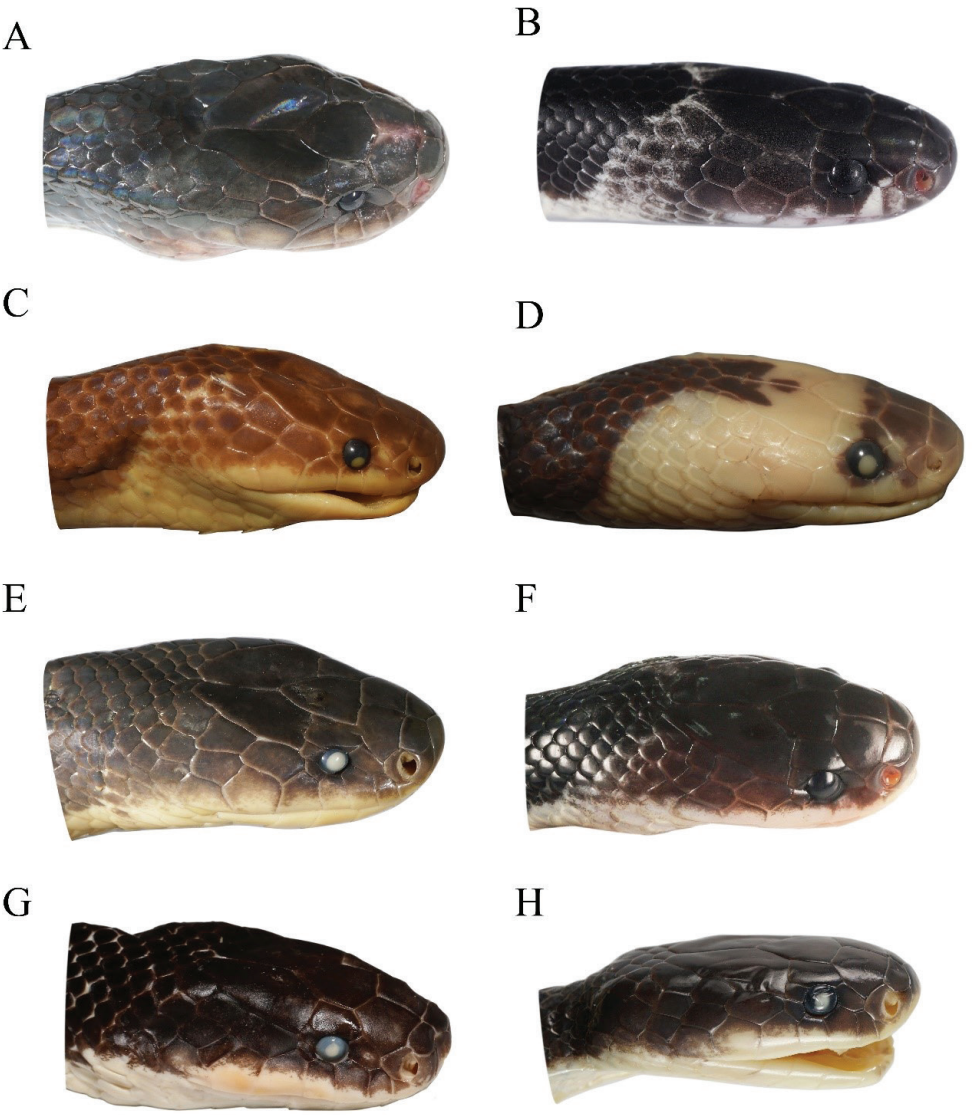

Figure 6. Dorsolateral head view of adults (left) and juveniles (right) of the *Bungarus candidus*/*multicinctus*/*wanghaotingi* complex and *B. suzhenae* sp. nov. **A** *B. multicinctus*, adult male, CIB DL2019051701 from Lishui, Zhejiang, China **B** *B. multicinctus*, juvenile female, CIB DL18090209 from Fujian, China **C** *B. candidus*, adult female, NMW 9486:1 from Pelambang, Java **D** *B. candidus*, juvenile female, NMW 27730:4 from Tasikmalaya, Java **E** *B. wanghaotingi*, adult male, CIB MLML20170801 from Jiangcheng, Yunnan, China **F** *B. wanghaotingi*, unknown sex juvenile, CIB JCR36 from Jiangcheng, Yunnan, China **G** *B. suzhenae* sp. nov. adult female, CIB 116090 **H** *B. suzhenae* sp. nov. subadult male, CIB 116088.

zone and spinous zones poorly defined. Most spines on the organ thick, papilla-shaped and blunt, each surmounted by minute, sharp, spine-like tip pointing towards base of hemipenes. The tips are weakly keratinized, concentrated in the shape of short bars; width consistent throughout organ, with a distinct boundary along the region between

Table 3. Teeth count of some members of subfamily Elapidae in this study.

Species	Maxilla	Palatine	Pterygoid	Dental
***Bungarus suzhenae* sp. nov. (n = 2)**	1+3	10–11	9–10	15–16
B. candidus	1+4	/	/	/
***B. wanghaotingi* (n = 1)**	1+4	12–13	10	16–17
***B. multicinctus* (n = 1)**	1+4	12	11	16
***B. fasciatus* (n = 2)**	1+3	13	11–13	17
***Ophiophagus hannah* (n = 3)**	1+3	8–9	10–12	15–16
***Naja melanoleuca* (n = 3)**	1+2	7–9	13–16	15–16
***N. atra* (n = 3)**	1+1	7–8	12–15	14–16
***Sinomicrurus kelloggi* (n = 1)**	1+1	8	4	11
***S. macclellandi* (n = 1)**	1+0	8	9	15

the main part of papilla-shaped spines and its tips. The morphology of large spines on hemipenes are similar to the morphology of a male from Changsha, Hunan Province, China, which was described by Pope (1935).

B. multicinctus differs from *B. candidus* by having (1) more white bands on the body (31–50, n = 24 vs. 18–26, n = 19) that are narrower in length (1–2 times of length of vertebral scales on middle body vs. 3–5 times); (2) different adult ventral surface (dense brown pigment vs. immaculate white); (3) different coloration of scales on the temporal and lateral neck regions (uniform black in adults and dim white edged in immatures vs. stained white in adults and creamy white in juveniles); (4) shape of the spines on the hemipenis (blunt, papilla-like vs. large spines that are sharp and fang-shaped); (5) and by the degree of keratinization of the hemipenial spines (tips of large spines not strongly keratinized, in shape of short bars, with a distinct boundary with the body of large spines vs. tips of large spines strongly keratinized, gradually wider towards base of large spines).

Distribution. This species is known from the following provinces in China based on specimens examined and/or DNA sequences data: Zhejiang, Fujian, Anhui, Guangdong, Guangxi, Hainan, Taiwan, Chongqing and Guizhou. It is also reported from Hunan Province (Pope 1935).

***Bungarus wanghaotingi* Pope, 1928**

Figs 4E, F, 5E, F, 6E, F, 7E, F, 8D, 9G–I
[English name: Wang's Krait]
[Chinese name: 云南环蛇]

Bungarus multicinctus wanghaotingi Pope 1928: 3.
Bungarus multicinctus wanghaotingi – Mell 1929; Zhao et al. 1998; Zhao 2006
Bungarus wanghaotingi – Leviton et al. 2003

Type locality. Yuankiang, Yunnan, China. ***Holotype*:** AMNH 35230.

The typical populations of this species possess the following characters based on 16 examined specimens from Yunnan and Guangxi, China (Appendix 1), squamation

Figure 7. Body patterns of adults (left) and juveniles (right) of the *Bungarus candidus*/*multicinctus*/*wanghaotingi* complex and *B. suzhenae* sp. nov. **A** *B. multicinctus*, adult male CIB DL2019051701 from Lishui, Zhejiang, China **B** *B. multicinctus* juvenile female, CIB DL18090209 from Fujian, China **C** *B. candidus*, adult male, NMW 27711:1 from Bandong, Java **D** *B. candidus*, juvenile male, RMNH 11416 from Pelambang, Java **E** *B. wanghaotingi*, adult male, CIB MLML20170801 from Mengla, Yunnan, China **F** *B. wanghaotingi*, unknown sex juvenile CIB JCR36 from Jiangcheng, Yunnan, China **G** *B. suzhenae* sp. nov. adult male, CIB 116089 from Yingjiang, Yunnan, China **H** *B. suzhenae* sp. nov. subadult male, CIB 116088 from Yingjiang, Yunnan, China.

data and body measurements of ten specimens from Yunnan, China (Yang and Rao 2008) and the holotype (Pope 1928): (1) 25.1 ± 3.2 (18–33, n = 27) narrow white dorsal body bands, 1.5–2.5 (n = 16) vertebral scales long at midbody (Yunnan population, n = 7; wider on specimens from Thailand) (Figs 4E, 5E); (2) ventral surface immaculate (Figs 4F, 5F); (3) scales on neck and head uniform black in adults, light brown in juveniles (Fig. 6E, F); (4) moderately elongate black bands on body (3.5–6.0 vertebral scales long) intruding to ventrals for 0.5 to 1.5 times of length of outer dorsal scales (Fig. 7E, F); (5) ventral tail white with one row of small light brown dots in the middle of the subcaudals (Figs 4F, 5F); (6) posterior maxilla teeth four, slightly folding backwards (Fig. 8D and Table 3); (7) fangs distinctly curved (Fig. 8D); (8) prefrontals suture 1.2–2.5 (n = 10) times the length of internasals suture; (9) VEN = 209–259 (n = 23), NSC = 32–64 (n = 22).

The hemipenes (Fig. 9G–I) are described based on the sequenced adult male specimen CIB MLMY20170801 (SVL 1170 mm) from Mengla, Yunnan Province and one

subadult male CIB DL2019051401 from, Yunnan Province, China; hemipenes reach 9th subcaudal, bilobed near apex, can be divided into three zones similar to *B. multicinctus*, the line of demarcation between the calyculate zone and the spinose zone is poorly defined; large spines thick, relatively short, mostly pointy, gradually thinning from the base to the tip; tips of large spines weakly keratinized, degree of keratinization highest at base, not in shape of short bars and not having a distinct boundary with main body of large spine.

B. wanghaotingi (typical populations from China) differs from *B. multicinctus* by having (1) fewer white bands on body; (2) ventral colouration of the body (immaculate vs. scattered with dense brown pigments in adults) (Fig. 5A, B); (3) coloration of the ventral surface of tail (immaculate or with dots vs. broad dark bands or patches); (4) the morphology of large spines on the hemipenes (large spines on hemipenes mostly pointy vs. papilla-like in shape and blunt); (5) the shape of the large spines on the hemipenes (without a distinct boundary with main body of large spines vs. with a distinct boundary); (6) fang shape (less distinctly curved vs. distinctly curved) (Fig. 7); and (7) posterior maxilla teeth less folding behind (Fig. 7).

B. wanghaotingi (typical populations from China) differs from *B. candidus* by having (1) narrower white bands in most specimens; (2) scales on neck and dorsal head uniform black in adults, light brown in juveniles vs. stained white, contrasting with neighbor scales on neck in adults, creamy white in juveniles; (3) ventral tail immaculate or with dots, rather than broad dark bands; (4) large spines on hemipenes relatively short, and weakly keratinized (vs. very elongated, and strongly keratinized).

Distribution. This species is known from the following localities based on specimens examined and/or DNA sequences data: Southern Yunnan, Southern Guangxi, China; Southern, Central and Northern Vietnam; Northern and Central Laos; Southern Thailand.

***Bungarus suzhenae* sp. nov.**

http://zoobank.org/8F3B0FA6-9B11-4CE3-AAD6-926D159D5220

Figs 6G, H, 7G, H, 8A–C, 9J–K, 10–13

Bungarus multicinctus multicinctus – Yang and Rao 2008, specimen from Yingjiang, Yunnan, China

Type material. ***Holotype*.** CIB 116088 (Fig. 9), subadult male, collected from a road through rice fields in Yingjiang County, Yunnan Province, China (97.584451, 24.662632, 922 m A.S.L), by Ding Li, in 2017. The holotype was a victim of roadkill and was fixed and stored in 80% ethanol.

***Paratypes*.** One adult male CIB 116089 (24.466941°N, 97.648691°E, 934 m A.S.L), one adult female CIB 116090 (24.634715°N, 97.762291°E, 1559 m A.S.L), one sub-adult male CIB 116091 from Yingjiang County (24.560296°N, 97.827170°E, 798 m A.S.L). The specimens were preserved in 80% ethanol.

Diagnosis. Assigned to genus *Bungarus* based on the presence of a row of enlarged, hexagonal scales on the vertebral scale row, enlarged prezygapophyseal accessory pro-

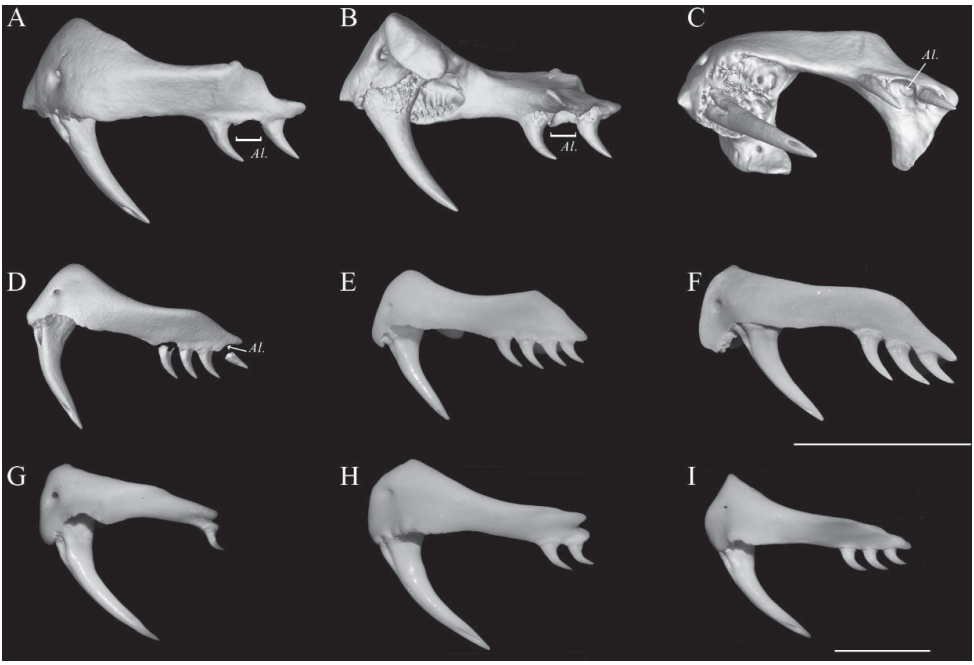

Figure 8. Maxilla morphology of seven members of subfamily Elapidae. Lateral (**A**) lingual (**B**), and ventral (**C**) view of the left maxilla of CIB 116090 (the paratype of *B. suzhenae* sp. nov.), compared with other members of the subfamily Elapinae **D** *B. wanghaotingi* SYNU R170408, from Yala, Thailand **E** *B. multicinctus*, from Guangdong, China **F** *B. fasciatus*, from Guangdong, China **G** *Naja atra* from Guangdong, China **H** *N. melanoleuca* from Kimpese, Congo **I** *Ophiophagus Hannah* from Guangxi, China. Scale bars: 5 mm, note that **H** and **I** had been scaled down at 1/2. Al = alveoli.

cess and relatively high neural spine (Slowinski 1994). The new species differs from its congeners by having a combination of the following characters: (1) posterior maxilla teeth three, slightly curved behind (Fig. 8A–C); (2) fangs feebly curved; (3) dorsal scales in 15 rows; (4) ventrals 220–229 (n = 4); (5) subcaudals undivided, 51–54 (n = 3); (6) anterior chin shields larger than the posterior ones (Fig. 10E); (7) prefrontal suture 2.7–3.4 (n = 3) times length of internasal suture (Fig. 10C, D); (8) adult and subadult heads uniform black (Figs 10–12); (9) dorsal body color black, with 39.3 ± 4.7 (26–38) white narrow bands present on midbody, covering 1.5 ± 0.4 (1.0–2.0) vertebral scales; (10) ventral surface uniform white, underside of tail white with tiny brown dots in the middle or immaculate (Figs 10–12); (11) ventral scales connected with the black bands of the dorsal body by small dark patches in lateral view, patches smaller than half the width of a dorsal scale; (12) tail relatively long, TaL/TL = 0.136–0.150 (n = 3); (13) hemipenes reaching 7th subcaudal; (14) large, elongated and pointed spines on hemipenes, in fang-shaped (Fig. 9J–L); (15) tips of the large spines strongly keratinized, without distinct boundary with the main body of large spines.

Comparison. Comparisons of *Bungarus suzhenae* sp. nov. with other *Bungarus* species are shown in Table 1. *Bungarus suzhenae* sp. nov. differs from *B. flaviceps* by: (1)

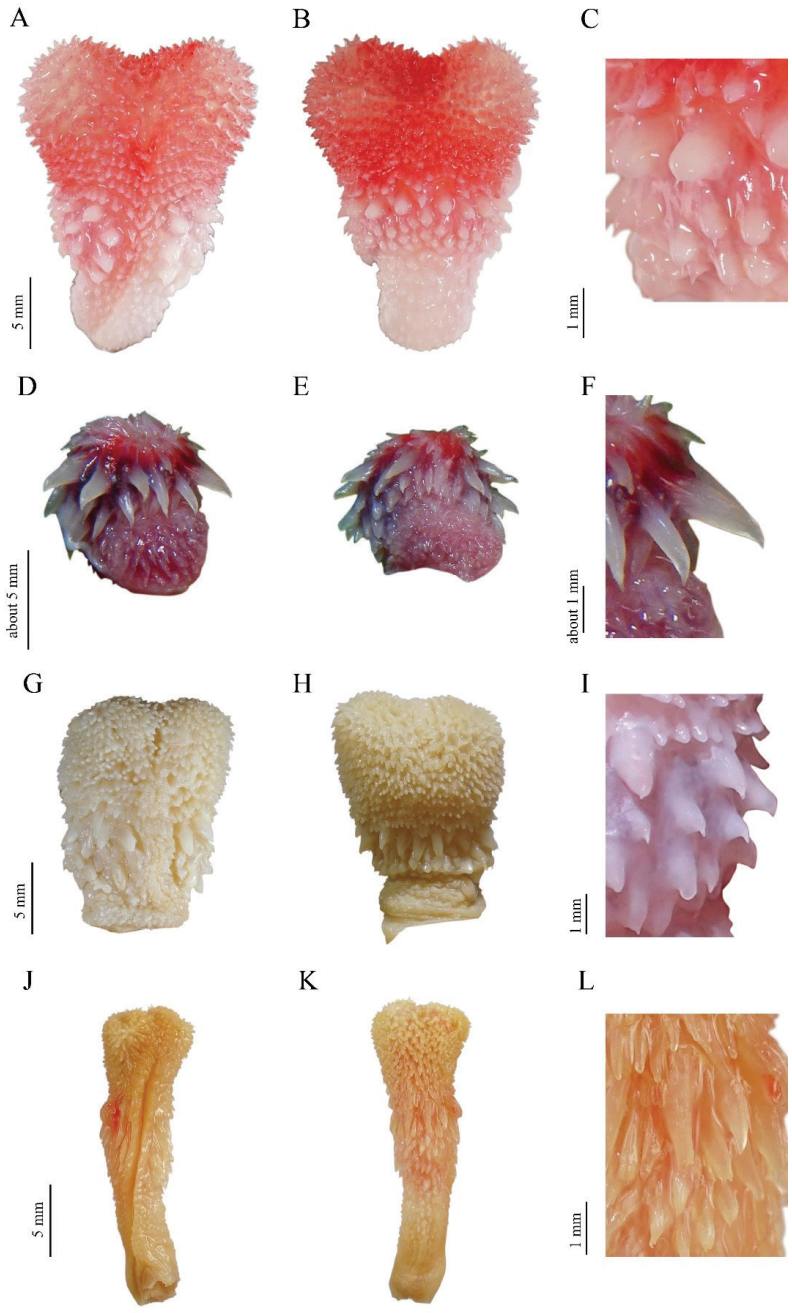

Figure 9. Hemipenial morphology of the *Bungarus candidus*/*multicinctus*/*wanghaotingi* complex and *B. suzhenae* sp. nov. Sulcate view (left), asulcate view (middle), spines (right) **A–C** *B. multicinctus*, CIB DL2019051701 from Lishui, Zhejiang, China, body length 993 mm **D–F** *B. candidus*, RH06153 from Quang Binh Province, Vietnam, body length 1200 mm **G–I** *B. wanghaotingi*, CIB MLML20170801 from Mengla, Yunnan, China, body length 1170 mm **J–L** *B. suzhenae* sp. nov., CIB 116089 from Yingjiang, Yunnan, China, body length 1140 mm.

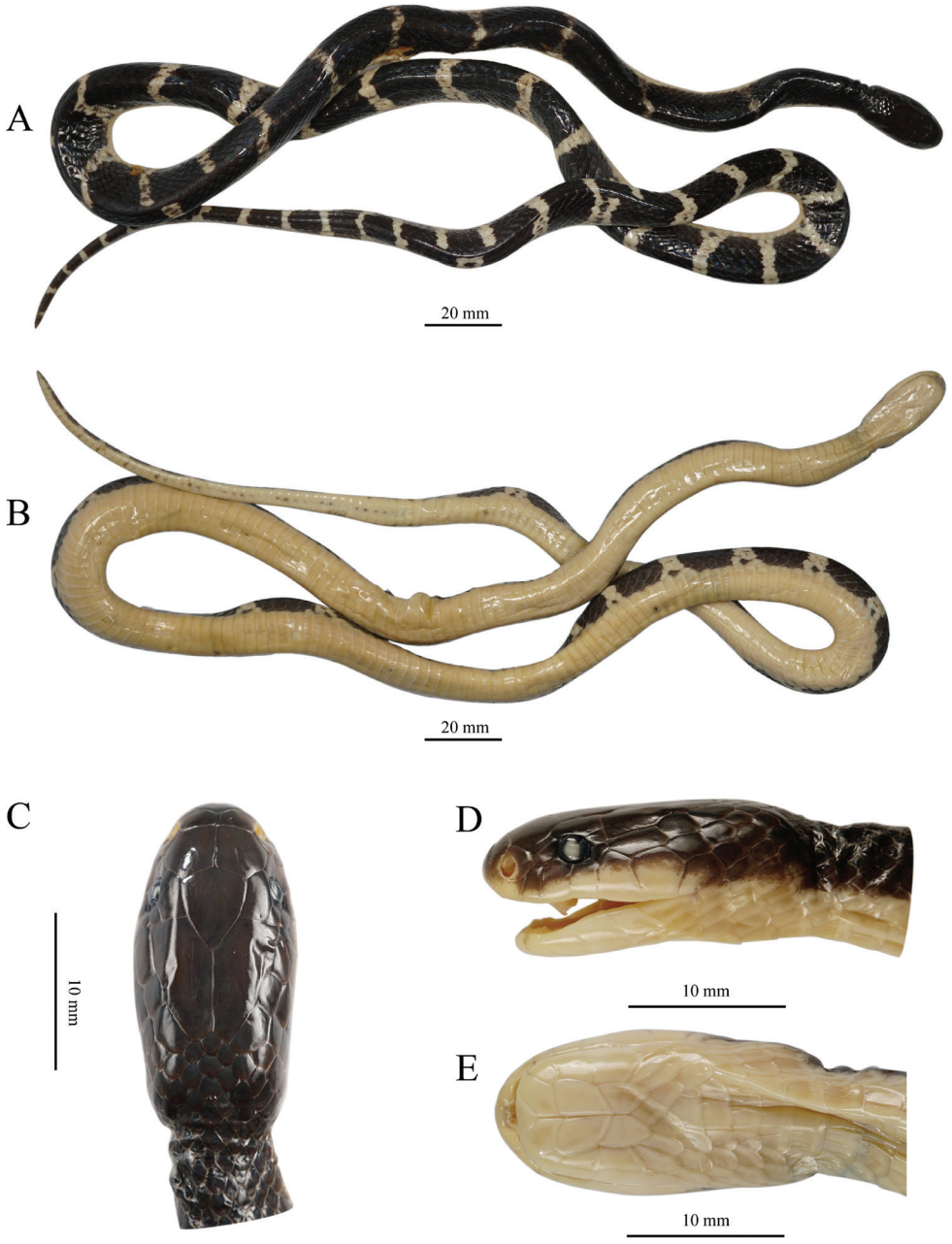

Figure 10. Holotype of *Bungarus suzhenae* sp. nov. (CIB 116088) **A** dorsal view of body **B** ventral view of body **C** dorsal view of head **D** left lateral view of head **E** right lateral view of head.

dorsal scales in 15 rows (vs. 13 rows); (2) dorsal body and tail black with white bands (vs. body black with or without light vertebral and paraventral stripes, tail bright red); (3) head uniform black (vs. head red or yellowish-tan).

Figure 11. Paratype of *Bungarus suzhenae* sp. nov. in life (Adult female CIB 116090).

Bungarus suzhenae sp. nov. differs from *B. fasciatus* by: (1) subcaudal scales 51–54 (n = 3) (vs. 23–39, n = ?); (2) dorsal body black with white bands (vs. with broad yellow rings between the dark rings); (3) dorsal head uniform black (vs. with V-shaped marking on the posterior of the head).

Bungarus suzhenae sp. nov. differs from *B. bungaroides* by: (1) subcaudals undivided (vs. divided); (2) Dorsum with 26–38 white bands (vs. 40–60 narrow white rings composing of small white spots); (3) ventral body uniform white (vs. blackish with irregular yellowish white pattern in every 3 to 4 scale intervals).

Bungarus suzhenae sp. nov. differs from *B. slowinskii* by: (1) subcaudals undivided (vs. divided); (2) anterior chin shields larger than the posterior chin shields (vs. anterior chin shields similar with posterior chin shields); (3) dorsal head uniform black (vs V-shaped marking present on head); (4) dorsal body and tail with black bands, ventral body uniform immaculate yellowish-white (vs. body with pattern of dark and white rings).

Bungarus suzhenae sp. nov. differs from *B. ceylonicus* by: (1) subcaudal scales 51–54 (n = 3) (vs. 34–40, n = ?); (2) ventral body uniform immaculate yellowish white (vs. ventral body with broad dark crossbands).

Bungarus suzhenae sp. nov. differs from *B. lividus* Cantor, 1839 by: (1) vertebral scales distinctly enlarged (vs. only slightly enlarged on the anterior body); (2) subcaudal scales 51–54 (n = 3) (vs. 41, n = 1); (3) dorsal body black with white bands (vs. no bands or rings or with narrow white rings).

Bungarus suzhenae sp. nov. differs from *B. niger* by: (1) dorsal body black with white bands (vs. no bands or rings on body) (Wall 1908); (2) tail relatively longer (TaL/TL = 0.136–0.150 n = 3 vs. 0.132 n = 1).

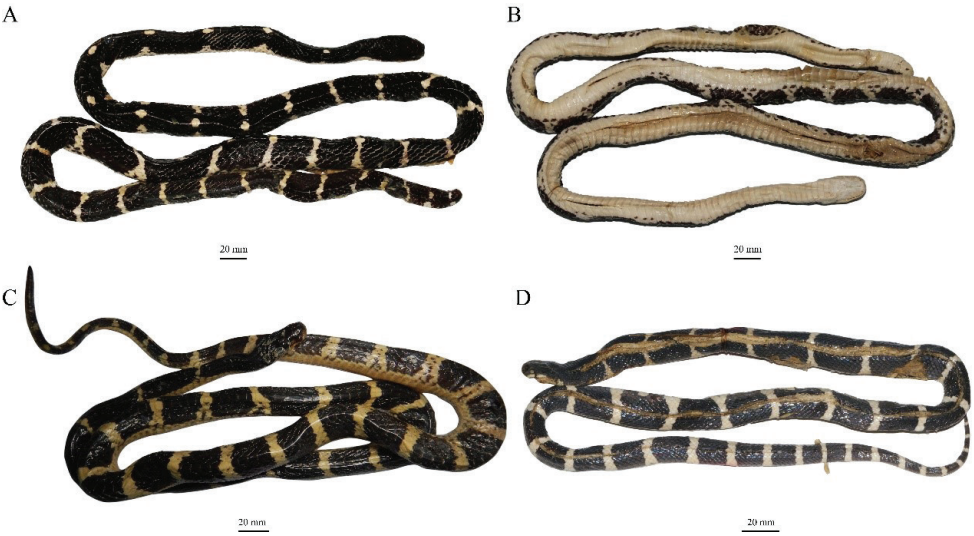

Figure 12. Paratypes of *Bungarus suzhenae* sp. nov. in preserve **A** dorsal and ventral **B** view of adult female CIB 116090 **C** dorsal view of adult male CIB 116089 **D** dorsal view of juvenile male CIB 116091.

Table 4. Main characters and measurements of *Bungarus suzhenae* sp. nov.

Character	CIB 116088	CIB 116089	CIB 116090	CIB 116091
Sex	M	M	F	M
DSR	15/15/15	15/15/15	15/15/15	15/15/15
VEN	221	229	222	220
SC	53	54	11+	51
SL	7/7	7/7	7/7	7/7
IL	7/7	7/7	7/7	7/7
BB+TB	38+12	34+12	34+3+	26+9
SVL	620	1140	1310	700
TaL	109	180	/	113
HL	21	39	30.2	/
HW	12.3	15.5	19.4	/
HH	8.7	12.8	14.2	/
ED	9.3	10.5	14.6	/

Abbreviations. – See in Material and methods.

Note: CIB 116088 is holotype, and other three is paratypes. The tail of CIB 116090 is incomplete. The head of CIB 116091 was flattened by roadkill.

Bungarus suzhenae sp. nov. differs from *B. magnimaculatus* by: (1) more subcaudal scales (51–54 n = 3 vs. 40–48); (2) dorsum with 26–38 white bands, narrower than black bands in between (vs. 11–14 broad, white crossbars, as wide as the black interspaces).

Bungarus suzhenae sp. nov. differs from *B. andamanensis* Biswas & Sanyal, 1978 by: (1) more ventral and subcaudal scales (220–229 n = 4 and 51–54 n = 3 vs. 192–197 n = 4 and 45–47 n = 4); (2) a shorter tail (TaL/TL = 0.136–0.150 n = 4 vs. 0.155–0.16 n = 4); (3) dorsum with 26–38 white bands (vs. 44 white linear arches or bars, mottled with brown); (4) head uniform black (vs. head is chocolate); (5) ventral body uniform white (vs. anterior and lateral margin of ventral scales tinged with brown).

Bungarus suzhenae sp. nov. differs from *B. sindanus* by: (1) fewer dorsal scale rows (15 vs. 17); (2) dorsal body colouration (black with white crossbands, and bands mostly complete vs. black with crossbands formed by series of white spots and interrupted).

Bungarus suzhenae sp. nov. differs from *B. walli* Wall, 1907 by: (1) fewer dorsal scale rows (15 vs. 17 rows); (2) dorsal body coloration (black with white crossbands, and bands mostly complete vs. body black above with crossbands formed by series of white spots and interrupted); (3) a higher number of ventral scales (220–229 n = 4 vs. 198–207 n = 8).

Bungarus suzhenae sp. nov. differs from *B. persicus* Abtin, Nilson, Mobaraki, Hooseini & Dehgannejhad, 2014 by: (1) fewer dorsal scale rows (15 vs. 17); (2) fewer ventral scales (220–229 n = 4 vs. 236–238 n = 2); (3) loreal plate absent (vs. present); (4) dorsal body coloration (black with white bands vs. body with crossbars ending in pairs of small rectangular whitish dots or short crossbars).

Bungarus suzhenae sp. nov. differs from *B. caeruleus* by: (1) dorsal body coloration (black with white crossbands, and bands mostly complete vs. narrow transverse white streaks or with small white spots); (2) white bands not in pairs (vs. at least some white bands occurring in pairs).

Bungarus suzhenae sp. nov. is morphologically most similar to phylogenetically closest congeners in *B. candidus*/*multicinctus*/*wanghaotingi* complex. However, it differs from the latter by multiple morphological characters. See hemipenis and maxilla comparisons in Tables 2, 3. The new species differs *B. multicinctus* by: (1) fang shape (less distinctly curved vs. distinctly curved); (2) lesser posterior maxilla teeth (three vs. four); (3) relatively longer prefrontals suture (length 2.7–3.4 times of internasals suture n = 3 vs. 1.3–2.3 times, n = 16); (4) ventral body coloration in adults (immaculate white, n = 4 vs. white scattered with dense brown pigments, n = 19); (5) black bands on body (large, length 4–7 times of vertebral scales on middle body, not reaching ventrals or just stained the edges of it, ventrals with black edges smaller than half of outer dorsal scales vs. black bands on body moderate, length 3–4 times of vertebral scales, intruding to ventrals for 1.2 to 2 times of width of outer dorsal scales); (6) ventral tail colouration (white with tiny brown dots in the middle or immaculate vs. with dense black bands or patches); (7) relatively shorter hemipenis (reaching 7th subcaudal vs. 9th subcaudal); (8) shape of large spines on hemipenes (elongated, fang-shaped, pointy vs. papilla-like and blunt); (9) tips of large spines on hemipenis (strongly keratinized, without distinct boundary with the main body of large spines vs. weakly keratinized, in shape of short bar, with a distinct boundary with main body of large spine).

Bungarus suzhenae sp. nov. differs *B. candidus* by: (1) fewer posterior maxilla teeth (three vs. four); (2) white bands on dorsal body more and narrower (26–38 white bands on dorsal body, width covering 1.0–1.5 vertebral scales on middle dorsum, n = 4 vs. 19–26 white bands on dorsal body, width covering 3.0–5.0 vertebral scales, n = 18); (3) prefrontal suture relatively longer (2.7–3.4 times length of internasals suture, n = 3 vs. 1.4–2.4 times, n = 17); (4) coloration on the upper head surface and neck (uniform black on adults and juvenile vs. temporal area and lateral neck light brown in adults, lateral necks and dorsal head posterior to eyes of immatures creamy white; (5) ventral tail

colouration (white with tiny brown dots in the middle or immaculate vs. with broad dark crossbands); (6) black bands on body (not intruding to ventral body, ventrals with narrow black edges smaller than half of outer dorsal scales vs. intruding to the ventral body, narrow black edges on ventrals with width 1–2 times of outer dorsal scales).

Bungarus suzhenae sp. nov. differs from typical *B. wanghaotingi* by: (1) slightly curved fangs (slightly curved and arc-like vs. distinctly curved); (2) fewer posterior maxilla teeth (three vs. four); (3) shorter hemipenis (reaches 7th subcaudal vs. 9th subcaudal); (4) shape of large spines on hemipenis (elongated, fang-shaped (vs. relatively short and blunt); (5) the degree of keratinization of the large hemipenial spines (strongly keratinized vs. weakly keratinized).

Description of holotype. (Fig. 10). Subadult male. Head relatively long, length 21.0 mm, maximal head width at anterior temporals 12.3 mm; maximal head height 8.7 mm, head 1.7 times longer than wide, distance between eyes 9.3 mm. Body length 620 mm; tail complete, 109 mm; total length 729 mm.

Body scalation. Ventrals 221, preventrals 3, anterior edge of first ventral starting at level of oral rictus; azygous scale immediately anterior to cloacal scale, half in width of the ventrals. Cloacal plate undivided. Subcaudals 53 undivided, tail complete. Dorsal scales smooth, in 15–15–15 rows; vertebral scales distinctly enlarged, largest and hexagonal at midbody, slightly wider than long.

Head. Cephalic scales smooth. Rostral near Λ-shaped, width 1.6 times of height visible from above. Nasals large, constricted and divided into one prenasal and one postnasal on both sides at border with internasals and first supralabial, prenasals irregular-shaped while postnasals crescent-shaped. External nares large, vertical oval-shaped, slightly smaller than eye diameter. Postnasal-preocular suture short and straight. Preocular hexagonal, bordered by third and fourth supralabials. Internasals two, 1.1 times wider than long, in contact with rostral, prenasals and postnasals, preoculars, and prefrontals. Prefrontals large, slightly wider than long; internasals suture short, prefrontals suture length 2.9 times of internasals suture and not aligned with latter. Frontal shield-shaped, pointing posteriorly, 1.3 times longer than wide, bordered by prefrontals, supraoculars and parietals; anterior suture of frontal pointed toward prefrontal suture, dividing posterior ends of prefrontals; supraoculars small, 1.7 times longer than wide, in contact with preoculars, upper postoculars, prefrontals, frontal and parietals. Parietals large and long, distance between end of parietals to preoculars 1.5 times the length of frontal; bordered by frontal, supraoculars, upper postoculars, one anterior temporal and two upper posterior temporals on each side, and three smalls nuchal scales on posterior margins. Posterolateral margins of parietals bordered by 1/1 enlarged elongate scales that anteriorly contact upper posterior temporals. Posterior extension of parietals pointed, divided in the middle by one of those three small dorsal scales. Preoculars 1/1, long hexagon, bordering with postnasal, second and third supralabials, prefrontal, and supraocular. Eyes small, oval, horizontal diameter 2.3 mm, vertical diameter 1.9 mm. Postoculars 2/2; relatively small with half size of preoculars; each lower postocular bordered by fourth and fifth supralabials, orbit, anterior temporal, upper postocular; each upper postocular bordered by lower postocular, orbit, supraocular, parietal but

not anterior temporal. Anterior temporals 1/1, long and hexagonal, length 2.9 times of width; each bordered by fifth and sixth supralabials, lower postocular, parietal, posterior temporals. Posterior temporals 2/2, bordering parietals, anterior temporals, sixth and seventh supralabials, and enlarged elongate scales bordering posterolateral margin of parietals. Supralabials 7/7, the third and fourth supralabials forming lower margin of orbit; first supralabials small, triangular, with pointed extension behind, not reaching preoculars, 1.4 times higher than wide; other supralabials in different subpentagonal shapes; second supralabials long and pentagonal-shaped, larger than the first, 1.8 times higher than wide; third supralabials larger than the former two, and the fourth, 1.5 times higher than wide; the fourth supralabials more or less rectangular, 1.6 times higher than wide; fifth and sixth supralabials are among the two largest, both 1.1 times higher than wide and similar in size, but fifth supralabials wider at lower part while the sixth supralabials is wider at the upper part; seventh supralabials height equal to width. Mentals moderate, width slightly shorter than width of rostral, triangular, bordering first infralabials, mental groove distinct. Infralabials 7/7 first infralabials pentagonal-shaped, long and narrow, in broad contact behind the mental and anterior chin shields; second infralabials in form of a square, half size of the first; the third and fourth enlarged; first, second, and third infralabials in broad contact with anterior chin shields, fourth infralabials in broad contact with posterior chin shields. Anterior chin shields larger than the posterior chin shields, the two pairs of chin shields in form of butterfly wings; anterior chin shield suture 3.5 times the length of the posterior chin shield suture; posterior chin shields 1.6 times longer than wide, bordered by anterior chin shields, fourth infralabials, 2/2 sublabials, and three gulars. Four gulars between first ventral and posterior most extension of each posterior chin shield; one gular and three preventrals between first ventral and suture of posterior chin shields, preventrals wider than half of first ventrals, gradually larger from first preventral to third.

Coloration in preservative. Dorsal surface of head, upper part of sides of the head, including upper part of supralabials, uniform black; lower half of head, including lower part of supralabials and rostral yellowish-white; ventral head uniform yellowish-white; iris dark black.

Dorsal body black with 38 white narrow crossbands (including incomplete bands). White bands on body scattered with tiny dark patches. Length of bands 1.0 to 2.0 times vertebral scales (average 1.2 ± 0.2), bands widening on flanks before joining the ventral surface, which is uniform white. 10 out of 38 bands incomplete, only present on one side of the dorsal body. First band starts at the 13th ventral, nine vertebral scales between first and second band; following bands gradually denser and brighter, three vertebral scales between 37th and 38th band. Most bands wider on outer row of dorsal scales, a dark spot present at junctions where the white bands meet the ventrals; black bands on body wide, covering 5–6 vertebral scales on middle body, not intruding to venter, ventrals with narrow black edges smaller than half of lateral dorsal scales. Venter immaculate yellowish-white, lateral edges of ventrals between dorsal white bands black.

Dorsal surface of tail black; 12 immaculate white bands present on dorsal part, width about equal to the width of one vertebral. Ventral portion of tail yellowish white,

23 of intermittent subcaudals with small brown dots; subcaudals between white bands margined with brown laterally (Fig. 10).

Variation. Paratypes largely resemble the holotype in scalation and color but differ in the following characters: upper postoculars of one adult male (CIB 116090) and one subadult male (CIB 116091) bordered by the anterior temporal on both sides. Ventral tail of CIB 116089, CIB 116090 (for remaining part) and CIB 116091 immaculate instead of mottled with small dots. First to 10th and the 12th white crossbands on dorsum of CIB 116090 disconnected, forming moderate white dots covering two vertebral scales. Posterior chin shields suture of CIB 116090 barely exist. The dorsal bands are fewer in CIB 116091 (Fig. 12).

Cranial osteology. The premaxilla of *B. suzhenae* sp. nov. is quite small and blunt, the ascending process of the premaxilla is well-developed, meeting the nasals at its dorsal edge. The nasal process of the premaxilla is not conspicuous. The nasal is peltate, with a blunt process on the lateral margin. The mesial process of the prefrontal is quite slender and pointed, narrowly reach the anterior tip of the frontal. Frontal triangular in shape from dorsal view. The distal process of the postorbital is slender and slightly anteriorly pointed, the basal part is in contact with the posterolateral marge of the frontal. A fenestra notch present on the posterolateral marge of the frontal. Two sides of the anterior surfaces of the parietal form the angle of approximately 120 degrees. The parietal is approximately "T" shaped; the lateral process is conspicuous and rectangular. The dorsal ridge of the parietal is more conspicuous in adults than in juveniles. The posterior end of the dorsal ridge merges at the mesial of the parietal in adults whereas separated in juveniles. The prefrontal surface of maxilla conspicuously upheaved. The supratemporal is flexed whereas the angular surface to the quadrate is obviously incrassated. The quadrate is quite short and stubby, the anterior angular surface to the supratemporal is extended. The ventral process of the basioccipital is trifurcate. The maxilla process (lateral process) of the palatine quite small whereas the choanal process is absent. The pterygoid is slender and medially curved, with the ectopterygoid process lost. The compound bone is quite stocky, the mesial crest and lateral crest are low and inconspicuous.

The first fang is canaliculated and feebly curved behind. There are four or five replacement fangs posterior to the first. Three small solid teeth ranged on the posterior end of maxilla, decrease in size posteriorly and separated from the fang by a very large diastema. Palatine teeth 10 (11), pterygoid teeth 10 (9); dentary teeth 16 (15), 2, 3 and 4 largest, decrease in size posteriorly. (Fig. 13).

The DOI numbers for ADMorph: 10.12112/R.0003 (CIB 116088, holotype) and 10.12112/R.0004 (CIB 116090, paratype).

Hemipenes. Description is based on the adult male paratype CIB 116089 (Fig. 9J–L; SVL 1,140 mm). Hemipenis reaches 7th subcaudal, slightly bilobed near top. Three zones of similar length of ornamentation exist: a distal calyculate zone, a spinose zone proximal to the sulcus bifurcation, and a basal zone. The line of demarcation between the calyculate zone and spinose zones is poorly defined. The

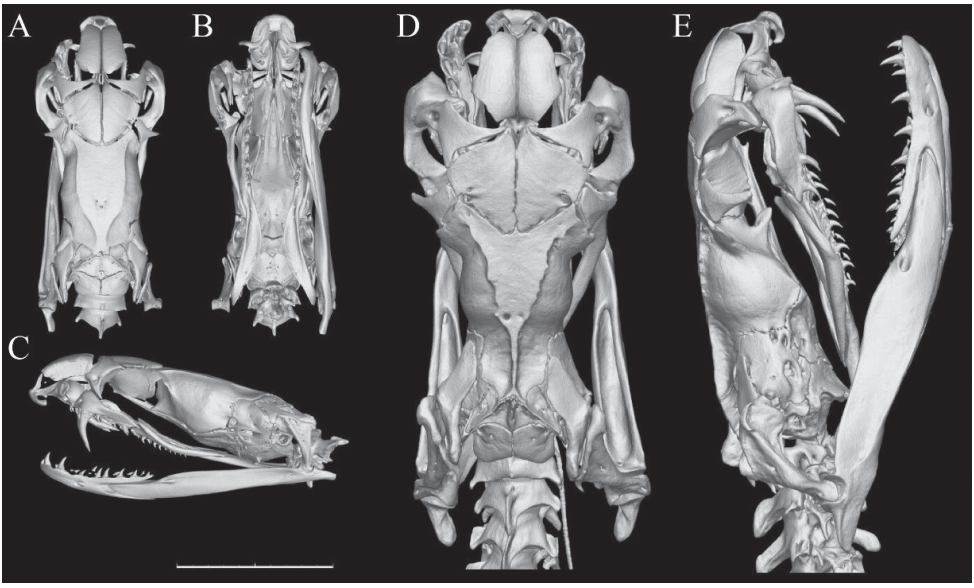

Figure 13. Three-dimensional reconstructed skull models of the holotype (**A–C** CIB 116088, subadult male) and paratype (**D, E** CIB 116090, adult female) of *Bungarus suzhenae* sp. nov. Dorsal (**A, D**), ventral (**B**), lateral (**C, E**) view. Scale bar: 10 mm.

calyculate zone is capitate; calyces well developed, gradually smaller and lesser keratinized towards the distal end; calyces nearest the sulcus intruding to the spinous zone by few ranks. The spinose zone is covered with large spines; large, elongated and pointed spines on hemipenes, in fang-shaped, gradually thinner from bases to tips; tips of large spine strongly keratinized, without distinct boundary with the main body of large spines; the spines adjacent to the calyces are nearly twice as large as the most proximal ones in a sulcate view. The hemipenis slightly constricts between the spinose zone and the basal zone. The basal zone is covered with numerous minute spines on the larger distal part, and smooth proximal region. The sulcus is forked distally along the spinose zone, with the bifurcation originating at a distance of about one large spine length; lips bearing calyces in calyculate zone, and small spines throughout the spinose region.

Etymology. The specific epithet of the new species was named after Su-Zhen Bai, a famous powerful goddess of Chinese myth *The legend of the White snake* (白蛇传), in honor of her courage to true love and kindness to people. The common name is suggested as "Suzhen's krait" in English and "素贞环蛇 (sù zhēn huán shé)" in Chinese.

Distribution and ecology. *Bungarus suzhenae* sp. nov. was found in rice fields, streams in monsoon forest at elevation from 800 m to 1,560 m. This species is distributed in Yingjiang Country, Yunnan Province, China and Kachin State, Myanmar (Fig. 1). In captivity, they prey on eels like *Monopterus albus* and small snakes such *Xenochrophis flavipunctatus*, *Pareas* spp., but refuse mice and frogs.

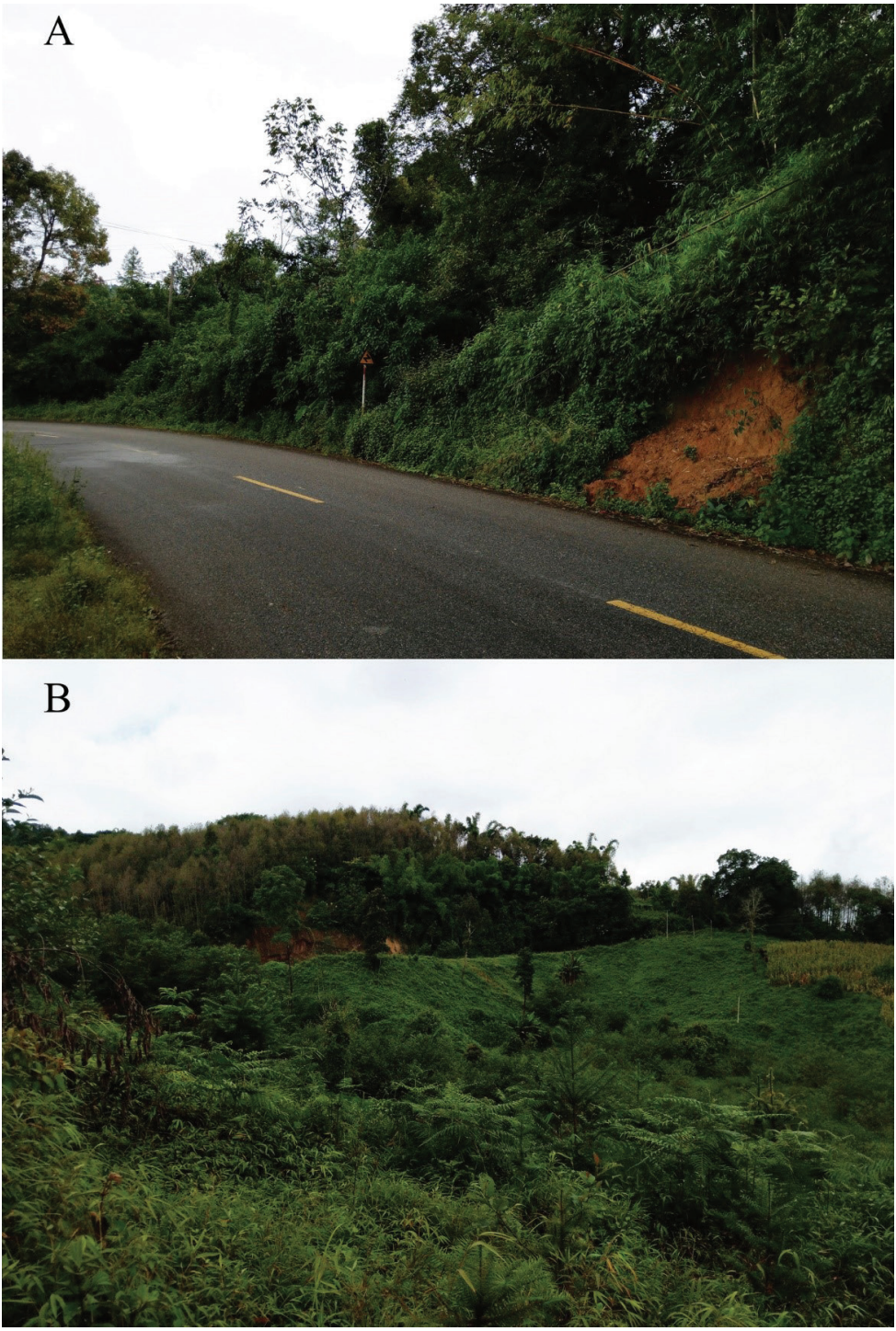

Figure 14. Habitats of *Bungarus suzhenae* sp. nov. Road **A** in Yingjiang County, Yunnan Province, China. Monsoon forest **B** in Yingjiang County, Yunnan Province, China.

Discussion

Since the members of *Bungarus* are a group of deadly snakes, understanding their species diversity, species boundaries and geographic distribution is vital for saving human lives. Snakebites from kraits are known to have a high mortality, and the toxicology of their venom has been the subject of numerous publications (e.g., Mebs et al. 1971; Liu et al. 1998; Chang et al. 1999; Nirthanan et al. 2002; Jiang et al. 2011). An extreme and sad case for krait bites is that one individual of *Bungarus suzhenae* sp. nov. (CAS 221526) led to the death of famous herpetologist Joe Slowinski (Justin L. Lee 2020; personal communication). Many studies have indicated that the venom composition of *B. candidus* is different from *B. multicinctus* (e.g., Nirthanan et al. 2002; Tsai et al. 2002). Thus, a sound understanding of the species boundaries between these two species is necessary to provide the essential underpinnings for future research on their venom composition and antivenin development (Fry et al. 2003; Barlow et al. 2009; Williams et al. 2011; Casewell et al. 2013, 2014). However, identification of these *Bungarus* is still challenging. Our examination of the specimens from the *B. candidus*/*multicinctus*/*wanghaotingi* complex shows that the traditional characters used to diagnose the three taxa from each other (i.e., by the number of the white/black bands and the ventral scales) only work for *B. candidus* and *B. multicinctus*. Furthermore, the range of the white body bands of *B. wanghaotingi* overlaps with that of *B. candidus* and *B. multicinctus* (Table 1) and may be unreliable for identification without further examination of other characters. As for *B. suzhenae* sp. nov., the range of the number of crossbands also overlaps with that of the *B. candidus*/*multicinctus*/*wanghaotingi* complex except *B. candidus* (Table 1).

Thorough morphological examination and comparisons are essential for taxonomy of *B. candidus*/*multicinctus*/*wanghaotingi* complex. The topology of molecular phylogeny in Xie et al. (2018) is similar to the topology in this study. The samples from Java, Indonesia, Thailand, and Vietnam form a lineage (*B. candidus* lineage) sister to the lineage (*B. wanghaotingi* lineage) including samples from southwestern and southern China, Laos, Thailand and Vietnam. However, Xie et al. (2018) concluded that the latter lineage is *B. candidus* without morphological comparisons with typical *B. candidus* from Indonesia and Peninsular Malaysia. Thus, the distribution report of "*B. candidus*" in the southwestern and southern China mentioned by Xie et al. (2018) should be revised into *B. wanghaotingi*. And similarly, the records of "*B. multicinctus*" in Vietnam, Laos, and Thailand (Uetz and Hošek 2017) are supposed to be *B. wanghaotingi*.

The "*B. candidus*" from Southern and Central Vietnam mentioned by Nguyen et al. (2017) are paraphyletic based on COI sequences data when *B. candidus* from Peninsular Malaysia (SYNU R180411, which is monophyletic with Javanese *B. candidus* in cyt *b* phylogeny) is included. Most specimens (e.g., ITBCZ 900) are monophyletic with typical *B. wanghaotingi* from China, Laos and Southern Thailand. But one specimen (KIZ 100) is monophyletic with two *B. candidus* from Peninsular Malaysian and Cambodia. This suggests a large sympatric zone from Southern Thailand to Southern Vietnam where *B. wanghaotingi* and *B. candidus* are morphologically similar in having wide crossbands but genetically paraphyletic (Fig. 1; Nguyen et al. 2017). However, the hemipenial mor-

phology of wide crossbanded *B. wanghaotingi* ITBCZ 900 (fig. 3 in Nguyen et al. 2017) is quite similar with typical *B. wanghaotingi* by large spines on hemipenes relatively short, and weakly keratinized. Southern Indochina populations of *B. wanghaotingi* have wider crossbands on body than typical *B. wanghaotingi* in the north and this is possibly due to different selective constraints from habitats at lower latitude. This is similar to the discussion on *B. candidus* and *B. javanicus* by Kuch and Mebs (2007). And similar scenario for that northern *Bungarus* species *B. suzhenae* and *B. multicinctus* which have narrower body bands. The difference between hemipenial morphology of *B. candidus* (RH06153) and *B. wanghaotingi* (both typical and Southern Indochina populations) further confirmed the identification of RH06153 when sequence data was unavailable.

Based on comprehensive morphological comparisons of specimens and molecular evidence, we identified additional morphological characters that can be used to be help identify these taxa (e.g., dental morphology, the patterns on head, ventral body and tail, and large spines on hemipenis). We note that the number of maxillary teeth is taxonomically significant in identifying species of *Bungarus* and might indicate divergences in feeding and/or defense behavior. *B. suzhenae* sp. nov. only possesses three posterior maxilla teeth, a character state shared by *B. fasciatus* and *Ophiophagus hannah*. However, all members of the *B. candidus*/*multicinctus*/*wanghaotingi* complex possess four posterior maxilla teeth, a character state that is likely a synapomorphy in comparison to *B. suzhenae* sp. nov. (Fig. 8).

The species of the *B. candidus*/*multicinctus*/*wanghaotingi* complex show feeble genetic divergences (Suppl. material 1: Table S3), with the uncorrected pairwise distances of cyt *b* between *B. candidus*, *B. multicinctus* and *B. wanghaotingi* ranging from 1.6%–3.3%. These distances are lower than those between other *Bungarus* species (ranging from 9.7% to 28.6%). However, morphological comparisons showed clear differences between these closely related species. According to Kuch (2007), *B. candidus*, *B. multicinctus* and *B. wanghaotingi* diverged between Middle to Late Pleistocene (> 0.8–1.5 MYA). During the Pleistocene, southeast Asia and southern China went through very frequent sea level oscillations (Voris 2000; Inger and Voris 2001) and the *B. candidus*/*multicinctus*/*wanghaotingi* complex may have experienced several hybridization events, introgression or incomplete lineage sorting. We encourage future studies to examine the *B. candidus*/*multicinctus*/*wanghaotingi* complex using genomic data, ecological niche modelling and broader sampling, which would help to better understand the evolutionary history of these medically important snakes.

For easier identification, an updated Key to Kraits based on Slowinski (1994) was compiled (note that the identification of this key is still experimental, confirmation by comparing more characters or by sequencing is strongly recommended):

1a	More than 13 dorsal scale rows	**2**
1b	13 dorsal scale rows	***Bungarus flaviceps***
2a	17 or 19 dorsal scale rows	**3**
2b	15 dorsal scale rows	**5**
3a	Loreal plate present	***B. persicus***
3b	Loreal plate absent	**4**

4a White bands on body ..... ***B. sindanus***
4b White spots on body..... ***B. walli***
5a Subcaudals divided **6**
5b Subcaudals single **7**
6a Inversely V-shaped light on dorsal head ..... ***B. slowinskii***
6b Without inversely V-shaped light on dorsal head ..... ***B. bungaroides***
7a Vertebral row of dorsal scales enlarged anteriorly..... **8**
7b Vertebral row of dorsal scales not enlarged anteriorly ..... ***B. lividus***
8a Bands or rings on body..... **9**
8b No bands or rings on body ..... ***B. niger***
9a Light bands or rings white **10**
9b Light bands yellow..... ***B. fasciatus***
10a Rings on body ..... ***B. ceylonicus***
10b Bands on body..... **11**
11a More than 20 white bands..... **12**
11b 11–14 white bands ..... ***B. magnimaculatus***
12a More than 26 white bands..... **13**
12b Less than 26 white bands..... ***B. candidus*****, or wide white crossbanded *B. wanghaotingi* from Southern Indochina and Peninsular Malaysia**
13a At least some white bands occurring in pairs..... ***B. caeruleus***
13b White bands not in pairs..... **14**
14a White bands equidistant from each other along body ..... ***B. andamanensis***
14b White bands closer to each other posteriorly than anteriorly..... **15**
15a Three posterior maxilla teeth..... ***B. suzhenae***
15b Four posterior maxilla teeth **16**
16a Ventral surface of tail immaculate white or with dots, large spines on hemipenes mostly pointy..... ***B. wanghaotingi*** **(typical populations from Northern Indochina and China)**
16b Ventral surface of tail with broad dark bands or patches, large spines on hemipenes papilla-like in shape and blunt ..... ***B. multicinctus***

Acknowledgements

We wish to thank Robert Jadin, Patrick David, Lee Grismer for their helpful comments and suggestions on our manuscript. We thank Justin L. Lee for his English revision and helpful suggestions. We thank Ralf Hendrix for sharing photos of hemipenes of *B. candidus*. We thank Peng Guo and Zhang Liang for providing partial samples. We are grateful for help from Yong-Sheng Zhang and Qiang-Bang Gong of Tongbiguan Nature Reserve. We thank Yi-Wu Zhu for sharing a specimen. This study is supported by Biodiversity Investigation, Observation and Assessment Program of Ministry of Ecology and Environment of China (2019–2023) and the Natural Science Foundation of Jiangsu Province, China (BK20160103), the Second Tibetan Plateau Scientific Expedition and Research Program (STEP, Grant

No. 2019QZKK05010503 and No. 2019QZKK0705) and the Strategic Priority Research Program of the Chinese Academy of Sciences (Grant No. XDA23080101) to Jian-Ping Jiang.

References

Abtin E, Nilson G, Mobaraki A, Hosseini AA, Dehgannejhad M (2014) A new species of krait, *Bungarus* (Reptilia, Elapidae, Bungarinae) and the first record of that genus in Iran. Russian Journal of Herpetology 21: 243–250.

Ahsan M, Rahman M (2017) Status, distribution and threats of kraits (Squamata: Elapidae: *Bungarus*) in Bangladesh. Journal of Threatened Taxa 9: 9903–9910. https://doi.org/10.11609/jott.2929.9.3.9903-9910

Arevalo E, Davis SK, Sites Jr JW (1994) Mitochondrial DNA sequence divergence and phylogenetic relationships among eight chromosome races of the *Sceloporus grammicus* complex (Phrynosomatidae) in central Mexico. Systematic Biology 43: 387–418. https://doi.org/10.1093/sysbio/43.3.387

Baig KJ, Masroor R, Arshad M (2008) Biodiversity and ecology of the herpetofauna of Cholistan Desert, Pakistan. Russian Journal of Herpetology 15: 193–205.

Barlow A, Pook CE, Harrison RA Wüster W (2009) Co-evolution of diet and prey-specific venom activity supports the role of selection in snake venom evolution. Proceedings of the Royal Society B 276: 2443–2449. https://doi.org/10.1098/rspb.2009.0048

Biswas S, Sanyal DP (1978) A new species of krait of the genus *Bungarus* Daudin, 1803 (Serpentes: Elapidae) from the Andaman Island. The journal of the Bombay Natural History Society 75(1): 179–183.

Blyth E (1860) Report of curator, Zoological Department. Journal and Proceedings of the Asiatic Society of Bengal 29: 87–100.

Boulenger GA (1890) The Fauna of British India, Including Ceylon and Burma. Reptilia and Batrachia. Taylor & Francis, London, 365–372. https://www.biodiversitylibrary.org/page/4388100

Boulenger GA (1896) Catalogue of the snakes in the British Museum (Vol. 3). Taylor & Francis: London, 727 pp.

Burbrink FT, Lawson R, Slowinski JB (2000) Mitochondrial DNA phylogeography of the polytypic North American rat snake (*Elaphe obsoleta*): a critique of the subspecies concept. Evolution 54: 2107–2118. https://doi.org/10.1111/j.0014-3820.2000.tb01253.x

Casewell NR, Wagstaff SC, Wüster W, Cook DAN, Bolton FMS, King SI, Pla D, Sanz L, Calvete JJ, Harrison RA (2014) Medically important differences in snake venom composition are dictated by distinct postgenomic mechanisms. Proceedings of the National Academy of Sciences of the USA 111: 9205–9210. https://doi.org/10.1073/pnas.1405484111

Casewell NR, Wüster W, Vonk FJ, Harrison RA, Fry BG (2013) Complex cocktails: the evolutionary novelty of venoms. Trends in Ecology and Evolution 28: 219–229. https://doi.org/10.1016/j.tree.2012.10.020

Chang LS, Lin SK, Huang HB, Hsiao M (1999) Genetic organization of α-bungarotoxins from *Bungarus multicinctus* (Taiwan banded krait): evidence showing that the production

of α-bungarotoxin isotoxins is not derived from edited mRNAs. Nucleic acids research 27(20): 3970–3975. https://doi.org/10.1093/nar/27.20.3970

Che J, Chen HM, Yang JX, Jin JQ, Jiang K, Yuan ZY, Murphy RW, Zhang YP (2012) Universal COI primers for DNA barcoding amphibians. Molecular Ecology Resources 12: 247–258. https://doi.org/10.1111/j.1755-0998.2011.03090.x

Chen YL, Lin YL, Lin TE (2016) Application of Species Identification via Mitochondrial COI DNA Barcoding for Viperidae and Elapidae Species in Taiwan. Taiwan Journal of Biodivers 18(2): 145–156.

Dowling HG (1951) A proposed standard system of counting ventrals in snakes. British Journal of Herpetology 1: 97–99.

Fry BG, Winkel KD, Wickramaratna JC, Hodgson WC, Wüster W (2003) Effectiveness of snake antivenom: species and regional venom variation and its clinical impact. Journal of Toxicology – Toxin Reviews 22: 23–34. https://doi.org/10.1081/TXR-120019018

Hillis DM, Bull JJ (1993) An empirical test of bootstrapping as a method for assessing confidence in phylogenetic analysis. Systematic biology 42(2): 182–192. https://doi.org/10.1093/sysbio/42.2.182

Hoang DT, Chernomor O, von Haeseler A, Minh BQ, Le SV (2017) UFBoot2: Improving the ultrafast bootstrap approximation. Moloecular Biology and Evolution 35: 518–522. https://doi.org/10.1093/molbev/msx281

Hou Y, Cui X, Canul-Ku M, Jin S, Hasimoto-Beltran R, Guo Q, Zhu M (2020) ADMorph: A 3d digital microfossil morphology dataset for deep learning. IEEE Access 8: 148744–148756. https://doi.org/10.1109/ACCESS.2020.3016267

Huelsenbeck JP, Ronquist F, Nielsen R, Bollback JP (2001) Bayesian inference of phylogeny and its impact on evolutionary biology. Science 294: 2310–2314. https://doi.org/10.1126/science.1065889

Inger RF, Voris HK (2001) The biogeographical relations of the frogs and snakes of Sundaland. Journal of Biogeography 28: 863–891. https://doi.org/10.1046/j.1365-2699.2001.00580.x

Jiang K (2010) A method for evaginating the hemipenis of Preserved snakes. Sichuan Journal of Zoology 29(1): 122–123. [In Chinese]

Jiang Y, Li Y, Lee W, Xu X, Zhang Y, Zhao R, Zhang Y, Wang W (2011) Venom gland transcriptomes of two elapid snakes (*Bungarus multicinctus* and *Naja atra*) and evolution of toxin genes. BMC genomics 12(1): 1–13. https://doi.org/10.1186/1471-2164-12-1

Khan MS (2002) A Guide to the Snakes of Pakistan. Frankfurt Contributions to Natural History (Vol. 16). Edition Chimaira, Frankfurt am Main.

Kharin VE, Orlov NL, Aranjeva NB (2011) New records and redescription of rare and little-known elapid snake *Bungarus slowinskii* (Serpentes: Elapidae: Bungaridae). Russian Journal of Herpetology 18(4): 284–294.

Kuch U, Kizirian D, Truong NQ, Lawson R, Donnelly MA, Mebs D, Lannoo MJ (2005) A New Species of Krait (Squamata: Elapidae) from the Red River System of Northern Vietnam. Copeia 2005: 818–833. https://doi.org/10.1643/0045-8511(2005)005[0818:ANSOKS]2.0.CO;2

Kuch U, Mebs D (2007) The identity of the Javan Krait, *Bungarus javanicus* Kopstein, 1932 (Squamata: Elapidae): evidence from mitochondrial and nuclear DNA sequence analyses and morphology. Zootaxa 1426: 1–26. https://doi.org/10.11646/zootaxa.1426.1.1

Kuch U (2007) The Effect of Cenozoic Global Change on the Evolution of a Clade of Asian Front-fanged Venomous Snakes: (Squamata: Elapidae: *Bungarus*). PhD thesis, Frankfurt am Main, Johann Wolfgang Goethe-Universität.

Kumar S, Stecher G, Tamura K (2016) MEGA7: molecular evolutionary genetics analysis version 7.0 for bigger datasets. Molecular biology and evolution 33: 1870–1874. https://doi.org/10.1093/molbev/msw054

Lanfear R, Calcott B, Ho SY, Guindon S (2012) Partition Finder: combined selection of partitioning schemes and substitution models for phylogenetic analyses. Molecular Biology and Evolution 29: 1695–1701. https://doi.org/10.1093/molbev/mss020

Leviton AE, Gibbs Jr RH, Heal E, Dawson CE (1985) Standards in herpetology and ichthyology: Part I. Standard symbolic codes for institutional resource collections in herpetology and ichthyology. Copeia 1985: 802–832.

Leviton AE, Wogan GO, Koo MS, Zug GR, Lucas RS, Vindum JV (2003) The Dangerously Venomous Snakes of Myanmar Illustrated Checklist with Keys. Proceedings of The California Academy of Sciences 54: 22–27.

Leviton AE, Zug GR, Vindum JV, Wogan GO (2008) Handbook to the dangerously venomous snakes of Myanmar. California Academy of Sciences, San Francisco.

Liu LF, Chang CC, Kuo KW, Liau MY (1998) Genetic characterization of the mRNAs encoding α-bungarotoxin: Isoforms and RNA editing in Bungarus multicinctus gland cells. Nucleic acids research 26(24): 5624–5629. https://doi.org/10.1093/nar/26.24.5624

Mebs D, Narita K, Iwanaga S, Samejima Y, Lee CY (1971) Amino acid sequence of α-bungarotoxin from the venom of *Bungarus multicinctus*. Biochemical and biophysical research communications 44(3): 711–716. https://doi.org/10.1016/S0006-291X(71)80141-9

Mell R ("1929" (1931)) List of Chinese snakes. *Lingnan science journal*, Canton 8: 199–219.

Nguyen SV, Ho CT, Nguyen TQ (2009) Herpetofauna of Vietnam. Chimaira, Frankfurt, 768 pp.

Nguyen L-T, Schmidt HA, von Haeseler A, Minh BQ (2015) IQ-TREE: a fast and effective stochastic algorithm for estimating maximum-likelihood phylogenies. Molecular biology and evolution 32: 268–274. https://doi.org/10.1093/molbev/msu300

Nguyen SN, Nguyen VDH, Nguyen TQ, Le NTT, Nguyen LT, Vo BD, Vindum JV, Murphy RW, Che J, Zhang YP (2017) A new color pattern of the *Bungarus candidus* complex (Squamata: Elapidae) from Vietnam based on morphological and molecular data. Zootaxa 4268: 563–572. https://doi.org/10.11646/zootaxa.4268.4.7

Nirthanan S, Charpantier E, Gopalakrishnakone P, Gwee MC, Khoo HE, Cheah LS, Bertrand D, Kini RM (2002) Candoxin, a novel toxin from *Bungarus candidus*, is a reversible antagonist of muscle (αβγδ) but a poorly reversible antagonist of neuronal α7 nicotinic acetylcholine receptors. Journal of Biological Chemistry 277(20): 17811–17820. https://doi.org/10.1074/jbc.M111152200

Pope CH (1928) Four new snakes and a new lizard from South China. American Museum novitates 325: 1–4.

Pope CH (1935) The reptiles of China: turtles, crocodilians, snakes, lizards (Vol. 10). In: Reeds CA (Ed.) Natural history of Central Asia. American Museum of Natural History, New York, 335–339.

Rao DQ, Zhao EM (2004) *Bungarus bungaroides*, A Record New to China (Xizang AR) with a Note on *Trimeresurus tibetanus*. Sichuan Journal of Zoology 23: 213–214.

Ronquist F, Teslenko M, Van Der Mark P, Ayres DL, Darling A, Höhna S, Larget B, Liu L, Suchard MA, Huelsenbeck JP (2012) MrBayes 3.2: efficient Bayesian phylogenetic inference and model choice across a large model space. Systematic Biology 61: 539–542. https://doi.org/10.1093/sysbio/sys029

Sivaperuman C, Venkataraman K (2018) Indian Hotspots: Vertebrate Faunal Diversity, Conservation and Management. Springer, 23–35. https://doi.org/10.1007/978-981-10-6983-3_16

Slowinski JB (1994) A Phylogenetic Analysis of *Bungarus* (Elapidae) Based on Morphological Characters. Journal of Herpetology 28: 440–446. https://doi.org/10.2307/1564956

Smith MA (1943) The Fauna of British India, Ceylon and Burma, Including the Whole of the Indo-Chinese Sub-Region. Reptilia and Amphibia. 3 (Serpentes). Taylor and Francis, London, 387–390.

Smits T, Hauser S (2019) First Record of the Krait *Bungarus slowinskii* Kuch, Kizirian, Nguyen, Lawson, Donelly and Mebs, 2005 (Squamata: Elapidae) from Thailand. Tropical Natural History 19: 43–50.

Stamatakis A (2014) RAxML version 8: a tool for phylogenetic analysis and post-analysis of large phylogenies. Bioinformatics 30: 1312–1313. https://doi.org/10.1093/bioinformatics/btu033

Tsai IH, Hsu HY, Wang YM (2002) A novel phospholipase A2 from the venom glands of *Bungarus candidus*: cloning and sequence-comparison. Toxicon 40(9): 1363–1367. https://doi.org/10.1016/S0041-0101(02)00150-2

Uetz P, Freed P, Hošek J [Eds] (2020) The Reptile Database. http://www.reptile-database.org [accessed on 3 November 2020]

Vogel G, David P, Pauwels OS (2004) A review of morphological variation in *Trimeresurus popeiorum* (Serpentes: Viperidae: Crotalinae), with the description of two new species. Zootaxa 727: 1–63. https://doi.org/10.11646/zootaxa.727.1.1

Voris H (2000) Maps of Pleistocene sea levels in Southeast Asia: shorelines, river systems and time durations. Journal of Biogeography 27: 1153–1167. https://doi.org/10.1046/j.1365-2699.2000.00489.x

Wall CF (1907) A new krait from Oudh (*Bungarus walli*). Journal of the Bombay Natural History Society 17: 608–611.

Wall F (1908) A popular treatise of the common Indian snakes. Part VIII. Journal of the Bombay Natural History Society 18: 711–735.

Whitaker R, Captain A (2004) Snakes of India. Draco Books, Chennai, 500 pp.

Williams DJ, Gutiérrez JM, Calvete JJ, Wüster W, Ratanabanangkoon K, Paiva O, Brown NI, Casewell NR, Harrison RA, Rowley PD, O'Shea M, Jensen SD, Winkel KD, Warrell DA (2011) Ending the drought: new strategies for improving the flow of affordable, effective antivenoms in Asia and Africa. Journal of Proteomics 74: 1735–1767. https://doi.org/10.1016/j.jprot.2011.05.027

Xie Y, Wang P, Zhong G, Zhu F, Liu Q, Che J, Shi L, Murphy RW, Guo P (2018) Molecular phylogeny found the distribution of *Bungarus candidus* in China (Squamata: Elapidae). Zoological Systematics 43: 109–117. https://doi.org/10.11865/zs.201810

Yang DT, Rao DQ (2008) Amphibia and Reptilia of Yunnan. Yunnan Science and Technology Press, Kuming, 343–352. [In Chinese]

Zhao EM (2006) Snakes of China. Anhui Science, Technology Publishing House, Hefei, 669 pp.

Zhao EM, Huang MH, Zong Y (1998) Fauna Sinica, Reptilia, Squamata. Serpentes (Vol. 3). Science Press, Beijing, 334–341.

Zhao EM, Yang DT (1997) Amphibians and Reptilies of the Hengduan Mountains Region. Science Press, Beijing, 290–293.

Appendix 1

Specimens examined for measurements and morphology; localities as originally stated

***B. caeruleus*.** (9 specimens). "Indes Orientalis" MNHN 7688. "Bengale" MNHN 3952, MNHN 7687. "Malabar" MNHN 7687. "Pondicheri" MNHN 7686. "Pakistan occ" MNHN 1962.239, MNHN 1962.236, MNHN 1962.238, MNHN 1962.237. "Birma" MNHN1893-413.

***B. ceylonicus*.** (1 specimens). "Sri Lanka" MNHN 4259 (1872-32).

***B. fasciatus*.** (1 specimens). "Bengkalis, Siak, Indonesia" RMNH 1667.

***B. candidus*.** (20 specimens). "Palembang, Sumatra, Indonesia" RMNH 11416. "Java, Indonesia" NMW 27730:2, NMW 27730:7, NMW 27730:3, NMW 27730:4; NMW 27740:5, NMW 27740:4, NMW 9486:4, NMW 9486:3, NMW 27730:5, NMW 27730:1, NMW 9486:1, NMW 9486:6, NMW 9486:5, NMW 9486:2, NMW 27711:1, NMW 27711:2, NMW 27711:3. "Johor, Malaysia" SYNU R180411. "Quang Binh, Vietnam" RH06153.

***B. multicinctus*.** China: (24 specimens). "Anhui, China" CIB 12209; "Chongqing, China" CIB 12215. "Fujian, China" CIB 12212, CIB 12204, CIB 12203, CIB 12207, CIB 12206, CIB 12205, CIB DL18090209, CIB DL18090210; "Guangdong, China" CIB 12191, CIB 12194; "Guangxi, China" CIB 12192, CIB 93924, CIB 93923, CIB 104228; "Zhejiang, China" CIB 12208; "Jiangxi, China" CIB 12210, CIB 12211; "Hainan, China" CIB 12197, SYNU R180305; "Guizhou, China" CIB 83793; "Hunan, China" CIB 12213, CIB 12214.

***B. wanghaotingi*.** China: (16 specimens). "Guangxi, China" CIB FCDZ20170806, CIB 104227. "Yunnan, China" CIB 12216, CIB 12201, CIB ML20170801, CIB MLMY20170801, CIB JCR36, CIB JCR36-2, CIB DL2019051401, CIB DL20190525, CIB DL2019070301, CIB DL20190522, CIB JCR2019062003, CIB JCR2019062311, CIB JCR2019061703, CIB JCR2019061807.

***B. suzhenae* sp. nov. China**. (4 specimens). "Yingjiang, Yunnan, China" CIB 116088–CIB 116091.

Specimens checked hemipenes:

***B. multicinctus*.** "Guangdong**,** China" CIB 12191. "Shangyou, Jiangxi, China" CIB 12211. "Nanning, Guangxi**,** China" CIB 104228. "Lishui, Zhejiang, China" CIB DL2019051701.

***B. wanghaotingi*. China.** "Luodian, Guizhou, China" CIB 83793. "Beiliu, Guangxi, China" CIB 104227. "Mengla, Yunnan**,** China" CIB MLML20170801.

***B. suzhenae* sp. nov.** "Yingjiang, Yunnan, China" CIB 116089.

B. candidus "Phong Nha-Ke Bang National Park Administration, Quang Binh Province, Vietnam" RH06153.

Supplementary material 1

Tables S1–S4

Authors: Ze-Ning Chen, Sheng-Chao Shi, Gernot Vogel, Li Ding, Jing-Song Shi

Data type: phylogenetic data

Explanation note: **Table S1.** DNA sequences used in this study. **Table S2.** Best evolution models of each partition combination. **Table S3.** Uncorrected p-distances between Bungarus species based on 1069 base pairs from the mitochondrial genes cyt b. **Table S4.** Uncorrected p-distances between Bungarus species based on 613 base pairs from the mitochondrial genes COI.

Link: https://doi.org/10.3897/zookeys.1025.62305.suppl1

ZooKeys 1025: 73–89 (2021)
doi: 10.3897/zookeys.1025.60972
https://zookeys.pensoft.net

RESEARCH ARTICLE

A peer-reviewed open-access journal
ZooKeys
Launched to accelerate biodiversity research

Effects of season and food on the scatter-hoarding behavior of rodents in temperate forests of Northeast China

Dianwei Li[1,2,3], Yang Liu[1], Hongjia Shan[1], Na Li[4], Jingwei Hao[1], Binbin Yang[1], Ting Peng[1], Zhimin Jin[1]

1 *College of Life Sciences and Technology, Mudanjiang Normal University, No. 191 Wenhua Road, Mudanjiang, Heilongjiang 157011, China* **2** *College of Wildlife and Protected Area, Northeast Forestry University, No. 26 Hexing Road, Harbin 150040, China* **3** *Heilongjiang Academy of Forestry, No. 134 Haping Road, Harbin, Heilongjiang 150081, China* **4** *Mudanjiang Medical School No. 5 Fangzhier Road, Mudanjiang, Heilongjiang 157009, China*

Corresponding authors: Zhimin Jin (swxjzm@126.com); Dianwei Li (lidianwei@mdjnu.edu.cn)

Academic editor: N. Cáceres | Received 21 November 2020 | Accepted 15 February 2021 | Published 18 March 2021

http://zoobank.org/B6988E41-62B3-4901-A516-6CEE26C46658

Citation: Li D, Liu Y, Shan H, Li N, Hao J, Yang B, Peng T, Jin Z (2021) Effects of season and food on the scatter-hoarding behavior of rodents in temperate forests of Northeast China. ZooKeys 1025: 73–89. https://doi.org/10.3897/zookeys.1025.60972

Abstract

To explore the differences in hoarding strategies of rodents for different seeds in various seasons, we labeled and released the seeds of *Pinus koraiensis*, *Corylus mandshurica*, *Quercus mongolica* and *Prunus sibirica* in temperate forests of Northeast China and investigated the fate of the seeds in spring and autumn. The analysis showed that the hoarding strategies of the rodents varied substantially between seasons. The seeds were consumed faster in the spring than in the autumn. More than 50% of the seeds in the two seasons were consumed by the 16th day. It took 36 days to consume 75% of the seeds in the spring and 44 days in the autumn. The rate of consumption of the seeds in the spring was greater than in the autumn, and the rate of spread of the seeds was greater in the autumn. The distances of removal for the consumption and dispersal of seeds in the spring (3.26 ± 3.21 m and 4.15 ± 3.52 m, respectively) were both shorter than those in the autumn (3.74 ± 3.41 m and 4.87 ± 3.94 m, respectively). In addition, the fate of different seeds varied significantly owing to differences in hoarding strategies. The seeds of the three preferred species, *P. koraiensis*, *C. mandshurica*, and *Q. mongolica*, were quickly consumed. More than 90% of the seeds of these species were consumed. Only 21% of *Pr. sibirica* seeds were slowly consumed, and the two

seasons had the same seed consumption rate patterns: the consumption rate of *P. koraiensis* seeds was the highest, followed by *C. mandshurica*, then *Q. mongolica*, and finally *Pr. sibirica*. The median removal times of the two seasons were different, but the rules were the same: *P. koraiensis* was the shortest, followed by *C. mandshurica*, and the third was *Q. mongolica*. In both seasons, the most predated *in situ* seeds were those of *P. koraiensis*; the most hoarded seeds were those of *C. mandshurica*, and the most unconsumed seeds were those of *Pr. sibirica*.

Keywords
Murids, rodents, scatter-hoarding, seed fate, seed dispersal, voles

Introduction

Rodents play an important role in the process of plant seed dispersal and regeneration (Hughes and Croy 1993; Vander Wall 2001; Vander Wall 2003; Lichti et al. 2015). Seed dispersal is a key link that affects plant regeneration, species survival and distribution (Vander Wall 2001; Vander Wall 2003; Lichti et al. 2015), and plays a vital role in forest ecosystems. The carrier behavior of animals determines the pattern of seed dispersal, which fundamentally affects the dynamics of vegetation populations and communities, and even forest ecosystems (Vander Wall 1990; Clayton et al. 2001; Vander Wall 2001; Briggs et al. 2009; Lichti et al. 2015). Rodents often dominate the local dynamics of forest regeneration, since they are the main scatter dispersers of plant seeds (Morán-López et al. 2016; Morán-López et al. 2018). This results in their role as an important seed disperser in forest ecosystems (Morán-López et al. 2015; Morán-López et al. 2018).

The hoarding behavior of rodents is a special type of feeding behavior; it is a vital adaptive strategy for many rodents during periods of food scarcity (Chang et al. 2010; Luna et al. 2016; Li et al. 2018, 2020). The hoarding behavior is affected by many factors, including the characteristics of plant seeds, yield, distribution, temporal and spatial changes of food resources, as well as seasonal changes in environmental factors, such as climate and habitat structure (Willson and Whelan 1990; Vander Wall 2001; Preston and Jacobs 2005; Jenkins 2011; Lichti et al. 2015; Morán-López et al. 2018; Li et al. 2018). The community structure and the quantity of rodents display obvious seasonal fluctuations in temperate regions, and the intensity of food hoarding activities also varies significantly in different seasons of the year (Vander Wall 1990). A reasonable allocation of limited food resources, an adjustment of the temporal and spatial abundance, and the use pattern of food help animals utilize hoarded resources to ensure their survival or reproductive activities during food shortages (Smith and Reichman 1984; Vander Wall 2001; Lu and Zhang 2005; Chang et al. 2010; Wang et al. 2012; Lichti et al. 2015; Luna et al. 2016). Food resources fluctuate greatly, particularly in the Northeast China in which the seasonal changes in the habitat environment are significant; the climatic environment changes are significantly, and the habitat conditions are unstable (Li et al. 2019 and 2020). Hoarding food is an important way to manage severe environments, effectively save predation time and energy consumption, and ensure that the rodents successfully survive the winter (Zhang et al. 2014; Li et al. 2018, 2020).

The Northeast China temperate zone is rich in forest vegetation resources and is an important resource of species and bank for seeds. Rodents not only damage forest resources by their predation on vegetation and seeds, but also promote the regeneration of vegetation by scatter-hoarding food (Vander Wall 2001; Vander Wall 2003; Lichti et al. 2015). *Pinus koraiensis* (Pinaceae), *Corylus mandshurica* (Betulaceae), *Quercus mongolica* (Fagaceae) and *Prunus sibirica* (Rosaceae) are common forest trees in the study area, and their seeds are the main food resources for rodents. In this study, four types of labeled seeds were released in the spring and autumn to investigate the predation, dispersal, and hoarding of seeds by rodents to understand the patterns of utilization of various seeds by rodents and the existing seasonal laws in the natural environment. Our goals were to provide theoretical and practical guidance to explore the interaction between rodents and many large-seed plants. We hypothesized the following: i) Because of the lack of food resources in the spring and abundance of seeds in the autumn, there are seasonal differences in seed dispersal, and seeds released in the spring will be consumed more quickly and in greater quantities than those released in the autumn; ii) to meet the different needs, more food is taken in the spring, and the amounts of dispersal and distance are greater in the autumn; and iii) rodents have predation preferences, and different seeds have various fates with the preferred seeds being consumed faster.

Site and methods

Study area and research site selection

The study was conducted from April to November, 2018. The research site was located in a forested area of the Sandao Forest Farm (44°40'N–44°45'N, 129°24'E–129°32'E, elevation 380 to 550 m), Mudanjiang City, located at the northern end of the Changbai Mountains in northeastern China, the east vein of the main ridge of the Zhangguangcai Mountain. The climate is a temperate and cold continental monsoon climate with four distinct seasons and a hot rainy season. The maximum temperature is 37 °C. The minimum temperature is -44.1 °C, and the annual average temperature is 2.3–3.7 °C. Approximately 100–160 days in the year are frost free. The first frost in most areas appears is in late September, and the last frost is in late April to early May. Precipitation is concentrated in June to September and varies from 400 mm to 800 mm.

The experiment was conducted in secondary coniferous and broad-leaved mixed forest that had been least disturbed. Common canopy tree species included *P. koraiensis*, *Q. mongolica*, *Larix gmelinii*, *Picea koraiensis*, *Abies nephrolepis*, *Betula platyphylla*, *Tilia amurensis*, *T. mandshurica*, *Juglans mandshurica*, while the brush included primarily *C. mandshurica*, *Lonicera maackii*, *Acanthopanax senticosus*, *Trichosanthes kirilowii*, and *Syringa reticulata.* The rodents in forests were highly abundant and diverse, largely dominated by different combinations of species, with *Apodemus peninsulae*, *A. agrarius*, and *Clethrionomys rufocanus* being the dominant species.

Tagging and tracking of seeds

Healthy seeds of *P. koraiensis*, *C. mandshurica*, *Q. mongolica*, and *Pr. sibirica* that had been selected in the field study experiment were tagged using an electric drill whose bit is 0.5 mm in diameter, to make a hole at one end of the seed. A thin red plastic sheet was cut into a 3 cm × 1 cm rectangular plastic plate (Xiao et al. 2006a; Hirsch et al. 2013), and a small hole was introduced into the middle of short side. A soft steel wire, 0.3 mm in diameter and 8 cm long, was used to connect the perforated seeds to the plastic plate and mark the seed category, sample number, and seed number on each tag. Based on experiments, after rodents ate the seeds or buried them in the ground, under dead branches, or in shallow caves, the tags would be exposed, which were convenient for positioning during studies. Rodents could not bite off the steel wire; therefore, this tagging method had no significant impact on their seed dispersal (Xiao et al. 2006b; Chang and Zhang 2011; Vander Wall and Beck 2011; Yi et al. 2012; Luna et al. 2016; Li et al. 2018)

Release and investigation of the seeds

Food release stations in the forest were randomly arranged and spaced more than 50 m apart. Each release station released 20 seeds of each type for a total of 80. There were 15 release stations in the spring with 300 seeds of each type, totaling 1200. There were 9 release stations in the autumn with 180 seeds of each type, totaling 720.

The study was conducted on days 1, 2, 3, 4, 6, 8, 12, 16, 20, 28, 36, 44, and 60 after release. The fate and characteristics and dispersal distance of the seeds were measured.

Definition of seed fate

The fate of the seeds released in the field experiment is defined as follows (Li and Zhang 2003; Pons and Pausas 2006; Yang et al. 2011; Li et al. 2018):

1. Intact *in situ* (IS): seeds not eaten or removed from the station
2. Predation *in situ* (PS): seed kernels eaten at the seed station
3. Predation after removal (PR): seed kernels eaten after removal
4. Intact after removal (IR): seeds not eaten and abandoned on the surface of ground after removal
5. Hoarded after removal (HR): seeds buried in the soil or humus layer after removal
6. Missing after removal (MR): seeds removed but not found
7. Consumption: With the exception of IS seeds, the fate of other seeds is defined as consumption by rodents.
8. Predation: PS and PR are defined as predation (PS + PR)
9. Dispersal: IR, HR, and MR are defined as dispersal. However, there were no data records for the survey indicators of the missing seeds, so they could not be calculated during the inspection and comparison (IR + HR + MR)

10. Median removal time (MRT) of the seeds: the time at which 50% of the seeds were removed (expressed in days), which was used to compare the seed removal rates in both types of vegetation.

Statistical analysis

All statistical analyses were conducted in SPSS 22.0 for Windows (IBM, Inc., Armonk, NY, USA). Before the data analysis, the data was tested for normality and equality of variance using the Kolmogorov-Smirnov and Homogeneity-of-variance tests. Data were treated with respective nonparametric tests depending on whether they met the assumptions of normality. A Cox regression was used to analyze the seed survival rates, factoring in both seasons' type and seeds. The Kruskal–Wallis H test (nonparametric) was used to compare the significant differences among the four seed species. The Mann–Whitney U test (nonparametric) was used to test the differences between the different seasons and different seed species. The data are represented as the mean ± SD. The values are considered statistically significant at $P < 0.05$.

Results

Seed survival curves

According to the analysis of the seed survival curve (Fig.1), the early seeds were mostly consumed quickly. And in general, the rate of consumption gradually decreased after the 20th day. Most seeds (*P. koraiensis*, *C. mandshurica*, and *Q. mongolica*) preferred by rodents were depleted over time, and most of the seeds not favored (*Pr. sibirica*) were IS. Therefore, when the curve survival ratio approached 20%, the curve flattened, and the trend of seed consumption became smaller.

According to the analysis of seed survival curves in different seasons (Fig. 1), the trends of consumption of seeds in the spring and autumn were the same, but the rates of consumption were different. The rate of consumption in the spring was faster than that in the autumn ($W = 32.395$, df = 1, $P < 0.001$). Most of the seeds of *Pr. sibirica* were not consumed, and the trend of consumption gradually slowed at approximately 20% of the curve.

According to the analysis of survival curves of four types of seeds in the spring and autumn (Fig. 2), the consumption rates of different seeds varied. The three types of seeds from *P. koraiensis*, *C. mandshurica*, and *Q. mongolica* had similar trends of consumption, but the rates of consumption were different (Spring: $W = 43.215$, df = 2, $P < 0.001$; Autumn: $W = 31.710$, df = 2, $P < 0.001$), with *Pr. sibirica* seed consumption being slow. The consumption rate laws of the four types of seeds in the two seasons is as follows. The consumption rate of *P. koraiensis* was the highest, followed by *C. mandshurica*, then *Q. mongolica*, and finally *Pr. sibirica*. (Spring: $W = 259.542$, df = 3, $P < 0.001$; Autumn: $W = 114.104$, df = 3, $P < 0.001$).

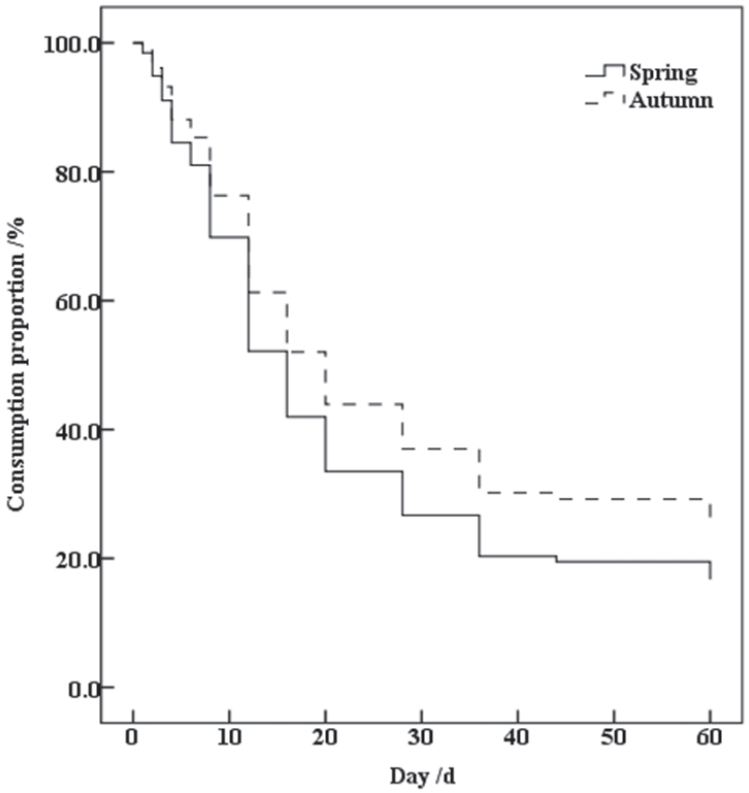

Figure 1. The total survival curve of the all seeds of *Pinus koraiensis*, *Corylus mandshurica*, *Quercus mongolica* and *Prunus sibirica* in the spring and autumn in temperate forests of Northeast China.

Seed consumption time of the rodents

There were no differences in the average time of the earliest food discovery between the two seasons (Z = -0.508, P > 0.05). After the animals found the seeds, they chose different ones based on their preferences and performed different operations, resulting in various fates of the seeds. The sequences of the earliest consumption time of seeds in the spring and autumn were both as follows: *C. mandshurica* was the earliest, followed by *P. koraiensis*, then *Q. mongolica*, and finally *Pr. sibirica*. There were no differences in the earliest consumption time among *P. koraiensis*, *C. mandshurica*, and *Q. mongolica* in different seasons (spring: χ^2 = 1.140, P > 0.05; autumn: χ^2 = 0.634, P > 0.05). The earliest time of consumption of *Pr. sibirica* was significantly later than that of the other types of seeds in the spring and autumn (all P < 0.05) (Table 1) .

Median removal time (MRT) of the seeds

When the seed species were not distinguished, the MRT was around the 16th day. Seventy percent of the seeds were consumed at approximately the 36th day, and 18.08% of

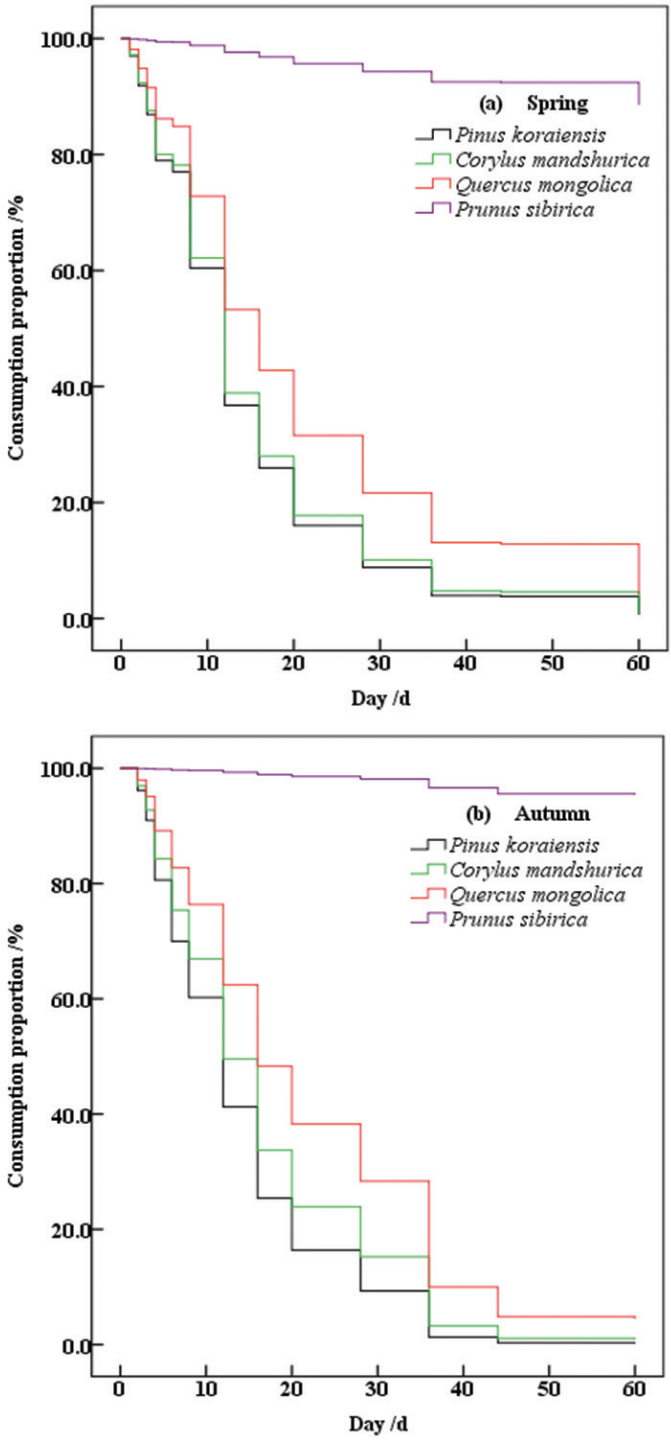

Figure 2. The survival curve of the four types of seeds of *Pinus koraiensis*, *Corylus mandshurica*, *Quercus mongolica* and *Prunus sibirica* respectively in spring and autumn in temperate forests of Northeast China

Table 1. The earliest discovery time and consumption time of the different seeds in spring and autumn in temperate forests of Northeast China. The different superscript letters represent significant differences from each other ($P < 0.05$), based on Mann–Whitney U testing differences in the earliest discovery time between the spring and autumn, based on Kruskal–Wallis H testing differences in the earliest consumption time among the four seed species.

Season	Earliest discovery time (range; day)	Earliest consumption time (range; day)			
		P. koraiensis	*C. mandshurica*	*Q. mongolica*	*Pr. sibirica*
Spring	7.2 ± 8.8 (1–36)[a]	10.7 ± 13.8 (1–60[b])b	9.4 ± 13.0 (1–60)[b]	9.6 ± 7.9 (1–[6]0)b	75.4 ± 38.1 (6–108[c])c
Autumn	5.8 ± 3.8 (2–12)[a]	10.3 ± 8.1 (2–28[b])b	9.1 ± 7.87 (3–28)[b]	11.1 ± 7.0 (4–20)[b]	70.7 ± 33.9 (12–92)[c]

Table 2. Median time of removal of the different seeds in spring and autumn in temperate forests of Northeast China. The same superscript letters represent nonsignificance ($P > 0.05$), based on Mann–Whitney U testing differences in MRT between the spring and autumn, based on Kruskal–Wallis H testing differences in MRT among the three seed species.

Season	Median removal time (day)			
	P. koraiensis	*C.mandshurica*	*Q. mongolica*	*Pr. sibirica*
Spring	13.6 ± 12.[9]a	14.4 ± 14.0[a]	18.5 ± 10.1[a]	–
Autumn	10.3 ± 8.1[a]	13.8 ± 7.0[a]	18.7 ± 12.4[a]	–

the seeds were still unconsumed after the 90th day (Fig. 1). *Pr. sibirica* comprised 90.46% of the unconsumed seeds. A statistical analysis of the data (Table 2, Fig. 2) indicated that the MRT was on the 16th day in the spring and autumn, and it took time for 75% of the seeds to be consumed. This did not happen until the 36th day in spring and the 44th day in autumn. However, the differences in MRT between spring and autumn were nonsignificant ($Z = -0.074$, $P > 0.05$). The times for 50% of the seeds to be consumed varied for different seeds. Spring and autumn showed the same pattern: *P. koraiensis* had the shortest time, followed by *C. mandshurica*, while *Q. mongolica* had the longest time. However, there was no significant difference between the three types of seeds (Spring: $\chi^2 = 4.480$, $P > 0.05$; Autumn: $\chi^2 = 3.089$, $P > 0.05$). The rates of consumption of the *Pr. sibirica* seeds did not exceed 50% during the spring and autumn studies. The autumn study led to the discovery that some of the *Pr. sibirica* seeds released in the spring remained at the seed station. The consumption curve estimated that the time when 50% of the *Pr. sibirica* seeds were consumed should exceed 150 d (Fig. 2).

Seed removal time

Less than 100% of the seeds were consumed during the study. Therefore, the average removal time of the three types of seeds (*P. koraiensis*, *C. mandshurica* and *Q. mongolica*) was estimated based on the survey data of the seed station after predation (Table 3). The latest time of *Q. mongolica* removal was significantly later than that of *P. koraiensis* in the spring ($Z = -2.283$, $P < 0.05$), while there was no difference for *C. mandshurica* ($Z = -1.395$, $P > 0.05$). The latest time of *Q. mongolica* removal was significantly later than those of *P. koraiensis* ($Z = -3.446$, $P < 0.001$) and *C. mandshurica* ($Z = -2.650$, $P < 0.01$) in the autumn.

Table 3. The latest consumption time of the different seeds in spring and autumn in temperate forests of Northeast China. The different superscript letters represent significant differences from each other ($P < 0.05$), based on Mann–Whitney U testing differences in the latest consumption time between the spring and autumn, based on Kruskal–Wallis H testing differences in the latest consumption time among the three seed species.

Season	The latest consumption time (range; day)			
	P. koraiensis	*C. mandshurica*	*Q. mongolica*	*Pr. sibirica*
Spring	18.3 ± 12.5(2–60)^{a}	22.1 ± 17.0(4–76)^{ab}	28.5 ± 17.7(12–76)^{b}	–
Autumn	17.3 ± 7.2(8–28)^{a}	24.0 ± 12.8(4–44)^{a}	46.7 ± 17.9(28–76)^{b}	–

Seed fate

Different seeds had varied fates, and the seasonal differences in the seed fates were significant. More seeds were consumed in the spring than in the autumn. With the exception of *Pr. sibirica* seeds, the rates of consumption of the seeds of the other three species all exceeded 90%. In the spring, the rate of consumption of *P. koraiensis* seeds reached 99.56%, *C. mandshurica* seeds 100%, and *Q. mongolica* seeds 92.35%. In the autumn, the rate of consumption of *P. koraiensis* seeds reached 99.44%, *C. mandshurica* seeds 99.44%, and *Q. mongolica* seeds 97.22%. The rates of consumption of *Pr. sibirica* seeds in the spring and autumn were 21.0% and 3.33%, respectively (Fig. 3)

In the spring, the proportions of seeds that were intact *in situ* (IS), predation *in situ* (PS), predation after removal (PR), intact after removal (IR), hoarded after removal (HR), and missing after removal (MR) were 14.20%, 41.52%, 13.59%, 1.45%, 11.07% and 18.17%, respectively. In the autumn, the proportions of seeds with corresponding fates were 25.14%, 8.47%, 7.92%, 5.28%, 19.58% and 33.61%, respectively (Fig. 4). The unconsumed seeds were primarily *Pr. sibirica* (comprising 84.95% in the spring and 96.13% in the autumn). *P. koraiensis* accounted for the most predation *in situ* seeds (57.90% in the spring and 44.26% in the autumn), followed by *Q. mongolica* (31.62% in the spring and 34.43% in the autumn). *C. mandshurica* had the largest proportion among the hoarded seeds (64.17% in the spring and 46.10% in the autumn) (Fig. 5).

The total predation rate of seeds was higher in the spring (55.11%) than in the autumn (16.39%). The total seed dispersal rate of seeds was higher in the autumn (58.47%) than in the spring (30.69%) (Fig. 5). This pattern was also evident in the three types of seeds of *P. koraiensis*, *C. mandshurica*, and *Q. mongolica*. In the spring, the predation rate of *P. koraiensis*, *C. mandshurica*, and *Q. mongolica* was 80.0%, 30.38%, and 67.94%, respectively, and the dispersal rate was 19.56%, 60.32%, and 24.41%, respectively. In the autumn, the predation rate of *P. koraiensis*, *C. mandshurica*, and *Q. mongolica* was 16.67%, 12.77%, and 35.56%, respectively, and the dispersal rate was 82.77%, 86.67%, and 61.66%, respectively (Fig. 6).

Transport distance of predation after removal

The transport distances of seeds by PR in the spring and autumn were 3.26 ± 3.21 m and 3.74 ± 3.41 m, respectively, with no significant difference ($Z = -1.276$, $P = 0.202 > 0.05$).

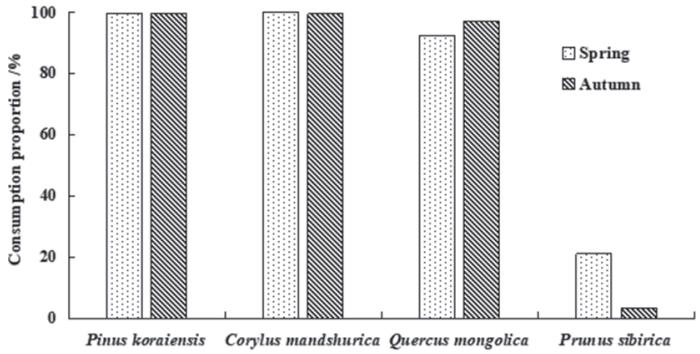

Figure 3. The consumption proportion of the four types of seeds in spring and autumn in temperate forests of Northeast China.

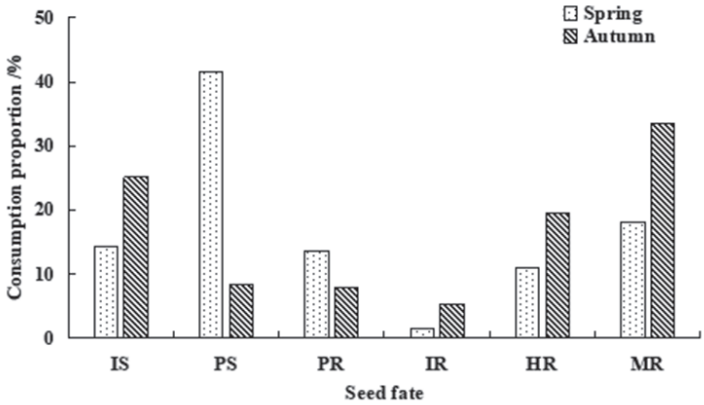

Figure 4. Statistics of the fate of seeds in the spring and autumn in temperate forests of Northeast China. Abbreviations: IS–Intact *in situ*, PS–Predation *in situ*, PR–Predation after removal, IR–Intact after removal, HR–Hoarded after removal, MR–Missing after removal.

The three species of seeds *P. koraiensis* (3.51 ± 3.25 m in the spring, 3.30 ± 2.03 m in the autumn), *C. mandshurica* (3.17 ± 2.91 m in the spring, 3.88 ± 2.19 m in the autumn), *Q. mongolica* (2.72 ± 3.37 m in the spring, 3.74 ± 3.76 m in the autumn) showed no seasonal differences in the transport distances of PR. *Pr. sibirica* seeds (7.73 ± 3.36 m in the spring) showed no PR of data records during the autumn study.

Dispersal distance

The seed dispersal distances in the spring and autumn were 4.15 ± 3.52 m and 4.87 ± 3.94 m, respectively, and the dispersal distance in the spring was significantly shorter than that in the autumn (Z = -2.008, P < 0.05). The dispersal distance of *P. koraiensis*

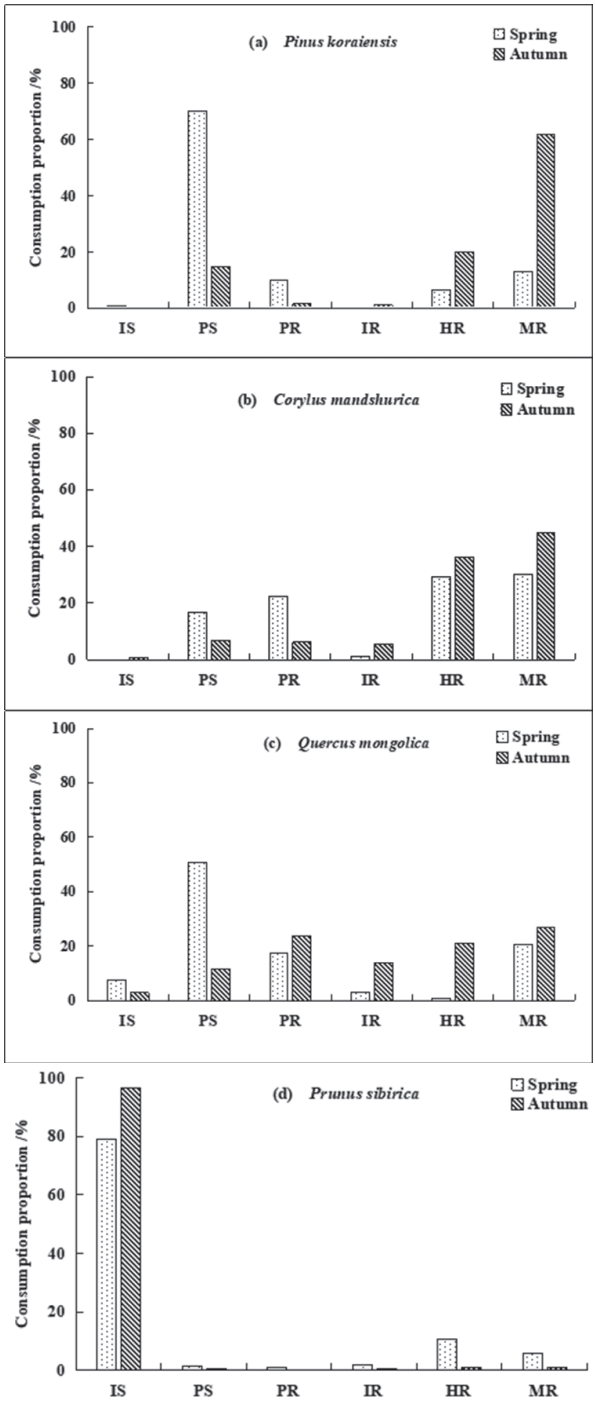

Figure 5. Statistics on the fate of the four types of seeds combined in spring and autumn in temperate forests of Northeast China. Abbreviations: IS–Intact *in situ*, PS–Predation *in situ*, PR–Predation after removal, IR–Intact after removal, HR–Hoarded after removal, MR–Missing after removal.

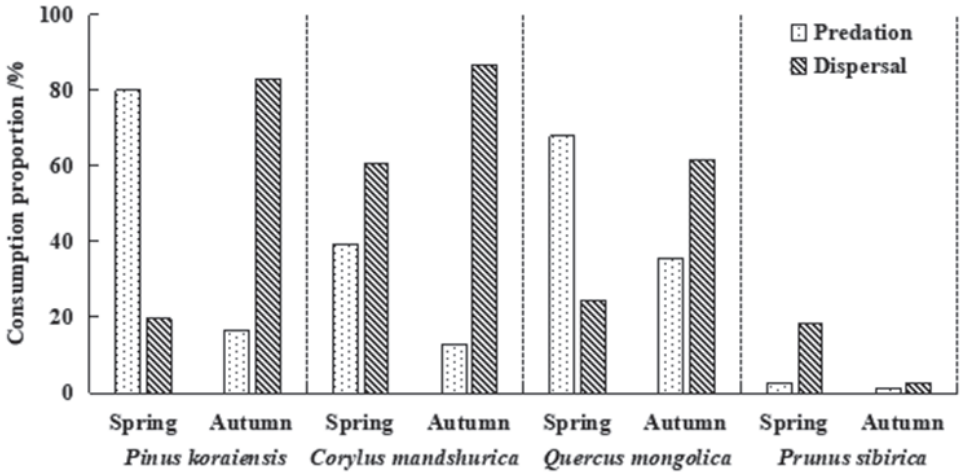

Figure 6. Predation rate and dispersal rate of four kinds of seeds combined in spring and autumn in temperate forests of Northeast China.

seeds was significantly greater than that of the other three types (χ^2 = 24.975, P < 0.001), and there was a difference between the other three types (all P > 0.05). The dispersal distance of *P. koraiensis* seeds in the spring (3.89 ± 2.05 m) was significantly shorter than that in the autumn (7.97 ± 5.33 m) (Z = -3.762, P < 0.001). *C. mandshurica* seeds (4.42 ± 3.72 m in the spring, and 4.12 ± 2.49 m in the autumn), *Q. mongolica* seeds (6.16 ± 6.27 m in the spring, 3.69 ± 3.31 m in the autumn) and *Pr. sibirica* seeds (2.29 ± 1.50 m in the spring, 3.18 ± 2.66 m in the autumn) showed no seasonal differences in the diffusion distances (all P > 0.05). The dispersal distances of seeds were greater than the transport for predation distances (all P < 0.05).

Discussion

Seasonal differences in the food hoarding strategies of rodents

Some studies have shown that feeding and hoarding behavior of rodents had significant seasonal differences and were seen as an adaptation strategy in response to seasonal changes in food and the environment in Northeast China (Li et al. 2020). Our results about survival curves, consumption time, MRT, removal time and fate of seeds also indicated that the hoarding strategies of rodents varied substantially between seasons. For example, seeds were consumed faster and the rate of consumption of seeds was greater in the spring than in the autumn, however, the rate of spread of seeds was greater in the autumn than in the spring. The availability of food resources serves as the core factor that affects predation strategy, so dynamic hoarding strategy is an adaptation to changes in food resources and food quality (Vander Wall 1995; Vander Wall 2001;

Chang et al. 2010; Lichti et al. 2015). Consequently, the rodent's own demands show seasonal changes.

In response to the seasonal changes and the impacts on food resources, coupled with the north temperate climate, some rodents showed different requirements to meet different life activities at different times (Li et al. 2018). In the spring, the seed intake is greater, and the food is consumed faster, reflecting the crucial importance of obtaining food resources as soon as possible to supplement energy in the spring. This type of countermeasure is an important guarantee for survival, so that the rodents can readily enter the summer season with abundant resources and a favorable environment. In the autumn, food abundance weakens the predation strategy, but the dispersal is greater, indicating that more food must be hoarded to survive the winter successfully. These are the adaptation strategies of animals to the seasonal changes in food and environment, which are meaningful for their current and future survival and reproduction (Vander Wall 1990; Vander Wall 2001; Murray et al. 2006; Chang et al. 2010; Lichti et al. 2015).

Earlier results indicated that environment temperature has an important effect on changes in the activity behavior in rodents, with rodent species adjusting their foraging times and activities in response to changes in temperature (Corp et al. 1997; Li et al. 2020). The temperature is similar in the spring (April–May, 1–21°C) and autumn (September–October, 0–21°C) in the research area in 2018. However, the trend of temperature change is the opposite. Seasonal temperature changes send a strong signal to rodents, inducing different predation and hoarding behavior strategies (Corp et al. 1997; Li et al. 2020). The temperature gradually increased after April, rodents began spending more time on feeding activities. On the contrary, when temperatures began to cool after September, some rodents began spending more time on scatter-hoarding activities, suggesting that they were storing food in order to successfully overwinter (Vander Wall 2001; Chang et al. 2010; Lichti et al. 2015; Li et al. 2020).

Differences in the selection of seeds by rodents

The differences in seed characteristics and the animal's needs will affect the hoarding behavior of animals, which manifests as preference for food selection (Takahashi and Shimada 2008; Xiao et al. 2009; Ribeiro and Vieira 2016). Small animals have higher requirements for food quality, and food selectivity is more obvious (Fortin et al. 2004; Courant and Fortin 2012). The selection preference of rodents for seeds is the result of co–evolution between animals and plants. Seeds attract animals through morphological characteristics and nutritional components and induce animals to predate on, disperse, or hoard them, forming a mutually beneficial relationship (Vander Wall 1990; Vander Wall 2001; Chang et al. 2010; Zhang et al. 2014; Lichti et al. 2015). The four types of seeds used in the experiment induced differences in the predation and hoarding strategies of the rodents, such as more predation on *P. koraiensis* and *Q. mongolica* seeds, the more hoarding of *C. mandshurica* seeds, and a lack of selection of most *Pr. sibirica* seeds (Li et al. 2019). According to the Handling Costs hypothesis (Vander Wall 2010;

Vander Wall and Beck 2011), seeds of *Q. mongolica* and *P. koraiensis*, which have higher contents of starch and fat, are prioritized to obtain the greatest energy benefits (Wang and Chen 2012; Li et al. 2018). *C. mandshurica* also has a high fat content, but the seed shell is thick and hard; the processing takes longer, and the cost, and risk of predation will increase. Therefore, hoarding is the optimal strategy. Moreover, *C. mandshurica* does not easily become moldy or be infested by moths, and it is more suitable for long-term hoarding than *Q. mongolica* (Vander Wall 2001; Yu et al. 2001). Therefore, the amount of *C. mandshurica* dispersed is the highest (60.32% in the spring, 86.67% in the autumn) in both the spring and autumn. *Pr. sibirica* has a small amount of predation and dispersal, indicating that there are some key factors that cause animal rejection. We hypothesize that it may be caused by the amygdalin compounds contained in almonds. This hypothesis requires an in–depth study. Different seeds vary in their diffusion distances, which is another type of selection difference exhibited by the rodents for different seed characteristics.

Conclusions

Rodents change their predation and hoarding behavior strategies based on different seasons and foods. These animals adopt different foraging strategies so that the consumption of seeds has obvious seasonal differences. Food resources are scarce in the spring, and rodents spend more time foraging than in the autumn. Spring seeds are consumed in greater numbers and more quickly than in the autumn. In the spring, to meet the immediate demand for a supply of energy, rodents predate on more seeds. In the autumn, the abundance of seeds increases. To ensure the necessary food demand for winter survival, rodents disperse more seeds to different locations for hoarding, and the dispersal distance is relatively larger. For different seeds distributed in the same region, rodents will identify and judge the characteristics of the seeds, resulting in various fates for the seeds. Handling seeds in different ways leads to obvious predation preferences, and usually seeds that are rich in nutrients and easily handled are prioritized. Seeds with hard and thick seed coats are hoarded the most intensively.

Acknowledgements

This research was supported by the Innovation Research Project of Mudanjiang Normal University (GP2019004), the Natural Science Foundation of Heilongjiang Province of China (LH2020C071), the Doctoral Research Fund of Mudanjiang Normal University (MNUB201907) and the Undergraduate Innovation and Entrepreneurship Training Program (202010233012). We thank Zhulin Han, Man Jiang and LEXIS (Scientific editorial experts, United States, LEXIS Academic Service, LLC) for its linguistic assistance during the preparation of this manuscript.

References

Briggs JS, Vander Wall SB, Jenkins SH (2009) Forest rodents provide directed dispersal of Jeffrey pine seeds. Ecology 90: 675–687. https://doi.org/10.1890/07-0542.1

Chang G, Xiao Z, Zhang Z (2010) Effects of burrow condition and seed handling time on hoarding strategies of Edward's long–tailed rat (*Leopoldamys edwardsi*). Behavioural Processes 85: 163–166. https://doi.org/10.1016/j.beproc.2010.07.004

Chang G, Zhang Z (2011) Differences in hoarding behaviors among six sympatric rodent species on seeds of oil tea (*Camellia oleifera*) in Southwest China. Acta Oecologica 37: 165–169. https://doi.org/10.1016/j.actao.2011.01.009

Clark DA, Clark DB (1984) Spacing dynamics of a tropical rain forest tree: evaluation of the Janzen-Connell model. The American Naturalist 124: 769–788. https://doi.org/10.1086/284316

Clayton NS, Yu KS, Dickinson A (2001) Scrub jays (*Aphelocoma coerulescens*) form integrated memories of the multiple features of caching episodes. Journal of Experimental Psychology Animal Behavior Processes 27: 17–29. https://doi.org/10.1037/0097-7403.27.1.17

Courant S, Fortin D (2012) Search efficiency of free–ranging plains bison for optimal food items. Animal Behaviour 84: 1039–1049. https://doi.org/10.1016/j.anbehav.2012.08.003

Corp N, Gorman ML, Speakman JR (1997) Ranging behaviour and time budgets of male wood mice *Apodemus sylvaticusin* different habitats and seasons. Oecologia 109: 242–250. https://doi.org/10.1007/s004420050079

Fortin D, Boyce MS, Merrill EH, Fryxell JM (2004) Foraging costs of vigilance in large mammalian herbivores. Oikos 107: 172–180. https://doi.org/10.1111/j.0030-1299.2004.12976.x

Gómez JM, Puerta–Piñero C, Schupp EW (2007) Effectiveness of rodents as local seed dispersers of Holm oaks. Oecologia 155: 529–537. https://doi.org/10.1007/s00442-007-0928-3

Hirsch BT, Kays R, Jansen PA (2013) Evidence for cache surveillance by a scatter–hoarding rodent. Animal Behaviour 85: 1511–1516. https://doi.org/10.1016/j.anbehav.2013.04.005

Hughes RN, Croy MI (1993) An experimental analysis of frequency–dependent predation (Switching) in the 15–Spined Stickleback, Spinachia spinachia. The Journal of Animal Ecology 62: 341–352. https://doi.org/10.2307/5365

Jenkins SH (2011) Sex differences in repeatability of food–hoarding behaviour of kangaroo rats. Animal Behaviour 81: 1155–1162. https://doi.org/10.1016/j.anbehav.2011.02.021

Li DW, Jin ZM, Yang CY, Yang CW, Zhang MH (2018) Scatter–hoarding the seeds of sympatric forest trees by *Apodemus peninsulae* in a temperate forest in northeast China. Polish Journal of Ecology 66: 382–394. https://doi.org/10.3161/15052249PJE2018.66.4.006

Li DW, Hao JW, Yao X, Liu Y, Peng T, Jin ZM, Meng FX (2020) Observations of the foraging behavior and activity patterns of the Korean wood mouse, *Apodemus peninsulae*, in China, using infra-red cameras. ZooKeys 992: 139–155. https://doi.org/10.3897/zookeys.992.57028

Li HJ, Zhang ZB (2003) Effect of rodents on acorn dispersal and survival of the Liaodong oak (*Quercus liaotungensis* Koidz.). Forest Ecology and Management 176: 387–396. https://doi.org/10.1016/S0378-1127(02)00286-4

Lichti NI, Steele MA, Swihart RK (2015) Seed fate and decision–making processes in scatter-hoarding rodents. Biological Reviews 92: 474–504. https://doi.org/10.1111/brv.12240

Lima SL (1998) Stress and decision making under the risk of predation: recent developments from behavioral, reproductive, and ecological perspectives. Elsevier 27: 215–290. https://doi.org/10.1016/S0065-3454(08)60366-6

Lu J, Zhang Z (2005) Food hoarding behaviour of large field mouse *Apodemus peninsulae*. Acta Theriologica 50: 51–58. https://doi.org/10.1007/BF03192618

Luna CA, Loayza AP, Squeo FA (2016) Fruit size determines the role of three scatter–hoarding rodents as dispersers or seed predators of a fleshy–fruited Atacama Desert Shrub. PLoS ONE 11: e0166824. https://doi.org/10.1371/journal.pone.0166824

Morán–López T, Fernández M, Alonso CL, Flores-Rentería D, Valladares F, Díaz M (2015) Effects of forest fragmentation on the oak-rodent mutualism. Oikos 124: 1482–1491. https://doi.org/10.1111/oik.02061

Morán–López T, Valladares F, Tiribelli F, Pérez–Sepúlveda JE, Traveset A, Díaz M (2018) Fragmentation modifies seed trait effects on scatter–hoarders' foraging decisions. Plant Ecology 219: 325–342. https://doi.org/10.1007/s11258-018-0798-2

Morán-López T, Wiegand T, Morales JM, Valladares F, Díaz M (2016) Predicting forest management effects on oak-rodent mutualisms. Oikos 125: 1445–1457. https://doi.org/10.1111/oik.02884

Murray AL, Barber AM, Jenkins SH, Longland WS (2006) Competitive environment affects food-hoarding behavior of Merriam's kangaroo rats (*Dipodomys merriami*). Journal of Mammalogy 87: 571–578. https://doi.org/10.1644/05-MAMM-A-172R1.1

Pons J, Pausas JG (2006) Rodent acorn selection in a Mediterranean oak landscape. Ecological Research 22: 535–541. https://doi.org/10.1007/s11284-006-0053-5

Preston SD, Jacobs LF (2005) Cache Decision Making: The Effects of Competition on Cache Decisions in Merriam's Kangaroo Rat (*Dipodomys merriami*). Journal of Comparative Psychology 119: 187–196. https://doi.org/10.1037/0735-7036.119.2.187

Ribeiro JF, Vieira EM (2016) Microhabitat selection for caching and use of potential landmarks for seed recovery by a neotropical rodent. Journal of Zoology 300: 274–280. https://doi.org/10.1111/jzo.12380

Smith CC, Reichman OJ (1984) The evolution of food caching by birds and mammals. Annual Review of Ecology & Systematics 15: 329–351. https://doi.org/10.1146/annurev.es.15.110184.001553

Takahashi A, Shimada T (2008) Selective consumption of acorns by the Japanese wood mouse according to tannin content: a behavioral countermeasure against plant secondary metabolites. Ecological Research 23: 1033–1038. https://doi.org/10.1007/s11284-008-0473-5

Vander Wall SB (1990) Food Hoarding in Animals. University of Chicago Press, 445 pp.

Vander Wall SB (1995) Sequential patterns of scatter hoarding by yellow pine chipmunks (*Tamias amoenus*). American Midland Naturalist 133: 312–321. https://doi.org/10.2307/2426396

Vander Wall SB (2001) The evolutionary ecology of nut dispersal. The Botanical Review 67: 74–117. https://doi.org/10.1007/BF02857850

Vander Wall SB (2003) Effects of seed size of wind–dispersed pines (*Pinus*) on secondary seed dispersal and the caching behavior of rodents. Oikos 100: 25–34. https://doi.org/10.1034/j.1600-0706.2003.11973.x

Vander Wall SB (2010) How plants manipulate the scatter-hoarding behaviour of seed-dispersing animals. Philosophical Transactions of the Royal Society of London 365: 989–997. https://doi.org/10.1098/rstb.2009.0205

Vander Wall SB, Beck MJ (2011) A comparison of frugivory and scatter–hoarding seed–dispersal syndromes. The Botanical Review 78: 10–31. https://doi.org/10.1007/s12229-011-9093-9

Wang B, Chen J (2012) Effects of fat and protein levels on foraging preferences of tannin in scatter-hoarding rodents. PLoS ONE 7: e40640. https://doi.org/10.1371/journal.pone.0040640

Wang B, Ye C-X, Cannon CH, Chen J (2012) Dissecting the decision making process of scatter-hoarding rodents. Oikos 122: 1027–1034. https://doi.org/10.1111/j.1600-0706.2012.20823.x

Willson MF, Whelan CJ (1990) Variation in postdispersal survival of vertebrate-dispersed seeds: effects of density, habitat, location, season, and species. Oikos 57: 191–198. https://doi.org/10.2307/3565939

Xiao Z, Gao X, Steele MA, Zhang Z (2009) Frequency-dependent selection by tree squirrels: adaptive escape of nondormant white oaks. Behavioral Ecology 21: 169–175. https://doi.org/10.1093/beheco/arp169

Xiao Z, Jansen PA, Zhang Z (2006a) Using seed-tagging methods for assessing post-dispersal seed fate in rodent–dispersed trees. Forest Ecology and Management 223: 18–23. https://doi.org/10.1016/j.foreco.2005.10.054

Xiao Z, Wang Y, Harris M, Zhang Z (2006b) Spatial and temporal variation of seed predation and removal of sympatric large-seeded species in relation to innate seed traits in a subtropical forest, Southwest China. Forest Ecology and Management 222: 46–54. https://doi.org/10.1016/j.foreco.2005.10.020

Yang Y, Yi X, Yu F (2011) Repeated radicle pruning of Quercus mongolica acorns as a cache management tactic of Siberian chipmunks. Acta Ethologica 15: 9–14. https://doi.org/10.1007/s10211-011-0102-0

Yi X, Yang Y, Curtis R, Bartlow AW, Agosta SJ, Steele MA (2012) Alternative strategies of seed predator escape by early-germinating oaks in Asia and North America. Ecology and Evolution 2: 487–492. https://doi.org/10.1002/ece3.209

Yu X, Zhou H, Luo T, He J, Zhang Z (2001) Insect infestation and acorn fate in *Quercus liaotungensis*. Acta Entomologica Sinica 44: 518–524

Zhang YF, Wang C, Tian SL, Lu JQ (2014) Dispersal and hoarding of sympatric forest seeds by rodents in a temperate forest from northern China. iForest–Biogeosciences and Forestry 7: 70–74. https://doi.org/10.3832/ifor1032-007

ZooKeys 1025: 91–137 (2021)
doi: 10.3897/zookeys.1025.57806
https://zookeys.pensoft.net

MONOGRAPH

A peer-reviewed open-access journal
ZooKeys
Launched to accelerate biodiversity research

Revision of the southern Andean genus *Sadocus* Sørensen, 1886 (Opiliones, Gonyleptidae, Pachylinae)

Marília Pessoa-Silva[1], Marcos Ryotaro Hara[2], Ricardo Pinto-da-Rocha[1]

1 *Departamento de Zoologia, Instituto de Biociências, Universidade de São Paulo, São Paulo, São Paulo, Brazil*
2 *Escola de Artes, Ciências e Humanidades, Universidade de São Paulo, Av. Arlindo Béttio, 1000, Ermelino Matarazzo, 03828-000, São Paulo, SP, Brazil*

Corresponding author: Marília Pessoa-Silva (marilia.pessoasilva@gmail.com)

Academic editor: G. Giribet | Received 27 August 2020 | Accepted 11 February 2021 | Published 22 March 2021

http://zoobank.org/231B6931-2787-496E-B6B4-B87D59F5AC02

Citation: Pessoa-Silva M, Hara MR, Pinto-da-Rocha R (2021) Revision of the southern Andean genus *Sadocus* Sørensen, 1886 (Opiliones, Gonyleptidae, Pachylinae). ZooKeys 1025: 91–137. https://doi.org/10.3897/zookeys.1025.57806

Abstract

Species of the genus *Sadocus* Sørensen, 1886 are conspicuous gonyleptids that occur in Chile and Argentina. Here, the genus is revised for the first time and the cladistic analysis based on morphological characters does not corroborate its monophyly unless a phylogenetically unrelated species is excluded (explained further on). A new classification is proposed for the seven species left in the genus and considered valid, of the 13 nominal species previously recognized. Two out of the seven valid species are considered as species inquirendae: *Sadocus allermayeri* (Mello-Leitão, 1945) [= *Carampangue allermayeri* Mello-Leitão, 1945] and *Sadocus nigronotatus* (Mello-Leitão, 1943) [= *Carampangue nigronotatum* Mello-Leitão, 1943]. The following synonymies are proposed: *Sadocus bicornis* (Gervais, 1849) [original combination = *Gonyleptes bicornis* Gervais, 1849] is a junior synonym of *Sadocus asperatus* (Gervais, 1847) [= *Gonyleptes asperatus* Gervais, 1847]; *Sadocus conspicillatus* Roewer, 1913, *Sadocus exceptionalis* (Mello-Leitão, 1946) [= *Araucanoleptes exceptionalis* Mello-Leitão, 1946] and *Sadocus guttatus* Sørensen, 1902 are junior synonyms of the valid name *Sadocus polyacanthus* (Gervais, 1847) [= *Gonyleptes polyacanthus* Gervais, 1847]; and *Sadocus calcar* (Roewer, 1913) [= *Lycomedes calcar* Roewer, 1913] is a junior synonym of the valid name *Gonyleptes horridus* Kirby, 1819. *Sadocus brasiliensis* Soares & Soares, 1949 is not congeneric with Argentinean/Chilean species of the genus according to the cladistic analysis and is here synonymized with *Discocyrtus catharinensis* (Mello-Leitão, 1923 [= *Sadocus catharinensis* Mello-Leitão, 1923]).

Keywords

Argentina, Chile, harvestmen

Introduction

Harvestman systematics has advanced greatly in the last few decades, especially in the Neotropical region, with many supraspecific groups being recently revised, such as for example Stygnidae Simon, 1879 (Pinto-da-Rocha 1997), Sodreaninae Soares & Soares, 1985 (Pinto-da-Rocha and Bragagnolo 2010), Goniosomatinae Mello-Leitão, 1935 (DaSilva and Gnaspini 2010), Hernandariinae Sørensen, 1884 (DaSilva and Pinto-da-Rocha 2010), among others. Gonyleptidae Sundevall, 1833, the largest Neotropical family in number of species, includes two taxonomically challenging and species-rich subfamilies pending revision: Gonyleptinae Sundevall, 1833 and Pachylinae Sørensen, 1884. The lack of revisions is possibly due to the considerable number of species and their great morphological variation.

Pachylinae is the most species-rich subfamily of Gonyleptidae, and is currently considered polyphyletic (Pinto-da-Rocha 2002; Pinto-da-Rocha et al. 2014; Benavides et al. 2021). A phylogenetic analysis, based on molecular data (Pinto-da-Rocha et al. 2014), recovered a clade including *Pachylus* Koch (1839), the type genus of the subfamily. This clade was named Pachylinae sensu stricto and includes mainly Chilean species. This result was the first step towards the dismemberment of this large subfamily into smaller monophyletic units.

The sister group of Pachylinae sensu stricto is a clade that includes the genus *Sadocus* Sørensen, 1886, composed of rather large-sized (5.5–13.8 mm of dorsal scutum length) and colorful harvestmen. Although conspicuous and relatively common in Chilean preserved areas, it was never revised in more than 130 years of existence. Historically (see below), the genus has been subjected to many taxonomic acts, resulting in confusing species identities. One has to use poor (for modern standards), hundred-year-old descriptions to identify a given species. In addition, similar species are difficult to distinguish, raising doubts about their identities. Therefore, the revision of *Sadocus* focuses on determining the identity of the included species, which in turn will allow further understanding of their relationships, and more precise inferences of their distribution and diversity (Acosta 2002). The goals of this article are also to test the monophyly of the genus and propose a classification based on cladistic analysis.

Historical aspects of *Sadocus* Sørensen, 1886

The history of *Sadocus* Sørensen, 1886 can be quite confusing because many of its species were described before the proposition of the genus. Therefore, this historical section mentions many species in different genera and subfamilies that were later transferred to *Sadocus* (Kury 2003; Kury et al. 2020a, b), as explained further on in this article.

Guérin-Méneville (1844) described the eldest species related to *Sadocus*, *Gonyleptes planiceps* in Cuvier's 'Iconographie du Règne Animal'. However, the publication of this issue was delayed, and Gervais' (1842) "redescription" was actually published first. Gervais (1842) did credit the authorship of *G. planiceps* to Guérin-Méneville, and he

redescribed that species in 1844. Gervais also described the next five species relevant to *Sadocus*: *Gonyleptus asperatus*, *G. polyacanthoides*, and *G. polyacanthus* in 1847, and *G. bicornis* and *G. subsimilis* in 1849. Butler (1873) mistakenly proposed *G. subsimilis* as a senior synonym of *G. polyacanthoides.* A year later, Butler (1874) described *Gonyleptes funestus*. In 1884, Simon transferred *G. planiceps* to *Pachylus.*

In 1886, Sørensen proposed the monotypic genus *Sadocus*, to include the type and new species *S. vitellinosulcatus.* In 1899, Loman described *Discocyrtus calcitrosus* and *Gonyleptes platei*, which are relevant to *Sadocus*, and transferred *G. funestus* to *Discocyrtus* Holmberg, 1878.

In 1902, Sørensen: (i) synonymized *S. vitellinosulcatus* and *G. platei* Loman, 1899 with *G. polyacanthus*; (ii) created the new genus *Lycomedes* (without indication of a type species), to which he transferred *G. asperatus*, *G. bicornis*, *D. calcitrosus*, *D. funestus* and *Pachylus planiceps*; and (iii) described *Sadocus guttatus*. On that paper, Sørensen placed these species in Gonyleptidae, but without assigning them to any subfamily. Therefore, at the beginning of the 20th century, named species relevant to *Sadocus* were placed in both *Sadocus*, comprising two species (S. *polyacanthus* and *S. guttatus*) and *Lycomedes*, with five species (*L. asperatus*, *L. bicornis*, *L. calcitrosus*, *L. funestus* and *L. planiceps*).

Roewer (1913) designated *L. asperatus* as the type species of *Lycomedes*, and placed it in the Pachylinae. In that same work, he: (i) proposed the synonymy of *G. subsimilis* and *L. calcitrosus* with *L. asperatus*; (ii) described *Lycomedes calcar*; (iii) placed *Sadocus* in the Gonyleptinae and described *S. dilatatus* and *S. conspicillatus*. In his large work of 1923, Roewer proposed *Lycomedicus* as a replacement name for *Lycomedes*, which was preoccupied, and described as new the genus *Eubalta*.

Mello-Leitão (1937) described the genus *Carampangue* for his new species *C. ingens*, placing it in the Pachylinae, and in 1943, he described *C. nigronotatum*. In that same year, Roewer (1943) described the monotypic genus *Jighas* for the new species *J. vastus*, and placed it in the Pachylinae.

In 1945, Mello-Leitão described *Carampangue allermayeri*, and in the next year (1946), he described *Araucanoleptes* for the new species *A. exceptionalis*, and placed it in the Gonyleptinae. A few years later, Mello-Leitão (1949) synonymized *J. vastus* with the older *Carampangue ingens.* In that same year, Soares and Soares (1949) described *Lycomedicus brasiliensis*, and later, H. Soares (1968) transferred *Sadocus dilatatus* to *Lycomedicus*. During the next 30 years, only few catalogues (Cekalovic 1968, 1976, 1985) mentioned the species related to *Sadocus*. 154 years after its first description, Acosta (1996) studied the collection of type material of Pachylinae described by Roewer and found differences between Guérin-Méneville's (1844) description of *L. planiceps* and the redescription by Roewer (1913).

At the beginning of the 21st century (prior to this study), species relevant to *Sadocus* were placed in the following genera and subfamilies: the monotypic *Araucanoleptes* (Gonyleptinae); *Carampangue* (Pachylinae), with three species (*C. allermayeri*, *C. ingens* and *C. nigronotatum*); *Lycomedicus* (Pachylinae), with seven species (*L. asperatus*, *L. bicornis*, *L. brasiliensis*, *L. calcar*, *L. dilatatus*, *L. funestus* and *L. planiceps*); and *Sadocus* (Gonyleptinae), with three species (*S. conspicillatus*, *S. guttatus*, and *S. polyacanthus*).

Kury (2003), in his complete catalogue of New World Laniatores, proposed the synonymy of *Lycomedicus*, *Carampangue*, and *Araucanoleptes* with *Sadocus*. Hence, *Sadocus* comprised 14 species (actually, there are entries for 15 species, but that of *S. subsimilis* is clearly a mistake, which should be listed as a junior synonym under *S. asperatus*). Finally, Pessoa-Silva et al. (2020), transferred *S. planiceps* to *Eubalta*. *Sadocus* hitherto was composed of 13 species (Kury et al. 2020b). In the present publication, we accept only seven species of *Sadocus* as valid.

Materials and methods

Material examined belongs to the following institutions (curators in parentheses) listed below:

AMNH American Museum of Natural History, New York, USA (L. Prendini);
NHM The Natural History Museum, London, England (J. Beccaloni);
CAS California Academy of Sciences (Entomology), San Francisco, California, USA (L. Esposito);
MCZ Museum of Comparative Zoology, Cambridge, Massachusetts, USA (G. Giribet);
MNHN Muséum National d'Histoire Naturelle, Paris, France (M. Judson);
MNRJ Museu Nacional, Universidade Federal do Rio de Janeiro, Rio de Janeiro, Brazil (A.B. Kury);
MZSP Museu de Zoologia, Universidade de São Paulo, São Paulo, Brazil (R. Pinto-da-Rocha). CGPC = Carlos Nicolau Gofferjé Private Collection was transferred to MZSP;
SMF Senckenberg Research Institute and Museum, Frankfurt am Main, Germany (P. Jäger);
UFMG Universidade Federal de Minas Gerais, Belo Horizonte, Brazil (A.J. Santos);
URMU Museo Nacional de Historia Natural de Montevideo, Montevideo, Uruguay (M. Simó);
ZMB Museum für Naturkunde Leibniz-Institut für Evolutions- und Biodiversitätsforschung, Berlin, Germany (J. Dunlop);
ZMUC Zoologisk Museum Universität København, Copenhagen, Denmark (N. Scharff).

The following abbreviations are used throughout the text, including synonymic listings:

cat catalogue;
cit citation;
coll collected;
desc description;
eco ecology;
rdesc redescription;
syst systematic discussion.

In the examined material:

fe female;
ma male;
juv juvenile;

MS A–E penis ventral plate pairs of macrosetae A–E.
[X(y)] where X is the character number and y, the character state.

The topological nomenclature follows Acosta et al. (2007), nomenclature of integumentary ornamentation of dorsal scutum and legs, dorsal scutum outline and ventral plate penial macrosetae follows DaSilva and Gnaspini (2010), Kury and Medrano (2016) and Kury and Villarreal (2015), respectively. Nomenclature of ovipositor morphology generally follows Townsend et al. (2015). We adopted the orientation of the captured images to reference the ovipositor lobes, because we had no topological reference after detaching it. It is unlike the penis, which has a sclerotized ventral feature, thus being easily referenced topologically. In *Sadocus*, we realized that leg IV is twisted retro-laterad from the trochanter (gradually untwisting along the femur), rendering the otherwise prolateral structures as dorsal (Fig. 3A, E). To standardize the topological nomenclature, we opted to consider (and call) those as prolateral, despite being functionally dorsal (in situ). We illustrated the external morphology using a stereomicroscope with a camera lucida and the material immersed in 70% ethanol. We prepared male and female genitalia according to Pinto-da-Rocha (1997) to take pictures using a scanning electron microscope (SEM) or to illustrate using a compound microscope with a camera lucida. The generic characteristics are not repeated in the specific (re)descriptions. Only characters differing from those of the males are listed in the female (re)descriptions. The variation on the number of tubercles on the dorsal scutum and other parts of the body or legs were included in the intraspecific variation. The color descriptions are based on specimens preserved in 70% ethanol and living photograph examples presented in the section "variation in males (or females)" under each species. Many species of *Sadocus* present a white patch on the body, commonly known as a dry-mark (Kury in DaSilva and Gnaspini 2009). It is an external serose layer of the cuticle that often forms white patches/shapes. Distribution maps for *Sadocus* species were prepared using QGIS 3.10 (QGIS.org 2019). The identification key is only for males. Synonymic listings follow Kury's catalogue (2003), to which we add the category of its content between parentheses (see abbreviations section above). All measurements are in millimeters. We followed the view of Kury et al. (2020a) regarding the use of the correct inflection of specific epithets that are adjectives throughout the article to avoid inviting further confusion for the reader. Therefore, despite Kury himself (2003) proposing the combination *Sadocus funestis* (Butler, 1874), we use *Sadocus funestus* (Butler, 1874) as Kury et al. (2020b) in all sections (except for synonymic listing), including the historical aspects of *Sadocus*.

We chose the outgroups based on available hypotheses including Pachylinae, such as Pinto-da-Rocha et al. (2014), Hara et al. (2012) and Hara (2016). We rooted the tree in Stygnidae (*Stygnus polyacanthus* (Mello-Leitão, 1923)) based on Kury (1994). We added other taxa to account for the morphological diversity of Pachylinae sensu stricto and its sister group.

List of outgroups analyzed, with respective vouchers

Acanthopachylus aculeatus (Kirby, 1819) (Gonyleptidae: Pachylinae) (MZSP 76419)
Acanthoprocta conica Maury, 1991 (Gonyleptidae: Pachylinae) (AMNH)
Goniosoma varium Perty, 1833 (Gonyleptidae: Goniosomatinae) (MZSP 76421)
Gonyleptes horridus Kirby, 1819 (Gonyleptidae: Gonyleptinae) (MZSP 59820)
Metagyndes pulchella (Loman, 1899) (Gonyleptidae: Pachylinae) (AMNH)
Nanophareus polyhastatus Hara, 2016 (Gonyleptidae: Pachylinae) (AMNH)
Neogonyleptes docilis (Butler, 1876) (Gonyleptidae: Pachylinae) (AMNH)
Neogonyleptes karschii (Sørensen, 1902) (Gonyleptidae: Pachylinae) (AMNH)
Pachylus chilensis (Gray, 1833) (Gonyleptidae: Pachylinae) (AMNH)
Pachyloides thorellii Holmberg, 1878 (Gonyleptidae: Pachylinae) (MZSP 59880)
Roeweria bittencourti Mello-Leitão, 1923 (Gonyleptidae: Roeweriinae) (MZSP 76420)
Stygnus polyacanthus (Mello-Leitão, 1923) (Stygnidae: Stygninae) (MZSP 59951)

We include records of distribution in maps only for vials with males. We used LibreOffice Calc to edit the character matrix and TNT 1.0 (Goloboff, Farris and Nixon 2008) to perform an implicit enumeration search under parsimony using equal weights. No character was ordered. We calculated Absolute and Relative Bremer support (Bremer 1994) to evaluate the support of clades using the Bremer Support Script for TNT 1.0 written by Pablo Goloboff (available at http://tnt.insectmuseum.org/index.php/Scripts/bremer). We used Winclada 1.00.08 (Nixon 1999) to edit the tree under ACCTRAN optimization and the notation of taxon+ proposed by Amorim (1982).

Results and discussion

Cladistic analysis

To test the monophyly of *Sadocus*, we used a matrix of morphological characters composed of 18 taxa (13 outgroups and five ingroups) and 64 characters (Table 1). The 64 characters are distributed as follows: 18 from dorsal scutum, four from free tergites, one from the chelicera, 23 from male legs, 17 from male genitalia, and one from coloration. We only included the valid *Sadocus* species with known males, as most of the characters are based on armature of male leg IV and penis. The cladistic analysis resulted in a single most parsimonious tree (182 steps, L = 182; C.I. = 45; R.I. = 53, Fig. 1).

According to the retrieved tree, *Sadocus* is not monophyletic, as it excludes *Sadocus brasiliensis* (Soares & Soares, 1949). Acosta (2020) first mentioned that *S. brasiliensis* may not belong to this genus based on the overall distribution of the other *Sadocus* species. That suspicion is corroborated here, and we propose its synonymy with the Brazilian *Discocyrtus catharinensis* (Mello-Leitão, 1923) (see taxonomic notes in this species' entry). In turn, the close relationship of *D. catharinensis* with *Roeweria bittencourti*

Table 1. List of character and character states used in the cladistic analysis. All characters of legs and genitalia refer to male.

	Character	State
1	(DS) Ocularium (Hara 2016):	0. Divided, each eye placed onto different elevations; 1. Single.
2	(DS) Ocularium, unpaired armature:	0. Absent; 1. Present.
3	(DS) Ocularium, paired armature:	0. Absent; 1. Present.
4	(DS) Anterior margin of carapace, frontal hump	0. Inconspicuous; i.e., straight from ocularium to anterior margin of DS in lateral view 1. Conspicuous; i.e., clear elevation from ocularium to anterior margin of DS in lateral view
5	(DS) Mesotergum: placement of the maximum width	0. Maximum width in the middle of the mesotergum; 1. Maximum width placed posteriorly to the middle of mesotergum
6	(DS) Dorsal scutum length and width ratio	0. Wider than long; 1. Longer than wide
7	(DS) Posterior margin, shape	0. Straight; 1. Concave; 2. Convex
8	(DS) Area I, state of fusion	0. Divided in right and left halves by a longitudinal groove between scutal areas I – II (even though the groove of area II slightly invades area I) 1. Divided in right and left halves by invasion of scutal area II into middle of scutal area I.
9	(DS) Scutal area I,paramedian armature (Hara 2016)	0. Absent or with similar sized granules; 1. With a pair of tubercles
10	(DS) Scutal area II, paramedian paired armature (Hara 2016)	0. Absent or with similar sized granules; 1. With a pair of tubercles
11	(DS) Scutal area III, paramedian paired armature (Hara 2016)	0. Absent or with similar sized granules; 1. With a paramedian pair of tubercles
12	(DS) Scutal area IV, presence	0. Absent; 1. Present.
13	(DS) Scutal area IV, degree of division	0. Incompletely divided; i.e., interrupted scutal groove IV; 1. Completely divided
14	(DS) Scutal area IV, paramedian paired armature	0. Absent; 1. Present.
15	(DS) Lateral margin, type of integumentary ornamentation	0. Covered with granules; 1. With tubercles, sometimes clustered
16	(DS) Lateral margin, type of armature	0. Large tubercles or apophyses; 1. similar sized tubercles
17	(DS) Posterior margin of the DS, paramedian armature	0. Absent; 1. Present.
18	(DS) Posterior margin of the DS, central unpaired armature	0. Absent; 1. Present.
19	(DS) Free tergites I, paramedian armature	0. Absent; 1. Present.
20	(DS) Free tergites II, paramedian armature	0. Absent; 1. Present.
21	(DS) Free tergites II, unpaired armature	0. Absent; 1. Present.
22	(DS) Free tergites III, paramedian paired armature	0. Absent; 1. Present.
23	(Chelicerae) Chelicerae, sexual dimorphism (#30, Hara 2016)	0. Isomorphic in both sexes 1. Large in male
24	(Pedipalp) Tibia, type of retro-lateral apical seta	0. Single; 1. Bifid
25	(Leg) Coxa IV, branch of the prodorsal apophysis	0. Single; 1. Bifid
26	(Leg) Coxa IV, insertion of the prodorsal apical apophysis in relation to the DS main axis (Hara et al. 2012)	0. Almost transversal; i.e., almost 90 degrees in relation to DS main axis; 1. Oblique; i.e., more than 120 degrees in relation to DS main axis; 2. Parallel to femur IV
27	(Leg) Coxa IV, retro-apical apophysis:	0. Absent; 1. Present.
28	(Leg) Leg IV, torsion that begins at the trochanter and ends at the patella	0. Untwisted; 1. Strongly twisted; i.e., prolateral features becoming dorsal in situ and gradually untwisting towards patella; 2. Strongly twisted from coxa IV towards the patella (Fig. 3A, E).
29	(Leg) Trochanter IV, Prolateral basal apophysis (# 30 Hara & Pinto–da–Rocha 2010)	0. Absent; 1. Present.
30	(Leg) Trochanter IV, dorso-median subapical apophysis	0. Absent; 1. Present.
31	(Leg) Trochanter IV, prodorsal apical apophysis	0. Absent; 1. Present.

	Character	State
32	(Leg) Trochanter IV, type of prodorsal apical apophysis	0. As a wart; 1. As a hook-like pointed apophysis of large base, smoothly becoming pointed apically; 2. As a moderate size blunt cone; 3. As a finger shaped, robust apophysis, basal half of ca. uniform diameter
33	(Leg) Trochanter IV, retro-dorsal apical apophysis (# 29 Hara & Pinto–da–Rocha 2010)	0. Absent; 1. Present.
34	(Leg) Trochanter IV, retro-apical armature (Hara & PdR 2010)	0. Absent; 1. Present.
35	(Leg) Trochanter IV, type of retro-apical armature	0. Pointed tubercle; 1. Moderate apophysis (ca. a quarter of podomere width); 2. Huge apophysis (as long as podomere width).
36	(Leg) Trochanter IV, proapical apophysis	0. Absent; 1. Present.
37	(Leg) Trochanter IV, length-width ratio (modified from Hara 2016)	0. As long as wide; 1. Twice longer than wide; 2. Wider than long.
38	(Leg) Femur IV, curvature in dorsal view	0. Straight; 1. Sinuous
39	(Leg) Femur IV, size of granules on retro-lateral row	0. Similar sized granules; 1. Tubercles, twice the size of granules.
40	(Leg) Femur IV, spiniform apophyses on basal half of the retro-lateral row of granules	0. Absent; 1. Present.
41	(Leg) Femur IV, the pattern of apophyses distribution at the ⅔ basal region of the retro-lateral row	0. Just an apophysis in the basal ⅓; 1. Growing from the median region to the basal region; 2. Very high apophyses alternating with low apophyses; 3. Apophyses distributed in the median region; 4. A basal apophysis and one or more in the distal ⅔; 5. An average apophysis; 6. Decreasing from the median region to the basal region.
42	(Leg) Patella IV, ventral row of granules	0. Similar sized granules; 1. Granules becoming tubercles or spines.
43	(Leg) Tibia IV, ventro-basal long spine	0. Absent; 1. Present.
44	(Leg) Tibia IV, size of granules on retro-ventral row	0. Tubercles of similar sizes; 1. Granules increasing in size apically, becoming tubercles.
45	(Leg) Tibia IV, proventral row of tubercles size	0. Tubercles of similar sizes; 1. Larger tubercles, which grows in size apically.
46	(Leg) Tibia IV, size of granules on ventral row	0. Similar sized granules; 1. Increasing in size apically.
47	(Penis) Ventral plate, shape of the distal margin	0. Straight; 1. Slightly concave; 2. Very concave, forming a “U”.
48	(Penis) Ventral plate, basal lobes	0. Inconspicuous; 1. Conspicuous.
49	(Penis) Ventral plate, plate format	0. Rectangular; 1. Hexagonal.
50	(Penis) Ventral plate, number of MS C	0. Three pairs; 1. Four pairs or more.
51	(Penis) Glans, dorsal prominence in the distal region of the sac	0. Absent; 1. Present.
52	(Penis) Glans, sac texture	0. Smooth and turgid; 1. Wrinkled.
53	(Penis) Glans, latero-apical region	0. Without projections; 1. With projections covering part or all of the pedestal in lateral view.
54	(Penis) Glans, dorsal process	0. Absent; 1. Present.
55	(Penis) Glans, ventral process	0. Absent; 1. Present.
56	(Penis) Ventral process, presence of stem	0. Absent; 1. Present.
57	(Penis) Ventral process, apex shape	0. As a flabellum ; 1. Tapered at the apex and rolled; 2. Flattened circular; 3. Flattened quadrangular; 4. Fringed triangular; 5. Large rectangular; 6. Rectangular bifid; 7. Rectangular with pointed projections.
58	(Penis) Stylus, ventral process length ratio	0. Stylus shorter than ventral process; 1. Stylus longer than ventral process.
59	(Penis) Stylus, apical lateral projections	0. Absent; 1. Present.
60	(Penis) Stylus, apex shape (DaSilva and Gnaspini 2010)	0. Rounded; 1. With an apical back beak.
61	(Penis) Stylus, trichomes on median apical region	0. Absent; 1. Present.
62	(Penis) Insertion on the glans in lateral view	0. Ventral; 1. Median
63	(Penis) Trunk of the penis, subapical region	0. Truncated; 1. Projected on the glans
64	(Color) Carapace, presence of dry-mark	0. Absent; 1. Present.

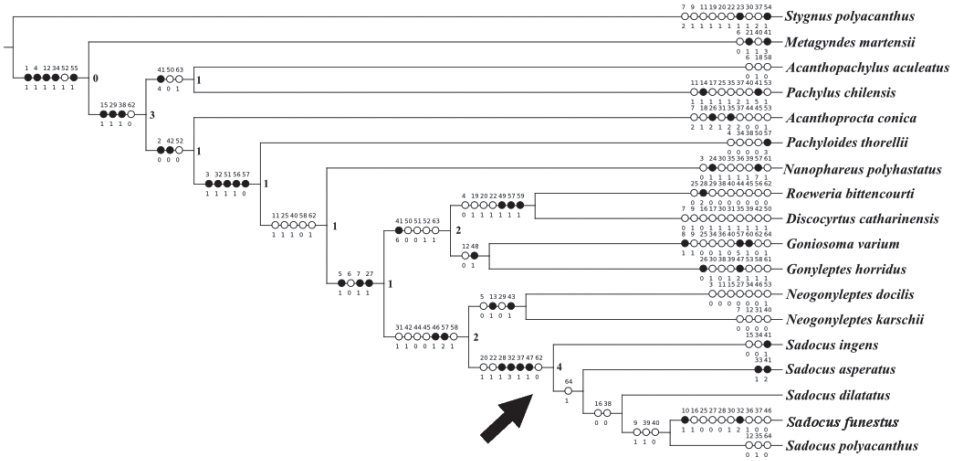

Figure 1. The single most parsimonious tree retrieved in the cladistic analysis representing *Sadocus* relationships (182 steps, L = 182; C.I. = 45; R.I. = 53). Number at the nodes are Goodman-Bremer support. Black circles indicate unique transformations, while white circles indicate homoplastic transformations, the arrow indicates the position of the genus *Sadocus*. The character number is above each circle, and the character state is below. The characters are optimized in ACCTRAN. The character and character states are given in Table 1, and the data matrix is in Table 2.

(Roeweriinae Brazilian species) is supported by seven synapomorphies, three of them exclusive: hexagonal shape of the penial ventral plate [49(1)]; penial ventral process apex tapering distally, becoming rolled [57(1)]; and penial stylus with latero-apical projections [59(1)]. *Discocyrtus catharinensis* is probably a Roeweriinae especially based on the shape of the penial ventral plate as well as the overall penial morphology. However, we refrained further taxonomic actions as Roeweriinae diversity grows further fueled by the dismemberment of *Discocyrtus*, which is currently under revision (Kury and Carvalho 2016; Carvalho and Kury 2018, 2021).

Once we settled the issue related to *S. brasiliensis*, we propose a new concept of *Sadocus*. Under the new definition, *Sadocus* is monophyletic and supported by seven synapomorphies, four of which are exclusive: leg IV twisted from the trochanter to patella [28(0)]; trochanter IV with a finger shaped, robust prodorsal apical apophysis, its basal half of ca. uniform diameter [32(3)], trochanter IV twice longer than wide [37(1)] (modified from Hara 2016); and penis ventral plate with slightly concave distal margin [47(1)]. *Sadocus* is also the best supported clade of the analysis, with a high Goodman-Bremer support (4).

So far, *Sadocus* (represented especially by *S. polyacanthus*, its type species) has often been used in cladistic analysis as outgroups (Hara et al. 2012; Hara 2016) or as an ingroup taxon of a more comprehensive analysis testing monophyly of Gonyleptidae or Gonyleptoidea (Pinto-da-Rocha et al. 2014; Benavides et al. 2021). According to the analyses based on morphological characters (Hara et al. 2012; Hara 2016), *Sadocus* is nes-

Table 2. Matrix of character states for the cladistic analysis of the *Sadocus* (Gonyleptidae: Pachylinae).

Stygnus polyacanthus	0 1 0 0 0 1 2 0 1 0 1 0 – – 0 1 0 0 1 1 0 1 1 0 0 1 0 0 0 1 0 – 0 0 – 0 2 0 0 0 – 1 0 1 1 0 0 0 0 1 0 0 0 1 0 – – – – 0 0 1 0 0
Acanthopachylus aculeatus	1 1 0 1 0 0 0 0 0 0 0 1 0 0 1 1 0 1 0 0 0 0 0 0 0 1 0 0 1 0 0 – 0 1 0 0 0 1 0 0 4 1 0 1 1 0 0 0 0 0 0 1 0 0 1 0 4 0 0 0 0 0 1 0
Acanthoprocta conica	1 0 0 1 0 1 2 0 0 0 0 1 0 0 1 1 0 1 0 0 0 0 0 0 0 0 2 0 0 1 0 1 0 0 1 2 0 2 1 0 0 – 0 0 0 0 0 0 0 0 0 1 0 0 1 0 1 0 4 1 0 0 0 0 0 0
Goniosoma varium	1 0 1 1 1 0 1 1 1 0 1 0 – – 1 1 0 0 0 0 0 0 0 0 0 0 0 1 1 0 1 0 0 – 0 0 – 1 0 1 0 0 – 0 0 1 1 0 0 1 0 0 0 1 0 0 1 1 5 0 0 1 0 0 1 1
Gonyleptes horridus	1 0 1 1 1 0 1 0 0 0 1 0 – – 1 1 0 0 0 0 0 0 0 0 0 1 0 1 0 1 1 0 – 0 1 0 0 0 0 1 1 6 0 0 1 1 0 2 1 0 0 0 1 1 0 1 1 0 1 0 0 1 1 1 0
Metagyndes martensii	1 1 0 1 0 0 0 0 0 0 0 1 0 0 0 1 0 0 0 0 1 0 0 0 0 1 0 0 0 0 0 0 – 0 1 0 0 0 0 0 0 1 3 1 0 1 1 0 0 0 0 1 0 1 0 0 1 0 4 1 0 0 0 1 0 0
Nanophareus polyhastatus	1 0 0 1 0 1 0 0 0 0 1 1 0 0 1 1 0 0 0 0 0 0 0 0 1 1 1 0 0 1 1 0 – 0 1 1 1 0 1 1 1 0 0 0 1 1 0 0 0 0 1 1 0 0 0 1 1 7 0 0 0 1 1 0 0
Neogonyleptes docilis	1 0 0 1 0 0 1 0 0 0 0 1 1 0 0 1 0 0 0 0 0 0 0 0 0 1 1 0 0 0 0 1 1 0 0 – 0 0 1 0 1 0 1 1 0 0 0 0 0 0 1 1 0 1 0 1 1 2 1 0 0 0 1 0 0
Neogonyleptes karschii	1 0 1 1 0 0 0 0 0 0 1 0 – – 1 1 0 0 0 0 0 0 0 0 0 1 1 1 0 0 0 0 1 0 1 0 0 0 1 0 0 – 1 1 0 0 1 0 0 0 1 1 0 0 0 1 1 2 1 0 0 0 1 0 0
Pachyloides thorellii	1 0 1 0 0 1 0 0 0 0 0 1 0 0 1 1 0 0 0 0 0 0 0 0 0 0 1 0 0 1 0 0 – 0 0 – ? 0 0 0 0 – 0 0 1 1 0 0 0 0 0 0 1 0 0 0 1 1 3 1 0 0 0 0 0 0
Pachylus chilensis	1 1 0 1 0 1 0 0 0 0 1 1 0 1 1 1 1 0 0 0 0 0 0 0 0 1 1 0 0 1 0 0 – 0 1 1 0 2 1 0 1 5 1 0 1 1 0 0 0 0 0 0 0 1 1 0 1 0 4 1 0 0 0 0 1 0
Roeweria bittencourti	1 0 1 0 1 0 1 0 0 0 1 1 0 0 1 1 0 0 1 1 0 1 0 0 0 1 1 2 0 0 0 – 0 1 0 0 0 0 0 0 0 – 0 0 0 0 0 0 0 0 1 0 0 1 0 0 1 0 – – 1 0 0 0 1 0
Discocyrtus catharinensis	1 0 1 0 1 0 0 0 1 0 1 1 0 0 1 0 1 0 1 1 0 1 0 0 1 1 1 0 1 1 1 1 0 1 1 0 0 1 1 1 6 1 0 1 1 0 0 0 1 1 0 1 0 0 1 1 1 0 1 0 0 1 1 0
Sadocus asperatus	1 0 1 1 1 0 1 0 0 0 1 1 0 0 1 1 0 0 0 1 0 1 0 0 1 1 1 1 1 0 1 3 1 1 0 0 1 1 0 1 2 1 0 0 0 1 1 0 0 1 1 0 0 0 1 1 2 1 0 0 0 0 0 1
Sadocus dilatatus	1 0 1 1 1 0 1 0 0 0 1 1 0 0 1 0 0 0 0 1 0 1 0 0 1 1 1 1 1 0 1 3 0 1 0 0 1 0 0 1 0 1 0 1 0 0 0 1 1 0 0 1 1 0 0 0 1 1 2 1 0 0 0 0 0 1
Sadocus funestus	1 0 1 1 1 0 1 0 1 1 1 1 0 0 1 1 0 0 0 1 0 1 0 0 0 1 0 0 1 1 1 2 0 1 0 1 0 0 1 0 – 1 0 0 0 0 1 0 0 1 1 0 0 0 1 1 2 1 0 0 0 0 0 1
Sadocus ingens	1 0 1 1 1 0 1 0 0 0 1 1 0 0 0 1 0 0 0 1 0 1 0 0 1 1 1 1 1 0 1 3 0 0 – 0 1 1 0 1 1 1 0 0 0 1 1 0 0 1 1 0 0 0 1 1 2 1 0 0 0 0 0 0
Sadocus polyacanthus	1 0 1 1 1 0 1 0 1 0 1 0 – – 1 0 0 0 0 1 0 1 0 0 1 1 1 1 1 0 1 3 0 1 1 0 1 0 1 0 – 1 0 0 0 1 1 0 0 1 1 0 0 0 1 1 2 1 0 0 0 0 0 0

tled in a clade mainly composed of Brazilian species. However, we have to stress that the clade with *Sadocus* in Hara's analyses is not well supported (Bremer support: 1), its sole homoplastic synapomorphy being the proventral apical armature of tibia IV as a tubercle. In the present analysis, we have a roughly similar outcome, as the clade including *Sadocus* (*Sadocus* + *Neogonyleptes*) is sister group to a clade composed of solely Brazilian species. This outcome differs considerably from Pinto-da-Rocha et al. (2014) or Benavides et al. (2021): in those analyses based on molecular data, *Sadocus* is often retrieved closely related to Chilean Pachylinae genera. Regarding this, Pinto-da-Rocha et al. (2014) indicate that *Sadocus* is in a clade with other Chilean species (*Neogonyleptes karschii* and *Tumbesia aculeata*), which in turn is sister group to Pachylinae sensu stricto. Benavides et al. (2021) also corroborates a close relationship of *Sadocus* with Chilean genera.

The sister taxon closest to *Sadocus* is also an unsettled issue, mainly because different taxa are employed in those analyses. In the present analysis, *Sadocus* sister group is the Chilean genus *Neogonyleptes*, supported by seven synapomophies, two of them exclusive: ventral row of granules increasing in size apically on tibia IV [46(1)]; and apex of glans ventral process flattened circle shaped [57(2)]. This sister group relationship is similar to Pinto-da-Rocha et al. (2014) sampling wise. On the other hand, Benavides et al. (2021) did not include *Neogonyleptes* in their analysis, and the Chilean *Eubalta planiceps* is the sister taxon to *Sadocus*. It is interesting to note that *Sadocus* sister taxon is strongly affected by the Chilean Pachylinae sampling not belonging to Pachylinae sensu stricto.

The main goals of this study were to revise and to test the monophyly of *Sadocus*, a hundred-year-old genus, with a convoluted taxonomic history. We believe that we succeeded in those, and the present study is an important step towards the understanding the evolution of the genus. Considering all the evidence (including the taxonomic history), *Sadocus* seems to be related to the Chilean-Argentinean Pachylinae. We understand that *Sadocus* relationship within Gonyleptidae is still an unsettled issue that deserves further investigation. As a mean to tackle that, we can suggest the inclusion of more Chilean Pachylinae genera (especially those already used in previous analyses and not belonging to Pachylinae sensu stricto) and Brazilian species as well, such as DRMN (Carvalho and Kury 2018) and K92 (Kury 1992). The latter suggestion is because of the Brazilian clade closest to Chilean Pachylinae clade depicted by Pinto-da-Rocha et al. (2014) and Benavides et al. (2021).

Taxonomic accounts

Gonyleptidae Sundevall, 1833
Pachylinae Sørensen, 1884

***Sadocus* Sørensen, 1886**

Gonyleptes [part]: Gervais, 1842: 2 [rdesc]; 1844: 105 [rdesc]; 1847: 576–577 [cit]; 1849: 21, 24–26 [desc, rdesc]; Butler 1873: 113–114 [cat]; 1876: 153 [desc].
Discocyrtus [part]: Loman, 1899: 6 [desc].

Sadocus Sørensen, 1886: 85 [desc]; 1902: 14–20 [rdesc]; Hogg 1913: 48 [cit]; Roewer 1913: 244–245 [cit, key]; 1923: 492 [cit, key]; Mello-Leitão 1923: 190 [cit]; 1926: 31 [key]; Roewer 1930: 381 [key, cit]; Mello-Leitão 1931a: 136 [cit]; 1932: 348 [rdesc]; 1935: 105 [key]; Canals 1936: 70 [cat]; Kästner 1937: 389 [desc]; Roewer 1938: 02 [cit]; Mello-Leitão 1939: 625 [cit]; B. Soares 1944a: 166 [syst]; Soares and Soares 1949: 211 [rdesc]; Ringuelet 1955a [cit]: 438; Ringuelet 1959: 409 [rdesc]; Roewer 1961: 102 [cat]; Cekalovic 1985: 14 [cat]; Kury 2003: 191 [cat]; Hara et al. 2012: 38–39 [syst]; Pinto-da-Rocha et al. 2012: 61 [cit]; Pinto-da-Rocha et al. 2014: 18 [syst]; Hara 2016: 106–109 [syst]; Pérez-Schultheiss et al. 2019, 4, 12–15 [cit]; Kury et al. 2020a: 5[cit]; Acosta 2020 [cit]; Kury et al. 2020b [cat]. (Type species *Sadocus vitellinosulcatus* Sørensen 1886, by monotypy).

Lycomedes Sørensen, 1902: 17 [desc]; Roewer 1913: 126–127 [rdesc, key]; Mello-Leitão 1926: 31 [key]; Muñoz-Cuevas 1973: 226–228 [cit]. (Type species *Gonyleptes asperatus* Gervais, 1847, by subsequent designation by Roewer 1913).

Lycomedicus Roewer, 1923: 442 (*nom. nov.* for *Lycomedes* Sørensen, 1902, rdesc); 1925: 17 [cit]; 1929: 213 [cat]; Mello-Leitão; 1931b: 84 [cit]; 1932: 216 [rdesc]; 1935: 101 [cit]; Canals 1936: 69 [cat]; Roewer 1943: 28 [cit]; Ringuelet 1959: 329 [rdesc]; Cekalovic 1985: 18 [cat]. Synonym established by Kury 2003.

Lycomedius [lapsus]: Kästner, 1937: 389 [rdesc]; Strand 1942: 397 [cit].

Carampangue Mello-Leitão, 1937: 152 [desc]; 1945: 156 [cit]; 1949: 17 [syst]; Soares and Soares 1954: 241 [rdesc, cat]; Cekalovic 1985: 16 [cat]. (Type species *Carampangue ingens* Mello-Leitão, 1937 by monotypy). Synonymy established by Kury 2003.

Jighas Roewer, 1943: 28 [desc]; Mello-Leitão 1949: 17 [syst]. (Type species *Jighas vastus* Roewer, 1943 by monotypy). Synonymy established with *Carampangue* by Mello-Leitão 1949.

Araucanoleptes Mello-Leitão, 1946: 4 [desc]; Soares and Soares 1949: 160 [rdesc]. (Type species *Araucanoleptes exceptionalis* Mello-Leitão, 1946 by monotypy). Synonymy established by Kury 2003.

Arauconoleptes [*lapsus*]: Cekalovic, 1985: 12 [cat].

Type species. *Sadocus vitellinosulcatus* Sørensen, 1886, by monotypy. Synonymized with *S. polyacanthus* by Sørensen (1902).

Other species included. *S. asperatus* (Gervais, 1847), *S. dilatatus* Roewer, 1913, *S. funestus* (Butler, 1874), *S. ingens* (Mello-Leitão, 1937) and *S. polyacanthus* (Gervais, 1847).

Diagnosis. *Sadocus* are large Pachylinae (dorsal scutum maximum length 5.5–13.8 mm) with paired spines on ocularium and prominent frontal hump on dorsal scutum anterior margin. Dorsal scutum shape types gamma triangular and gamma pyriform, its posterior margin concave. Dorsal scutum mid-bulge placed close to scutal groove IV (scutal groove III in *S. funestus*) and transversal (*S. funestus*, *S. ingens*, *S. polyacanthus*) or oblique (*S. asperatus*, *S. dilatatus*); free tergites II and III each with a pair of spines. Legs IV are twisted retro-laterad from the trochanter and gradually distorted along the femur and patella (except in *S. funestus*). Coxa IV bearing a long, large prodorsal apical apophysis and a short, retro-apical one (except in *S. funestus*, in which is lacking). Trochanter IV with a short, blunt prolateral sub-basal apophysis and a long,

robust prodorsal apical one. Penis glans turgid and dorsally projected (with antero-lateral projections), with ventral process (half stylus length) and without dorsal process. General color (in living specimens) of the body and most parts of legs and ventral area dark brown, with lighter tones at the tips of podomeres. Yellowish to reddish tone in scutal area, scutal posterior margin, free tergites, part of legs and apophysis. Green on the arthrodial membranes between the free tergites.

Redescription. Male: ***Dorsum.*** Anterior margin of carapace with a prominent median frontal hump (bell shaped in dorsal view). Ocularium with one pair of spines posterior to the eyes. Dorsal scutum type varying from gamma to gamma triangular and gamma pyriform, its posterior margin concave, mid-bulge slightly asymmetrical and displaced posteriorly, widest at the scutal groove IV (scutal groove III in *S. funestus*). The curvature of mid-bulge can be transversal (*S. funestus*, *S. ingens*, and *S. polyacanthus*) or oblique (*S. asperatus* and *S. dilatatus*). Four scutal areas (three in *S. polyacanthus*); scutal area I divided into right and left halves by a longitudinal median groove. Scutal area III with one pair of paramedian spiniform tubercles or spines. Two pairs of ozopores close to coxa II. Lateral margin of dorsal scutum with an external and internal rows of tubercles (the external row of slightly larger tubercles) (except *S. asperatus*, with granules covering most of the lateral margin of dorsal scutum and *S. ingens*, smooth or with only few granules). Posterior margin of dorsal scutum and free tergite I each with one paramedian pair of tubercles (except *S. funestus* and *S. polyacanthus*, unarmed). Free tergites II and III each with one paramedian pair of spines. ***Venter.*** Coxa I–IV granulate; coxa I with a median longitudinal row of granules increasing in size apically, becoming tubercles. ***Chelicerae.*** Isomorphic in males and females. Segment I with well-marked bulla. Segment II fixed finger and segment III toothed. ***Pedipalps.*** Trochanter dorsal face inflated; ventral face with one or two setiferous tubercles. Femur bearing sub-apical mesal seta; dorsal face with few granules; ventral face with one basal setiferous tubercle. Tibiae and tarsi dorsal and lateral faces with few minute granules and variable setation. ***Legs.*** Coxae I–III each with one prodorsal and one retro-dorsal spiniform tubercles, ventral faces granulate (except *S. polyacanthus*, coxa I with tubercles and others with setae). Coxa IV dorso-lateral face with sparsely distributed granules, ventral face entirely granulated, with one long, oblique, bifid prodorsal apical apophysis (transversal in *S. dilatatus*, uniramous in *S. funestus*), dorsal branch longest and curved ventrad and ventral branch short and blunt; and one ventro-apical retro-lateral spine. Trochanters I–III granulate. Leg IV twisted retro-laterad from the trochanter, gradually untwisting along the femur (except *S. funestus*, straight). Trochanter IV longer than wide; prolateral face with one short, conical, blunt sub-basal apophysis, and one robust, blunt dorso-apical apophysis. Femora I–IV with granules roughly organized in six longitudinal rows (prodorsal, retro-dorsal, pro- and retro-lateral, proventral and retro-ventral rows); femora I and II unarmed. Femur IV curved, with marked inner curvature on the distal half (*S. asperatus* and *S. ingens*) or almost straight (*S. dilatatus*, *S. funestus*, and *S. polyacanthus*). Patellae I–III granulate, unarmed; patella IV dorsal face granulate, ventral face tuberculate. Tibiae I–III granulate, unarmed (except *S. dilatatus* and *S. funestus*, tibia III dorsal face granulate with retro-ventral row of tubercles increasing in size apically). Tibia IV dorsal face granulate, ventral face with tubercles sparsely distributed. Metatarsi I–IV minute granulate, unarmed. Tarsus III and IV each

with ventral process, tarsal claws smooth. ***Penis***. Ventral plate distal margin with slight (but conspicuous) to moderate concavity, two or three pairs of MS A, one pair of MS B or entirely absent, four or five pairs of MS C, one or two pairs of MS D, and one or two pairs of MS E. Glans sac tall, turgid, dorsally projected with antero-lateral projections, forming a sheath for the stylus. Glans without dorsal process; stylus inserted ventrally and smooth. Glans ventral process is short (half of stylus length), parallel to the stylus, apex curved ventrad, with a short semi-circular antero-lateral projection.

Geographic distribution (Fig. 2). Central Chile, Región XIV Los Ríos; Metropolitan Region of Santiago; Región V Valparaíso; Región VIII Bio-Bío; Región IX Araucanía; and Region X Los Lagos. There are other localities mentioned in the literature besides the material studied here for *S. polyacanthus* in Neuquén (Argentina) and Magallanes, in the extreme south of Chile, however, we did not examine any material from there. The record of *Sadocus funestus* for Ecuador (Chimborazo, Riobamba) by Roewer (1913) is certainly a mislabeling because it does not agree with the known generic distribution (Cekalovic 1985; Kury 2003). Two species are widely distributed (*S. asperatus* and *S. polyacanthus*) and three others occur mainly in coastal mountains of Central Chile (*S. funestus*, *S. dilatatus*, and *S. ingens*).

Key to males of *Sadocus* species

1 Coxa IV with a bifid prodorsal apical apophysis (Fig. 3A, C) and one retro-ventral apical apophysis (Fig. 3A) **2**

– Coxa IV with an unbranched prodorsal apical apophysis (Fig. 5A, C), without retro-ventral apical apophysis (Fig. 5A) ..... ***S. funestus***

2 Lateral margin of the dorsal scutum with a posterior large tubercle (Figs 4A, 7A) 3

– Lateral margin of the dorsal scutum only with similar sized tubercles (Fig. 6C) 4

3 Dorsal scutum with four areas (Fig. 4A), femur IV with a long, retro-lateral sub-basal apophysis (Fig. 4D) ..... ***S. dilatatus***

– Dorsal scutum with three areas (Fig. 7A), femur IV retro-lateral face with spines of similar size (Fig. 7B) ..... ***S. polyacanthus***

4 Trochanter IV dorso-apical face only with one prolateral apophysis of similar length as the podomere, strongly curved (in lateral view), pointing frontwards (Fig. 6C) ..... ***S. ingens***

– Trochanter IV dorso-apical face with two apophyses, both shorter than the podomere length, femur IV slightly curved (Fig. 3B, E) ..... ***S. asperatus***

***Sadocus asperatus* (Gervais, 1847)**

Figures 2, 3A–E, 8A, B, 9A–C, E, 11A, B, 12A–C

Gonyleptes asperatus Gervais, 1847: 577 [desc]; 1849: 26, pl. 1, fig 9 [rdesc]; Butler 1873: 113 [cat]; Sørensen 1902: 17 [syst]. Transferred to *Lycomedes* by Sørensen

1902. (MNHN, type lost, not examined) (RPR visited the museum but the curator was unable to find the type material)

Lycomedes asperatus: Sørensen, 1902: 17 [syst]; Roewer 1913: 127–130, fig 57 [key, rdesc].

Lycomedicus asperatus: Roewer, 1923: 442, fig 556 [rdesc]; 1925: 17 [cit]; 1929: 213 [cat]; Mello-Leitão 1931b: 84 [cit]; Canals 1936: 69 [cat]; Roewer 1938: 6 [cat]; Mello-Leitão 1939: 624 [cat]; Soares and Soares 1954: 270 [cat]; Ringuelet 1959: 329, fig 44 [rdesc]; H. Soares 1968: 264 [cit]; Cekalovic 1968: 8 [cat]; 1985: 18 [cat].

Sadocus asperatus: Kury, 2003: 191 [cat]; Kury et al. 2020b [cat].

Sadocus (?) *subsimilis:* Sørensen, 1902: 17 [cit]; Roewer 1913: 127–130, fig 57 [syst]. Synonymy with *L. asperatus* established by Roewer 1913.

Gonyleptes polyacanthoides Gervais, 1847: 577 [desc]; Butler 1873: 114 [cat]. Synonymy with *G. subsimilis* established by Butler 1873. (MNHN, type lost, material not examined) (RPR visited the Museum but the curator was unable to find the type material)

Gonyleptes subsimilis Gervais, 1849 [desc]: 25, pl. 1, fig 8; Butler 1873: 114 [cat]; Sørensen 1902: 6 [syst], 16 [syst]. Synonymy with *Sadocus* (?) *subsimilis* established by Sørensen 1902 (MNHN, type lost, material not examined) (RPR visited the museum but the curator was unable to find the type material)

Gonyleptes bicornis Gervais, 1849: 21, pl. 1, fig 4a–b [desc]; Butler 1873: 114 [cat]; Sørensen 1902: 19 [syst]. (type material depository unknown). syn. nov.

Lycomedes bicornis: Sørensen, 1902: 20, fig 4–4b [rdesc]; Roewer 1913: 136–137, fig 62 [rdesc].

Lycomedicus bicornis: Roewer, 1923: 445, fig 561 [cit]; Canals 1936: 69 [cat]; Soares and Soares 1954a: 270 [cat]; Cekalovic 1968: 7 [cat], 1985: 18 [cat].

Sadocus bicornis: Kury, 2003: 191 [cat]; Kury et al. 2020b [cat].

Discocyrtus calcitrosus Loman, 1899: 7, fig 5 [desc]; Sørensen 1902: 19 [syst]. (type ZMB 7837, ma holotype – examined by detailed photographs).

Lycomedes calcitrosus: Sørensen, 1902: 19 [syst]. Synonymy with *L. asperatus* established by Roewer 1913.

Lycomedicus calcitrosus: Moritz, 1971: 193 [cat].

Material examined. Chile, date and collector unknown, 1 ma (MCZ 31267). Región Metropolitana de Santiago, *Santiago*, date or collector unknown, 6 ma, 3 fe (SMF 1369); Same, *El Canelo*, 16.I.1980, collector unknown, 2 ma (AMNH); Same, 16.I.1980, collector unknown, 1 ma, 1 fe (AMNH). Región de Valparaíso, collection date or collector unknown, 8 ma, 19 fe (SMF 5382). Región de Biobío, *Provincia de Concepción*, 22.I.1985, N.I. Platnick & O.F. Francke coll., 1 ma (AMNH); Same, Estero Nonguén (-36.831501, -73.008374), 13.III.1977, T. Cekalovic coll., 1 ma (MCZ 31275); Same, Cerro Caracol, Mirador Aleman (-36.834167, -73.047778), 15.IX.1968, T. Cekalovic coll., 1 ma, 3 fe (MZSP 9965); Same, *Provincia de Arauco*, Parque Nacional Nahuelbuta (-37.800000, -73.033333), 30.XI.2003, I. Avila, S. Ocares & D. Silva coll., 1 ma (CAS 9055050); Same, Parque Nacional Nahuelbuta (-37.8043374259, -73.0344813614, date or collector unknown, 1 ma, 1 fe (CAS 9052227); Same, Parque Nacional Nahuelbuta (-37.827500, -73.009722), 9.XII.2010, F. Marques, F.

Cadiz & F. Carbayo coll., 5 ma (MZSP 36839); Same, Parque Nacional Nahuelbuta, (-37.827500, -73.009722), 9.XII.2010, F. Marques, F. Cadiz & F. Carbayo coll., 6 ma, 1 fe (MZSP 36840); Same, Cayucupil, Pichinahuel, 23.XII.1976, collector unknown, 1 ma (AMNH); Same (-37.766667, -73.333333), 9.II.1965, T. Cekalovic coll., 1 ma (MZSP 27695). Región de Nuble, *Provincia Diguillín*, Chillán, Las trancas Nuble, XII.1976, collector unknown, 1 ma, 3 fe (AMNH); Same, ?.XII.1976, collector unknown, 1 ma, 2 fe (AMNH); Same, 11–17.I.1983, L.E. Pena coll., 1 ma (AMNH); Same, XII.1974, collector unknown, 1 ma, 3 fe (AMNH); Same, Las Trancas, (-36.600, -72.117), I.1967, L. Peña coll, 1 ma (MCZ 38272); Same, Los Lleuques (-36.85800, -71.61700), 11–7.V.1975, G. Moreno coll., 1 ma, 4 fe (MCZ 3125). Región de Araucanía, *Provincia de Cautín*, 27.I.1985, N.I. Platnick & O.F. Francke coll., 1 ma (AMNH); Same, 6.XII.1992, T. Cekalovic & S. Gonzalez coll., 1 ma (AMNH); Same, Fundo de las Selvas, 16–20.II.1981, L.E. Pena coll., 3 ma, 1 fe (AMNH); Same, Fundo de las Selvas, 16–20.II.1981; L.E. Pena coll., 3 ma, 1 fe (AMNH); Same, Villarrica (-39.03, -72.121), 1–30.I.1965, L. Peña coll., 1 ma (MCZ 38265); Same, (-39.03, -72.121), 1–30.I.1965, L. Peña coll., 5 ma (MCZ 31263); Same, 1 ma (MCZ 31264); Same, 6 fe, 4 ma (MCZ 31232); Same, 1 ma, 3 fe (MCZ 31270); Same, Flor del Lago Ranch (-39.2044664427, -72.1279383487), 11.XII.2003, I. Avila & D. Silva coll., 1 ma, 2 fe (CAS 9055035); Same, 2 ma (CAS 9055009); Same, Pucón, 12.I.1951, E. Ross & A. Michelbacher coll., 3 ma, 7 fe (CAS 9055052); Same, Angol, Sierra Nahuelbuta, 13.I.1951, E. Ross & A. Michelbacher coll., 1 ma (CAS, 9055400); Same, Angol (-37.829000, -73.007278), 25–27.XII.2016, A. Anker & P.H. Martins coll., 1 fe (UFMG 22643); Same, 2 fe (UFMG 22644); same, 1 ma (UFMG 22645); Same, 1 ma, 1 fe (UFMG 22646); same, 2 fe (UFMG 22647); Same, 1 ma (UFMG 22649); Same, Temuco, 8.I.1951, E. Ross & A. Michelbacher coll., 1 ma (CAS 9052224); Same, Cerro Ñielol (-38.726389, -72.590833), 26.I.2010, R. Pinto-da-Rocha, F. Cádiz L. & D. Cádiz L. coll., 5 ma, 5 fe (MZSP 36836); Same, *Provincia de Malleco*, Caracatín, VI.1975, collector unknown, 1 ma, 1 fe (AMNH); Same, Purén, Monumento Natural Contulmo, (-38.01256, -73.18517), 12.XI.2014, G. Giribet, G. Hormiga & A. Pérez-González coll., 1 ma, 1 fe (MCZ 138066); Same, Monumento Nacional Contulmo (-38.012778, -73.187500), 12.XII.2010, F. Marques, F. Cádiz & F. Carbayo coll., 9 ma, 10 fe, 3 juvs. (MZSP 36967). Región de Los Lagos, *Provincia de Llanquihue*, 13.II.1994, T. Cekalovic coll., 6 ma, 9 fe (AMNH). Región de Los Ríos, *Provincia de Valdivia*, date or collector unknown, 2 ma, 4 fe (SMF 783); Same, 2 ma, 3 fe (SMF 778); Same, 28.II.1993, T. Cekalovic coll., 2 ma (AMNH); Same, (-39.81389, -73.24583), 15–20.XI.1978, E. Krahmer coll., 3 ma, 4 fe (MCZ 31274); Same, Panguipulli, Puerto Fuy, 24.II.1978, collector unknown, 1 ma (AMNH); Same, Valdivia, Isla Teja (-39.81389, -73.24583), 6.III.1965, H. Levi coll., 1 ma (MCZ 31231).

Diagnosis. *Sadocus asperatus* resembles *S. ingens*, *S. polyacanthus*, and *S. dilatatus* by the bifid prodorsal apical apophysis on coxa IV. *S. asperatus* can be distinguished from the latter species by the combination of the following characters: lateral margin of dorsal scutum covered by granules; trochanter IV with a blunt retro-dorsal apical apophysis being half of the podomere length, and a rhombus retro-ventral apical tubercle; femur IV curved (in dorsal view), with a retro-lateral row of spiniform apophysis (the middle one longest).

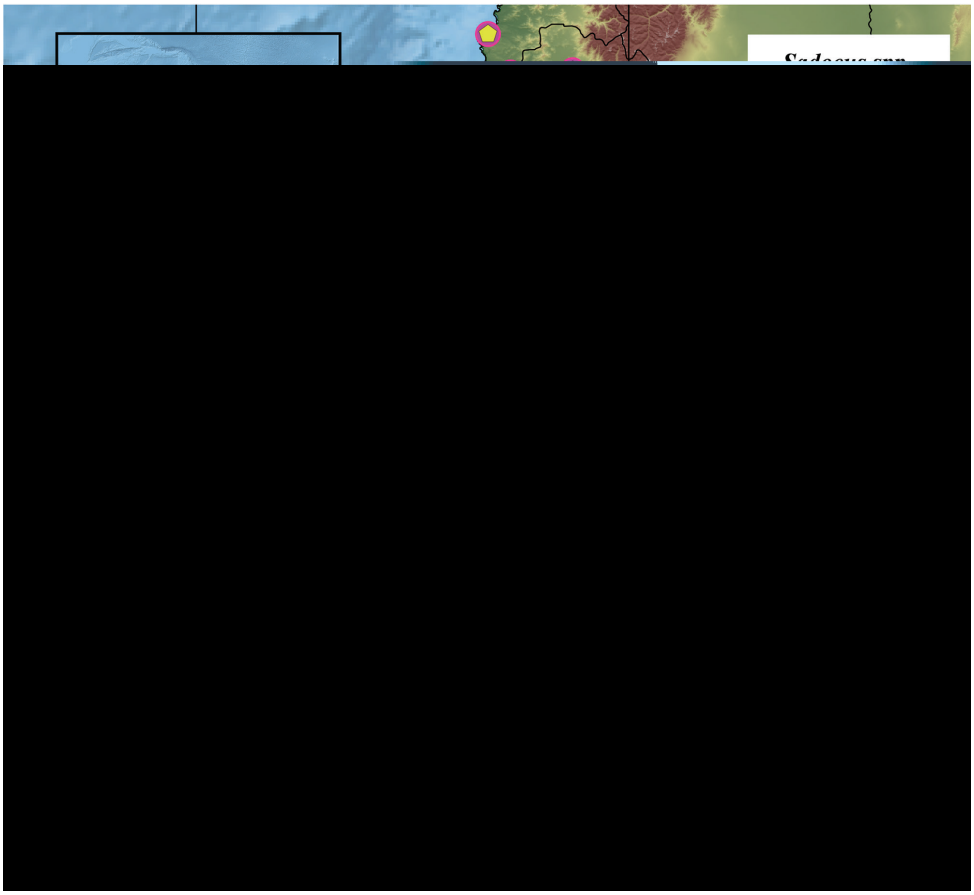

Figure 2. Geographical records of distribution of *Sadocus* species.

Redescription. Male (CAS 9055035). Measurements. Dorsal scutum maximum length 6.3; dorsal scutum maximum width 7.2; prosoma maximum length 2.5; prosoma maximum width 3.2; leg femora I 3.2; II 6.5; III 5.5; IV 7.2. ***Dorsum*** (Fig. 3A). Dorsal scutum type gamma triangular. Carapace with granules sparsely distributed. Scutal areas I–IV with eight, four, two and four granules, respectively; scutal area III with one pair of paramedian spiniform tubercles; scutal area IV incompletely divided. Lateral margin of dorsal scutum mostly covered in granules (from posterior half of carapace to posterior margin of dorsal scutum). Posterior margin of dorsal scutum and free tergite I each with a pair of paramedian tubercles. ***Chelicerae.*** Segment I with basal tubercle, bulla with small setae, each finger with five teeth. ***Pedipalps.*** Coxa dorsal face smooth, ventral face with two apical tubercles. Trochanter dorsal and ventral faces smooth. Femur ventral face granulate. Patella with sparsely distributed setae. Tibial setation: prolateral IiiiIi/IiiiIi; retro-lateral iIiIi/IiIi. Tarsal setation: prolateral and retro-lateral IiIi/IiIi. ***Legs*** (Fig. 3B–E). Coxa IV with one long, oblique, bifid prodorsal apical apophysis and one retro-ventral apical spine. Trochanters I and II each with one pair of prodorsal spiniform tubercles. Trochanter III with one medio-ventral

tubercle and three retro-lateral ones. Trochanter IV prodorsal and proventral faces with few granules, the prodorsal apical apophysis long (ca. half the podomere length); retro-lateral face with one basal, one central, and one apical tubercles; one retro-dorsal apical spiniform apophysis (ca. ¼ podomere length); ventral face with setiferous tubercles sparsely distributed. Femur III with one retro-basal tubercle. Femur IV sigmoid, with dorsal row of apophysis on the basal half abruptly decreasing in size apically, becoming granules; prolateral row with central–subapical tubercles; retro-lateral row of granules with spiniform apophysis (basal most and central one longer than the others, apical most oblique, curved ventrad); ventral face with two short retro-lateral sub-apical spiniform apophyses and one proapical spiniform apophysis. Patella IV ventral face mostly smooth, with one probasal, one proapical and one retro-apical large, spiniform tubercles. Tibia IV roughly with two ventral rows of granules increasing in size from central to apical becoming spines. Tarsal counts: 6, 9, 7, 8. ***Penis*** (Fig. 11A, B). Ventral plate of penis with moderate cleft on anterior margin, three pairs of MS A, one pair of MS B, four or five pairs of MS C and one pair of MS D, without MS E.

Coloration. Immersed in ethanol: carapace, trochanter–patella IV brown, tibia light brown, legs I–III, pedipalps, and chelicerae yellowish-brown. Live specimens (Fig. 9A–C, E): carapace, coxa, and trochanter black, light gray spot (inverted T shape) from ocularium to scutal area II; femora I–III orange; patellae–tibiae I–IV brown.

Variations (n = 56). Scutal area I–IV tubercles (5 minimum, 16 maximum per site), Measurements. Dorsal scutum maximum length 6.0–8.5; dorsal scutum maximum width 6.7–11.6; prosoma maximum length 2.5–3.5; prosoma maximum width 3.2–4.8; leg femora: I 3.2–5.0; II 6.5–10.0; III 5.5–8.5; IV 7.2–11.0.

Female (CAS 9055035). Measurements. Dorsal scutum maximum length 6.3; dorsal scutum maximum width 8.1; prosoma maximum length 2.6; prosoma maximum width 3.7; leg femora: I 3.7; II 7; III 6.1; IV 7.2.

Redescription. ***Dorsum*** (Fig. 8A, B). Scutal areas I, II, and IV with three, five, and two granules, respectively. ***Legs.*** Coxa IV with one prodorsal apical apophysis and one retro-ventral apical spine shorter than on the male, trochanter IV with retro-lateral row of tubercles, the apical one longest, femur IV with pro- and retro-ventral rows of tubercles, patella–metatarsi IV unarmed. Tarsal counts: 6, 9, 7, 8. ***Ovipositor*** (Fig. 12A–C). Two main groups of lobes delimited by a constriction, ovipositors peripheral setae inserted into sockets that are a mixture of dorsal and ventral sockets, the dorsal lobe with five setae and the ventral one with six; each main group of lobes divided by a fissure.

Variations (n = 66). Tubercle variation in the scutal areas: I 2–7; II 1–8; III 2–8; IV 3–5. Free tergites I–III each with one pair of blunt or pointed spiniform tubercles. Measurements. Dorsal scutum maximum length 5.9–8.2; dorsal scutum maximum width 8.0–9.6; prosoma maximum length 2.4–3.5; prosoma maximum width 3.7–4.5; leg femora: I 3.5–4.5; II 6.7–8.7; III 5.7–7.0; IV 7.0–8.9.

Type locality. Of *Gonyleptes asperatus* and *Gonyleptes subsimilis*: CHILE. Of *Discocyrtus calcitrosus*: CHILE, Región de Los Rios, *Provincia de Valdivia*, Corral.

Geographical distribution (Fig. 2). Chile, Región de Los Ríos, *Valdivia*, Corral; Región Metropolitana de Santiago, *Santiago*; Región de Valparaíso; Región de

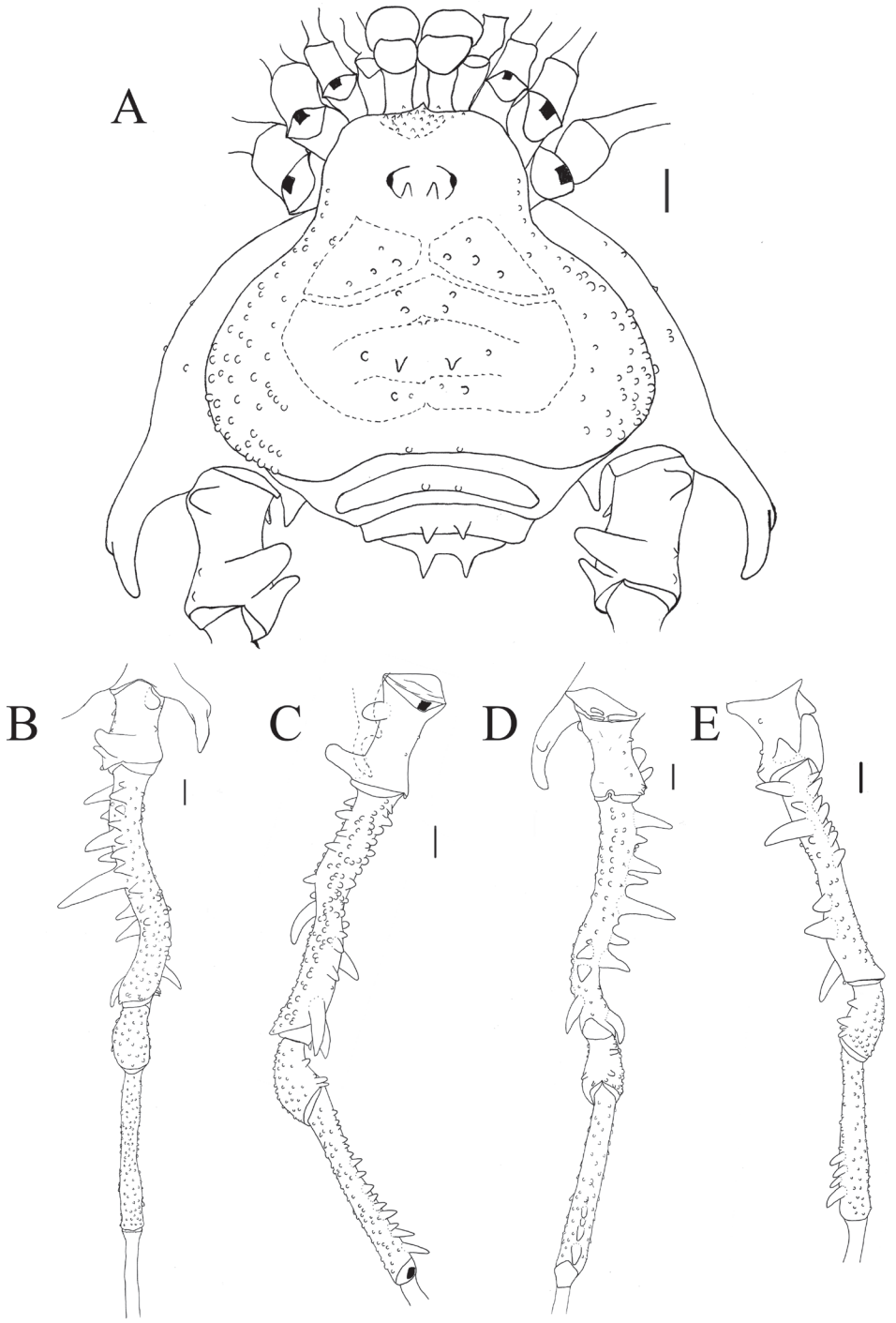

Figure 3. *Sadocus asperatus* (Gervais). Male (CAS 9055035) **A** Habitus, dorsal view **B–E** right leg IV, Trochanter–tibia IV **B** dorsal view **C** prolateral view **D** ventral view **E** retro-lateral view. Scale: 1 mm.

Biobío, *Provincia de Concepción*, *Provincia de Arauco*, *Provincia de Nuble*; Región de Araucanía, *Provincia de Cautin*, *Provincia de Malleco*; Región de Los Lagos, *Provincia de Llanquihue*.

Taxonomic notes. After examining the original description and the drawing of *Gonyleptes bicornis*, we concluded that it is of a male of *S. asperatus*. In the original description, the spines on the free tergite, the two apical apophyses on the trochanter IV and uneven spines in the inner part of the "leg" (referring to the femur IV) are mentioned. Those characters lead us to conclude that it is *S. asperatus*.

Sadocus dilatatus Roewer, 1913

Figures 2, 4A–E, 8C, D, 9D, 11G, H

Sadocus dilatatus Roewer, 1913: 249, fig 102 [desc]; 1923: 493–494, fig 620 [rdesc]; Canals 1936: 70 [cat]; Soares and Soares 1949: 211 [cat]; Cekalovic 1968: 7 [cat]; Acosta 1996: 223 [cat]; Kury 2003: 191 [cat]; Kury et al. 2020b [cat] (SMF RI, 886, ma holotype – examined).

Lycomedicus dilatatus: H. Soares, 1968: 264 [rdesc]; Cekalovic 1985: 18 [cat].

Material examined. Chile, Región de Biobío, *Provincia Concepción*, date or, collector unknown, 1 ma (SMF 886 – Holotype); Same, 1.XI.1964, T. Cekalovic coll., 2 ma, 1 fe (MZSP 7875); Same, Quebrada Pinares, 4.XI.1964, T. Cekalovic coll., 1 ma (MZSP 7876); Same, Reserva Nacional Nonguén (-36.878430, -72.994350), G. Giribet, G. Hormiga & A. Pérez-González coll., 11.XI.2014, 1 ma, 2 fe (MCZ 140078).

Diagnosis. *Sadocus dilatatus* resembles *S. polyacanthus* by the lesser-armed femur IV (compared to other species) and by the posterior large tubercle on the lateral margin of dorsal scutum. *Sadocus dilatatus* can be distinguished from the other species of the genus by the single retro-ventral central apophysis on femur IV and the very long prodorsal apical apophysis on coxa IV (ca. ⅔ of the scutum width).

Redescription. Male (SMF 886). ***Measurements.*** Dorsal scutum maximum length 7.5; dorsal scutum maximum width 10.4; prosoma maximum length 3.2; prosoma maximum width 4.2; leg femora: I 6.0; II 13.0; III 10.3; IV 11.0. ***Dorsum*** (Fig. 4A). Dorsal scutum type gamma triangular. Anterior margin of dorsal scutum with median frontal hump bearing six tubercles and three granules on each side. Carapace with granules sparsely distributed. Scutal areas I–IV with 13, 16, eight and six granules, respectively; scutal area III with one pair of paramedian spines; scutal area IV completely divided (from area III). Lateral margin of dorsal scutum mostly covered by granules (from the posterior half of carapace to posterior margin of dorsal scutum), with one large tubercle near scutal area IV. Posterior margin of dorsal scutum and free tergite I each with few granules on the corners. ***Chelicerae.*** Segment I with one seta on mesal side of the bulla, each finger with five or six teeth. ***Pedipalps.*** Coxa mostly

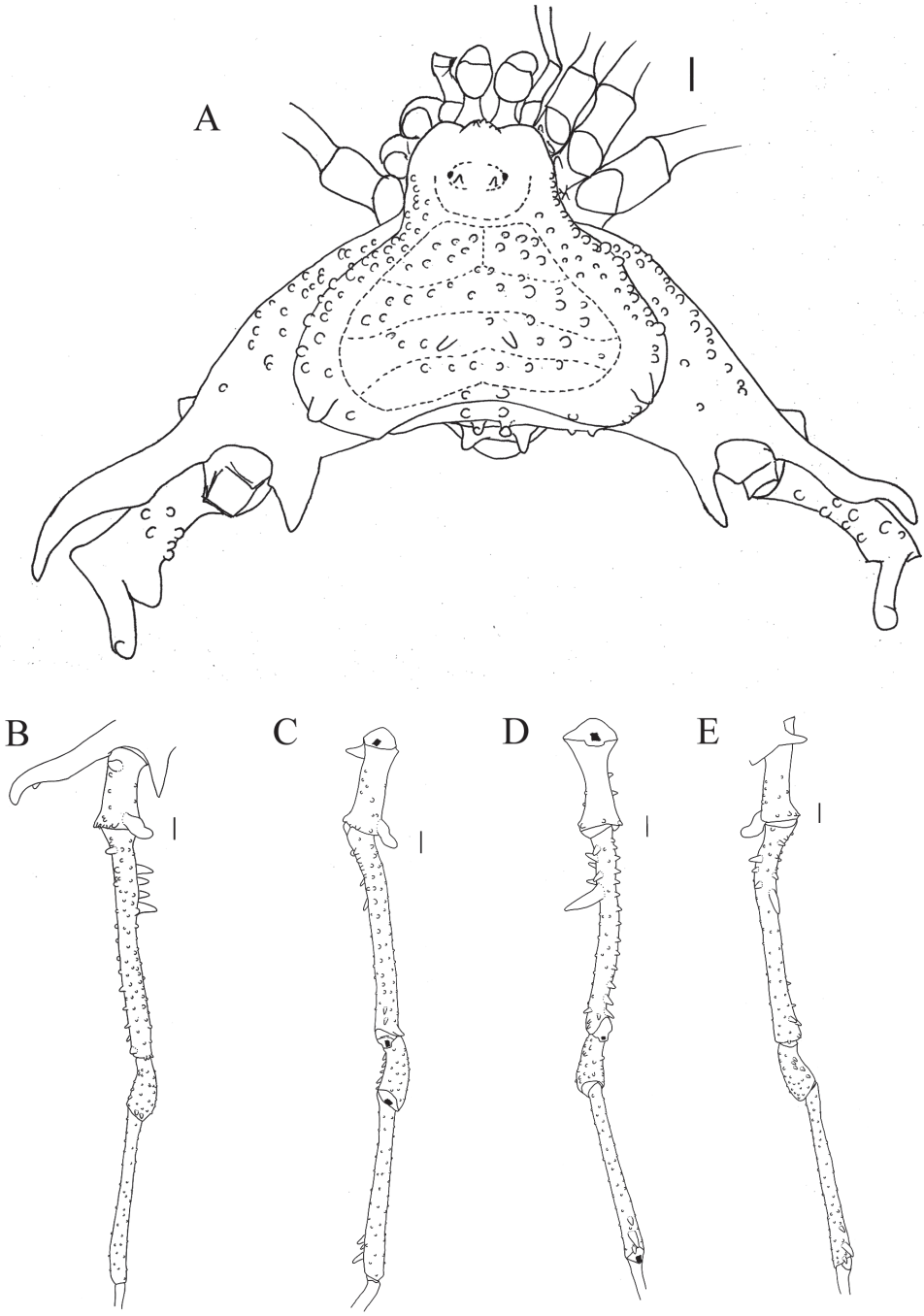

Figure 4. *Sadocus dilatatus* Roewer. Male holotype (SMF 886) **A** habitus, dorsal view **B–E** male left trochanter–tibia IV **B** dorsal view **C** prolateral view **D** ventral view **E** retro-lateral view. Scale bars: 1 mm.

smooth, with one ventro-central tubercle. Trochanter dorsal face smooth, with one retro-ventral apical tubercle and one retro-apical spine. Femur dorsal face smooth, ventral row of few granules and one retro-ventral spine. Patella smooth. Tibial setation: prolateral Iiii/IiiIi; retro-lateral IiIi/IiIi. Tarsal setation: prolateral IiIii/IiIi; retro-lateral iiIiIii/iIiIii. ***Legs*** (Fig. 4B–E). Coxa IV with one long, oblique, bifid prodorsal apical apophysis and one retro-ventral apical spine. Trochanters I–III granulate; trochanter III with one retro-apical spine. Trochanter IV with sparse granules, the prodorsal apical apophysis long, (ca. ⅓ of podomere length), pointing prolaterad. Femur III with proventral and retro-ventral rows of granules increasing in size apically, becoming tubercles. Femur IV with three blunt dorsal spines on basal ⅓; proventral row of pointed granules increasing in size apically becoming spines; retro-lateral row with two spines and one central apophysis and one proventral basal spine. Patella IV with ventral row of tubercles. Tibia IV with three retro-ventral apical spines (apical one the largest). Tarsal counts: 6, 11, 7, 10. ***Penis*** (Fig. 11G, H). Ventral plate of penis with attenuated cleft on anterior margin; three pairs of MS A, one pair of MS B, four pairs of MS C, one pair of MS D, and two pairs of ventral MS E.

Coloration. Immersed in ethanol: carapace and leg IV dark brown; legs I–III, pedipalps and chelicerae light brown. Specimen color badly preserved. Live specimens (Fig. 9D): carapace, coxa, and trochanter black, dry-mark on carapace; femora I–III, patellae–tibiae I–IV brown; border of dorsal scutum and free tergite green; free tergite yellowish.

Variations (n = 4). Scutal areas I–IV with 10–13, 14–16, 8–10, 5–6 granules, respectively. In smaller males, the lateral margin of dorsal scutum may bear cluster of tubercles instead of a large tubercle. Measurements. Dorsal scutum maximum length 7.0–8.1; dorsal scutum maximum width 8.5–11.5; prosoma maximum length 3.0–3.4; prosoma maximum width 4.1– 4.4; leg femora: I 5.5–6.5; II 11.4–14.5; III 9.0–11.5; IV 9.7–12.0.

Female (MZSP – 8022). ***Measurements.*** Dorsal scutum maximum length 7.5; dorsal scutum maximum width 8.9; prosoma maximum length 3.4; prosoma maximum width 4.5; leg femora: I 5.0; II 11.4; III 9.0; IV 11.0. ***Dorsum*** (Fig. 8C, D). Lateral margin of dorsal scutum with five slightly large granules. Scutal areas I–IV with ten, twelve, eleven, and seven granules, respectively. ***Legs.*** Coxa IV with moderate prodorsal spiniform apophysis (as long as the podomere width, but shorter than male) and one retro-ventral apical spine shorter than on the male. Trochanter IV with a retro-apical apophysis. Femur III with proventral and retro-ventral row of granules increasing in size apically, becoming tubercles; femur IV with prolateral row of pointed granules on distal half and a retro-lateral row of pointed granules on basal half. Tarsal counts: 6, 11, 7, 9.

Type locality. Chile, Región de Biobío, *Provincia Concepción*.

Geographical distribution (Fig. 2). Chile. Región de Biobío, *Provincia Concepción*, Quebrada Pinares.

Note. The allotype MZSP 7874 was not used for the variation or in the distribution maps because it is a female, which lacks the diagnostic characters of the species (solely based on male characters).

Erratum. H. Soares (1968) incorrectly cited the collection number 7676 for the vial labelled: CHILE, Región de Biobío, *Provincia Concepción*, Quebrada Pinares, 4.XI.1964, T. Cekalovic coll., 1 ma. It is in fact 7876. The vial with number 7875 mentions 2 ma, when in fact, it includes 2 ma and 1 fe, and vial 7874 mentions only 1 ma, when it is in fact 1 fe.

***Sadocus funestus* (Butler, 1874)**
Figures 2, 5A–E, 8E, F, 9F, 11I–J, 12D–F

Gonyleptes funestis Butler, 1874: 153, figs 5, 5a [desc]; Loman 1899: 6, fig 3 [cit]; Sørensen 1902: 20 [cit]. (Type material NHM, ma holotype, examined by detailed photographs).
Discocyrtus funestus: Loman, 1899: 6, fig 3 [syst]; Sørensen 1902: 20 [syst].
Lycomedes funestus: Sørensen, 1902: 20 [syst]; Roewer 1913: 127, 130, fig 58 [rdesc].
Lycomedicus funestus: Roewer, 1923: 443, fig 557 [rdesc]; 1929: 214 [cat]; Canals 1936: 69 [cat]; Soares and Soares 1954: 271 [cat]; Muñoz-Cuevas 1973: 232, fig 4 [cit]; Cekalovic 1968: 7 [cat]; 1985: 18 [cat]; Cokendolpher 1993: 136 [eco].
Sadocus funestis: Kury, 2003: 191 [cat]; Pérez-González et al. 2020: 3 [cit].
Sadocus funestus: Kury et al., 2020b [cat].

Material examined. Chile, Región de Los Ríos, *Provincia de Valdivia*, Corral, date or collector unknown, 1 ma (SMF 766); Same, Valdivia, date or collector unknown, 1 ma (SMF 276); Same, Curiñanco, 12.I.2006, Elizabeth Arias et al. coll., 1 ma, 2 fe, 3 juvs. (AMNH); Same, Oncol Park (-39.70025, -73.0), 12.I.2006, Elizabeth Arias et al. coll., 2 ma, 3 fe (AMNH); Same, 7.II.2004, T. Cekalovic coll., 2 ma (CAS 9026265); Same, 1 ma (AMNH); Same, 10.I.2006, Elizabeth Arias et al. coll., 1 ma, 2 fe (AMNH); Same, 7.II.2004, T. Cekalovic coll., 4 ma, 1 fe (AMNH); Same, (-39.712333, -73.307278), 01.I.2017, A. Anker & P.H. Martins coll., 1 ma (UFMG 22650); Same, 1 ma (UFMG 22651); Same, 2 ma (UFMG 22652); Same, 2 ma (UFMG 22653); Same, on the way to Oncol Park, 15.II.2004, T. Cekalovic coll., 1 ma (AMNH); Same, Chiguayco, I.1980, collector unknown, 1 ma (AMNH); Same, Las Lajas, Las Tablas, 9.I.1989, L.S. Kimsey coll., 1 ma, 3 fe (MCZ 31262); Región da Araucanía, Villarrica (-39.03 -72.121), 1–30.I.1965, L. Peña coll., 1 ma (MCZ 38272); ECUADOR, Canelos [doubtful record], date or collector unknown, 1 ma (SMF 777).

Diagnosis. *Sadocus funestus* can be distinguished from other species of the genus by the following characters: uniramous prodorsal apical apophysis on coxa IV; leg IV straight; and trochanter IV with four apophyses.

Redescription. Male (CAS 9026265). ***Measurements.*** Dorsal scutum maximum length 9.3; dorsal scutum maximum width 10.0; prosoma maximum length 3.9; prosoma maximum width 5.0; leg femora: I 4.5; II 8.3; III 7.0; IV 8.0. ***Dorsum*** (Fig. 5A). Dorsal scutum type gamma pyriform. Dorsal scutum anterior margin with nine granules, lateral margins with a row of granules and cluster of granules near scutal groove I.

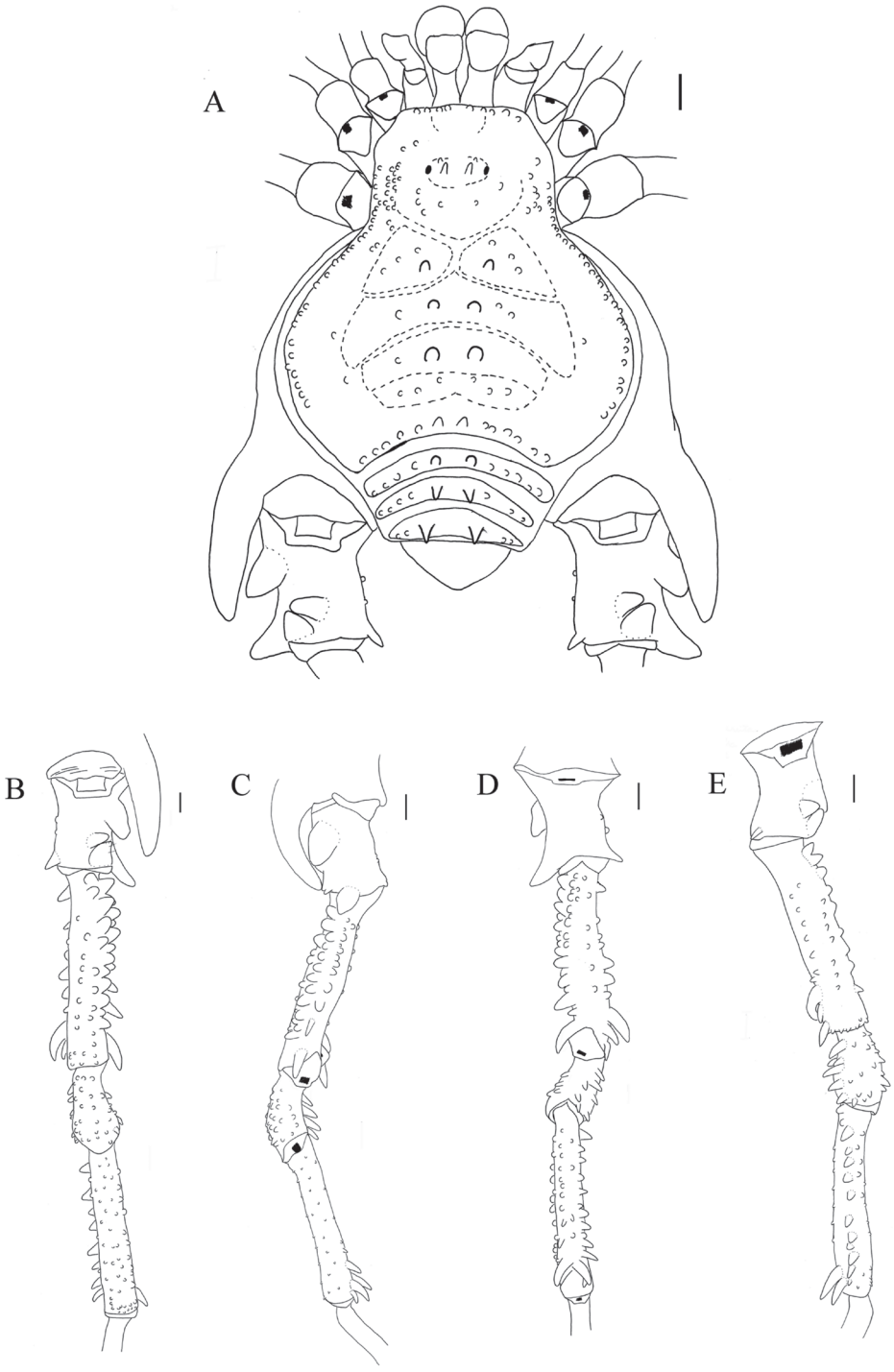

Figure 5. *Sadocus funestus* Butler. Male (CAS 9026265) **A** habitus, dorsal view **B–E** male right trochanter–tibia IV **B** dorsal view **C** prolateral view **D** ventral view **E** retro-lateral view. Scale bar: 1 mm.

Ocularium with one pair of granules on anterior face. Scutal areas I–IV with six (three on each side), three, one, and six granules, respectively; scutal areas I–III each with one pair of paramedian tubercles. Scutal area IV completely divided. Lateral margin of dorsal scutum with row of granules between ozopore area and anterior part of scutal area IV. Posterior margin of dorsal scutum and free tergites I–III each with a row of granules. ***Chelicerae.*** Segment I with setae on bulla; fixed finger with four teeth, movable finger with three teeth. ***Pedipalps.*** Coxa with one ventro-apical spine. Trochanter dorsal face smooth, with one pair of geminated ventro-apical setiferous tubercles. Femur with a row of ventro-basal granules. Patella smooth. Tibial setation: prolateral IiIi/IiiI; retro-lateral iIiIi/iIiIi. Tarsal setation: prolateral IiIii/IiIi; retro-lateral iiIIIiii/iiIiiIii. ***Legs*** (Fig. 5B–E). Coxa IV with one long, oblique, uniramous prodorsal apical apophysis, without retro-ventral apical spine. Trochanters I and III granulate; trochanter III with one retro-apical spine. Trochanter IV proapical spiniform apophysis with large base (ca. ⅓ of podomere length); additionally with two retro-dorsal apical apophyses with the ridges touching each other; retro-lateral face with two central granules and one apical spine. Femur III dorsal face granulate; ventral face with two rows of granules increasing in size apically. Femur IV with prodorsal row of large tubercles decreasing in size apically; prolateral row of tubercles; one retro-ventral row of granules; proventral row of granules increasing in size apically; one proventral apical spiniform apophysis, one retro-sub-apical spiniform apophysis, and two or three retro-ventral apical apophyses. Patella IV with five retro-ventral spines. Tibia III with ventral row of tubercles. Femur IV with retro-lateral row of spines and four ventro-apical spines. Tarsal counts: 6, 12, 7, 8. ***Penis*** (Fig. 11I, J). Ventral plate of penis with deeper (than moderate) cleft on anterior margin, three pairs of MS A, four pairs of MS C, one pair of MS D, without MS B or E.

Coloration. Immersed in ethanol: carapace, trochanter, and leg IV brown; legs I–III, pedipalps fading from brown to yellowish. Tubercles and spines of dorsal scutum and free tergites yellowish. Live specimens (Fig. 9F): carapace, coxa, and trochanter black, dry-mark on dorsal scutum; femora I–III, patellae–tibiae I–IV brown; free tergite green.

Variations (n = 21). Granules between lateral margin of carapace and ocularium varying from none to 4–19. Color of granules on carapace range from brown to yellowish. Measurements. Dorsal scutum maximum length 8.3–10.0; dorsal scutum maximum width 8.6–10.5; prosoma maximum length 3.4–4.0; prosoma maximum width 4.7–5.5; leg femora: I 4.5–5.0; II 8.3–9.4; III 7.0–7.9; IV 7.5–8.5.

Female (AMNH CHILE, Región de Los Rios, *Provincia Valdivia*, Parque Oncol, 10.I.2006, Elizabeth Arias et al. coll., 1 ma, 2 fe). ***Measurements.*** Dorsal scutum maximum length 8.4; dorsal scutum maximum width 10.0; prosoma maximum length 3.4; prosoma maximum width 5.0; leg femora: I 5.0; II 9.5; III 7.8; IV 9.7. ***Dorsum*** (Fig. 8E, F). Lateral margin of dorsal scutum with two rows of tubercles. ***Legs.*** Coxa IV with short prodorsal apical apophysis, seen in a ventral view. Trochanter IV prolateral and dorsal faces unarmed, with one retro-lateral spiniform apophysis. Femora III–IV with a prolateral and a retro-lateral rows of tubercles, increasing in size apically. Tarsal counts: 5, 11, 7, 8.

Variations (n = 8). Dorsal scutum with 10–24 granules, the armature on the free tergites varying from one paramedian pair of blunt to pointed tubercles. Measurements. Dorsal scutum maximum length 5.5–8.3; dorsal scutum maximum width 8.7–10.0; prosoma maximum length 3.4–3.5; prosoma maximum width 4.5–5.0; leg femora: I 4.8–5.0; II 9.0–9.5; III 7.5–7.8; IV 9.3–9.7.

Geographical distribution (Fig. 2). Chile, Región de Los Ríos, Provincia de Valdivia, Curiñanco & Chiguayco. The record for Ecuador is doubtful (Kury 2003).

Sadocus ingens **(Mello-Leitão, 1937)**
Figures 2, 6A–E, 8G, H, 10A, B, 11C, D, 12G–I

Carampangue ingens Mello-Leitão, 1937: 152–153, figs 14–15 [desc]; B. Soares 1945: 370 [cat]; Mello-Leitão 1949: 17 [syst]; Soares and Soares 1954: 242 [cat]; Cekalovic 1968: 7 [cat]; 1985: 17 [cat] (type MNRJ 5263, 1 ma, 1 fe, syntype, previously preserved in dry collection, examined).

Sadocus ingens: Kury, 2003; 191 [cat]; Kury et al. 2020b [cat].

Jighas vastus Roewer, 1943: 28, pl. 3, fig 22 [desc]; Mello-Leitão 1949: 17 [syst]; Acosta 1996: 217 [cat]. (type SMF RII 1380/73, 2 ma, 2 fe, syntypes, examined). Synonymy established by Mello-Leitão 1949.

Material examined. Chile, Región de Araucanía, *Provincia de Malleco*, Contulmo Natural Monument (-38.012778, -73.187500), 12.XII.2010, F. Marques, F. Cadiz & F. Carbayo coll., 1 ma, 1 fe (MZSP 36965); Same, Purén, Salto el Rayen (-38.013528, -73.162639), 04.I.2017, A. Anker & P.H. Martins coll., 1 ma (UFMG 22654); Same, 1 ma (UFMG 22655); Same, *Provincia de Cautín*, Temuco, 1943, collector unknown, 2 ma, 2 fe (SMF 1380/73); Same, Región de Biobío, *Provincia de Arauco*, Carampangue, 1937, W. Feed coll., 1 ma 1 fe (MNRJ 5263 – Syntypes).

Diagnosis. *Sadocus ingens* can be distinguished from the other species of the genus by being the largest among them (and quite large among gonyleptid harvestmen); by the prodorsal apical apophysis on trochanter IV of the same length as the podomere (in other *Sadocus* species, that apophysis length is up to ½ the podomere length); lateral margin of dorsal scutum smooth posterior to scutal area II.

Redescription. Male (MZSP 36965). ***Measurements.*** Dorsal scutum maximum length 12.0; dorsal scutum maximum width 15.5; prosoma maximum length 4.5; prosoma maximum width 7.2; leg femora: I 8.7; II 17.4; III 11.7; IV 19.4. ***Dorsum*** (Fig. 6A). Dorsal scutum type gamma pyriform. Anterior margin of dorsal scutum with 13 granules, lateral margin of dorsal scutum with three to nine granules on carapace, seven granules behind ocularium. Scutal areas I–IV with four or five, nine, six, and four granules, respectively; scutal area III with one paramedian pair of spines. Scutal area IV completely divided by fading scutal groove IV. Lateral margin of dorsal scutum and free tergites I and II with three or four, eight and two granules, respectively. Free tergite III smooth. ***Chelicerae.*** Segment I with one probasal spine on bulla, one retro- and

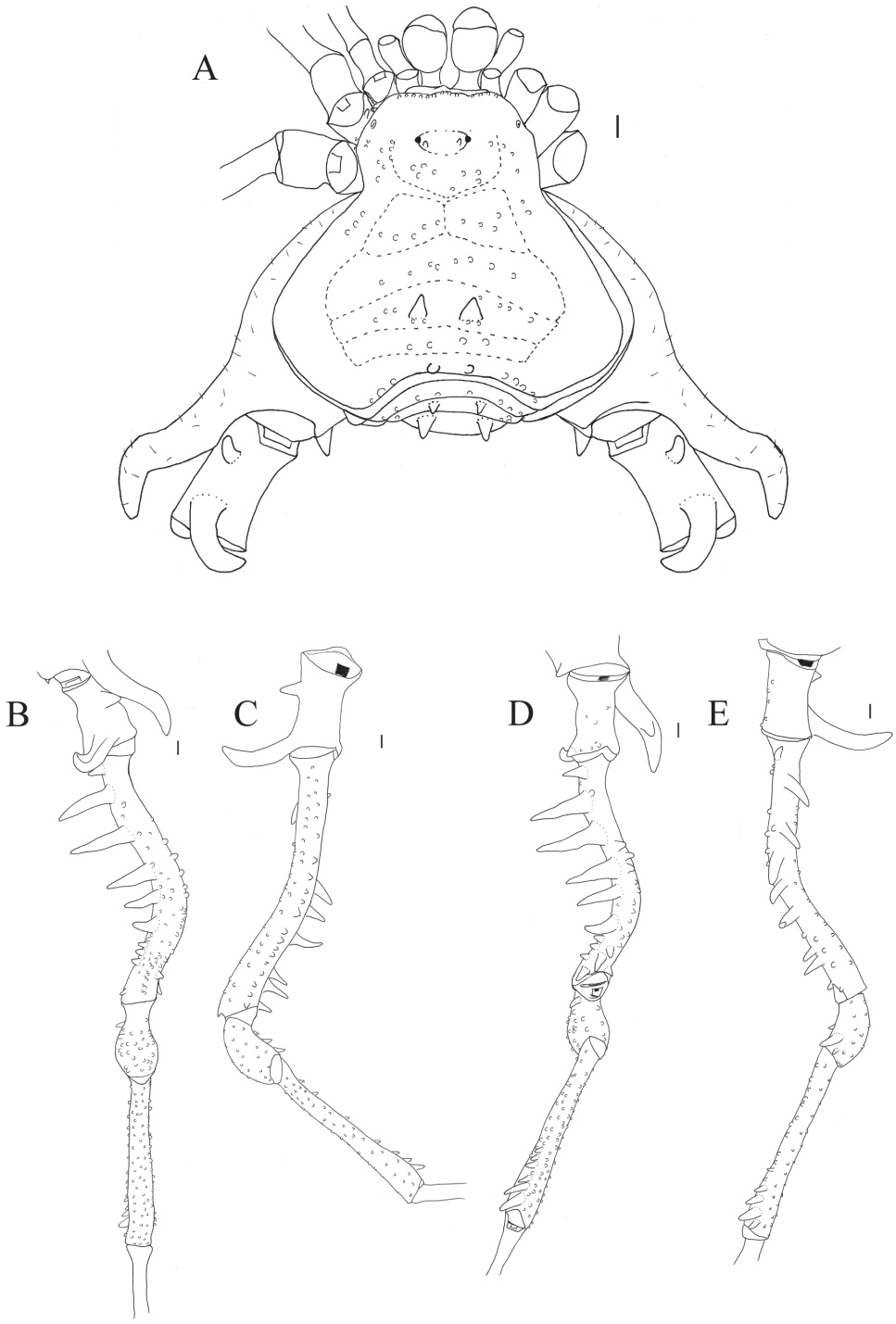

Figure 6. *Sadocus ingens* (Mello-Leitão). Male (MZSP 36965) **A** habitus, dorsal view **B–E** male right trochanter–tibia IV **B** dorsal view **C** prolateral view **D** ventral view **E** retro-lateral view. Scale bars: 1 mm.

one prolateral pair of filiform spines; segment II, fixed finger with four teeth, movable finger with three teeth. ***Pedipalps.*** Coxa smooth and barely visible. Trochanter ventral face with one retro-apical tubercle and one prolateral spine. Femur dorsal face granulate, one ventro-basal tubercle, retro-ventral row of granules and a ventral row of tubercles. Patella smooth. Tibial setation: prolateral IiIi/IiiIi; retro-lateral iIiIi. Tarsal setation: prolateral iIiIi; retro-lateral iIiIii/iiIiIii. ***Legs*** (Fig. 6B–E). Coxa IV covered by setae, with one robust, long, bifid prodorsal apical apophysis and one short retro-ventral spiniform apophysis. Trochanters I–III granulate; trochanters I and III dorsal face smooth. Trochanter IV with few granules on ventral central and apical areas; one retro-lateral tubercle; the prodorsal apical apophysis long, curved, as long as the podomere length. Femur IV with retro-lateral row of spines (five prominent) decreasing in size apically, becoming blunt tubercles; retro-ventral row of granules with one basal pointed tubercle, few tubercles on the middle ⅓ and two spines on apical area; ventro-apical face with one retro-lateral spine and one pointed, prolateral tubercle. Patella IV with three or four retro-ventral spines. Tibia IV dorsal face granulate and with retro-ventral row of granules increasing in size apically, becoming spines on distal half. Tarsal counts: 8, 16, 8, 8. ***Penis*** (Fig. 11C, D). Ventral plate of penis with moderate cleft on anterior margin, two or three pairs of MS A, four or five pairs of MS C and one pair of MS D.

Coloration. Immersed in ethanol: carapace, trochanters, femora, patella IV, and tibia IV dark brown. Scutal areas II and III, free tergites, patellae and tibiae I–III orange. Live specimens (Fig. 10A, B): carapace, scutal areas and legs I–IV black; lateral margin of dorsal scutum dark brown with green pleurites; posterior margin of dorsal scutum and free tergites orange, arthrodial membranes green.

Variations (n = 6) – Free tergites II and III with one paramedian pair of spines which length varies from similar to slightly longer than the tergite length, its apex varying from blunt to pointed; femur IV with granules in between the retro-lateral spines. Measurements. Dorsal scutum maximum length 12.0–13.8; dorsal scutum maximum width 12.7–16.5; prosoma maximum length 4.5–5.4; prosoma maximum width 7.2–7.8; leg femora: I 8.7–10.0; II 16.8–18.5; III 11.7–15.0; IV 16.0–20.0.

Female (MZSP 36965). ***Measurements.*** Dorsal scutum maximum length 12.0; dorsal scutum maximum width 11.5; prosoma maximum length 5.0; prosoma maximum width 7.0; leg femora: I 8.4; II 16.2; III 12.0; IV 17.0. ***Dorsum*** (Fig. 8G, H). Scutal areas I–IV with six, six, four, and four granules, respectively. ***Legs.*** Coxa IV with discreet apophysis, not seen in ventral view. Tarsal counts: 8; 15; 8; 9. ***Ovipositor*** (Fig.12 G–I). Two main groups of lobes delimited by constriction, ovipositors peripheral setae inserted into sockets that are a mixture of dorsal and ventral sockets, left lobe with six setae and right lobe with six. Each main group of lobes divided by a fissure.

Variations (n = 4). Tubercle variation in the areas: I–2–8, II–4–6, III–3–6, IV–2–4. Measurements. Dorsal scutum maximum length 11.0–12.0; dorsal scutum maximum width 10.0–11.7; prosoma maximum length 4.5–5.0; prosoma maximum width 6.4–7.2; leg femora: I 7.1–8.4; II 13.8–16.2; III 11.0–12.0; IV 13.0–17.0.

Type locality. Chile, Región de Araucanía, Provincia de Malleco, Monumento Nacional Contulmo.

Geographical distribution (Fig. 2). Chile. Región de Araucanía, Provincia de Cautín; Idem, Provincia de Malleco, Temuco; Región de Biobío, Provincia de Arauco.

***Sadocus polyacanthus* (Gervais, 1847)**
Figures 2, 7A–E, 8I, J, 10C–F, 11E, F, 12J–L

Gonyleptes polyacanthus Gervais, 1847: 576 [desc]; 1849: 24, pl. 1, figs 7–7c [rdesc]; Butler 1873: 114 [cat]. (Syntypes MNHN, 1 ma, 1 fe examined by detailed photographs). Transferred to *Sadocus* by Sørensen 1902.

Sadocus polyacanthus: Sørensen, 1902: 14 [syst; rdesc]; Roewer 1913: 245–246, fig 101 [key, rdesc]; 1923: 493, fig 619 [rdesc]; 1930: 381 [cit]; Canals 1934: 6 [cit]; 1936: 70 [cat]; Roewer 1938: 02, 06 [cat]; Mello-Leitão 1939: 625 [cit]; Soares and Soares 1949: 212 [cat]; Ringuelet 1955b: 113 [cit]; 1957: 13, 19 [cit]; 1959: 409, figs XVIII-1, 2 [rdesc]; Cekalovic 1968: 7 [cat]; 1976: 24 [cat]; 1985: 15 [cat]; Acosta and Maury 1998: 569 [cit]; Kury 2003: 191 [cat]; Hara et al. 2012: 38–39 [syst]; Pinto-da-Rocha et al. 2012: 61 [cit]; Pinto-da-Rocha et al. 2014: 18 [syst]; Hara 2016: 106–109 [syst]; Kury et al. 2020b [cat].

Sadocus vitellinosulcatus Sørensen, 1886: 85, pl. 6, fig 7 [desc]. (Type depository unknown, fe). Synonymy with *S. polyacanthus* established by Sørensen 1902.

Gonyleptes platei Loman, 1899: 5, pl. 5, fig 3–3a [desc]. (Holotype ZMB 7843, 1 ma examined). Synonymy with *S. polyacanthus* established by Sørensen 1902.

Araucanoleptes exceptionalis Mello-Leitão, 1946: 5, fig 5 [desc]; Soares and Soares 1949: 160 [cat] (Syntypes – URMU 703, 1 ma, 3 fe examined). Transferred to *Sadocus* by Kury 2003. syn. nov.

Arauconoleptes exceptionalis [spelling mistake]: Cekalovic, 1968: 7 [cat]; 1985: 12 [cat].

Sadocus platei: Moritz, 1971: 207 [cat].

Sadocus conspicillatus Roewer, 1913: 251 – 253, pl. 1, fig 3 [desc]; 1923: 495 [rdesc]; Canals 1936: 70 [cat]; Soares and Soares 1949: 211 [cat]; Cekalovic 1968, 7 [cat]; 1985: 14 [cat]; Pinto-da-Rocha et al. 2012: 61 [cit]; Kury et al. 2020b [cat]. (Syntypes – SMF, 1 ma 1 fe examined). syn. nov.

Sadocus guttatus Sørensen, 1902: 15 [desc]; Roewer 1913: 248 [rdesc]; 1923: 494 [rdesc]; Canals 1936: 70 [cat]; Soares and Soares 1949: 211 [cat]; Roewer 1961: 102 [cit]; Cekalovic 1968, 7 [cat]; 1985: 14 [cat]; Kury 2003: 191 [cat]; Kury et al. 2020b [cat] (Holotype – ZMUC, ma examined). syn. nov.

Sadocus exceptionalis: Kury, 2003: 191 [cat]; Kury et al. 2020b [cat].

Material examined. Chile, Región Metropolitana de Santiago, *Santiago*, date or collector unknown, 4 ma, 2 fe (SMF 1384); Región de Valparaíso, 13.II.89, collector unknown, 1 ma (ZMUC– holotype of *S. guttatus*); Región de Biobío, *Provincia de Arauco*, Parque Nacional Nahuelbuta (-37.805567, -73.03505), 30.XI.2003, I. Avila, S. Ocares & D. Silva coll. (CAS 9055055); Same (-37.806433, -73.036333), date or collector unknown (CAS 9055038); Same (-37.810556, -73.0575), 13.XII.2010, F.

Marques, F. Cádiz & F. Carbayo coll., 4 ma, 4 fe (MZSP 36964); Same (-37.8275, -73.009722), 9.XII.2010, F. Marques, F. Cadiz & F. Carbayo coll., 3 ma (MZSP 36838); Same, *Provincia Concepción*, date or collector unknown, 2 ma (SMF 906; holotype of *S. conspicillatus*); Región de la Araucanía, *Provincia de Vilarrica*, Las Ochocientas (-39.1668, -71.98755), 14.XII.2003, E. Arias & D. Silva et al. coll. (CAS 9055047); Same, *Provincia de Malleco*, Lonquimay, 23–24.XII.1976, collector unknown, 1 ma, 1 fe (AMNH); Same (Las Raices), collector unknown, 1 ma (AMNH); Same, Contulmo Natural Monument, 23.I.1985, N.I. Platnick & O.F. Francke coll., 3 ma, 1 fe (AMNH); Same (-40.73715, -72.31062), 12.XI.2014, G. Giribet, G. Hormiga & A. Pérez-González coll., 2 ma, 3 fe (MCZ 138065); Same, Parque Nacional de Tolhuaca (-38.226111, -71.730833), 18.I.2008, R. Pinto-da-Rocha coll., 4 ma, 3 fe, 1 juv (MZSP 29076); Same, 12.XII.2010, F. Marques, F. Cádiz & F. Carbayo coll., 5 ma, 2 fe (MZSP 36966); Curacatín, Salto del Indio no Rio Cautín (-38.46125, -71.741333), 28.XII.2016, A. Anker & P.H. Martins coll., 1 ma, 1 fe (UFMG 22632); Purén, Salto el Rayen (-38.013528, -73.162639), 04.I.2017, A. Anker & P.H. Martins coll., 1 ma (UFMG 22637); Same, 1 fe (UFMG 22640); Same, 1 ma (UFMG 22641); Same, 1 ma (UFMG 22642); Same, *Provincia de Cautin*, Angol, Parque Nacional Nahuelbuta (-37.829000, -73.007278), 25–27.XII.2016, A. Anker & P.H. Martins coll., 1 ma, 1 fe (UFMG 22628); Same, 1 fe (UFMG 22629); Same, 1 ma (UFMG 22630); Same, 1 fe (UFMG 22631); Same, Fundo de las Selvas, 16–20.II.1981, L.E. Peña coll., 3 ma (AMNH); Same, Vulcão Villarrica, 15–29.XII.1982, A. Newton & M. Thayer coll., 1 ma (AMNH); Same, Villarrica (-39.03 -72.121), 16–31.XII, L. Peña coll., 1 ma, 1 fe (MCZ 38270); Same, 1–30.I.1965, 4 ma, 3 fe (MCZ 38271); Same, 5 ma, 4 fe (MCZ 38273); Same, 4 ma (MCZ 38272); Same, 2 ma (MCZ 31240); Same, Lago Conguillio, Parque Nacional Conguillio (-38.647778, -71.610278), 24–25.I.2010, R. Pinto-da-Rocha, F. Cádiz L. & D. Cádiz L. coll., 8 ma, 1 fe (MZSP 36799); Same, 2 ma, 1 fe (MZSP 36803); Same, Puesco, Parque Nacional Villarica (-39.565000, -71.513889), 22.I.2010, R. Pinto-da-Rocha, F. Cádiz L. & D. Cádiz L. coll., 9 ma, 6 fe (MZSP 36802); Región de Los Lagos, *Provincia de Osorno*, Pucatrihue, 23.III.1963, Tha & Lep coll., (AMNH); Same, Parque Nacional Puyehue, 12–22.II.1979, L.E. Peña coll., 2 ma, 4 fe (AMNH); Same, 5–12.II.1978, collector unknown, 1 ma (AMNH); Same (-40.666389, -72.171944), 15.I.2003, S.E. Lew & K.W. Will coll., 1 ma, 1 fe (CAS 9017709); Same, 31.I.1985, N.I. Platinick & O.F. Francke coll., 2 ma, 1 fe, 1 juv (AMNH); Same, Puyehue, 5–12.II.1978, collector unknown, 1 ma (AMNH); Same (-40.73715 -72.31062), 16.XI.2014, G. Giribet, G. Hormiga & A. Pérez-González coll., 2 ma, 2 fe (MCZ 138128); Same, Puyehue, Parque Nacional Puyehue (-40.665583, -72.175694), 30–31.XII.2016, A. Anker & P.H. Martins coll., 1 ma (UFMG 22633); Same, La Picada, 15–20.I.1980, L.E. Peña coll., 1 ma (AMNH); Same, Entre Lagos, 14–17.II.1978, collector unknown, 1 ma (AMNH); Same, 14–17.II.1978, collector unknown, 1 ma (AMNH); Same, *Provincia de Chiloé*, Ilha Chiloé, Chepu, 2.II.1985, N.I. Platnick & O.F. Francke coll., 1 ma (AMNH); Same, 20.II.2000, T. Cekalovic coll., 2 ma (AMNH); Same, Chepu, 14.II.2002, T. Cekalovic coll., 1 ma (AMNH); Same, Parque Nacional Chiloé (-42.574417, -74.077350), 3.XII.2009, H. Wood, L. Almeida & C. Griswold coll., 1 ma (CAS 9036299); Same, Termas de Puyehue

(-40.7 -72.3; 250 masl), 12.III.1965, H. Levi coll., 4 ma (MCZ 38289); Pucatrihue (-40.54389 -73.71778; near the coast of Osorno), 3–21.III.1967, H. Levi coll., 6 ma, 2 fe (MCZ 38288); Same, XII.1967, L. Peña coll., 3 ma, 13 fe (MCZ 34212); Same, 2 ma (MCZ 38280); Same, 1 ma, 2 juvs (MCZ 38268); Same, 1 ma, 3 fe (MCZ 38282); Same, 1 ma, 2 fe (MCZ 38284); Same, 2 ma (MCZ 31244); Same, 1 ma (MCZ 31242); Same, 2 ma (MCZ 31245); Same, Parque Nacional Puyehue (-40.659722, -72.174167), 21.I.2010, R. Pinto-da-Rocha, F. Cádiz L. & D. Cádiz L. coll., 6 ma, 8 fe, 3 juv (MZSP 36800); Same (-40.659722, -72.174167), 20.I.2010, R. Pinto-da-Rocha, F. Cádiz L. & D. Cádiz L. coll., 1 ma, 1 fe (MZSP 36841); Same, *Provincia de Llanquihue*, Chamiza (-41.467 -72.85), 25.II.1976, T. Cekalovic coll., 4 ma, 6 fe (MCZ 31261); Same, Puerto Montt, Parque Nacional Alerce Andino (-41.593611, -72.593889), 15.XII.2010, F. Marques, F. Cadiz & F. Carbayo coll., 1 ma (MZSP 36842); Same (-41.59351, -72.59359), 15.XI.2014, G. Giribet, G. Hormiga & A. Pérez-González coll., 1 ma (MCZ 138113); Same, Monumento Nacional Lahuen Nadi (-37.810556, -73.057500), 14.XII.2010, F. Marques, F. Cadiz & F. Carbayo coll., 1 ma (MZSP 36837); Same, Los Muermos (-41.329167, -73.825278), 16.XII.2010, F. Marques, F. Cadiz & F. Carbayo coll., 1 ma, 2 fe (MZSP 36801); Región de Los Rios, *Provincia Valdivia*, Parque Oncol (-39.700250, -73.000000), 10.I.2007, E. Arias coll., 1 ma (CAS 9026268); Parque Nacional Oncol (-39.712333, -73.307278), 01.I.2017, A. Anker & P.H. Martins coll., 1 fe (UFMG 22634); Same, 1 fe (UFMG 22635); Same, 1 ma, 1 fe (UFMG 22636); Same, 1 ma (UFMG 22638); Same, 4 ma, 1 fe (UFMG 22639); Same, Rio Bueno, II.1945, R. Vaz-Ferreira coll., (MNHN 703; holotype of *S. exceptionalis*); Same, Neltume, I.1978, collector unknown, 1 ma, 1 fe (AMNH); Same, Parque Oncol, 7.II.2004, T. Cekalovic coll., 2 ma, 1 juv (AMNH); Same, 15.II.2004, T. Cekalovic coll., 2 ma, 2 fe (AMNH); Same, 7.II.2004, T. Cekalovic coll., 2 ma (AMNH); Same, 12.I.2006, Elizabeth Arias coll., 1 ma (AMNH); Same, 12.I.2006, Elizabeth Arias coll., 3 ma, 1 fe (AMNH); Same, Curiñanco, 15.II.2004, T. Cekalovic coll., 2 ma, 2 fe (AMNH); Same, Puerto Fuy, 16–20.II.1978, collector unknown, 1 ma (AMNH); Same (-39.81389 -73.24583), 15–20.XI.1978, E. Krahmer coll., 1 ma (MCZ); Same, Corral (-39.867 -73.433), 30.XII.1905, R. Thaxter coll., 1 ma (MCZ 38279); Same, date or collector unknown, 1 ma, 2 fe (MCZ 38286).

Diagnosis. *Sadocus polyacanthus* resembles *S. dilatatus* by the posterior apophysis on the lateral margin of dorsal scutum, and femur IV almost straight. It is distinguished from the latter by the lack of a long, single retro-central apophysis (present in *S. dilatatus*) on femur IV, and by the presence of prolateral and retro-lateral rows of similar sized tubercles on femur IV and coxa IV being closer to the body (instead of spread to the sides as *S. dilatatus*).

Redescription. Male (CAS 9055047). ***Measurements.*** Dorsal scutum maximum length 8.0; dorsal scutum maximum width 10.0; prosoma maximum length 3.3; prosoma maximum width 4.5; leg femora: I 4.9; II 9.6; III 8.2; IV 8.5. ***Dorsum*** (Fig. 7A). Dorsal scutum type gamma pyriform. Anterior margin of dorsal scutum with 15 granules, few closer to ocularium on carapace, lateral margin of carapace with a row of granules. Three scutal areas; scutal areas I–III with four, five, and eight granules, respectively. Scutal area III with one pair of spines. Lateral margin of dorsal scutum with row

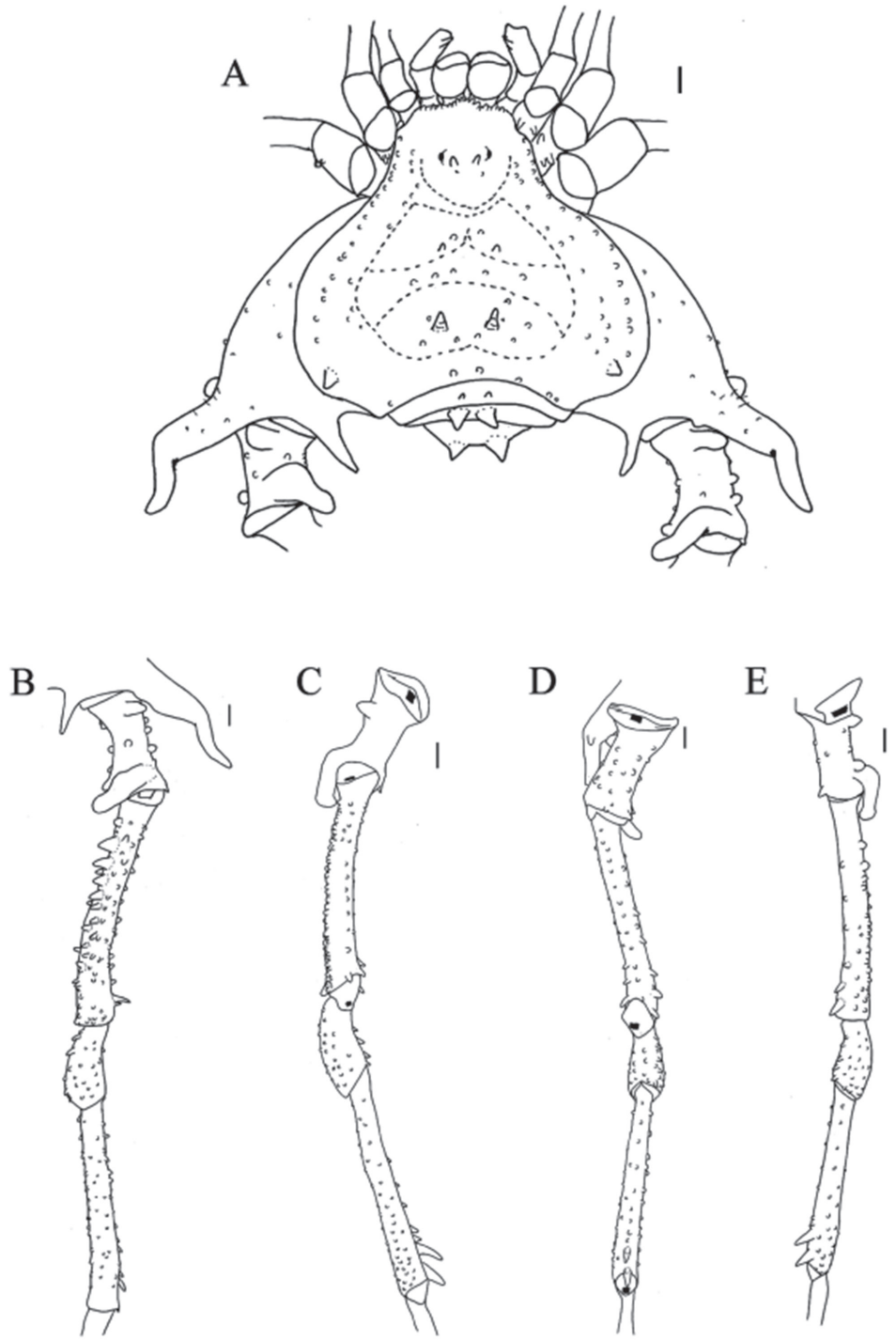

Figure 7. *Sadocus polyacanthus* (Gervais). Male (CAS 9055047) **A** habitus, dorsal view **B–E** male right trochanter–tibia IV **B** dorsal view **C** prolateral view **D** ventral view **E** retro-lateral view. Scale bars: 1 mm.

of granules increasing in size from the ozopore area to scutal area III, ending in a large spiniform tubercle. Posterior margin of dorsal scutum with a row of ten tubercles. ***Chelicerae.*** Segment I with a pair of retro-apical setae; fixed finger with three teeth, movable finger with four teeth. ***Pedipalps.*** Coxa with one central ventral spine. Trochanter with one ventro-apical tubercle. Femur with one ventro-basal seta and three ventro-basal granules. Patella covered with setae. Tibial setation: prolateral IiiIi/IiiiIi; retro-lateral: iIiIi. Tarsal setation: prolateral IiIii; retro-lateral IiIi. ***Legs*** (Fig. 7B–E). Trochanters I–IV granulate; trochanter II with one retro-lateral tubercle; trochanter III with one retro-apical spine; trochanter IV with one dorso-central tubercle, one retro-central tubercle, one retro-apical tubercle, one retro-dorsal apical spine; prodorsal apical apophysis with a rounded apex extending towards the dorsal region. Femur III ventral face with two rows of granules increasing in size apically. Femur IV with retro-dorsal row of spines decreasing in size towards the center; retro-lateral row of sparse spines increasing in size apically; ventro-apical face with a prolateral spine and retro-lateral granule. Patella IV with retro-lateral row of spines, the apical one curved, pointing towards tibia IV. Tibia IV with two retro-ventral apical spines. Tarsal counts: 6, 11, 7, 8. ***Penis*** (Fig. 11E, F). Ventral plate of penis with attenuated cleft on anterior margin; three pairs of MS A, two pairs of MS B, four or five pairs of MS C, two or three pairs of MS D.

Coloration. Immersed in ethanol: carapace, trochanters I–IV and femur IV dark brown. Legs with a gradient from brown to caramel. Live specimens (Fig. 10C–F): carapace, patellae, and tibiae I–IV black, except the areas of dorsal scutum that can vary (yellow, orange or red). Coxa and trochanters black. Femora I–IV varying between black and orange. Posterior margin of dorsal scutum to free tergite III arthrodial membranes green.

Variations (n = 58). Even in ethanol there is a great variation of coloration, which ranges from orange to caramel and yellow. The number of granules on the anterior margin of dorsal scutum varying from few sparsely distributed to completely covered. Measurements. Dorsal scutum maximum length 5.6–9.8; dorsal scutum maximum width 6.0–11.9; prosoma maximum length 2.2–4.0; prosoma maximum width 3.0–5.4; leg femora: I 3.5–6.9; II 6.4–13.0; III 5.3–11.4; IV 6.0–11.5.

Female (AMNH – 11- Chile, Region de Los Lagos, Oncol Parque, 12.I.2006, Luma Arias et al. coll., Berkeley). ***Measurements.*** Dorsal scutum maximum length 9.3; dorsal scutum maximum width 9.4; prosoma maximum length 3.6; prosoma maximum width 5.0; leg femora: I 6.0; II 11.5; III 9.5; IV 11.5. ***Dorsum*** (Fig. 8I, J). Scutal areas I and II with three and five granules, respectively. ***Legs.*** Coxa IV granulate, with short prodorsal apical spiniform apophysis, not visible in ventral view. Trochanter IV with one retro-lateral spiniform tubercle. Tarsal counts: 6, 11, 7, 8. ***Ovipositor*** (Fig. 12J–L). Two main groups of lobes delimited by constriction, ovipositors peripheral setae inserted into sockets that are a mixture of dorsal and ventral sockets, left lobe with four setae and right lobe with six; each main group of lobes divided by a fissure.

Variations (n = 25). Color in dorsal scutum and femur varying between black and orange. Dorsal scutum with 10–30 granules. Measurements. Dorsal scutum maximum

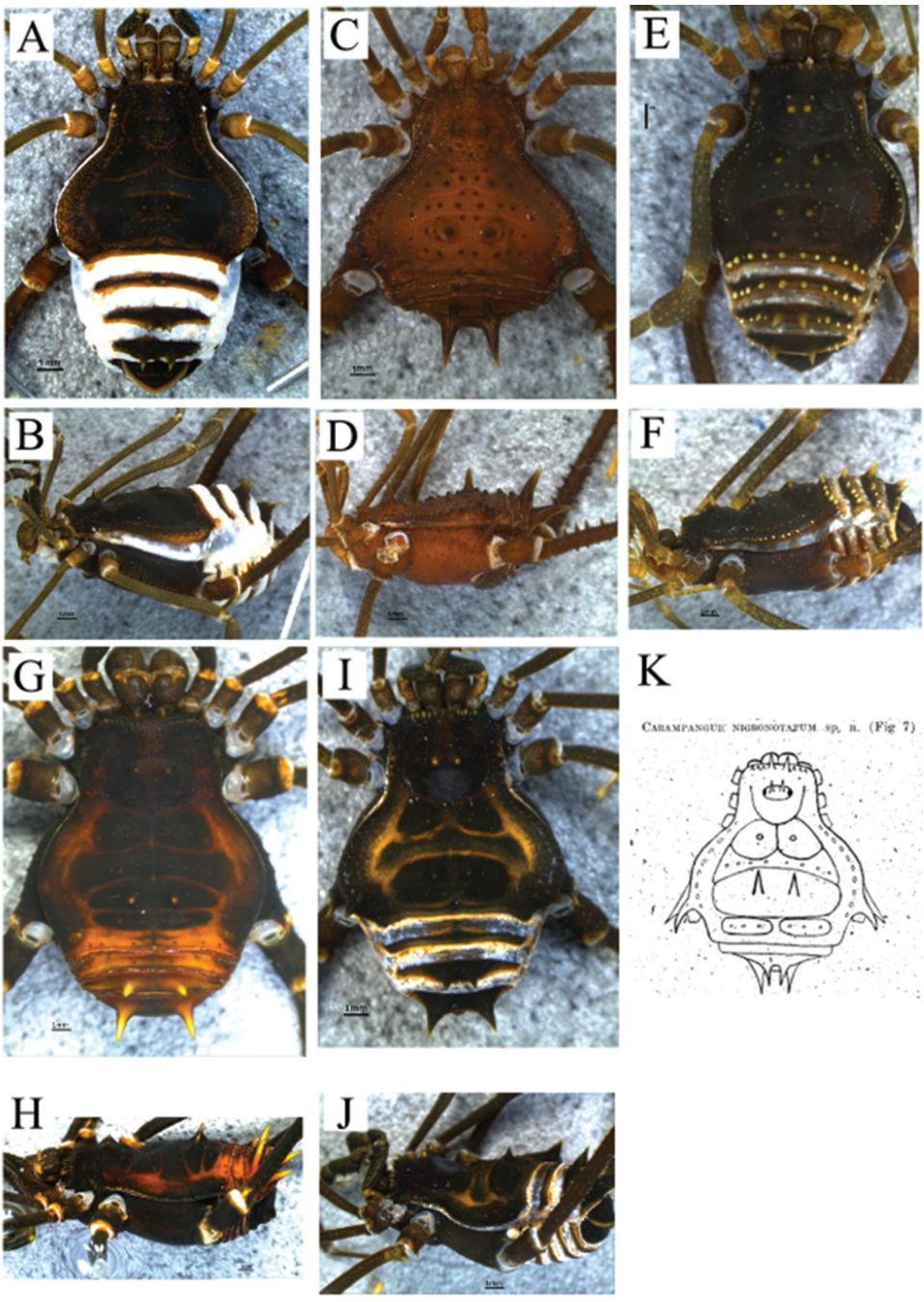

Figure 8. Female specimens of *Sadocus* **A, B** *S. asperatus* (CAS–9055035) **A** dorsal view **B** lateral view **C, D** *S. dilatatus* (MZSP–8022) **C** dorsal view **D** lateral view **E, F** *S. funestus* (AMNH) **E** dorsal view **F** lateral view **G, H** *S. ingens* (MZSP–36965) **G** dorsal view **H** lateral view **I, J** *S. polyacanthus* (AMNH) **I** dorsal view **J** lateral view **K** Drawing of species inquirenda *Carampangue nigronotatum* extracted from Mello-Leitão 1943.

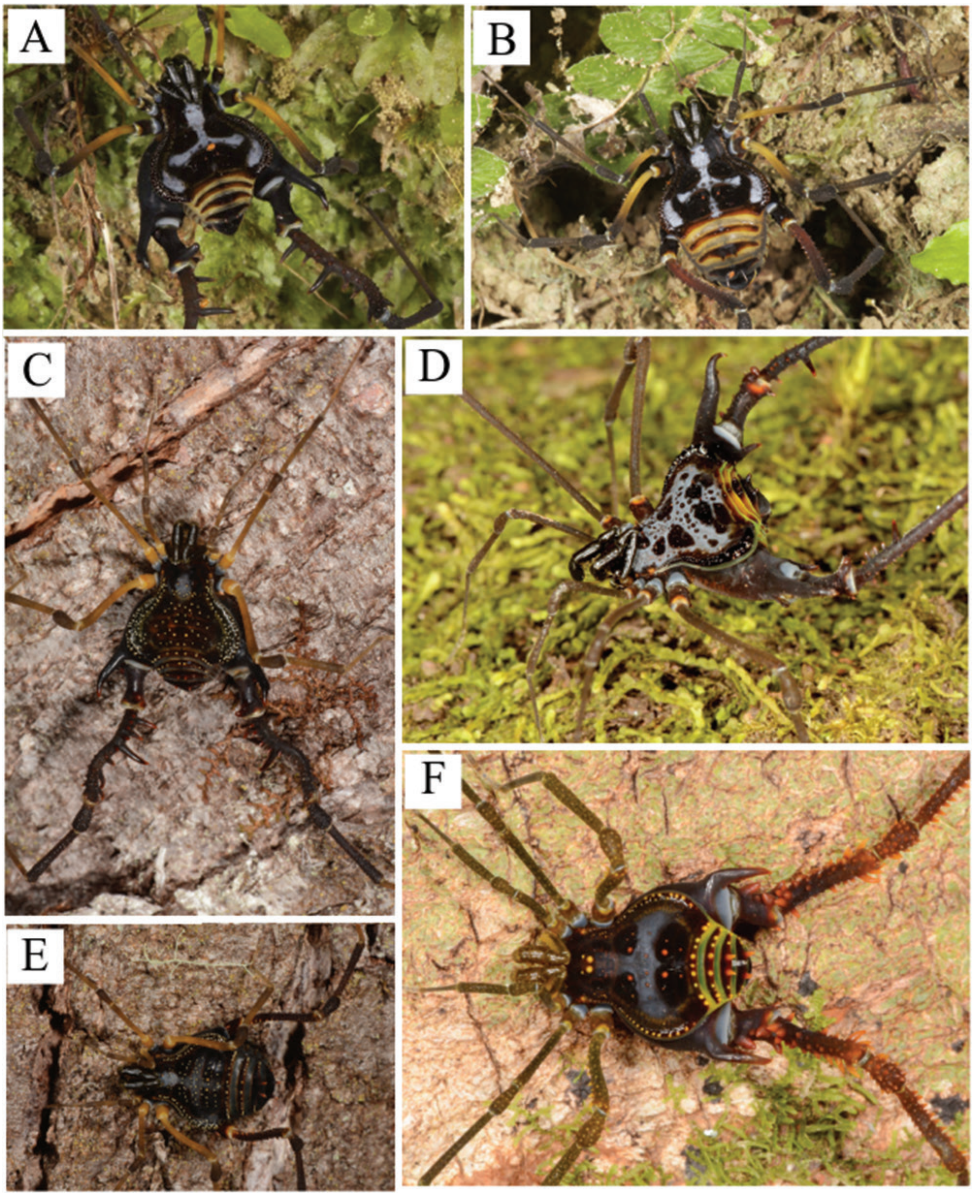

Figure 9. Photographs of living specimens of *Sadocus* **A** *S. asperatus* (ma) **B** *S. asperatus* (fe) **C** *S. asperatus* (ma) **D** *S. dilatatus* (ma) **E** *S. asperatus* (fe) **F** *S. funestus* (ma). **A, B** taken by R. Pinto-da-Rocha, **C–F** taken by Pedro H. Martins.

length 7.6–9.3; dorsal scutum maximum width 8.3–10.0; prosoma maximum length 3.0–3.6; prosoma maximum width 4.2–5.0; leg femora: I 4.5–6.0; II 7.0–13.0; III 7.0–11.4; IV 8.4–11.5.

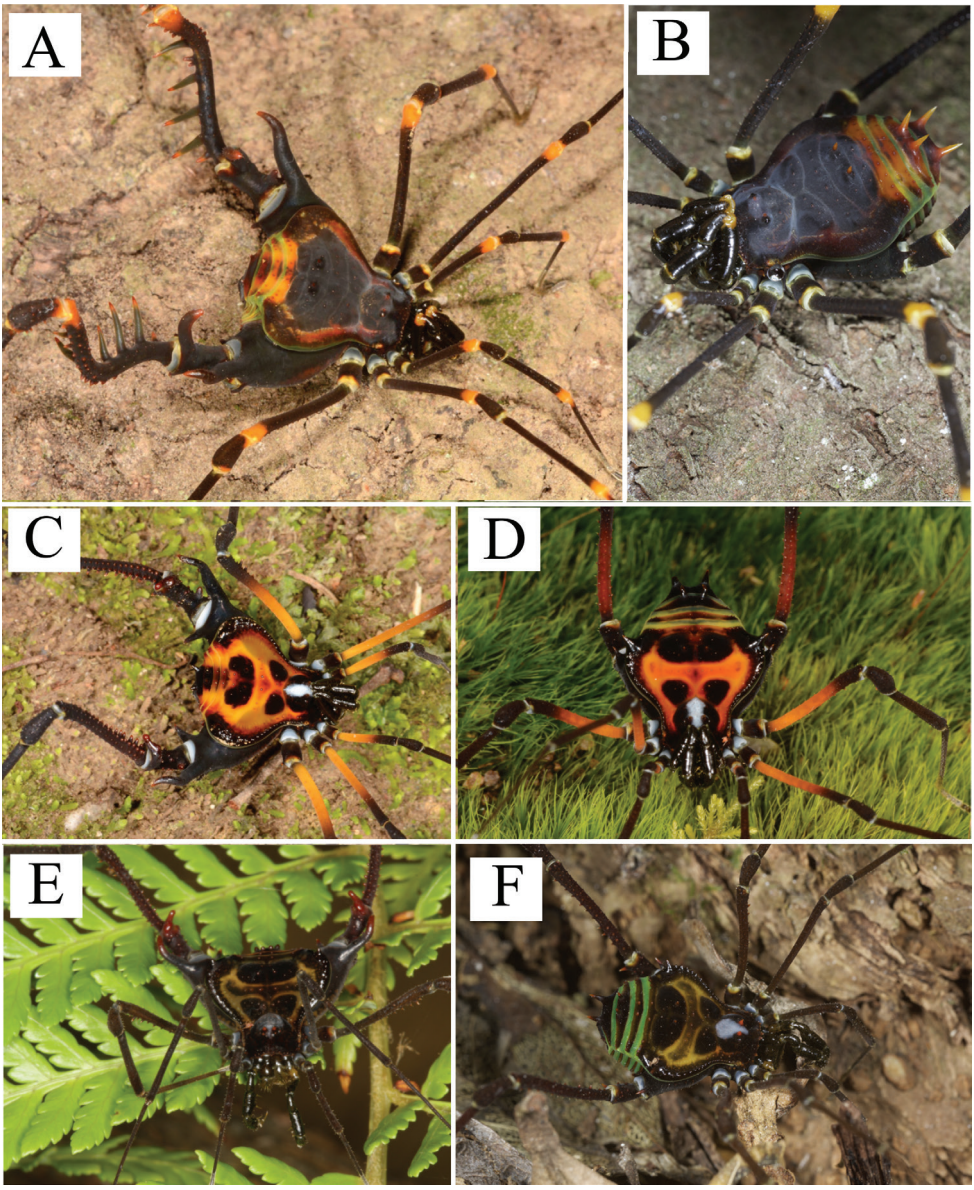

Figure 10. Photographs of living specimens of *Sadocus* **A** *S. ingens* (ma) **B** *S. ingens* (fe) **C** *S. polyacanthus* (ma) **D** *S. polyacanthus* (fe) **E** *S. polyacanthus* (ma) **F** *S. polyacanthus* (fe). **B, E** taken by R. Pinto-da-Rocha; **A, C, D, F** taken by Pedro H. Martins.

Type locality. Of *G. polyacanthus*: Chile. Provincias del Sur. Of *S. vitellinosulcatus*: either Australasia or South America. Of *G. platei*: Chile. Región de Los Lagos. *Provincia de Valdivia*. Corral. Of *A. exceptionalis* Chile. Región de Los Lagos. Osorno. Barra del Rio Bueno. Of *S. conspicillatus*: Chile. Región de Biobío. *Provincia de Concepción*. Concepción. Of *Sadocus guttatus*: Chile. Región de Biobío. *Provincia de Arauco*. Lebu.

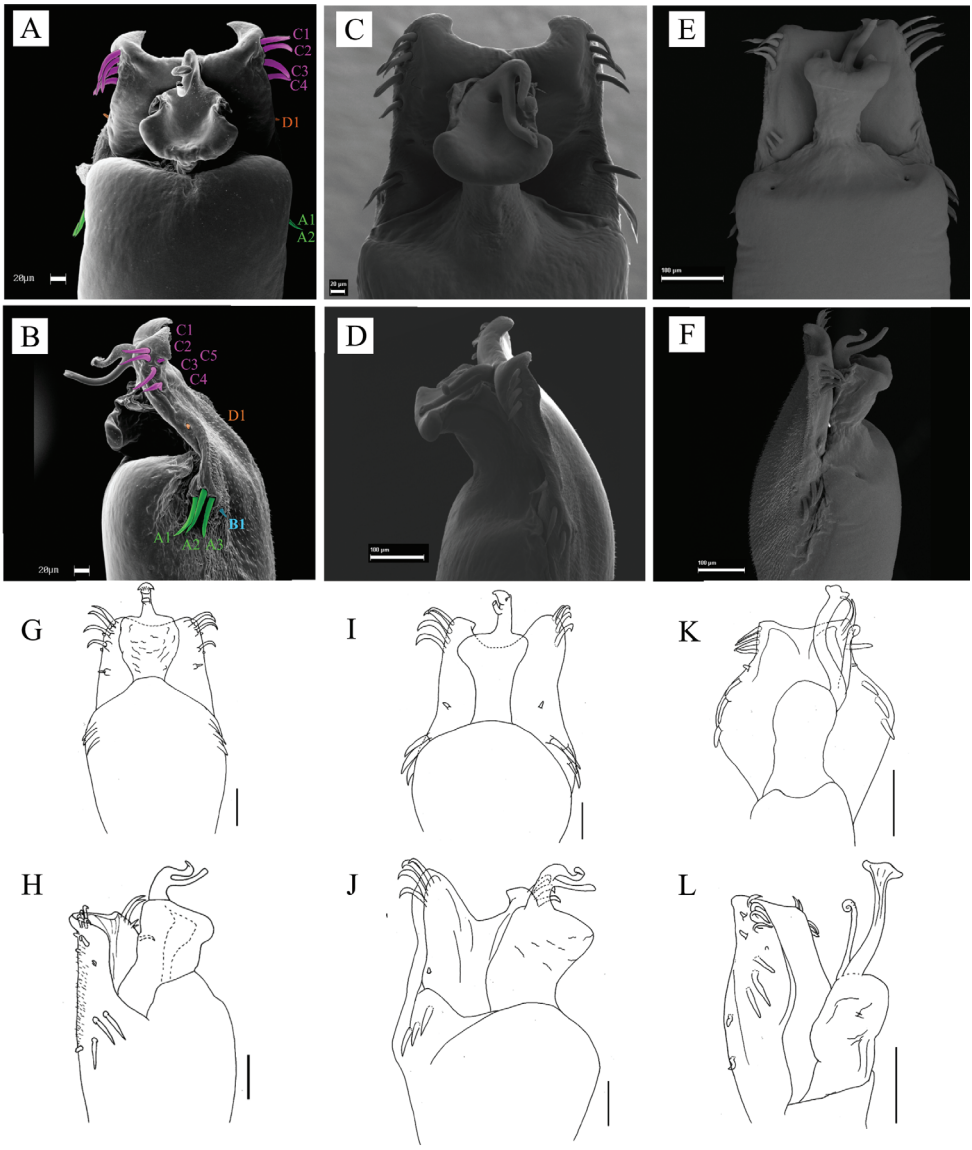

Figure 11. Distal part of penis *Sadocus* and *Discocyrtus*, dorsal and ventral views, respectively **A, B** *S. asperatus*, macrosetae colorized and numbered **C, D** *S. ingens* **E, F** *S. polyacanthus* **G, H** *S. dilatatus* **I, J** *S. funestus* **K, L** *D. catharinensis*. Scale bar of drawings: 0.1mm.

Geographical distribution (Fig. 2). Chile, *Región Metropolitana de Santiago*; Región de Biobío; Región de Araucanía; Región de Los Lagos; Ilha Chiloé; Región de Los Rios.

Taxonomic notes. After examining the holotypes of *S. conspicillatus*, *S. guttatus*, and *S. exceptionalis*, we concluded that they were males within *S. polyacanthus* size variation. The apophyses size and shape on trochanter IV and the armature of femur IV (especially the retro-dorsal and retro-lateral row of spines size pattern) of all species are the same.

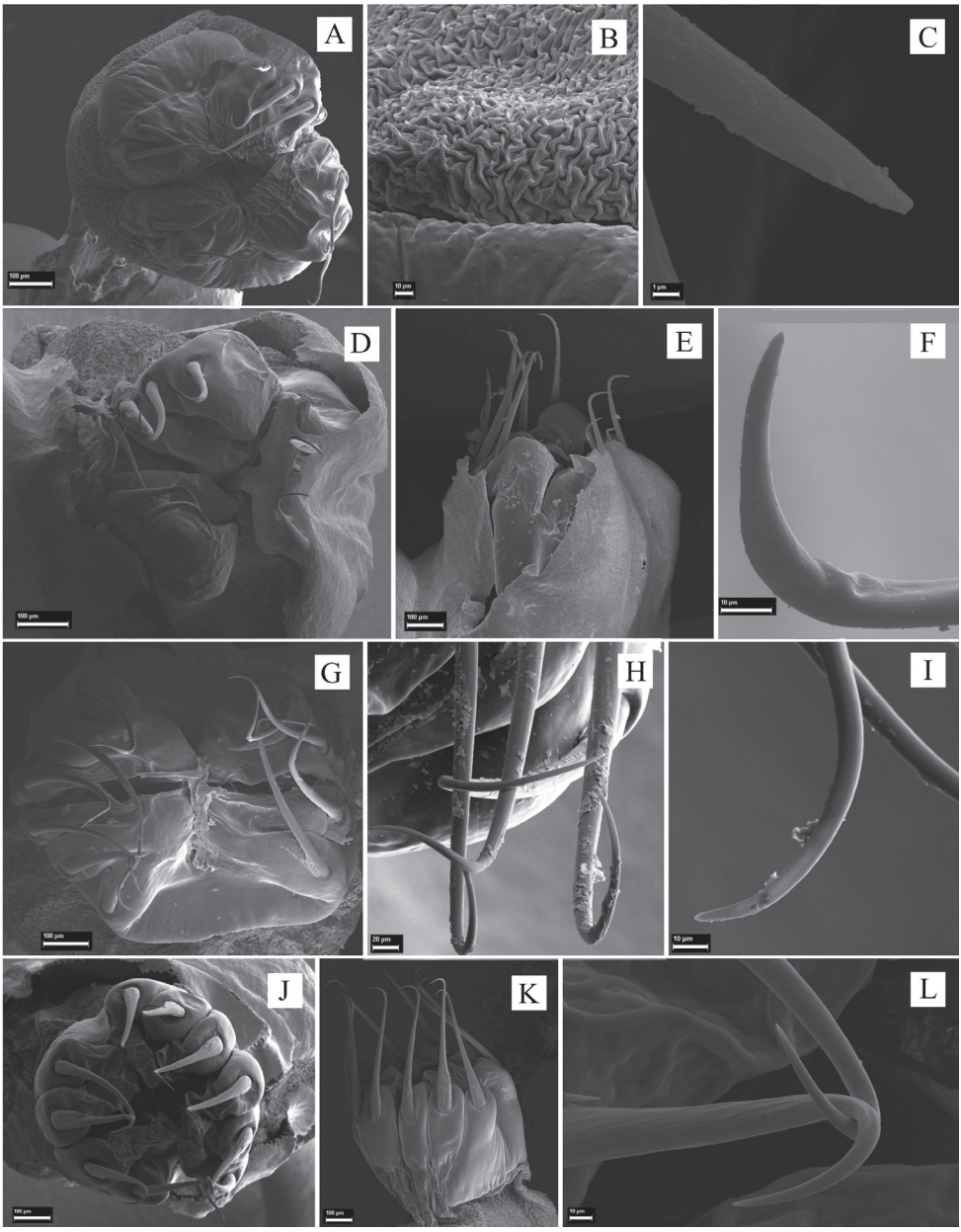

Figure 12. Distal part of ovipositor of *Sadocus* **A–C** *S. asperatus* **A** upper view **B** villi **C** setae **D–F** *S. funestus* **D** upper view **E** lateral view **F** seta **G–I** *S. ingens* **G** upper view **H, I** setae **J–L** *S. polyacanthus* **J** upper view **K** lateral view **L** setae.

Species inquirendae

Sadocus allermayeri (Mello-Leitão, 1945)

Carampangue allermayeri Mello-Leitão, 1945: 158 [desc]; Soares and Soares 1954: 241 [cat]; Cekalovic 1968: 7 [cat]; 1985: 16 [cat] (type material MNRJ, 1 ma & 1 fe syntypes, destroyed, not examined).
Sadocus allermayeri: Kury, 2003: 191 [cat]; Kury et al. 2020b [cat].

Type locality. Chile. Región de Biobío. Concepción. Concepción.

Taxonomic notes. The type material, belonging to MNRJ, was lost in the fire that destroyed most of the arachnid collection (Kury, pers. comm.; Kury et al. 2018). The original description is poor for modern standards and it has no illustrations. However, the description allows to be diagnosed by: the presence of scutal area IV on dorsal scutum, coxa IV with one prodorsal apical bifid apophysis; trochanter IV with one retro-basal apophysis and three proapical apophyses. *Sadocus asperatus*, *S dilatatus*, and *S. ingens* have the scutal area IV in dorsal scutum and coxa IV with a bifid prodorsal apical apophysis; but none of them has three apical apophyses on trochanter IV. The only species with four scutal areas on the dorsal scutum and trochanter IV with three apical apophyses is *S. funestus*, but the prodorsal apical apophysis on coxa IV is uniramous. Assuming that the description is correct, it implies that this is a valid species that we have not yet located among the material gathered for this revision of *Sadocus*.

Sadocus nigronotatus (Mello-Leitão, 1943)

Figure 8K

Carampangue nigronotatum Mello-Leitão, 1943: 8, fig 7 [desc]; Soares and Soares 1954: 242 [cat]; Cekalovic 1968: 7 [cat]: 1985: 17 [cat] (type material MNRJ, 1 fe holotype lost, not examined).
Sadocus nigronotatus: Kury, 2003, 191 [cat]; Kury et al. 2020b [cat].

Type locality. Chile. *Provincia de Llanquihue*. Región de Los Lagos. Maullín.

Taxonomic notes. The type material, belonging to the MNRJ, is lost (for the same reason as *S. allermayeri*). The original description is poor for modern standards, and both description and figure are based on a female. The females of the different *Sadocus* species are very similar and difficult to identify unequivocally. According to the original description, *S. nigronotatus* resembles *S. polyacanthus* in the presence of a spiniform apophysis on the lateral margin of the dorsal scutum, but can be distinguished by the presence of scutal area IV.

Species removed from *Sadocus*

***Discocyrtus catharinensis* (Mello-Leitão, 1923)**
Figure 11K, L

Sadocus catharinensis Mello-Leitão, 1923: 152 [desc]; B. Soares 1944a: 166 [syst]; 1944b: 222 [cit]; 1945: 364 [cat]; Soares and Soares 1949: 211 [cat]; H. Soares 1966: 90 [cat] (Types MNRJ 1510, syntypes examined by detailed photographs).
Parasadocus catharinensis: Mello-Leitão, 1927: 8 [syst]; Roewer 1930: 425 [rdesc]; Mello-Leitão 1932: 329 [rdesc].
Discocyrtus catharinensis: Soares & Soares, 1987: 458, figs 3–6 [syst, rdesc].
Sadocus aquifugus Mello-Leitão, 1931a: 136, fig 8 [desc]; 1935: 106 [cit] (Types MNRJ 11390 syntypes, male genitalia examined by photographs).
Gonyleptes pugilator Mello-Leitão, 1932: 303, fig 163 [desc]; B. Soares 1944b: 222 [cit]; Soares and Soares 1949: 180 [cat] (Type MNRJ – lost).
Gonyleptes acanthopus Mello-Leitão, 1945: 156 [cit] [nec Quoy and Gaimard 1824] – misidentification: Soares and Soares 1987].
Lycomedicus brasiliensis Soares & Soares, 1949: 52, figs 6–8 [desc]; 1954: 271 [cat] (type material – old collection CGPC, 1 ma, 1 fe – MZSP 36165, holotype, MZSP 1029 paratype, examined). syn. nov.
Sadocus brasiliensis: Kury, 2003: 191 [cat]; Kury et al. 2020b [cat].

Material examined. Brazil, Paraná, *Piraquara*, Banhado, IV.1946, Goffergé coll., 1 ma holotype, 1 fe paratype (MZSP 36165); same, 1 ma paratype (MZSP 1029); Santa Catarina, *Joinville*, III.1947, Goffergé coll., 1 ma (MZSP 36419).

Type locality. *S. catharinensis* and *S. aquifugus*: BRAZIL. Santa Catarina. Joinville. Of *G. pugilator*: BRAZIL. Santa Catarina. Of *Lycomedicus brasiliensis*: BRAZIL. Paraná. Piraquara: Banhado.

Taxonomic notes. We examined the type material of *Sadocus brasiliensis* and its external and penial morphology did not match that of other Chilean species of the genus. Based on its type locality, we examined other Brazilian Pachylinae genera and found striking similarities between *S. brasiliensis* and *D. catharinensis*. We examined detailed pictures of the type material kindly shared by Rafael N. Carvalho and additional material from the MZSP collection. Those species are the same, and we propose that *S. brasiliensis* is the junior synonym of *D. catharinensis*. Many *Discocyrtus* spp. have been transferred to revalidated genera or newly created subfamilies, such as Roeweriinae (Carvalho and Kury 2018) or Neopachylinae (Carvalho and Kury 2021). Indeed, the penial features of *D. catharinensis* (Fig. 15K, L) resembles those of that subfamily, which is corroborated in the present analysis: *D. catharinensis* is the sister species of *R. bittencourti*. Based on male genitalia and leg IV (see Carvalho and Kury 2018), *D. catharinensis* seems to belong to *Discocyrtanus* Roewer, 1929. However, because there is an ongoing study revising *Discocyrtus* conducted by Rafael N. Carvalho (MNRJ) and taking into account that it will have serious taxonomic consequences, we opted to propose only the synonymy of *S. brasiliensis* with *D. catharinensis.*

***Gonyleptes horridus* Kirby, 1819**

Gonyleptes horridus Kirby, 1819: 452, pl. 22, fig 16 [desc]; Kury 2003: 128 [cat]; Hara et al. 2012: 38–39 [syst]; Pinto-da-Rocha et al. 2012: 26, 41–45 [syst]; Pinto-da-Rocha et al. 2014: 4, 17 [syst]; Hara 2016: 106–109 [syst]. (Type holotype NHM 1863.41, ma examined by detailed photographs).
Lycomedes calcar Roewer, 1913: 132, fig 59 [desc]; Acosta 1996: 218 [cit] (Type holotype SMF RI, 782, ma examined). syn. nov.
Lycomedicus calcar: Roewer, 1923: 444, fig 558 [rdesc]; Canals 1936: 69 [cat]; Soares and Soares 1954: 271 [cat]; Cekalovic 1968: 8 [cat], 1985: 18 [cat].
Sadocus calcar: Kury, 2003, 191 [cat]; Kury et al. 2020b [cat].

Taxonomic note. The holotype of *Sadocus calcar* is in a very bad state of preservation; only part of the carapace, with the ozopores, and leg IV remain. The rest of the prosoma and all of the other legs are absent. Even in this condition, we noted that *S. calcar* lacks the large tubercles and spines on the free tergites, which are diagnostic of *Sadocus*. Furthermore, the armature of trochanter IV and the long, bifid, C-shaped dorso-basal apophysis on femur IV are strikingly similar to those of *Gonyleptes horridus*, a common species in the state of Rio de Janeiro. Therefore, we propose *S. calcar* as a junior synonym of *G. horridus*. This synonymy made us conclude that the provenance of *S. calcar* is mistaken, because *G. horridus* is endemic to the Brazilian Atlantic rainforest. It is widely known that Roewer, unfortunately, indicated wrong provenance of a few species, and this seems to be the case for this species.

***Eubalta planiceps* (Gervais, 1842)**

Remarks. *Sadocus planiceps* (originally *Gonyleptes planiceps* Gervais, 1842) has a convoluted taxonomic history, with many previously unknown synonyms detected, which will be published elsewhere (briefly commented in Pessoa-Silva et al. 2020). We excluded it from *Sadocus* because it lacks the synapomorphies of the genus. It also lacks the diagnostic characters of the genus, such as the typical ocularium shape and type of armature, dorsal scutum shape, just to name a few. Comparing with other species of Chilean Pachylinae, we detected striking similarities with *Eubalta meridionalis*. This synonymy did not go unnoticed by Kury et al. (2020a) in his catalogue, who also detected this in parallel with this revision. Finally, Kury et al. kindly invited us to publish this synonymy that resulted in a publication of that synonymy (Pessoa-Silva et al. 2020).

Acknowledgements

This study was supported by the project Dimensions US–BIOTA–São Paulo (Fapesp 2013/50297–0, NSF–DOB 1343578 and NASA), and the first author is also grateful for a M.Sc. fellowship (CAPES). MRH thanks the Fundação de Amparo à Pesquisa

do Estado de São Paulo (Fapesp 2018/07193-2). We also thank the financial support from CNPq (304933/2014–7). Rafael Carvalho kindly shared pictures of *Discocyrtus catharinensis* that resulted its synonymy with *Sadocus brasiliensis*. We are grateful to the editor Gonzalo Giribet and reviewers of an early version, Cristina Rheims, Cibele Bragagnolo, and James Cokendolpher.

References

Acosta LE (1996) Die Typus-Exemplare der von Carl-Friedrich Roewer beschrieben en Pachylinae (Arachnida: Opiliones: Gonyleptidae). Senckenbergiana biologica 76(1/2): 209–225.

Acosta LE (2002) Patrones zoogeográficos de los opiliones argentinos (Arachnida: Opiliones). Revista Ibérica de Aracnología 6: 69–84.

Acosta LE (2020) *Qorimayus*, a new genus of relictual, high-altitude harvestmen from western Argentina (Arachnida, Opiliones, Gonyleptidae) reveals trans-Andean phylogenetic links. Zootaxa 4722(2): 129–156. https://doi.org/10.11646/zootaxa.4722.2.2

Acosta LE, Pérez-González A, Tourinho AL (2007) Methods for taxonomic study. In: Pinto-da-Rocha R, Machado G, Giribet G (Eds) Harvestmen: The Biology of Opiliones. Harvard University Press, Cambridge, Massachusetts, 494–510.

Acosta LE, Maury EA (1998) Opiliones. In: Morrone JJ, Coscarón S (Eds) Biodiversidad de Artrópodos argentinos, Una perspectiva biotaxonómica. Ediciones Sur, La Plata, 569–580.

Amorim DS (1982) Classificação por sequenciação: uma proposta para a denominação dos ramos retardados. Revista Brasileira de Zoologia 1(1): 1–9. https://doi.org/10.1590/S0101-81751982000100001

Benavides LR, Pinto-da-Rocha R, Giribet G (2021) The phylogeny and evolution of the flashiest of the armored harvestmen (Arachnida: Opiliones). Systematic Biology, syaa080. https://doi.org/10.1093/sysbio/syaa080

Bremer K (1994) Branch support and tree stability. Cladistics 10: 295–304. https://doi.org/10.1111/j.1096-0031.1994.tb00179.x

Butler AG (1873) A monographic list of the species of the genus *Gonyleptes*, with descriptions of three remarkable new species. Annals and Magazine of Natural History (series 4) 11(62): 112–117. https://doi.org/10.1080/00222937308696775

Butler AG (1874) Descriptions of five new species of *Gonyleptes*. Zoological Journal of the Linnean Society 12: 151–155. https://doi.org/10.1111/j.1096-3642.1875.tb02579.x

Canals J (1934) Opiliones de la Argentina. Descripción de "*Diconospelta Gallardoi*", n. gen., n. sp., y nómina de otros opiliones, nuevos para nuestro país. Estudios aracnológicos (V). 10.

Canals J (1936) Los Opiliones de Chile. Revista Chilena de Historia Natural 39: 68–71.

Carvalho RN, Kury A (2018) Further dismemberment of *Discocyrtus* with description of a new Amazonian genus and a new subfamily of Gonyleptidae (Opiliones, Laniatores). European Journal of Taxonomy 393: 1–32. https://doi.org/10.5852/ejt.2018.393

Carvalho RN, Kury AB (2021) A new subfamily of Gonyleptidae formed by false *Discocyrtus* Holmberg, 1878 from Brazil, with revalidation of *Pachylobos* Piza, 1940 and description of a new genus. Zoologischer Anzeiger 290: 79–112. https://doi.org/10.1016/j.jcz.2020.11.004

Cekalovic-K TN (1968) Conocimiento actual de los opiliones chilenos. Noticiario Mensual 12(138): 5–11.

Cekalovic-K TN (1976) Catalogo de los Arachnida: Scorpiones, Pseudoscorpiones, Opiliones, Acari, Araneae y Solifugae de la XII Region de Chile, Magallanes Incluyendo la Antartica Chilena (Chile). Gayana 37: 11–107.

Cekalovic-K TN (1985) Catálogo de los Opiliones de Chile (Arachnida). Boletin de la Sociedad de Biologia de Concepción 56: 7–29.

Cokendolpher JC (1993) Pathogens and parasites of Opiliones (Arthropoda: Arachnida). Journal of Arachnology 21(2): 120–146.

DaSilva MB, Pinto-da-Rocha R (2010) Systematic review and cladistic analysis of the Hernandariinae (Opiliones: Gonyleptidae). Zoologia (Curitiba) 27(4): 577–642. https://doi.org/10.1590/S1984-46702010000400010

DaSilva MB, Gnaspini P (2010) A systematic revision of Goniosomatinae (Arachnida: Opiliones: Gonyleptidae), with a cladistic analysis and biogeographical notes. Invertebrate Systematics 23(6): 530–624. https://doi.org/10.1071/IS09022

Gervais P (1842) Arachnides. Description et figures de quatre espèces nouvelles de Phalangiens. Magasin de Zoológie, Série 2, 4: 1–5.

Gervais P (1844) Acères Phrynéides, Scorpionides, Solpugides, Phalangides et Acarides; Dicères pizoïques, Aphaniptères et Thysanoures. In: Walckenaer CA (Org.) Histoire naturelle des Insectes Aptères 3: 94–131.

Gervais P (1847) Phalangides. In: Walckenaer CA, Gervais P (Eds) Histoire naturelle des Insectes Aptères 4: 344–345. [576–577.]

Gervais P (1849) Arácnidos. Orden IV Falangidos. In: Gay C (Org.) Historia fisica y politica de Chile, Zoologia IV: 18–2.

Goloboff PA, Farris JS, Nixon KC (2008) TNT, a free program for phylogenetic analysis. Cladistics 24: 774–786. https://doi.org/10.1111/j.1096-0031.2008.00217.x

Gray GR (1833) Arachnida. Animal Kingdom (Conversio Britannica operis illustris Cuvier) (Vol. 13). Whittaker, Treacher & Co., London, 540 pp.

Guérin-Méneville FÉ (1844) Iconographie du Règne-Animal de G. Cuvier: ou Représentation d'après nature de l'une des espèces les plus remarquables et souvent non encore figurées, de chaque genre d'animaux. 3. Texte explicatif (Vol. 3). Baillière, Paris, 930 pp.

Hara MR (2016) Cladistic analysis and description of three new species of the Chilean genus *Nanophareus* (Opiliones: Gonyleptidae: Pachylinae). Zootaxa 4105: 101–123. https://doi.org/10.11646/zootaxa.4105.2.1

Hara MR, Pinto-Da-Rocha R (2010) Systematic review and cladistic analysis of the genus *Eusarcus* Perty 1833 (Arachnida, Opiliones, Gonyleptidae). Zootaxa 2698(1): 1–136. https://doi.org/10.11646/zootaxa.2698.1.1

Hara MR, Pinto-da-Rocha R, Kury AB (2012) Revision of *Nanophareus*, a mysterious harvestman genus from Chile, with descriptions of three new species (Opiliones: Laniatores: Gonyleptidae). Zootaxa 3579: 37–66. https://doi.org/10.11646/zootaxa.3579.1.2

Hogg HR (1913) 2. Some Falkland Island spiders. Proceedings of the Zoological Society of London 1913: 37–50. https://doi.org/10.1111/j.1096-3642.1913.tb01981.x

Holmberg EL (1878) Notas aracnologicas sobre los Solpugidos argentinos. El naturalista argentino 1(1): 69–74.

Kästner A (1937) Chelicerata. 7. Ordnung der Arachnida: Opiliones Sundeval = Weberknechte. In: Kukenthal W, Krumbach T (Eds) Handbuch der Zoologie 3(2): 300–393.

Kirby W (1819) A century of insects, including several new genera described from his Cabinet. Transactions of the Linnean Society of London 12(27): 375–453. https://doi.org/10.1111/j.1095-8339.1817.tb00239.x

Koch CL (1839) Uebersicht des Arachnidensystems 2. C. H. Zeh'sche Buchhandlung, Nürenberg, 38 pp.

Kury AB, Carvalho RN (2016) Revalidation of the Brazilian genus *Discocyrtanus*, with description of two new species (Opiliones: Gonyleptidae: Pachylinae). Zootaxa 4111(2): 126–144. https://doi.org/10.11646/zootaxa.4111.2.2

Kury AB, Giupponi APL, Mendes AC (2018) Immolation of Museu Nacional, Rio de Janeiro – unforgettable fire and irreplaceable loss. Journal of Arachnology 46: 556–558. https://doi.org/10.1636/JoA-S-18-094.1

Kury AB, Villarreal MO (2015) The prickly blade mapped: establishing homologies and a chaetotaxy for macrosetae of penis ventral plate in Gonyleptoidea (Arachnida, Opiliones, Laniatores). Zoological Journal of the Linnean Society 174(1): 1–46. https://doi.org/10.1111/zoj.12225

Kury AB, Medrano M (2016) Review of terminology for the outline of dorsal scutum in Laniatores (Arachnida, Opiliones). Zootaxa 4097(1): 130–134. https://doi.org/10.11646/zootaxa.4097.1.9

Kury AB, Mendes AC, Cardoso L, Kury MS, Granado Ade A (2020a) WCO-Lite: online world catalogue of harvestmen (Arachnida, Opiliones). Version 1.0 – Checklist of all valid nomina in Opiliones with authors and dates of publications up to 2018. Self published, Rio de Janeiro, 237 pp.

Kury AB, Mendes, AC, Cardoso, L, Kury, MS, Granado Ade A, Giribet, G (2020b) World Catalogue of Opiliones. WCO-Lite version 1.2.1. https://wcolite.com/

Kury AB (1994) Early lineages of Gonyleptidae (Arachnida Opiliones Laniatores). Tropical Zoology 7: 343–353. https://doi.org/10.1080/03946975.1994.10539264

Kury AB (2003) Annotated catalogue of the Laniatores of the New Word (Arachnida, Opiliones). Revista Ibérica de Aracnologia. Volumen especial monográfico 1: 5–337.

Loman JCC (1899) Die Opilioniden der Sammlung Plate. Zoologische Jahrbücher, Jena, Supplement, 5 (Fauna Chilensis. Zweiter Band), 1–14.

Maury EA (1991) Gonyleptidae (Opiliones) del bosque subantartico chileno-argentino I. El genero *Acanthoprocta* Loman, 1899. Boletin de la Sociedad de Biología de Concepción 62: 107–117.

Mello-Leitão CF (1923) Opiliones Laniatores do Brasil. Archivos do Museu Nacional 24: 107–197.

Mello-Leitão CF (1926) Notas sobre Opiliones Laniatores sul-americanos. Revista do Museu Paulista 14: 327–383.

Mello-Leitão CF (1927) Generos novos de Gony-leptideos. Boletim do Museu Nacional do Rio De Janeiro 3(2): 13–22.

Mello-Leitão CF (1931a) Opiliões novos ou criticos. Archivos do Museu Nacional 33: 115–145.

Mello-Leitão CF (1931b) Nota sobre arachnideos argentinos. III. Opiliões novos ou críticos. IV. Aranhas novas. Annaes da Academia brasileira de Sciencias 3(2): 83–97.

Mello-Leitão CF (1932) Opiliões do Brasil. Revista do Museu Paulista 17(2): 1–505.
Mello-Leitão CF (1935) Algumas notas sobre os Laniatores. Archivos do Museu Nacional 36(4): 87–116.
Mello-Leitão CF (1937) Cuatro géneros nuevos de Pachylinae. Revista Chilena de Historia natural 41: 149–156.
Mello-Leitão CF (1939) Les arachnides et la zoogeographie de l'Argentine. Physis 17: 601–630.
Mello-Leitão CF (1943) Aracnidos de Maullín. Revista Chilena de Historia natural 46: 1–8.
Mello-Leitão CF (1945) Considerações sobre o gênero *Eusarcus* Perty e descrição de quatro novos Laniatores. Anais Academia brasileira de Ciências 7(2): 149–162.
Mello-Leitão CF (1946) Nuevos aracnidos sudamericanos de las colecciones del Museo de Historia Natural de Montevideo. Comunicaccones Zoologicas del Museu de Historia natural de Montevideo 35(2): 1–11.
Mello-Leitão CF (1949) Famílias, subfamília, espécies gêneros novos de opiliões e notas de sinonimia. Boletim do Museu Nacional 94: 1–33.
Moritz M (1971) Die Typen der Arachniden-Sammlung der zoologischen Museums Berlin I. Opiliones. Mitteilungen aus dem Zoologischen Museum in Berlin 47(1): 189–214. https://doi.org/10.1002/mmnz.19710470116
Muñoz-Cuevas A (1973) Sur les caractères génériques de la famille des Gonyleptidae (Arachnida, Opiliones, Laniatores). Bulletin du Muséum National d'Histoire Naturelle 87(113): 225–234.
Nixon KC (1999) Winclada (beta) ver. 0.9. Published by the author, rearrangements are optimal for slight perturba. Ithaca. http://www.cladistics.com
Pérez-González A, Cotoras DD, Acosta LE (2020) Early detection of an invasive harvestman in an oceanic island? Remarkable findings of *Parabalta reedii* (Opiliones, Gonyleptidae) in the Juan Fernández archipelago, Chile. Studies on Neotropical Fauna and Environment, 8 pp. https://doi.org/10.1080/01650521.2020.1809611
Pérez-Schultheiss J, Urra F, Otárola A (2019) Opiliones Laniatores (Arachnida) de la Cordillera de Nahuelbuta: un desconocido hotspot de diversidad. Boletín Nahuelbuta Natural 4: 1–24.
Perty M (1833) Delectus animalium articulorum quae in itinere per Brasilia annni 1817–1820 peracta collegerunt J.B. Spix et de Martius, Monachii, 205 pp.
Pessoa-Silva M, Hara M, Pinto-da-Rocha R (2020) Chapter 12. Pachylinae at their southernmost extreme (Laniatores: Gonyleptidae). In: Kury AB, Mendes AC, Cardoso L, Kury MS, Granado AA (Eds) WCO-Lite: online world catalogue of harvestmen (Arachnida, Opiliones). Version 1.0 – Checklist of all valid nomina in Opiliones with authors and dates of publication up to 2018. Self published, Rio de Janeiro, 58–59.
Pinto-da-Rocha R, Bragagnolo C (2010) Review of the Brazilian Atlantic Rainforest harvestman *Longiperna* (Opiliones: Gonyleptidae: Mitobatinae). Zoologia (Curitiba) 27(6): 993–1007. https://doi.org/10.1590/S1984-46702010000600023
Pinto-da-Rocha R (1997) Systematic review of the Family Stygnidae (Opiliones: Laniatores: Gonyleptoidea). Arquivos de Zoologia 33(4): 163–342. https://doi.org/10.11606/issn.2176-7793.v33i4p163-342
Pinto-Da-Rocha R (2002) Systematic review and cladistic analysis of the Caelopyginae (Opiliones, Gonyleptidae). Arquivos de Zoologia 36(4): 357–464.

Pinto-da-Rocha R, Benedetti A, Vasconcelos E, Hara M (2012) New systematic assignments in Gonyleptoidea (Arachnida, Opiliones, Laniatores). ZooKeys 198: 25–68. https://doi.org/10.3897/zookeys.198.2337

Pinto-da-Rocha R, Bragagnolo C, Marques FPL, Junior MA (2014) Phylogeny of harvestmen family Gonyleptidae inferred from a multilocus approach (Arachnida: Opiliones). Cladistics 20(5): 519–539. https://doi.org/10.1111/cla.12065

QGIS (2019) QGIS Geographic Information System. Open Source Geospatial Foundation Project. http://qgis.org

Quoy JRC, Gaimard JP (1824) Division 3° Zoologie. Section II. Des Arachnides et des Insectes. In: Freycinet L de (Ed.) Voyage autour du Monde entrepris par ordre du Roi exécuté sur les corvettes de S. M. l'Uranie et la Physicienne, pendant les années 1817, 1818, 1819 et 1820. Pillet Aîné, Paris, 542–558.

Ringuelet RA (1955a) Ubicación zoogeográfica de las Islas Malvinas. Revista del Museo de La Plata 6(48): 419–464.

Ringuelet RA (1955b) Vinculaciones faunisticas de la zona boscosa de Nahuel Huapi y el domino zoogeografico austral-Cordillerano. Notas del Museo de La Plata 18(160): 81–121.

Ringuelet RA (1957) Bioeografia de los aracnidos Argentinos del orden Opiliones. Contribuciones Cientificas Facultad Ciencias Exactas y Naturales Universidad de Buenos Aires, Serie Zoologia 1(1): 1–33.

Ringuelet RA (1959) Los aracnidos Argentinos del orden Opiliones. Revista del Museo Argentino de Ciencias Naturales "Bernardino Rivadavia." Ciencias Zoologicas 5(2): 127–439.

Roewer CF (1913) Die Familie der Gonyleptiden der Opiliones-Laniatores. Archiv für Naturgeschichte. 79A(4–5): 1–473.

Roewer CF (1923) Die Weberknechte der Erde. Systematische Bearbeitung der bisher bekannten Opiliones. Gustav Fischer, Jena, 1116 pp.

Roewer CF (1925) Opilioniden aus Süd-Amerika. Bollettino dei Musei di Zoologia e di Anatomia Comparata della Reale Università di Torino 40(34): 1–34.

Roewer CF (1929) Weitere Weberknechte III. (3. Ergänzung der: Weberknechteder Erde", 1923). Abhandlungen der Naturwissenschaftlichen Verein zu Bremen 27(2): 179–284.

Roewer CF (1930) Weitere Weberknechte IV. (4. Ergänzung der Weberknechte der Erde, 1923). Abhandlungen der Naturwissenschaftlichen Verein zu Bremen 27(3): 341–452.

Roewer CF (1938) Opiliones aus dem Naturhistorischen Reichsmuseum in Stockholm. Arkiv för zoologi, Series B. 30(10): 1–8. https://doi.org/10.5962/bhl.part.1498

Roewer CF (1943) Über Gonyleptiden. Weitere Webernechte (Arachn., Opil.) XI. Senckenbergiana 26(1–3): 12–68.

Roewer CF (1961) Opiliones aus Süd-Chile. Senckenbergiana Biologica 42(1/2): 99–105.

Simon E (1879) Essai d'une classification des Opiliones Mecostethi. Remarques synonymiques et descriptions d'espèces nouvelles. Première partie. Annales de la Société Entomologique de Belgique 22: 183–241.

Simon E (1884) Arachnides recueillis par la mission du Cap Horn en 1882–1883. Bulletin de la Société Zoologique de France, Paris 9: 117–144.

Soares HEM, Soares BAM (1987) Opera Opiliologica Varia XVIII. (Opiliones, Cosmetidae e Gonyleptidae). Revista Brasileira de Entomologia 31(1): 1–11.

Soares HM, Soares BA (1985) Opera Opiliologica Varia XXII. Opiliones Gonyleptidae. Naturalia 10: 157–200.

Soares BAM (1944a) Notas sobre opiliões da coleção do Museu Nacional do Rio de Janeiro. Papéis avulsos do Departamento de Zoologia 6(15): 163–180.

Soares BAM (1944b) Notas sobre opiliões XIV. Papéis avulsos do Departamento de Zoologia 6(20): 221–224.

Soares BAM (1945) Opiliões da coleção do Museu Nacional do Rio de Janeiro. Arquivos de zoologia do Estado de São Paulo 4 (9): 341–394.

Soares BAM, Soares HEM (1954) Monografia dos gêneros de opiliões neotrópicos III. Arquivos de zoologia do Estado de São Paulo 8(9): 225–302.

Soares BAM, Soares HEM (1949) Monografia dos gêneros de opiliões neotrópicos II. Arquivos de zoologia do Estado de São Paulo 7(2): 149–240.

Soares BAM (1945) Opiliões da coleção do Museu Nacional do Rio de Janeiro. Arquivos de zoologia do Estado de São Paulo 4(9): 341–394.

Soares HEM (1966) Opiliões da coleção Gofferjè (Opiliones: Gonyleptidae, Phalangodidae). Papéis Avulsos do Departamento de Zoologia 18(10): 77–102.

Soares HEM (1968) Contribuição ao estudo dos opiliões do Chile (Opiliones: Gonyleptidae, Triaenonychidae). Papéis avulsos de Zoologia 21(27): 259–272.

Sørensen WE (1884) Opiliones Laniatores (Gonyleptides W.S. Olim) Musei Hauniensis. Naturhistorisk Tiddskrift 14(3): 555–646.

Sørensen WE (1886) Opiliones. In: Koch L, Keyserling E von (Eds) Die Arachniden Australiens nach der Natur beschrieben und abgebildet, vol. [Theil] 2 of two volumes & atlas, 1871–1889, fascicle [Lieferung] 33. Bauer & Raspe, Nürnberg, 53–86.

Sørensen WE (1902) Gonyleptiden (Opiliones, Laniatores). Ergebnisse der Hamburger Magalhaensischen Sammelreise 6(5): 1–36.

Strand E (1942) Miscellanea nomenclatoria zoologica et Paleontologica X. Folia zoologica et hydrobiologica 11(1): 386–402.

Sundevall CJ (1833) Conspectus Arachnidum. C.F. Berling, Londini Gothorum [Lund (Sweden)], 39 pp.

Townsend VR, Bertram MS, Milne MA (2015) Variation in ovipositor morphology among laniatorean harvestmen (Arachnida: Opiliones). Zoomorphology 134(3): 487–497. https://doi.org/10.1007/s00435-015-0269-4

ZooKeys 1025: 139–175 (2021)
doi: 10.3897/zookeys.1025.61385
https://zookeys.pensoft.net

RESEARCH ARTICLE

A peer-reviewed open-access journal
ZooKeys
Launched to accelerate biodiversity research

Illustrated keys to Scoliidae (Insecta, Hymenoptera, Scolioidea) from China

Zhen Liu[1], Cornelis Van Achterberg[2], Jun-Hua He[2], Xue-Xin Chen[2], Hua-Yan Chen[3]

1 *College of Life and Environmental Sciences, Hunan University of Arts and Science, Changde 415000, China* **2** *State Key Lab of Rice Biology, Ministry of Agriculture Key Lab of Molecular Biology of Crop Pathogens and Insects, Institute of Insect Sciences, Zhejiang University, Hangzhou 310058, China* **3** *State Key Laboratory of Biocontrol, School of Life Sciences / School of Ecology, Sun Yat-sen University, Guangzhou 510275, China*

Corresponding authors: Zhen Liu (qingniao8.27@163.com); Cornelis Van Achterberg (kees@vanachterberg.org)

Academic editor: A. Köhler | Received 26 November 2020 | Accepted 22 February 2021 | Published 22 March 2021

http://zoobank.org/F530AA74-3DB6-4375-8759-DEA3D5E28B22

Citation: Liu Z, Van Achterberg C, He J-H, Chen X-X, Chen H-Y (2021) Illustrated keys to Scoliidae (Insecta, Hymenoptera, Scolioidea) from China. ZooKeys 1025: 139–175. https://doi.org/10.3897/zookeys.1025.61385

Abstract

The Scoliidae occur predominantly in tropical and subtropical regions and are ectoparasitoids of Scarabaeoidea larvae (especially of Melolonthinae) which are immobilised, parasitised by the female wasp in their terrestrial larval gallery and buried deeper in a special cell by the female wasp. Herein, we provided, for the first time, illustrated keys to 11 genera and 52 species of Scoliidae from China, based on specimens in the Naturalis Biodiversity Center (RMNH, Leiden) and additional specimens from the Chinese Academy of Insect Science (Beijing), Zhejiang University (ZJUH, Hangzhou) and Sun Yat-sen University (SYSU, Guangzhou) and it is a first attempt to make keys available for all the Scoliidae species in China.

Keywords

China, illustrated keys, Scoliidae

Introduction

Scoliid wasps (Hymenoptera, Scoliidae) form a medium-sized family with approx. 560 species worldwide and occur predominantly in tropical and subtropical regions (Osten 2005). Scoliidae parasitise exclusively second and third instar beetle larvae of Scarabaeoidea (Illingworth 1919, 1921). There are few studies on this group from China, though several species are common in south and central China. Fabricius (1781–1804) described 41 species of Scoliidae, including six from China. In the 18th century, more than 20 species have been reported from China by several authors (Lepeletier 1845; Eversmann 1846, 1849; Smith 1855; de Saussure 1858; de Saussure et al. 1864; Morawitz 1889; Bingham 1896, 1897). In the 19th century, Betrem (1928) published a monograph on the Indo-Australian Scoliidae, including 72 species and subspecies, of which 20 were reported from China. Later, Betrem (1941) published a systematic study on the Chinese Scoliidae including 2 genera, 61 species, subspecies and varieties from China, which is the first overview of the Chinese fauna, but partly confusing, because of naming too many (overlapping) subspecies and varieties. The systematics is in a state of confusion, which is well summarised by Elliott (2011). In China, 52 species are known (Liu et al., submitted), all belonging to the subfamily Scoliinae. For the present key, we examined Chinese specimens of four major collections: Naturalis Biodiversity Center (RMNH, Leiden, Netherlands), Chinese Academy of Insect science (IOZ, Beijing, China), Zhejiang University (ZJUH, Hangzhou, China) and Sun Yat-sen University (SYSU, Guangzhou, China). In this paper, we provide illustrated keys for all taxa of Scoliidae from China for the first time. This paper is part of an ongoing project on the revision of the Chinese Scoliidae.

Material and methods

This work is based on specimens in the collections of the Naturalis Biodiversity Center (**RMNH**), Chinese Academy of Insect Science (**IOZ**), Zhejiang University (**ZJUH**) and Sun Yat-sen University (**SYSU**).

Examination and measurements were made using a stereomicroscope (Zeiss Stereo Discovery V8). Detailed images of specimens were taken and processed using a digital camera Zeiss Stereo Discovery V12 and with the software Axiovision SE64 Rel.49.1. Habitus images were taken with a Nikon D600 camera coupled with a Nikon 60 mm Macro lens and processed with the software Combine ZM. All images were further processed using Adobe Photoshop CS5. Morphological terms for body structures and measurements followed Betrem et al. (1972). Wing venation nomenclature followed a modified version of the Comstock-Needham (van Achterberg 1979) and Betrem et al. (1972) system. Abbreviations used are as follows: POL = postocellar line, OOL = ocular-ocellar line, OD = ocellar diameter; T1–T6 = 1st to 6th tergite of metasoma; S1–S5 = 1st to 5th sternite of metasoma.

The genitalia were removed, cleaned and pinned under the specimen in a genitalia tube as described by Prosvirov and Savitsky (2011).

Key to genera of the Scoliidae from China

1 Second recurrent vein (2m-cu) of fore wing present **and** connected to second submarginal cell, resulting in two discal cells (a), **if** rarely absent (aa), **then** length of body 5–15 mm; mesopleural crest low, often carina-like, directed approximately to posterior corner of pronotum and with a small horizontal area at upper corner (b); T2 and T3 often with subapical row of setae bearing punctures (c); volsella of males divided into two parts (d); basal elevation of S3 ("gradulus") or of T3 usually present (e); Campsomerini.....**2**

– Second recurrent vein (2m-cu) of fore wing absent, resulting in one discal cell (aa) and length of body more than15 mm **or** vein 2m-cu short and connected to first recurrent vein (1m-cu), thus resulting in a shorter second discal cell (aaa); mesopleural crest high, directed to the base of fore wing and with a large horizontal area (bb); T2 and T3 without subapical row of setae bearing punctures (cc); volsella of males not divided (dd); basal elevation of S3 or of T3 usually absent (ee); Scoliini **12**

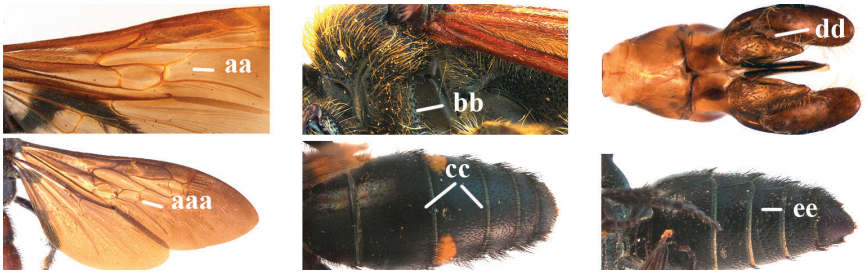

2 Fore wing with 3 submarginal cells (a); T1–T4 often without subposterior transverse setose bands (b); hypostomal carina of male bisected, with submandibular triangle (c); ventral mandibular furrow of female exposed in frontal view (d); ["Trielidini/Colpinae auct."; in China *C. tartara* (de Saussure, 1880)] ..... ***Colpa*** **Dufour**

– Fore wing with 2 submarginal cells (aa); T1–T4 often with subposterior transverse setose bands (bb); hypostomal carina of male simple, without submandibular triangle (cc); ventral mandibular furrow of female concealed in frontal view (dd) **3**

3 Females (antenna with 12 segments) **4**
– Males (antenna with 13 segments) **8**
4 Length of body 9–15 mm; base of hind wing without any carina below and upper plate of metapleuron smooth dorsally (a); metasomal tergites entirely black (b); metasomal setae white, except on apical tergite (c); wings subhyaline to pale brown (d) ..... ***Micromeriella*** **Betrem**

– Length of body 15–35 mm; base of hind wing with a carina below (aa) **or** upper plate of metapleuron more or less punctate dorsally, transition between its vertical and dorsal areas straight, with or without a carina below base of hind wing (aaa); metasomal tergites entirely black or with yellow or red pattern (bb); metasomal setae often differing in colour from the tegument (cc); wings subhyaline to dark brown (dd) **5**

5 Upper plate of metapleuron smooth, sometimes with fine, sparse punctures dorsally, transition between its vertical and dorsal areas straight and with an entirely or partially distinct carina below base of hind wing (a) **6**

– Upper plate of metapleuron punctate dorsally, transition between its vertical and dorsal areas usually straight anteriorly and gradually sloping posteriorly and without a distinct carina below base of hind wing (aa) **7**

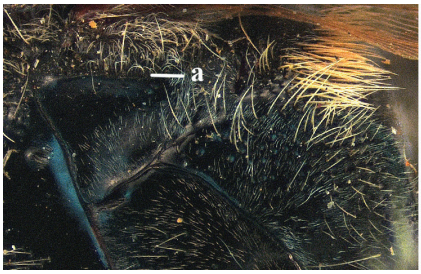

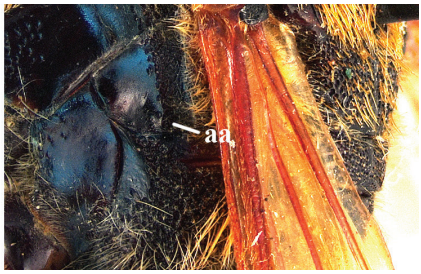

6 Lateral carina of propodeum at most extending up to level of spiracle (a); dorsal area of propodeum triangularly protruding medio-posteriorly and its posterior surface impunctate to remotely punctate (b); vertex behind posterior ocelli impunctate (c); body black, 20–30 mm long (d); wings entirely fuscous to yellowish subhyaline (e)..... ***Campsomeriella*** **Betrem**

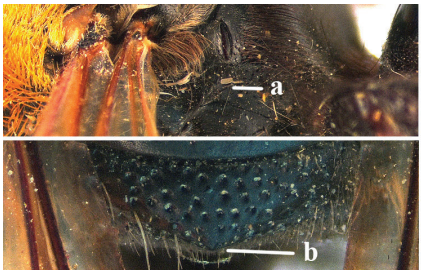

– Lateral carina of propodeum extended beyond level of spiracle (aa); dorsal area of propodeum truncated medio-posteriorly and its posterior surface densely punctate, at least dorsally (bb); vertex behind posterior ocelli with sparse to dense punctation (cc); metasoma partly yellow or red, body length more than 30 mm (dd); wings dark brown (ee) ..... ***Sericocampsomeris*** **Betrem**

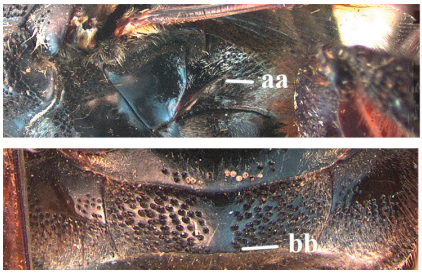

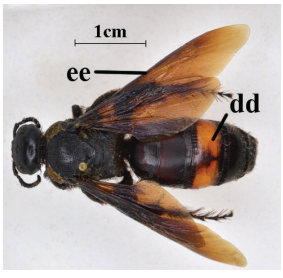

7 Frons with cluster of deep punctures in front of anterior ocellus (a); first submarginal cell of fore wing almost entirely setose (b); fore wing dark brown subapically (c) ..... ***Phalerimeris*** **Betrem**

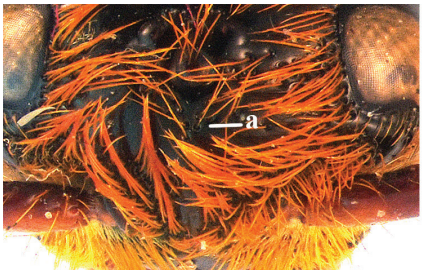

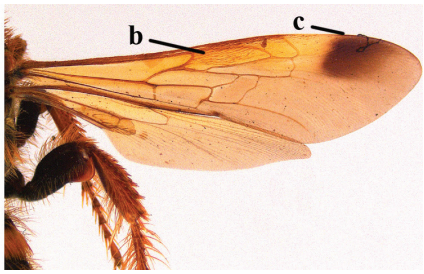

– Frons usually without deep punctures in front of anterior ocellus (aa); first submarginal cell fore wing glabrous, except for some setae anteriorly (bb); fore wing at most indistinctly smoky subapically (cc)..... ***Megacampsomeris*** **Betrem**

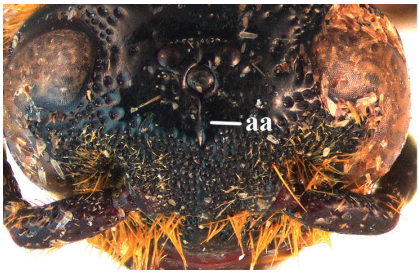

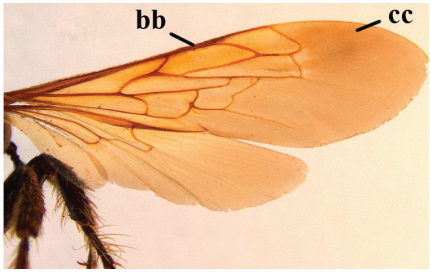

8 Length of body 5–15 mm; frontal spatium sparsely punctate, intervals between punctures larger than puncture diameters, especially medially (a); scutellum and metanotum usually marked with yellow spots; T1 always with yellow apical band which usually narrowed medially (b); parameres more slender, 4.6× longer than wide (c). [Note: As far as is known, vein 2m-cu of fore wing is always developed in Chinese species, but this vein is occasionally reduced or absent in some species] ..... ***Micromeriella*** **Betrem**

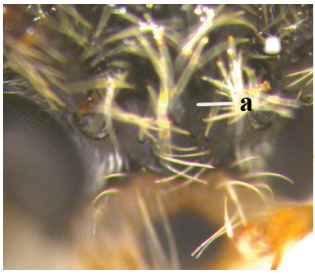

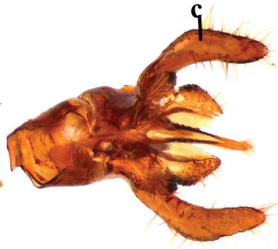

– Length of body 20–30 mm; frontal spatium with dense punctation, intervals mostly smaller than puncture diameter (aa); yellow spots absent or present on scutellum and metanotum and shape of yellow apical band of first tergite variable (bb); parameres robust, 3.2× longer than wide (cc) **9**

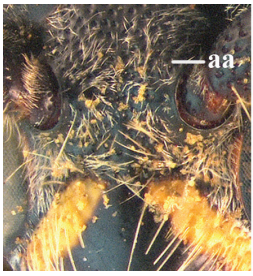

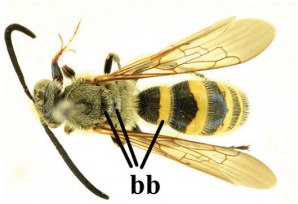

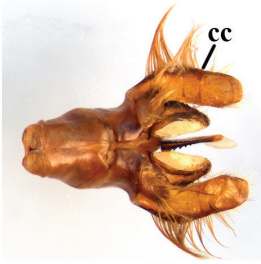

9 Head distinctly broader than high in frontal view (width approx. 1.3× height) (a); frons largely impunctate and with a large, flat, triangular area in front of anterior ocellus (b); apical metasomal sternites usually with dense erect setae (copulatory brushes) (c); parameres distinctly angled in middle, not narrowed apicad, basal part of volsellae lacking dense setae (d) ..... ***Campsomeriella*** **Beterem**

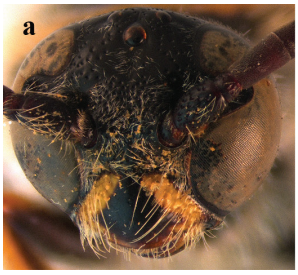

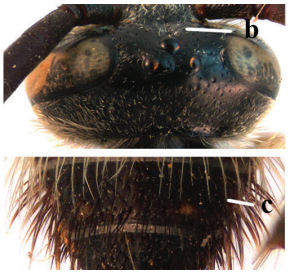

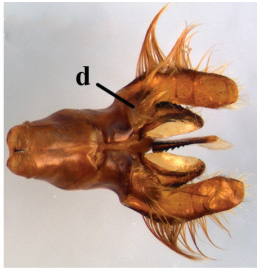

– Head almost as broad as high in frontal view (width at most 1.1× height) (aa); frons without a large impunctate area or triangular area in front of anterior ocellus (bb); apical metasomal sternites without dense erect setae (cc); parameres usually rounded in middle, narrower apicad, basal part of volsellae with sparse to dense setae (dd) **10**

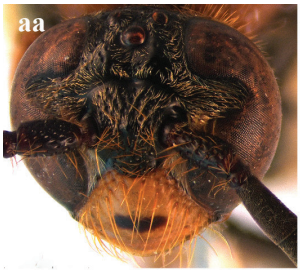

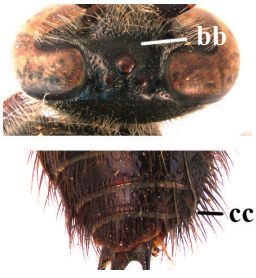

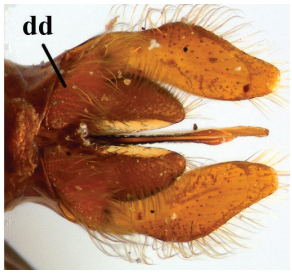

10 Clypeus, mandible, scapula, scutellum and metanotum entirely black, metasoma usually with wide reddish or orange bands on T1–3, often also on apical tergites (a); hind tibial spurs black (b); parameres less slightly converging apically (c) .....***Sericocampsomeris*** **Betrem**

– Clypeus, mandible, scapula, scutellum or metanotum often partly yellow, metasoma usually with narrow yellowish to reddish bands at least on basal four tergites (aa); hind tibial spurs white to pale yellowish (bb); parameres strongly converging apically (cc) **11**

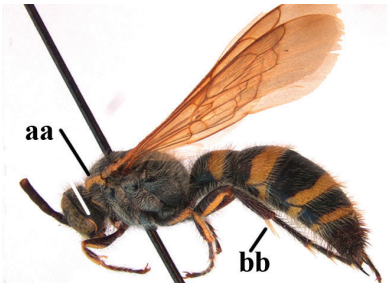

11 Basal part of volsellae with short sparse setae, distance between bases of these setae more than their own diameter (a); length of body less than 14 mm..... ..... ***Phalerimeris*** **Betrem**

– Basal part of volsellae with long dense setae, distance between the bases of these setae less than their own diameter (aa); length of body more than 15 mm, often 20–30 mm .....***Megacampsomeris*** **Betrem**

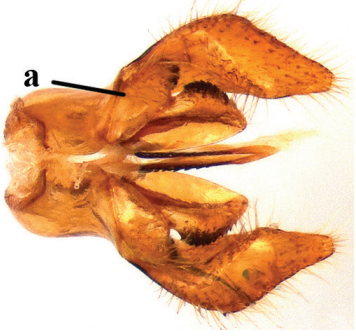

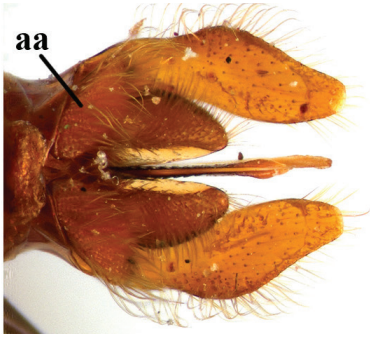

12 Fore wing with two discal cells (a)..... ***Liacos* Guérin-Méneville**
– Fore wing with one discal cell (aa)..... **13**

13 Fore wing with three submarginal cells (a) **14**
– Fore wing with two submarginal cells (aa)..... **15**

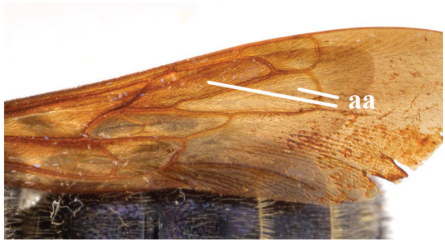

14 Length of body 15–20 mm; frons with an arched ridge, running from one ocular sinus to another and passing behind anterior ocellus, ridge prominent in male (a), but rather weak in female; ocelli on high triangle, posterior tangent to anterior ocellus far away from posterior ocelli in both sexes (b); metasomal setae black (c); T1 without tubercle (d); [only *Austroscolia ruficeps* (Smith, 1855) occurs in China] ..... ***Austroscolia* Betrem**

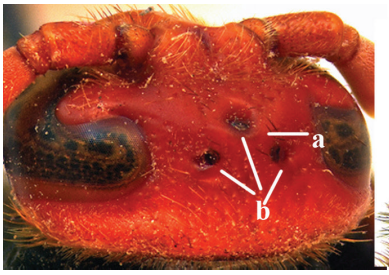

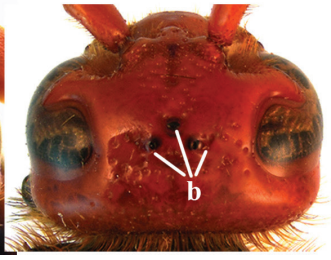

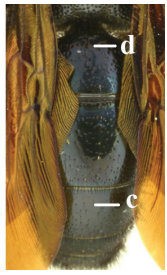

– Length of body 23–42 mm; frons without an arched ridge (aa); ocelli on low triangle, posterior tangent to anterior ocellus nearly touching posterior ocelli in both sexes (bb); setae of T3–6 or T4–6 reddish (cc); T1 with a strong tubercle antero-medially (dd); [only *Megascolia* (*Regiscolia*) *azurea* (Christ, 1791) occurs in China] ..... ***Megascolia*** **Betrem**

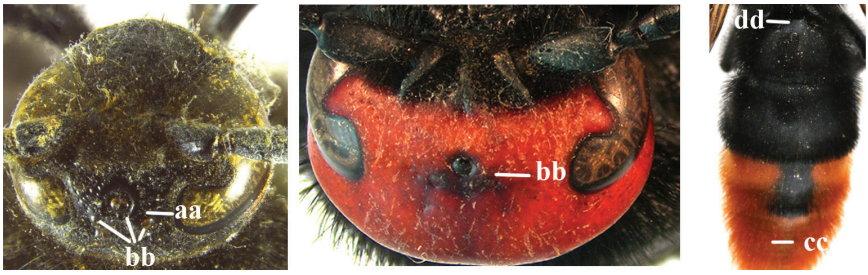

15 Frons often with a transverse ridge (or carina) on the males (a); posteriorly not strongly sloping vertex and temples less receding dorsally (b); metasoma black (c), at most T3 with yellow spots (cc), often with purple and blue reflections ..... ***Carinoscolia*** **Betrem**

– Frons without transverse carina on the males (aa); vertex strongly sloping posteriorly and temples more receding dorsally (bb); metasoma often with extensive yellow pattern (ccc) and with variable reflections ..... ***Scolia*** **Fabricius**

Key to species of genus *Campsomeriella* from China

1 Females, antenna with 12 segments (female of *C. ilanensis* (Tsuneki, 1972) unknown) **2**

– Males, antenna with 13 segments **5**

2 Lateral carina of propodeum short, not reaching spiracles (a); spurs of hind tibia black or testaceous (b); setae yellow to reddish on head and mesosoma (c); subgenus *Campsomeriella* Betrem **3**

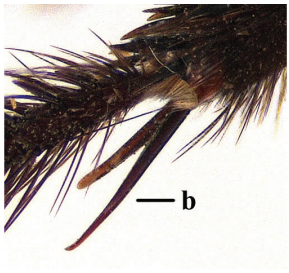

– Lateral carina of propodeum long, extending somewhat beyond the spiracles (aa); spurs of hind tibia white (bb); setae white on head and thorax (cc); subgenus *Annulimeris* Betrem ..... ***C.* (*A.*) *annulata* (Fabricius 1793)**

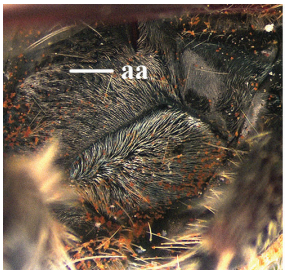

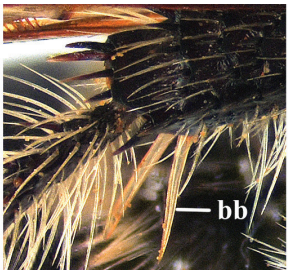

3 Setae of metasoma entirely black (a); setae on vertex and pronotum red (b); wings distinctly darkened apically (c), sometimes also basally and medially (cc) **4**

– Fringes of T1–T5 white (aa); setae on vertex and pronotum yellow (bb); wings subhyaline, at most, faintly darkened anteriorly (ccc) .... ***C.* (*C.*) *sauteri* (Betrem, 1928)**

4 Wings with distinctly darkened apical third and remainder subhyaline (a); vertex sparsely and distinctly punctate, densely pubescent (b); disc of clypeus with longitudinal ridge medially (c) ..... ***C.* (*C.*) *thoracica* (Fabricius, 1787)**

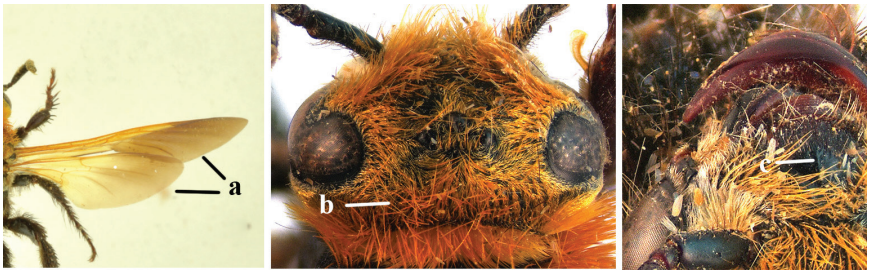

– Wings largely dark brown (aa); vertex smooth, except near occipital carina; disc of clypeus without ridge (cc); [syn. with *C.*(?) *ilanensis* (Tsuneki, 1972)] ..... ***C.* (*C.*) *collaris* (Fabricius, 1798)**

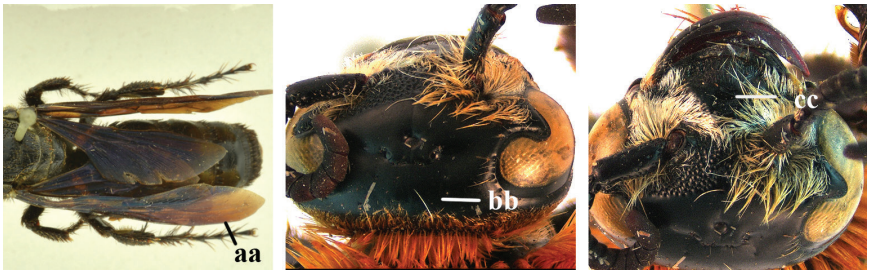

5 Base of volsella covered with sparse and short setae (a); metanotum black (b) and scutellum sometimes with two yellow spots; subgenus *Campsomeriella* Betrem **6**

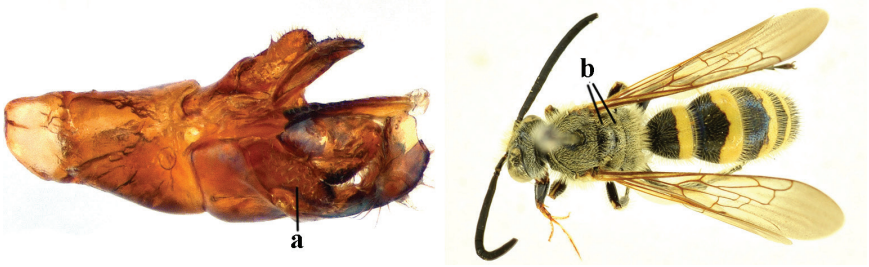

– Base of volsella covered with long and dense setae (aa); metanotum and scutellum always with yellow spots (bb); subgenus *Annulimeris* Betrem ..... ***C.* (*A.*) *annulata* (Fabricius 1793)**

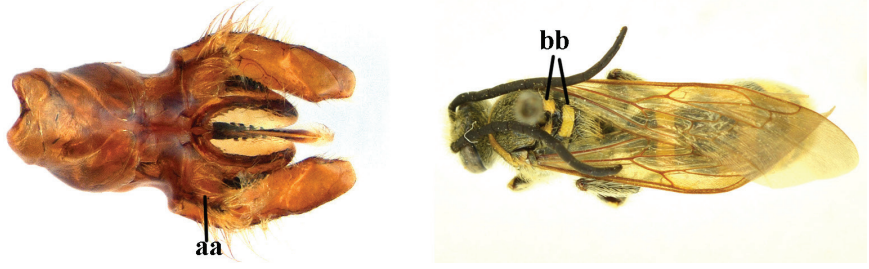

6 Bands of apical metasoma tergites red or orange, wide extending over half of tergites surface; coloured bands often absent on T1 (a); reddish setae covering most of metasoma coloured bands (b)... ***C.* (*C.*) *thoracica* (Fabricius, 1787)**

– Bands of apical metasoma segments yellow and often narrow, at most covering half of the tergites surface; T1 always with yellow apical band (aa); white setae covering yellow bands; brown to blackish-brown setae on T7 or T5–7 and T1–T6 or T1–T4 with white setae (bb) **7**

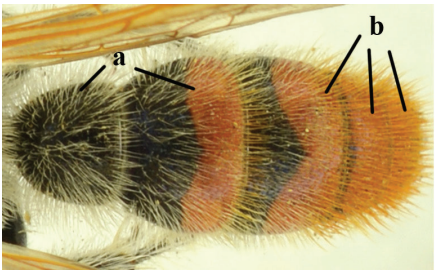

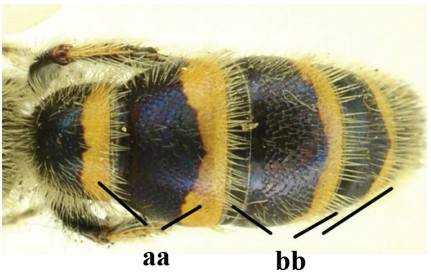

7 Pronotum yellow posterodorsally (a); middle femur marked with yellow apically; hind tibia extensively yellow (b); yellow band on T3 covering nearly half of its mid-length (c); [syn. with *C.*(?) *ilanensis* (Tsuneki, 1972)]..... ..... ***C.* (*C.*) *collaris* (Fabricius, 1798**

– Pronotum black posterodorsally (aa); middle femur nearly entirely black; hind tibia yellow basally (bb); yellow band on T3 occupying 1/4 of its mid-length (cc)..... ***C.* (*C.*) *sauteri* (Betrem, 1928)**

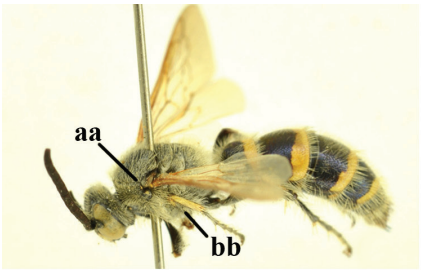

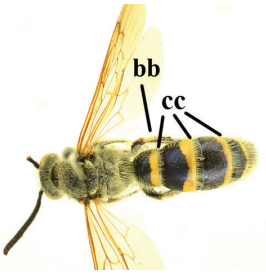

Notes. Only the male holotype of *Campsomeriella ilanensis* from Taiwan is known. According to the description and drawings by Tsuneki (1972a), *C. ilanensis* is very similar to *C.* (*C.*) *collaris quadrifasciata* (Fabricius, 1798) and it could be a synonym of the latter.

Key to species of *Megacampsomeris* from China

1 Female, antenna with 12 segments (female of *M. szetschwanensis* (Betrem, 1928) unknown) **2**

– Male, antenna with 13 segments (males of *M. bella* (Bingham, 1897), *M. grossa* (Fabricius, 1804) and *M. stoetzneri* (Betrem, 1928) unknown) **14**

2 Fringes of T1–T3 white or whitish (a) **3**

– Fringes of T1–T3 yellow, reddish-yellow or black (aa) **8**

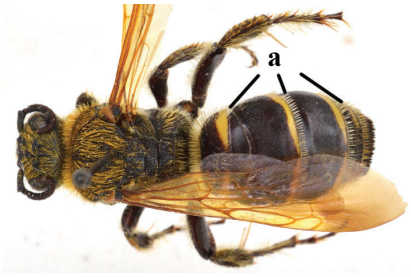

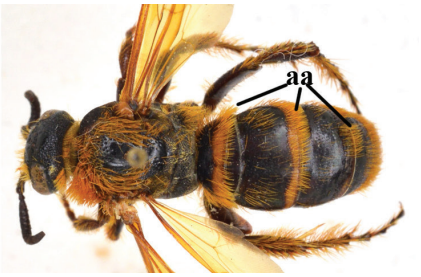

3 At least T1 more or less yellow or pale yellow posteriorly (a) **4**

– Metasomal tergites completely black (aa) **6**

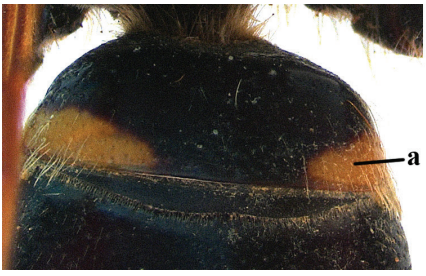

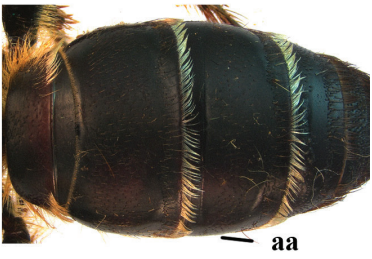

4 Vertex, behind ocelli, largely smooth (a); frons, in front of ocelli, narrowly smooth (b); mesoscutum smooth medially (c) ... ***M. schulthessi*** **(Betrem, 1928)**

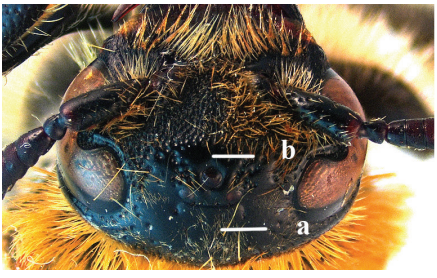

– Vertex (aa) and frons (bb) largely, densely and deeply punctate; mesoscutum entirely densely punctate (cc) **5**

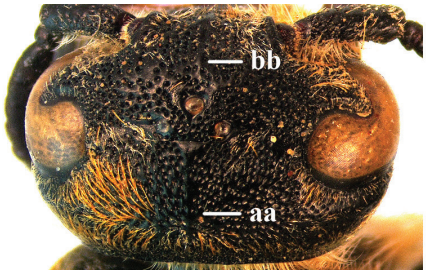

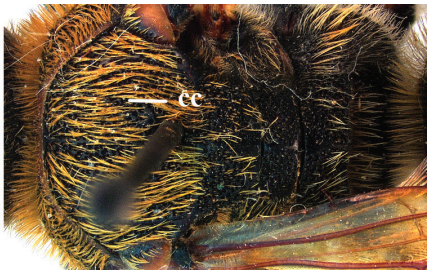

5 Spiracular corner (a) and vertical portion of upper plate of metapleuron (b) impunctate; upper plate of metapleuron divided by a well-defined ridge into a punctate dorsal portion and an impunctate vertical portion (c) .... ***M. bella*** **(Bingham, 1897)**

– Spiracular corner punctate (aa); vertical portion of upper plate of metapleuron punctate just below transition from dorsal portion and with few punctures along anterior and posterior sutures (bb); transition from dorsal to vertical portion of upper plate of metapleuron gradual, not carina-like (cc) .... ***M. stoetzneri*** **(Betrem, 1928)**

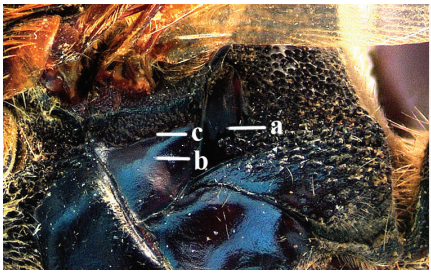

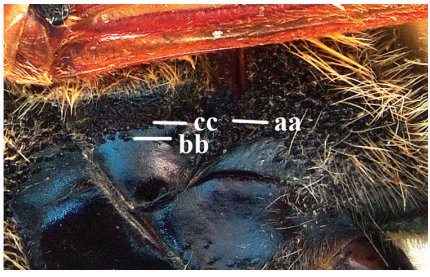

6 Vertex entirely smooth behind ocelli (a); setae blackish above antennal insertion and along inner margin of eyes (b) ..... ***M. grossiformis*** **Betrem, 1928**

– Vertex densely punctate behind ocelli (aa); head setae yellow or yellowish-brown (bb) 7

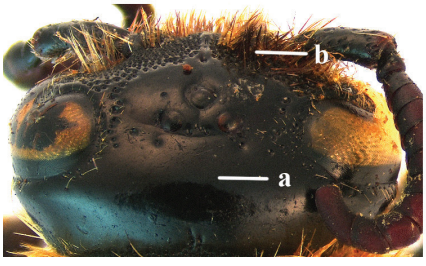

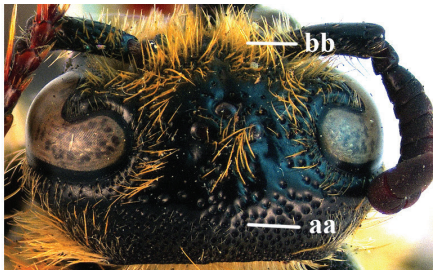

7 Mesoscutum and scutellum smooth, except for few punctures laterally (a); metanotum broadly smooth medially (b) ..... ***M. farrenwhitei*** **Betrem, 1928**

– Mesoscutum and scutellum nearly entirely densely punctate, except for more or less smooth area posteromedially (aa); metanotum densely punctate (bb) ..... ***M. grossa*** **(Fabricius, 1804)**

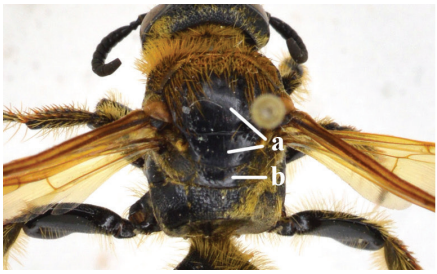

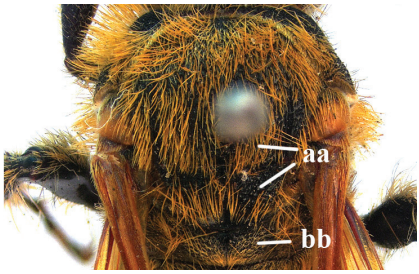

8 Fringes of T1–T4 blackish-brown to black; wings distinctly darkened .... ***M. binghami*** **(Betrem, 1928)**

– Fringes of T1–T4 brown or yellowish-brown (a); wings subhyaline and yellowish (b) **9**

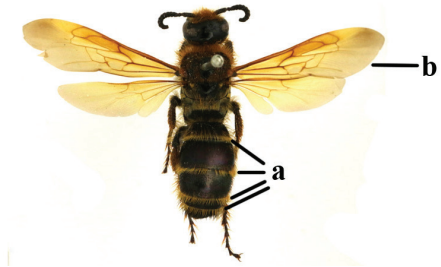

9 T1 and T2, sometimes including T3, with a yellow or pale yellow band posteriorly (a) **10**

– Tergites entirely black (aa) **11**

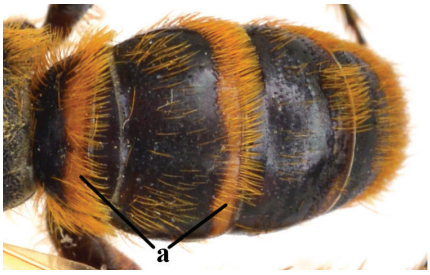

10 Bands on tergites distinct, T3 usually with yellow area posteriorly (a); scutellum largely smooth medially (b); basal elevation of T2 ("gradulus") distinctly developed (c) ..... ***M. formosensis*** **Betrem, 1928**

– Bands on tergites indistinct, T3 without yellow area (aa); scutellum evenly and densely punctate (bb); basal elevation of T2 absent (cc) .... ***M. limbata*** **(de Saussure & Sichel, 1864)**

11 Vertex smooth latero-posteriorly (a) ..... ***M. lindenii*** **(Lepeletier, 1845)**

– Vertex coarsely punctate latero-posteriorly (aa) **12**

12 Scutellum largely smooth (a); wings without infuscation subapically (b); median groove of frons distinct (c) ..... ***M. farrenwhitei*** **Betrem, 1928**

– Scutellum punctate anteriorly (aa), **if** largely smooth, then wings with subapical infuscation (bb); median groove of frons partly or almost completely missing (cc)..... **13**

13 Fringes of T1–T4 yellowish-brown and black on other tergites (a); antenna black (b); scutellum entirely or only anteriorly punctate (c) ..... ***M. prismatica*** **(Smith, 1855)**

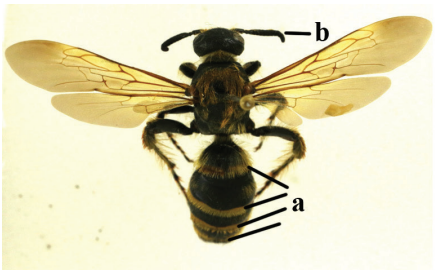

– Tergites setae yellowish-brown; antenna reddish-yellow; scutellum largely smooth ..... ***M. ceylonica*** **(Kirby, 1889)**

14 Tergites setae red or reddish-brown (a); legs yellowish-brown (b) ..... ***M. ceylonica*** **(Kirby, 1889)**

– Setae pale yellowish (aa) or reddish-brown and, on T6–T7, black (aaa); legs mainly black (bb)..... **15**

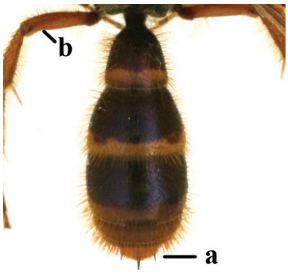

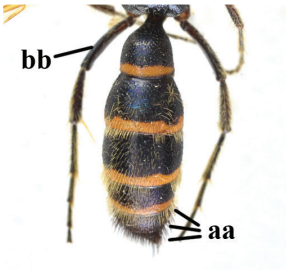

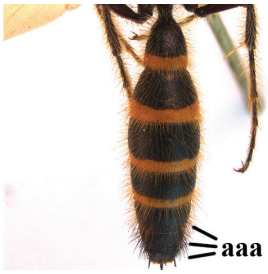

15 Clypeus mostly black, at most with two small lateral yellowish areas above mandible base..... **16**

– Clypeus at least broadly yellow laterally (a) **19**

16 Wings more or less darkened (a) ..... ***M. binghami*** **(Betrem, 1928)**
– Wings subhyaline (aa) **17**

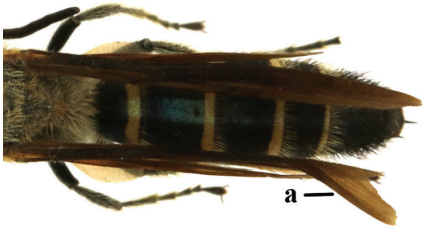

17 Posterodorsal margin of pronotum pale yellow; scutellum without medio-longitudinal carina ..... ***M. schulthessi*** **(Betrem, 1928)**
– Posterodorsal margin of pronotum only indistinctly narrowly yellow posteriorly (a); scutellum and metanotum with a more or less distinct medio-longitudinal carina (b) **18**

18 Setae on mesosoma yellowish and sparse (a); punctures sparse, intervals 1–2× larger than puncture diameter (b) ..... ***M. formosensis*** **(Betrem, 1928)**
– Setae on mesosoma reddish and dense (aa); punctures dense, intervals often smaller than puncture diameter (bb) .... ***M. szetschwanensis*** **(Betrem, 1928)**

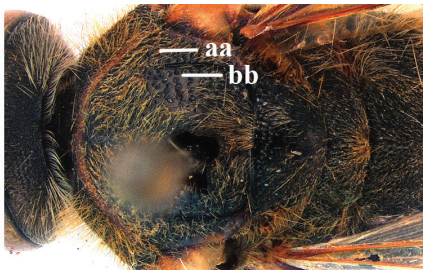

19 Clypeus always black medio-ventrally and remainder more or less yellow (a) **20**

– Clypeus always yellow medially (aa) **22**

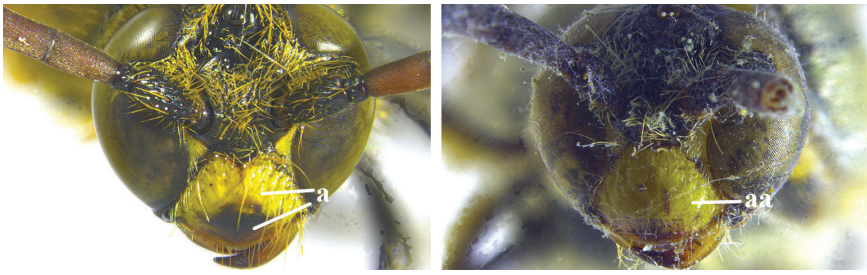

20 Yellow bands on T1 wide, covering nearly 1/3 of T1; scutellum always with two lateral yellow spots ..... ***M. limbata*** **(de Saussure & Sichel, 1864)**

– Yellow bands on T1 narrow, at most covering 1/5 of T1; scutellum often entirely black, rarely with yellow spots **21**

21 Hind femur yellow ventrally (a); S2–S4 often with yellow cuneate maculae lateroapically (b) ..... ***M. farrenwhitei*** **Betrem, 1928**

– Hind femur black ventrally (aa); S2–S4 rarely with yellow maculae (bb) ..... ***M. prismatica*** **(Smith, 1855)**

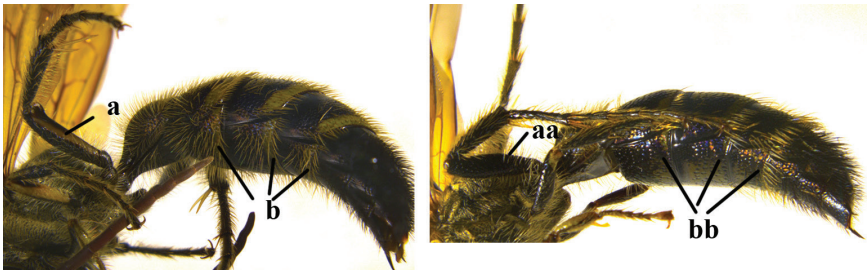

22 T5 usually with yellow band posteriorly; setae of mesosoma dirty white; pronotum black ..... ***M. grossiformis*** **Betrem, 1928**

– T5 without a yellow band (a); setae of mesosoma reddish or yellowish-brown (b); pronotum entirely or mostly reddish-yellow (c) ..... ***M. lindenii*** **(Lepeletier, 1845)**

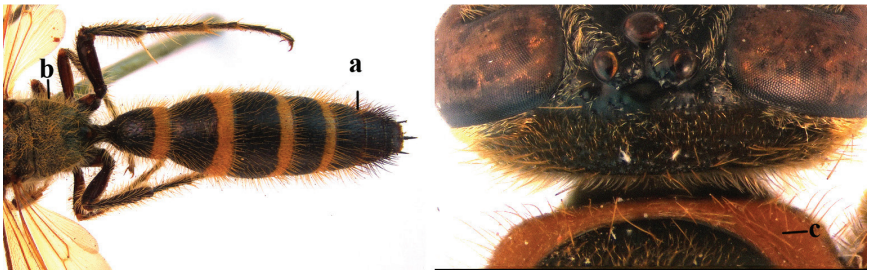

Notes. Males of this genus are difficult to recognise, the key above is a practical key to the males present in the material we have studied and is just a first attempt. The male of *M. farrenwhitei* Betrem, 1928 is here recorded for the first time worldwide. However, males identified as *M. szetschwanensis* (Betrem, 1928) could be the male of *M. stoetzneri* Betrem or another species, since the female of *M. szetschwanensis* and the males of *M. bella* (Bingham, 1897), *M. grossa* (Fabricius, 1804) and *M. stoetzneri* (Betrem, 1928) are unknown and the forma A (in Betrem 1941, typical forma of *C. szetschwanensis*) specimen of *M. szetschwanensis* carries an identical collection label as the holotype female of *M. stoetzneri* (Schulten 2011).

Key to species of *Sericocampsomeris*

1 Female, antenna with 12 segments **2**

– Male, antenna with 13 segments **3**

2 Pronotum posterodorsally and upper margin of clypeus with golden setae (a); metasoma setae dark brown, except indistinctly reddish-brown setae on epipygium (b); metanotum and propodeum densely punctate (c) .... ***S. degaullei*** **(Betrem, 1928)**

– Pronotum posterodorsally and clypeus with black setae (aa); setae on T2 or T5–T7 reddish-golden (bb); metanotum and median part of propodeum largely smooth (cc) ..... ***S. rubromaculata*** **(Smith, 1855)**

3 Posterior part of T3 and T4–T7 bright reddish-yellow (a); wings infuscate (b); scutellum and metanotum with a continuous medio-longitudinal carina (c) ..... ***S. degaullei*** **(Betrem, 1928)**

– T1–T3 predominantly reddish-yellow with pale yellow setae, except for black setae on T5/T6–T7 (aa); wings hyaline (bb); scutellum and metanotum without medio-longitudinal carina (cc) ..... ***S. rubromaculata*** **(Smith, 1855)**

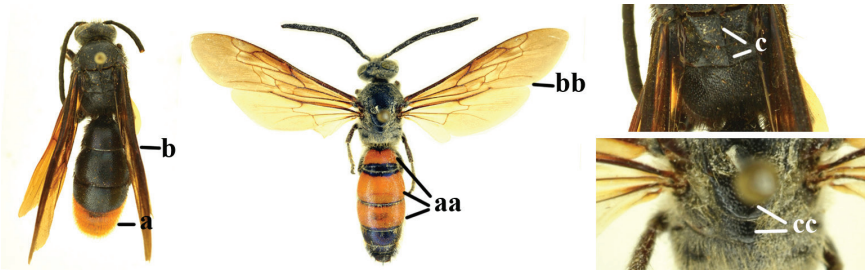

Key to species of *Carinoscolia* Betrem from China

1 Frons with a distinct transverse carina present in front of anterior ocellus in both sexes (a); head dark in female (b) ..... ***C. nipponensis*** **Uchida, 1933**

– Frons without transverse carina, at most with distinct transverse ridge present in males (aa), but often with more or less denser punctate depression before a relatively higher area in both sexes (aaa); head with more or less yellow areas (bb) **2**

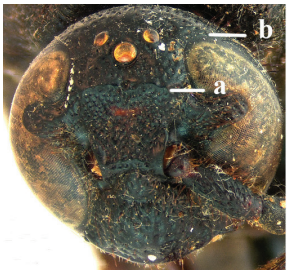

2 Frons with a distinct transverse ridge in male (a); pronotum in both sexes yellow laterally (b); T3 and sometimes also T4 in female yellow laterally (c), male metasoma wholly black..... ***C. yunnanensis*** **(Betrem, 1941)**

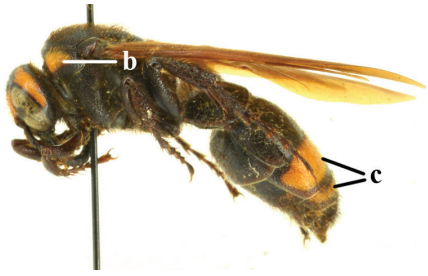

– Frons without distinct transverse ridge in male, often replaced by a more or less denser punctate depression (aa); pronotum in both sexes black laterally (rarely with small round yellow spot anteriorly in female); T3 of both sexes often with pale yellow lateral spot (cc) ..... ***C. vittifrons*** **(Sichel, 1864)**

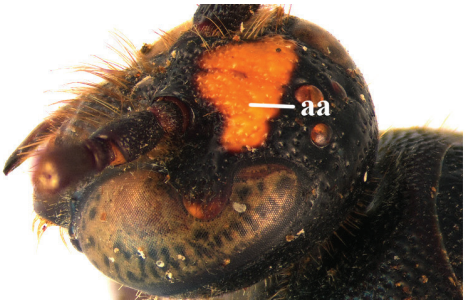

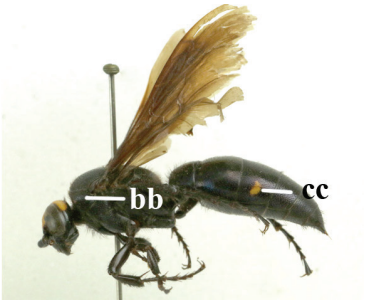

Key to species of the genus *Scolia* Fabricius from China

1 Base of volsella covered with a dense brush of silky setae (a); Chinese female either with metasoma entirely black and wings evenly infuscate, lacking purple or blue reflections (b) **or** with metasoma predominantly yellow and wings bright yellow basally (bb); mainly distributed in Palaearctic Regions of China; subgenus *Scolia s. str.* Fabricius **2**

– Base of volsella without dense brush of silky setae (aa); females either with metasoma predominantly black and wings dark brown with distinct purple or blue reflections (bbbb) **or** with red or yellow pattern and wings never bright yellow basally (bbb); mainly distributed in Oriental Regions of China; subgenus *Discolia* Saussure..... **4**

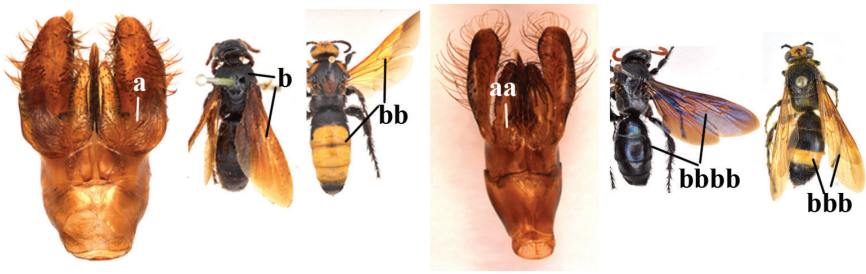

2 Body black (a); wings not distinctly darkened apically and evenly infuscate (b); clypeus nearly smooth medially (c) .... ***S.* (*S.*) *concolor* Eversmann, 1849**

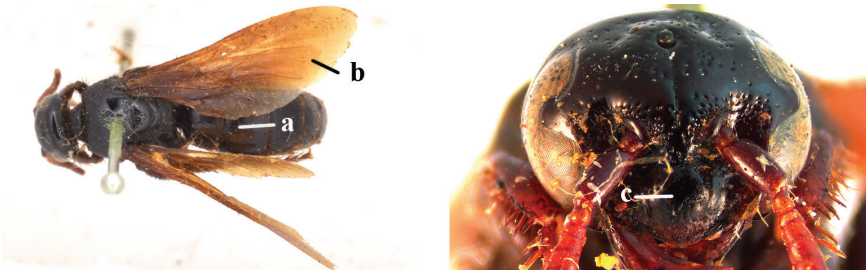

– Metasoma at least partly yellowish (aa); wings with distinct dark apical band and yellowish basally (bb); clypeus strongly rugose or densely punctate medially (cc) **3**

3 Vertex smooth behind ocelli (a); anterior ocellus situated in a narrow and shallow depression (b); vertex and frons yellow (c) .... ***S.* (*S.*) *flaviceps* Eversmann, 1846**

– Vertex densely punctate (aa); anterior ocellus in a broad and deep depression (bb); vertex and frons black (cc) ..... ***S.* (*S.*) *potanini* Morawitz, 1889**

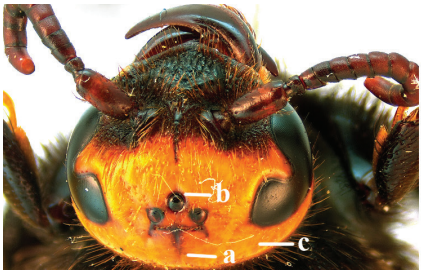

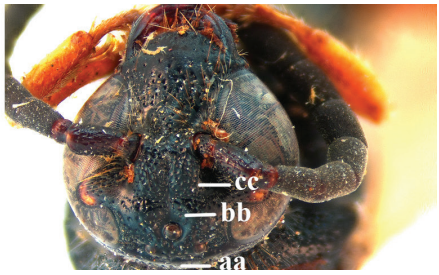

4 Setae red or yellowish-brown on T2–T7 (sometimes black on epipygium) and black on mesosoma (a) **5**

– Setae on T4–T7 usually black (aa), **if** setae pale, **then** mesosoma setae also pale **6**

5 Body entirely black, setae red on T2–T7 (a); fore wing without dark subapical spot (b); mesopleuron densely punctate, except partly anteriorly and posteriorly (c) ..... ***S.* (*D.*) *sinensis* de Saussure & Sichel, 1864**

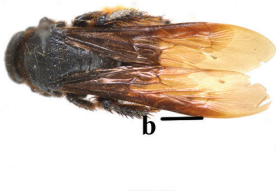

– T3–T6 largely reddish-yellow with red setae, fringes of T2 black; fore wing with a darker subapical spot; mesopleuron nearly smooth, with a few large punctures ..... ***S.* (*D.*) *minowai* Uchida, 1933**

6 Female, antenna with 12 segments (females of *S.* (*D.*) *bnun* Tsuneki, 1972 and *S.* (*D.*) *wusheensis* Tsuneki, 1972 unknown) **7**

– Male, antenna with 13 segments (males of *S.* (*D.*) *inouyei* Okamoto, 1924 and *S.* (*D.*) *tigrimaculosa* Yamane, 1995 unknown) **23**

7 Dorso-median area of propodeum smooth to superficially and sparsely punctate (intervals at least as large as puncture diameter) (a) **8**

– Dorso-median area of propodeum more or less strongly and densely punctate (intervals smaller than puncture diameter) (aa) **11**

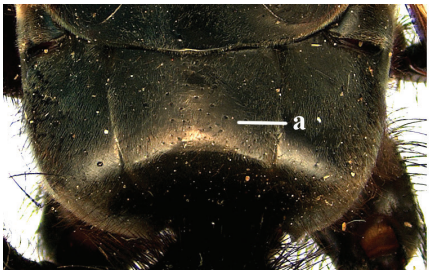

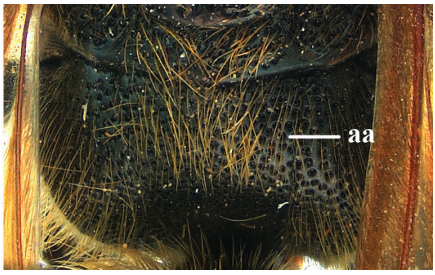

8 Metasoma and mesosoma completely black (a) **9**

– Metasoma and/or mesosoma often with yellow pattern (aa) **10**

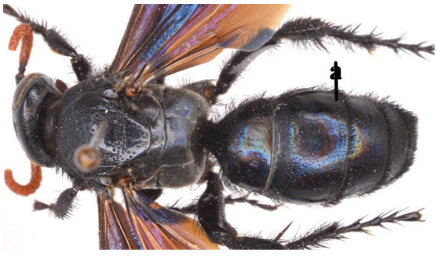

9 Vertex partially to almost entirely yellowish-red (a); metanotum with few, irregular punctures (b); POL:OD:OOL=183:54:251 (c); wings without reflection (d) ..... ***S.* (*D.*) *superciliaris* de Saussure, 1864**

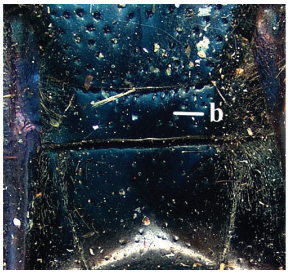

– Vertex entirely black (aa); metanotum and propodeal dorsally almost entirely smooth (bb); POL:OD:OOL=153:69:183 (cc); wings with distinct purple reflection (dd) ..... ***S.* (*D.*) *affinis* Guérin-Méneville, 1845**

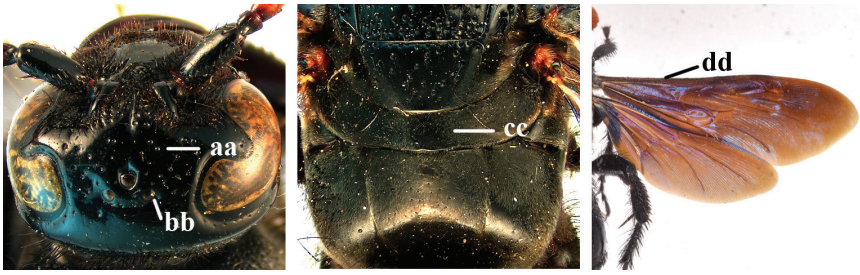

10 T4 black (a); lateral carina just reaching level of propodeal spiracle (b); median groove of frons distinct (c) ..... ***S.* (*D.*) *nobilis* de Saussure, 1858**

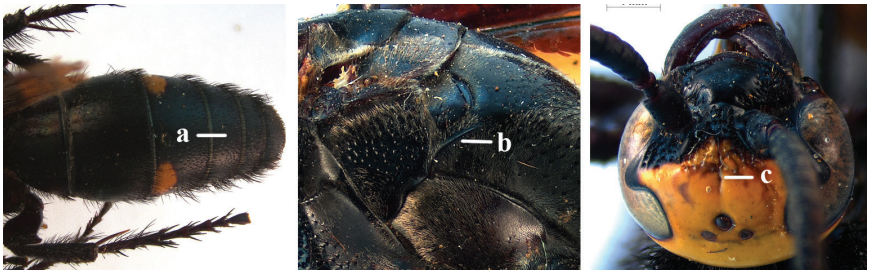

– T4 with a narrow apical yellow band or two lateral yellow spots (aa); lateral carina surpassing level of propodeal spiracle (bb); median groove of frons absent (cc) ..... ***S.* (*D.*) *inouyei* Okamoto, 1924**

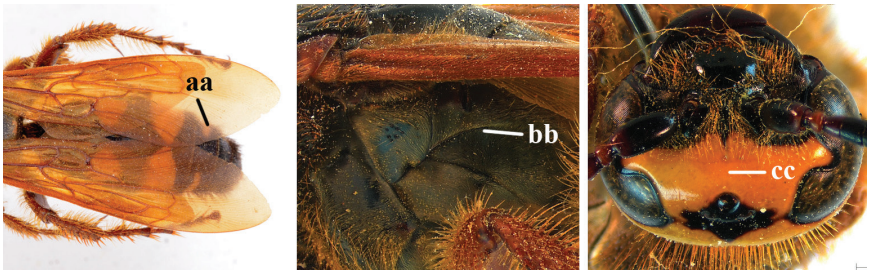

11 Body black (a)..... ***S.* (*D.*) *laeviceps* Smith, 1855**

– Metasoma often with red or yellow pattern (aa) **12**

12 Pronotum posterodorsally yellow or red (a) **13**
– Pronotum posterodorsally black (aa) **17**

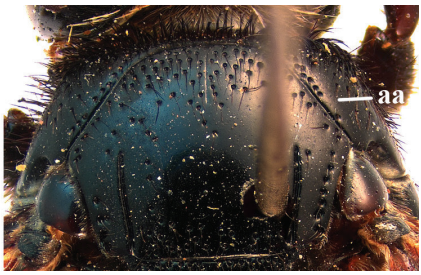

13 Middle of clypeus and anterior part of head above antenna sockets red; pronotum marked with red ..... ***S.* (*D.*) *clypeata* Sickman, 1894**
– Head black or only with yellow spots; pronotum marked with yellow..... **14**
14 Mesonotum often evenly densely punctate (a); spiracular corner often smooth (b); pronotum posterodorsally widely smooth (c); scutellum and/or metanotum always with yellow bands (d) ..... ***S.* (*D.*) *picteti* de Saussure, 1855)**

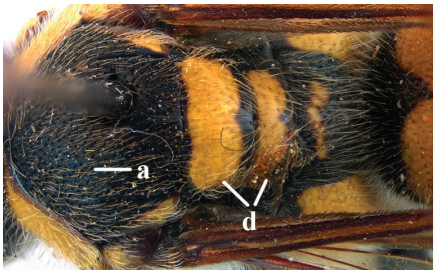

– Mesonotum narrowly to largely impunctate medially; spiracular corner punctate, **if** smooth, **then** pronotum posterodorsally largely sculptured; pale pattern on scutellum and metanotum less developed **15**
15 Area behind hind ocellus almost impunctate; gena with a yellow line behind eye **16**
– Area behind hind ocellus with well-defined punctures; gena without yellow line ..... ***S.* (*D.*) *desidiosa* Bingham, 1896**
16 Scutellum black; anterior half of mesopleuron almost impunctate; apical fringe of T2–4 and S5 dark brown..... ***S.* (*D.*) *taiwana* Tsuneki, 1972**
– Scutellum largely yellow; anterior half of mesopleuron extensively closely punctate; apical fringe of T2–4 and S5 pale golden..... ..... ***S.* (*D.*) *tigrimaculosa* Yamane, 1995**
17 Legs reddish (a); wings yellow hyaline, with dark tip (b); metasoma with reddish-brown setae throughout (c); T2–5 with yellow apical maculae (d).... ..... ***S.* (*D.*) *rufispina* Morawitz, 1889**

– Femora and tibiae black (aa); wings almost uniformly dark or yellow hyaline without dark tip (bb); metasoma setae not reddish-brown (cc); one to three tergites with yellow or reddish maculae (dd) **18**

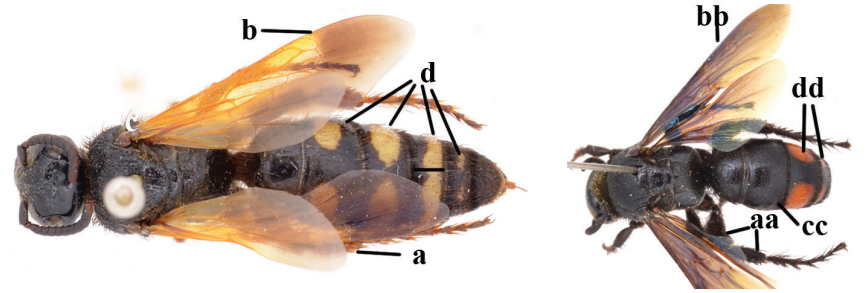

18 T3–T4 with pair of reddish spots (a); mesonotum and pronotum posterodorsally largely impunctate (b); dorso-lateral area of propodeum impunctate on its inner half (c) [= *S. quadripustulata* auctt. from China] .... ***S.* (*D.*) *binotata* Fabricius, 1804**

– T3 with yellow band and T4 black (aa); mesonotum and pronotum posterodorsally densely punctate (bb) or largely impunctate; dorso-lateral area of propodeum more or less punctate (cc) **19**

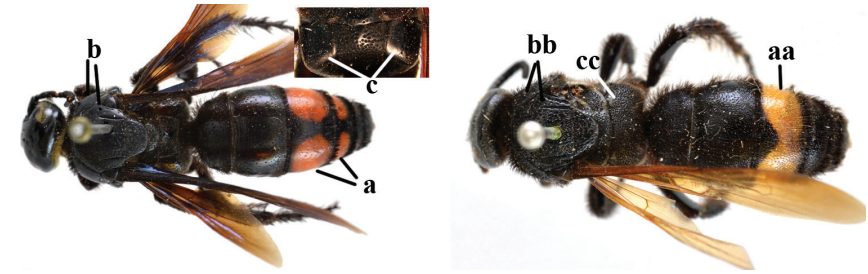

19 Mesonotum largely impunctate; frons and vertex impunctate; frons with transverse impressed line **20**

– Mesonotum densely punctate (a); frons and vertex largely smooth (b) to densely punctate (bb); frons without transverse impressed line (c) **21**

20 Transverse impressed line on frons slightly curved upwards laterally; intervals of punctures on posterior margin of pronotum broadly smooth and polished ..... ***S.* (*D.*) *apakaensis* Tsuneki, 1972**

– Transverse impressed line on frons straight; intervals of punctures on posterior margin of pronotum rugulose ..... ***S.* (*D.*) *schrenckii* Eversmann, 1846**

21 Head entirely black (a); median groove of frons more or less impressed (b).... **22**

– Head partly red or yellow (aa); median groove of frons absent (bb)..... ..... ***S.* (*D.*) *watanabei* (Matsumura, 1912)**

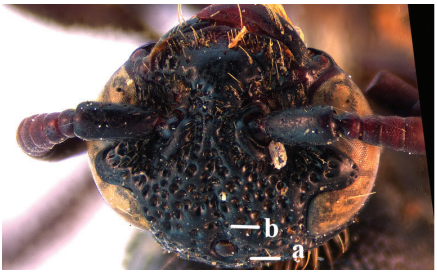

22 Vertex and frons with dense coarse punctation (a); median groove of frons distinct (b) ..... ***S.* (*D.*) *formosicola* Betrem, 1928**

– Vertex and frons largely smooth, without large punctures, (aa); median groove of frons indistinct (bb)..... ***S.* (*D.*) *oculata* Matsumura, 1911**

23 Metasoma entirely black (a) **24**

– Metasoma with variable whitish-yellow to reddish pattern (aa) **26**

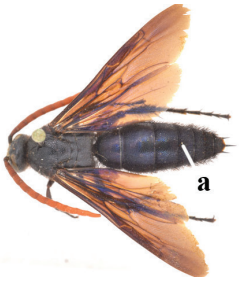

24 Antenna robust subapically, penultimate flagellomere 1.2× longer than wide (a); anterior ocellus in a broad deep pit (b) ....***S.* (*D.*) *laeviceps* Smith, 1855**

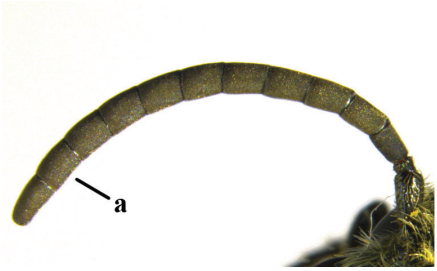

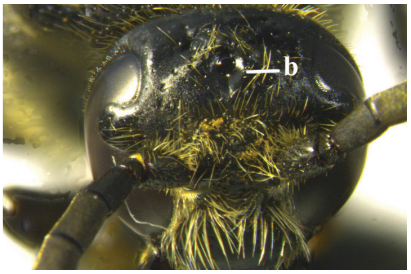

– Antenna slender subapically, penultimate flagellomere distinctly (1.6×) longer than wide (aa); anterior ocellus in a narrow pit (bb) **25**

25 Vertex entirely black (a); setae of metasoma entirely black (b) ..... ***S.* (*D.*) *affinis* Guérin-Méneville, 1845**

– Vertex partly to nearly entirely yellowish-red (aa); setae of metasoma yellowish, but black on T6–T7 (bb) ..... ***S.* (*D.*) *superciliaris* de Saussure, 1864**

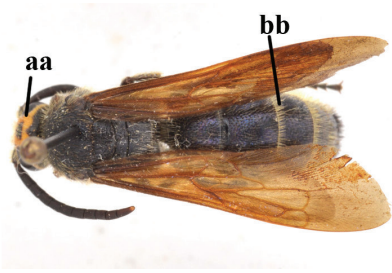

26 Head and mesosoma entirely black (a) **27**

– Head and/or mesosoma with variable yellow to reddish patterns (aa) **31**

27 Femora and tibiae red; metasoma with reddish-brown setae, even on black parts; T2–T5 with yellow band ..... ***S.* (*D.*) *rufispina* Morawitz, 1889**

– Femora and tibiae black; setae on metasoma not reddish-brown; often only T3 with yellow or reddish band **28**

28 Antenna shorter than head and mesosoma combined **29**
– Antenna longer than head and mesosoma combined (a) **30**

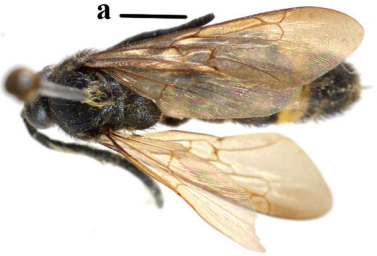

29 Wings not paler apically; mesoscutum narrowly impunctate medio-posteriorly ..... ***S.* (*D.*) *apakaensis* Tsuneki, 1972**
– Wings slightly paler apically; mesoscutum broadly impunctate medio-posteriorly..... ***S.* (*D.*) *schrenckii* Eversmann, 1846**
30 Lateral areas of propodeum almost smooth (a); yellow band of T3 uninterrupted or indistinctly interrupted (b); metasoma 3.0× longer than wide (c) .. .. ***S.* (*D.*) *formosicola* Betrem, 1928**
– Lateral areas of propodeum distinctly punctate (aa); yellow band of T3 distinctly interrupted (bb); metasoma 2.4× longer than wide (cc)..... ..... ***S.* (*D.*) *oculata* Matsumura, 1911**

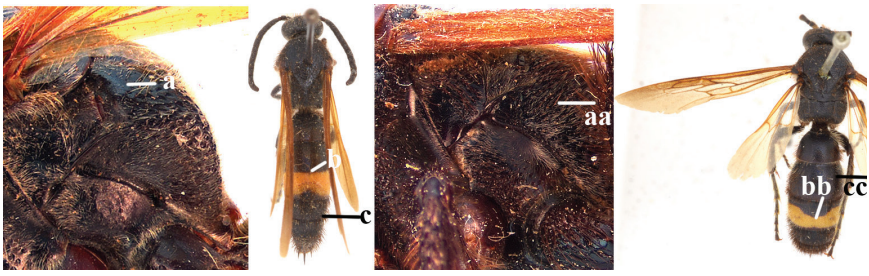

31 Dorso-median area of propodeum smooth to superficially and sparsely punctate (intervals at least as large as puncture diameter).....**32**
– Dorso-median area of propodeum more or less strongly and densely punctate (intervals smaller than puncture diameter) **34**
32 Mesonotum and scutellum uniformly punctate (a); often only T3 with a more or less interrupted pale band (b) ..... ***S.* (*D.*) *nobilis* de Saussure, 1858**

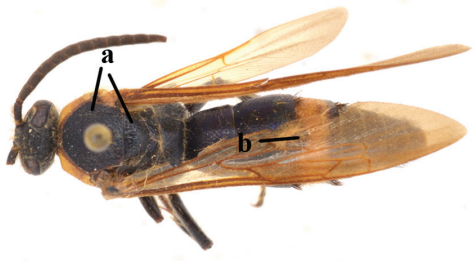

– Mesonotum and scutellum with impunctate area medio-posteriorly; tergites with variable pale pattern **33**

33 T3–T5 each with a medially constricted broad band (rarely also T2 with a pair of yellow spots, yellow band on T5 sometimes greatly reduced or absent); punctures on mesosoma and propodeum (including lateral face) smaller and closer; wings brownish-yellow; punctures on metasoma smaller .....
***S.* (*D.*) *wusheensis* Tsuneki, 1972**

– Only T3 with two large yellow spots and T4–T5 black; punctures on mesosoma and propodeum (including lateral face) much coarser and slightly sparser; wings pale yellow; punctures on metasoma larger.....
***S.* (*D.*) *bnun* Tsuneki, 1972**

34 Pronotum postero-dorsally yellow or red..... **35**

– Pronotum postero-dorsally black **38**

35 Body black and reddish (a): anterior part of head largely red; frontal spatium not separated from frons (b); frons with punctures as on frontal spatium, smooth laterally (c); median groove of frons indistinct (d); T1 densely punctate, posterior margin with extremely dense and fine punctures (e) .....
***S.* (*D.*) *clypeata* Sickman, 1894**

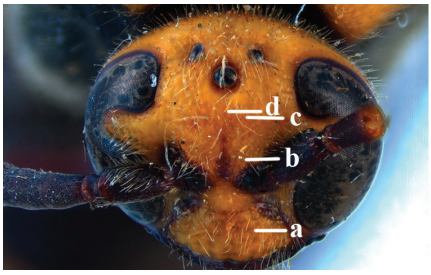

– Body black and yellow, head black or only with yellow spots (aa); frontal spatium usually separated from frons by a linear depression (bb), **if** not separated, then punctures on frons sparser than punctures on frontal spatium (cc); median groove of frons always distinct (dd); T1 usually sparsely punctate (ee) **36**

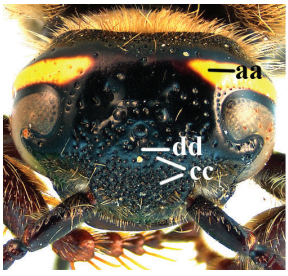

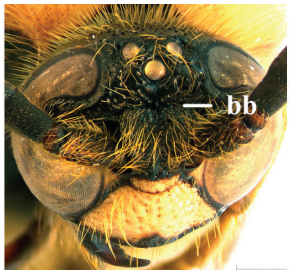

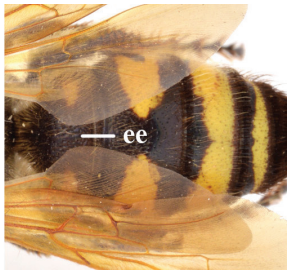

36 Three large yellow spots present on propodeum (a); spiracular corner punctate (b) ..... ***S.* (*D.*) *desidiosa* Bingham, 1896**

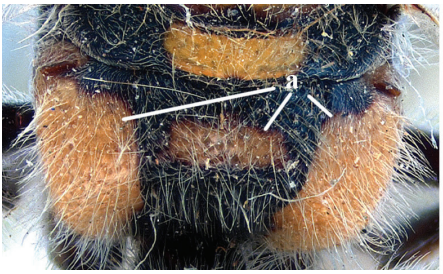

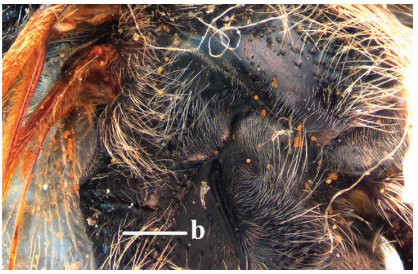

– Propodeum entirely black (aa); spiracular corner smooth (bb) **37**

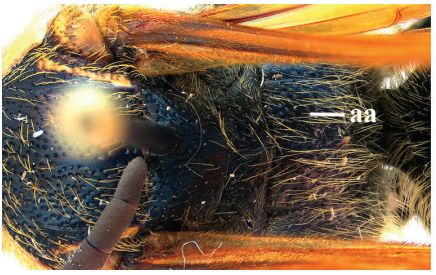

37 Mesonotum often evenly densely punctate (a); scutellum and/or metanotum always with yellow bands (b) ..... ***S.* (*D.*) *picteti* de Saussure, 1855)**

– Mesonotum narrowly to largely impunctate medially (aa); yellow pattern on scutellum and metanotum absent (bb) or less developed ..... ***S.* (*D.*) *taiwana* Tsuneki, 1972**

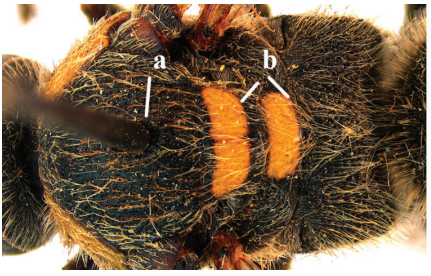

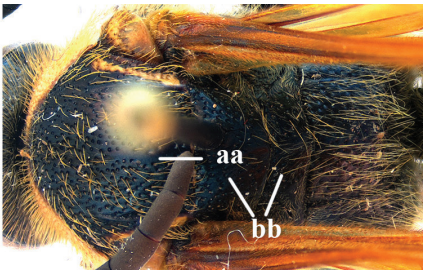

38 T3–T4 with paired reddish spots (a); flagellum somewhat widened towards apex (b) ..... ***S.* (*D.*) *binotata* Fabricius, 1804**

– T3 or T3–T4 with yellow bands (aa); flagellum not widened towards apex (bb) ..... ***S.* (*D.*) *watanabei* (Matsumura, 1912)**

Notes. The name *Scolia quadripustulata* Fabricius was misapplied for a long time to another species now known as *Scolia binotata* Fabricius (Gupta and Jonathan 2003). We checked all specimens from China in IOZ and RMNH and all were found to belong to *Scolia* (*Discolia*) *binotata* Fabricius. All reported records of *S. quadripustulata* from China concern *S. binotata*; therefore, we delete *S. quadripustulata* from the Chinese fauna.

Acknowledgements

The first author is very grateful to Frederique Bakker, the manager of RMNH Hymenoptera Collection (Leiden) and to Hong Liu (IOZ, Beijing) for facilitating her visit for examining specimens. This research was supported by the Scientific Research Foundation for Doctors of Hunan University of Arts and Science (19BSQD30), Scientific Research Fund of Hunan Provincial Education Department (20K089) and Hunan Provincial Natural Science Foundation of China (2020JJ5392).

References

Argaman Q (1996) Generic synopsis of Scoliidae (Hymenoptera, Scolioidea). Annals Historico-Naturales Musei Nationalis Hungarici 88: 171–222.

Betrem JG (1927) Een nieuwe indeeling der Scoliiden. Tijdschrift voor Entomologie 70 (verslag): XCIII–XCVIII.

Betrem JG (1928) Monographie der Indo-Australischen Scoliiden mit zoogeographischen Betrachtungen. Treubia 9 (suppl.): 1–388.

Betrem JG (1932) De Scoliiden-fauna van Banka. Entomologische Berichten 9: 412–415.

Betrem JG (1933) Die Scoliiden der indoaustralischen and palaearktischen Region aus dem Staatlichen Museum für Tierkunde zu Dresden (Hym.). Stettiner Entomologische Zeitung 94: 236–263.

Betrem JG (1935) Beitrage zur Kenntnis der Palaarktischen Arten des genus *Scolia*. Tijdschrift voor Entomologie 78: 1–78.

Betrem JG (1937) The males of the Indo-Australian *Campsomeris* species with yellow metanotum (Hym., Scoliidae). The Proceedings of the Royal Entomological Society of London (B) 6(5): 91–96. https://doi.org/10.1111/j.1365-3113.1937.tb00305.x

Betrem JG (1941) Étude systematique des Scoliidae de Chine et leurs relations avec les autres groups de Scoliidae. Notes d'Entomologie Chinoise 8(4): 47–188.

Betrem JG (1947 [1945]) Analyse van enkele fauna:-elementen van de Maleische Scoliiden. Tijdschrift voor Entomologie 88: 409–416.

Betrem JG (1962) The taxon *Trielis* (Hymenoptera: Scoliidae) and its type. Entomological News 73: 146.

Betrem JG (1967) The natural groups of *Campsomeriella* Betr., 1941 (Hymenoptera: Scoliidae). Entomologische Berichten 27: 25–29.

Betrem JG, Bradley JC (1972) The African Campsomerinae (Hym., Scoliidae). Mono-grafieën van de Nederlandse Entomologische Vereniging 6: 1–326.

Bingham CT (1896) On some Exotic Fossorial Hymenoptera in the Collection of the British Museum, with Descriptions of New Species and of a New Genus of the Pompilidæ. Zoological Journal of the Linnean Society 25(164): 422–445. https://doi.org/10.1111/0044-0124.00164-i1

Bingham CT (1897) The Fauna of British India, including Ceylon and Burma: Hymenoptera, 1 (Wasps and Bees). Taylor and Francis, London, 579 pp. https://doi.org/10.5962/bhl.title.100738

Bradley JC (1950) The most primitive Scoliidae. Eos (tomo extraord.): 427–437.

Bradley JC (1959) The Scoliidae of Africa. Annals of the Transvaal Museum 23: 331–362.

Bradley JC (1964a) The Fabrician types of Scoliidae (Hymenoptera), with notes and an appendix by J.G. Betrem. Spolia Zoologica Musei Hauniensis 21: 1–38.

Bradley JC (1964b) The type-specimens of the Scoliidae described by Amédée Lepeletier, Comte de Saint-Fargeau (with notes by J. G. Betrem) and by the Marchese Massimiliano Spinola. Estratto Dagli Annali Del Museo Civico Di Storia Naturale Di Genova 75: 16–196.

Bradley JC (1972) Scoliid types in the Museum für Naturkunde of the Humboldtuniversität zu Berlin. Zoologisches Museum und Institut für Spezielle Zoologie (Berlin) 48(1): 3–19. https://doi.org/10.1002/mmnz.19720480102

Bradley JC (1973) The scoliid types of Guérin-Méneville (Insecta: Hymenoptera: Scoliidae). Bulletin du Muséum National D'Histoire Naturelle (3) 112, Zoologie 86: 217–221.

Bradley JC (1974) The types of Scoliidae (Hymenoptera) described by Henri de Saussure or by Jules Sichel, or by them jointly. Revue Suisse Zoologie 81(2): 417–485. https://doi.org/10.5962/bhl.part.76015

Bradley JC, Betrem JG (1966) Burmeister's work on Scoliidae, with especial reference to types and synonymy (Hymenoptera: Scoliidae). Beiträge zur Entomologie 16: 73–84.

Bradley JC, Betrem JG (1967) The types of Scoliidae described by Frederick Smith (Hymenoptera). Bulletin of the British Museum (Natural History) Entomology 20 (7): 287–327.

Bradley JC, Betrem JG (1968) Friedrich Klugs material of Scoliidae with especial reference to his type specimens. Deutsche Entomologische Zeitschrift 15: 321–334. https://doi.org/10.1002/mmnd.4810150406

Day MC, George RE, David M (1981) The most primitive Scoliidae (Hymenoptera). Journal of Natural History 15: 671–684. https://doi.org/10.1080/00222938100770471

Elliott MG (2011) Annotated catalogue of the Australian Scoliidae (Hymenoptera). Technical Reports of the Australian Museum, Online, 22: 1–17. https://doi.org/10.3853/j.1835-4211.22.2011.1562

Eversmann E (1846) Hymenoptorum rossicorum species novae vel parum cognitae. Bulletin de la Société Impériale des Naturalistes de Moscou XXII (2): 441–442.

Eversmann E (1849) Fauna hymenopterologica Volgo-Uralensis III. Idem XXII (2): 430.

Gupta SK, Jonathan JK (2003) Fauna of India and the adjacent countries, Hymenoptera: Scoliidae. Zoological Survey of India, Kolkata, 277 pp.

He JH, Chen XX, Fan JJ, Li Q, Liu CM, Lou XM, Xu ZF (2004) Hymenopteran Insect Fauna of Zhejiang. Science Press, Beijing, 1373: 354–816.

Hua LZ (2006) List of Chinese Insects, Vol. IV. Sun Yat-sen University Press, Guangzhou, 540 pp.

Illingworth JF (1919) Monthly notes on grubs and other cane pests. Queensland Bur. BSES Division of Entomology Bulletins 7: 1–29.

Illingworth JF (1921) Natural enemies of sugar-cane beetles in Queensland. Bur. BSES Division of Entomology Bulletins 13: 1–47.

Jonathan JK (1976) Records of additional Campsomerinae from India (Hymenoptera: Aculeata). Newsletter of the Zoological Survey of India, Calcutta 2 (3): 112–114.

Kim JK (2009) Taxonomic review of the tribe Campsomerini (Scoliinae, Scoliidae, Hymenoptera) in Korea. Animal Systematics, Evolution and Diversity 25(1): 99–106. https://doi.org/10.5635/KJSZ.2009.25.1.099

Krombein KV (1978) Biosystematic studies of Ceylonese Wasps, II: A monograph of the Scoliidae (Hymenoptera: Scolioidea). Smithsonian Contributions to Zoology 283: 1–56. https://doi.org/10.5479/si.00810282.283

Krombein KV (1979) Superfamily Scolioidea. In: Krombein KV, Hurd Jr PD, Smith DR, Burks BD (Eds) Catalog of Hymenoptera in America North of Mexico. Smithsonian Institution Press, Washington, DC, 1253–1321.

Kumar PG, Rajmohana K (2017) Checklist of Scoliidae (Insecta: Hymenoptera: Vespoidea) of India. Zoological Survey of India: 1–9.

Lelej AS, Mokrousov MV (2017) The types of Scoliidae (Hymenoptera), described by Eduard Eversmann, with some taxonomic notes and checklist of Russian Scoliidae. Far eastern Entomologist 340: 1–17. https://doi.org/10.25221/fee.340.1

Lepeletier A (1845) Historie naturelle des insects. Hyménoptères 3: 1–646.

Liu Z, van Achterberg C, He JH, Chen XX (submitted) Checklist of Scoliidae (Insecta: Hymenoptera: Scolioidea) from China.

Matsumoto R, Hasegawa M, Ichikawa A (2019) *Scolia watanabei*, an adventive wasp newly discovered in Japan (Hymenoptera, Scoliidae, Scoliinae). Bulletin of the Osaka Museum of Natural History 73: 1–5.

Micha I (1927) Beitrag zur Kenntnis der Scoliiden (Hym. Acul.) (*Liacos* Guer., *Diliacos* Sauss. Sich. und *Triscolia* Sauss. Sich). Mitteilungen aus dem Zoologischen Museum in Berlin 13(1): 1–156.

Morawitz F (1889) Insecta, a Cl. G. N. Potanin in China et in Mongolia novissime lecta. IV. Hymenoptera Aculeata. Horae Societatis Entomologicae 23: 112–168.

Okamoto H (1924) The insect fauna of Quelpart Island. Bulletin of the Agricultural Experimental Station of the Government-General of Chosen 1: 1–233.

Osten T (2000) Die Scoliiden des Mittelmeer-Gebietes und angrenzender Regionen (Hymenoptera). Ein Bestimmungsschlüssel. Linzer Biologische Btrge 32(2): 537–593.

Osten T (2005) Checkliste der Dolchwespen der Welt (Insecta: Hymenoptera, Scoliidae). Naturforschende Gesellschaft 220: 1–62.

Osten T, Arens W (2004) Beitrag zur Kenntnis der Scoliiden-Fauna Griechenlands (ohne Zypern) (Hymenoptera, Scoliidae). Entomofauna 25(20): 305–320.

Ozbek H, Anlas S (2011) Distribution of Scoliidae (Hymenoptera: Aculeata) of Turkey with their zoogeographic characterization. Turkish Journal of Entomology 35(4): 627–639.

Prosvirov AS, Savitsky VY (2011) On the significance of genital characters in supraspecific systematics of the elaterid subfamily Agrypninae (Coleoptera, Elateridae). Entomological Review 91(6): e755. https://doi.org/10.1134/S0013873811060091

Samin N, Bağrıaçık N (2012) A contribution to the knowledge of Scoliidae (Hymenoptera) from Iran. Entomofauna 33(27): 389–396.

Samin N, Bağrıaçık N, Gadallah NS (2014) A checklist of Iranian Scoliidae (Hymenoptera: Vespoidea). Munis Entomology & Zoology 9(2): 713–723.

Saussure H de (1858) Description de diverses especes nouvelles ou peu connues du genre Scolia. Annales de la Societé entomologique de France 3(6): 193–249.

Saussure H de, Sichel J (1864) Catalogue des espèces de l'ancien genre Scolia, contenant les diagnoses, les descriptions et la synonymie des espèces, avec des remarques explicatives et critiques. Geneve et Paris, V. Mason, 350 pp. https://doi.org/10.5962/bhl.title.9323

Schulten GGM, Feijen HR, Feijen C (2011) The genus *Bellimeris* Betrem (Hymenoptera: Scoliidae, Campsomerinae). Zoologische Mededelingen 85: 887–903.

Smith F (1855) Mutillidae and Pompilidae. In: Catalogue of the Hymenopterous Insects in the collection of the British Museum. Taylor and Francis, London, 1–206.

Tsuneki K (1972a) Studies on the scoliid wasps of eastern Asia (Hymenoptera). Etizenia 62: 1–41.

Tsuneki K (1972b) Some scoliid wasps from South East Asia (Hymenoptera). Etizenia 63: 1–9.

Turner RE (1911) Further notes on the Thynnidae and Scoliidae: Notes on fossorial Hymenoptera V. Annals and Magazine of Natural History (8)8: 602–624. https://doi.org/10.1080/00222931108693069

Uchida T (1933) Revision der Japanischen Scoliiden mit Beschreibungen der neuen Arten und Formen. Journal of the Faculty of Agriculture, Hokkaido Imperial University 32: 229–262.

Uchida T (1936) Fauna Nipponica. 10(9/1) Family Scoliidae. Sanseido, Tokyo, 72 pp. [in Japanese]

van Achterberg C (1979) A revision of the subfamily Zelinae auct. (Hymenoptera, Braconidae). Tijdschrift voor Entomologie 122: 241–479.

Yasumatsu K (1946) Hymenoptera aculeata collected by Mr. K. Tsuneki in North China and Inner Mongolia 11. Vespoidea 1. Mushi 17(4): 13–14.

ZooKeys 1025: 177–201 (2021)
doi: 10.3897/zookeys.1025.60442
https://zookeys.pensoft.net

RESEARCH ARTICLE

A peer-reviewed open-access journal
ZooKeys
Launched to accelerate biodiversity research

Review of the New World *Notomicrus* Sharp (Coleoptera, Noteridae) I: Circumscription of species groups and review of the *josiahi* group with description of a new species from Brazil

Stephen M. Baca[1], Andrew Edward Z. Short[2]

1 *University of Kansas, Department of Ecology and Evolutionary Biology, Lawrence KS, USA* **2** *University of Kansas, Biodiversity Institute, Division of Entomology, Lawrence KS, USA*

Corresponding author: Stephen M. Baca (baca@ku.edu)

Academic editor: M. Michat | Received 6 November 2020 | Accepted 24 February 2021 | Published 22 March 2021

http://zoobank.org/C9D007A0-2385-4104-816C-F9177473ABBC

Citation: Baca SM, Short AEZ (2021) Review of the New World *Notomicrus* Sharp (Coleoptera, Noteridae) I: Circumscription of species groups and review of the *josiahi* group with description of a new species from Brazil. ZooKeys 1025: 177–201. https://doi.org/10.3897/zookeys.1025.60442

Abstract

The New World species of the minute aquatic beetle genus *Notomicrus* Sharp compose a much greater diversity than their Old World congeners, with 14 of the 17 known *Notomicrus* species occurring in the Neotropics. A recent phylogenetic study recovered four primary New World species groups and found that there are a number of undescribed species across all of these main lineages. Here, we provide a taxonomic key to these New World species groups, including two described species that we currently do not place in any group ("*incertae sedis*" species), complete with images and illustrations of diagnostic characters and taxonomic notes including a list of known species in each group. This work provides a scaffold for further planned taxonomic revisions within the genus. In addition, we review the first of the four New World groups, the *josiahi* species group and describe one new taxon, *N. interstinctus* **sp. nov.** from northern Brazil. Provided are descriptions, habitus images and illustrations of diagnostic characters.

Keywords

Aquatic beetles, Brazil, new species, South America, taxonomy

Introduction

Notomicrus Sharp is the most speciose genus of the minute aquatic beetle subfamily Notomicrinae (Coleoptera: Noteridae). Its distribution spans Indomalaya, Oceania and the New World, though the majority of *Notomicrus* diversity occurs in the Neotropics (14 of 17 described species). *Notomicrus* species occupy a wide range of habitats, including the margins of ponds, streams, marshes and swamps, drying stream beds, forest pools, hygropetric habitats and terrestrial leaf litter. Some species present a high specificity in their habitat preference, while others are found to be more generalists (Baca and Short 2020; personal observation). This ecological plasticity is a quality of the subfamily Notomicrinae as a whole. Both of the other notomicrine genera are subterranean specialists: *Phreatodytes* Uéno from aquifers in Japan and *Speonoterus* Spangler, a monotypic genus known only from a single collection in a shallow cave in Indonesia. *Speonoterus* appears to be a very close relative of *Notomicrus*, with *Phreatodytes* being their sister-group (Baca et al. 2017; Baca and Short 2020). It has been speculated that, given the plasticity of the habit preferences of *Notomicrus* and the aforementioned morphological similarity, *Speonoterus* may represent a specialized *Notomicrus* species (Baca and Short 2020). These relationships remain to be tested with molecular sequence data as *Speonoterus* is known only from the few specimens of the type series (Spangler 1996).

Since its establishment by Sharp (1882), the classification of *Notomicrus* and its species has been very stable. *Notomicrus nanulus* (LeConte, 1863) and *Notomicrus tenellus* (Clark, 1863) are the only species that have required nomenclatural recombination as these were described before the genus was established, thus necessitating transfer (Nilsson 2011; note that some synonyms of *N. tenellus* were also described before the erection of *Notomicrus*). Few junior synonyms of any *Notomicrus* species have been described (Nilsson 2011), and the genus itself has no current generic synonyms. Classification changes have occurred at higher levels, for example, tribe, subfamily and family levels, but the genus status of *Notomicrus* has remained unaltered.

The monophyly of *Notomicrus* has been previously supported, with the Old and New World clades each also being found to represent reciprocally monophyletic lineages (Baca et al. 2017; Baca and Short 2020). These studies have also revealed that, unsurprisingly, there remain many undescribed species in the genus, especially in South America. This is further indicated by recent descriptions of new Neotropical species (Miller 2013; Manuel 2015; Baca and Short 2018; Guimarães and Ferreira-Jr 2019). Together, these works have greatly strengthened our understanding of notomicrine diversity and evolution. However, in effect, Young's (1978) benchmark revision of the New World *Notomicrus* now includes just over half of the currently described species, amplifying the need for a comprehensive treatment of the group, especially with more diversity remaining to be described.

The species-level phylogenetic reconstruction of Baca and Short (2020) placed heavy emphasis on New World *Notomicrus* diversity. They recovered New World *Notomicrus* as diverging into four clades, the *josiahi*, *nanulus*, *meizon* and *traili* species groups, reciprocally supported by morphological characters. As such, Baca and Short (2020) provide an appropriate scaffold for taxonomic treatment of the groups.

Here, we (1) diagnose and provide a taxonomic key to the four primary species groups of New World *Notomicrus*. As part of this objective, we review morphological characters of importance, illustrate diagnostic characters and provide habitus images of exemplar species, taxonomic notes and a list of known species and references for each group. We then (2) present the first of four species-level revisionary works of New World *Notomicrus* by reviewing the *josiahi* species group. Included are a diagnosis of the group, a re-description of *N. josiahi* Miller, 2013 and a description of a new species from Brazil.

Materials and methods

Observations and measurements

Specimens were observed and measured using an Olympus SZX7 stereomicroscope. The microscope was equipped with 10× eyepieces, a DF PL $2\times_{-4}$ objective (16–112× magnification) and a calibrated ocular micrometer. Genitalia and tarsal claws were relaxed in hot water and dissected. Dissections were placed in glycerine on glass slides for observation. For additional observations and images of the prosternal process, aedeagi and tarsal claws, selected specimens were cleared in a warm 10% potassium hydroxide (KOH) solution and periodically checked multiple times an hour. Once desired elimination of soft tissue was achieved, specimens were thoroughly rinsed in DI (deionized) water. In some cases, DNA voucher specimens were used for observation and imaging of structures as the lysing process also dissolves soft tissue, effectively clearing the specimen and negating the need to damage additional specimens.

Images and illustrations

Dorsal habitus images were obtained with a Visionary Digital microphotography system equipped with an Infinity K2 microscope using a 5× objective and Helicon Focus imaging software. Photos were aligned and stacked using CombineZP (www.hadleyweb.pwp.blueyonder.co.uk) and refined in Adobe Photoshop. Ventral images and images of structures to be used for illustrations were taken with an Olympus DP72 camera system attached to either an Olympus SZX16 stereomicroscope with an SDF PLAPO 1×PF or 2×PF objective or an Olympus BX51 compound microscope with an UPlanFLN 40× oil immersion objective. The digital images were then stacked as above, with structures traced using Adobe Illustrator. Prolegs, prosterna, noterid platforms and male genitalia were imaged with the aforementioned stereomicroscope imagining system; illustrations were traced from these images. Male genitalia were placed in a depression slide with a drop of KY jelly and the remainder of the depression was filled with ethanol (EtOH). The KY jelly maintains its viscosity so that genitalia will hold its position for imaging. The EtOH eliminates obscuring refraction. Tarsal claws were imaged on the compound microscope. The fifth (V) pro- and metatarsomeres with tarsal claws were placed on a flat slide with EtOH and

a cover slip was applied and glycerine was then used the seal the outside of the slip. The lower surface tension of the EtOH allows the cover slip to press on the claws, flattening them against the slide.

Terminology

Descriptive terminology follows previous works (e.g. Manuel 2015; Baca and Short 2018).

Noterid platform. In *Notomicrus*, the noterid platform is formed by the raised projections of the inner metacoxal lamellae.

Genitalia and appendages. Following Miller and Nilsson (2003), genitalia and appendages are described in their fundamental homologous positions.

List of depositories

INPA Instituto Nacional de Pesquisas da Amazônia, Manaus, Brazil (N. Hamada);
MIZA Museo del Instituto de Zoología Agrícola, Maracay, Venezuela (L. Joly);
MSB Museum of Southwestern Biology, University of New Mexico (K. Miller);
NHM Natural History Museum, London, UK (M. Barclay, C. Taylor);
SEMC Snow Entomological Collection, University of Kansas, Lawrence, KS (A. Short);
USNM U.S. National Museum of Natural History, Smithsonian Institution, Washington, DC (C. Micheli).

Structures of taxonomic importance for diagnoses of *Notomicrus* species

Size. The total body length of *Notomicrus* species ranges between ca. 1.0 mm and 1.8 mm. Following Young (1978), size can, in combination with other characters, be very helpful in species determination. Size is quantified in terms of (1) total length (TL), as measured from anterior margin of head to apex of elytra, in dorsal aspect, (2) total length without head (TLPn), measured from medial anterior margin of pronotum to elytral apex (this is included to provide a consistent length measurement, as the degree to which the head is ventrally reflexed can affect the TL measurement) and (3) greatest width (GW), as measured transversely at the widest point of the beetle. Means of the measurements for each species, with standard deviations (SD) of the mean are also presented. Ratios of TL and GW are given as a way of quantifying the shape of the body outline. Means of the measurements for each species, with standard deviations (SD) of the mean for TL are also presented. Ratios of TL and GW are given as a way of quantifying the shape of the body outline.

Color. Most species of *Notomicrus* present dorsal coloration as varying shades from brown to yellow. However, individuals of some species present specific color patterns among sclerites. For example, some species appear bicolorous, with the elytra and head darker brown and contrasting against a lighter colored pronotum, for example, *N. traili* Sharp, 1882 (Fig. 1d, f). Other species, such as *N. nanulus* (LeConte, 1863) (Fig. 1a–c), are more uniformly brown, with little contrast between elytra, head and pronotum.

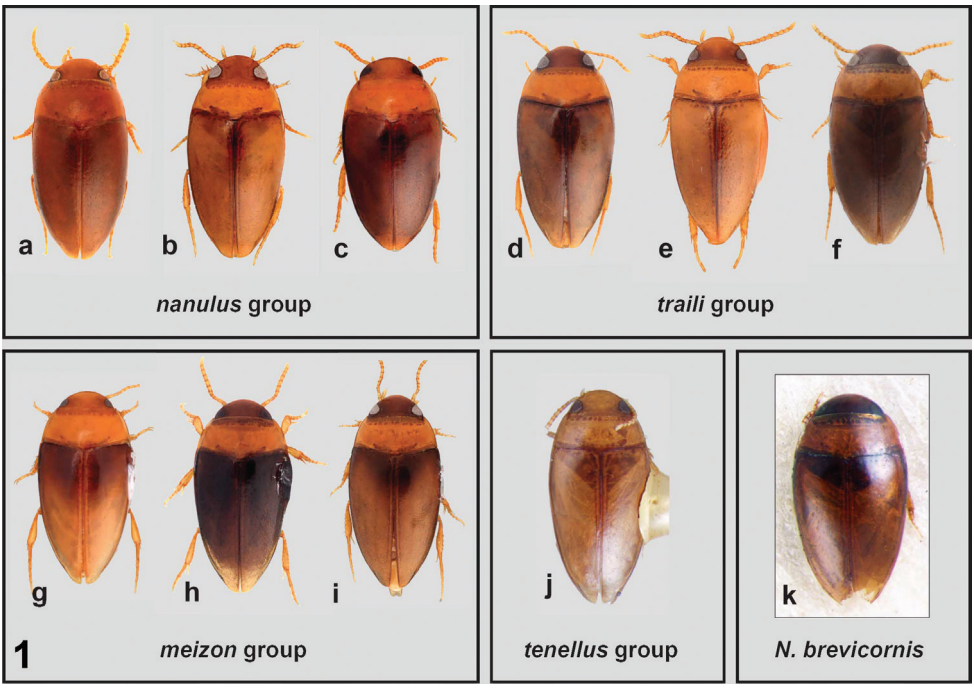

Figure 1. *Notomicrus* species groups. Dorsal habitus of representative *Notomicrus* species **a** *N. nanulus* **b** *N. sharpi* **c** *N.* sp. **d** *N.* cf. *traili* **e** *N.* cf. *gracilipes* **f** *N. petrareptans* **g** *N.* sp. **h** *N.* sp nr. *malkini* **i** *N.* sp. nr. *meizon* **j** *N. tenellus* **k** *N. brevicornis* male syntype.

Others still, such as *N. josiahi* Miller, 2013, present elytra with dark areas distinctly contrasting against lighter areas and/or may have a notable iridescent sheen (Fig. 5). Color patterns of the ventral surface can also be helpful in delimiting species. Color is best used in conjunction with other characters, as many species share similar coloration. Intraspecific variation is often present, with individuals appearing relatively lighter or darker in color, this variation being additionally present between mature and teneral individuals.

Punctation. Elytral punctation can be very helpful in diagnosing species of *Notomicrus*. Many species differ in the relative coarseness, density and patterns of punctation. Punctation should be used in combination with other characters to diagnose species as this character often presents similarly across multiple species.

Microsculpture. External microsculpture in *Notomicrus* varies among species and, in combination with other characters, can be helpful for diagnosis. In *Notomicrus*, the microsculpture consists of a microreticulation, where a superficially impressed mesh of very fine lines or grooves creates small cells. This is usually present on most external sclerites of the head, thorax, abdomen and legs, though it may not be uniform across these sclerites in an individual (e.g. the microsculpture of the noterid platform often differs from that of the elytra). In particular, the degree of impression and size or density of the meshes can be characteristic for a species or group of species.

Eye size. The size of the eyes, relative to the head capsule, can be very useful in identifying species. Here, the relative eye size is presented as a ratio of the greatest

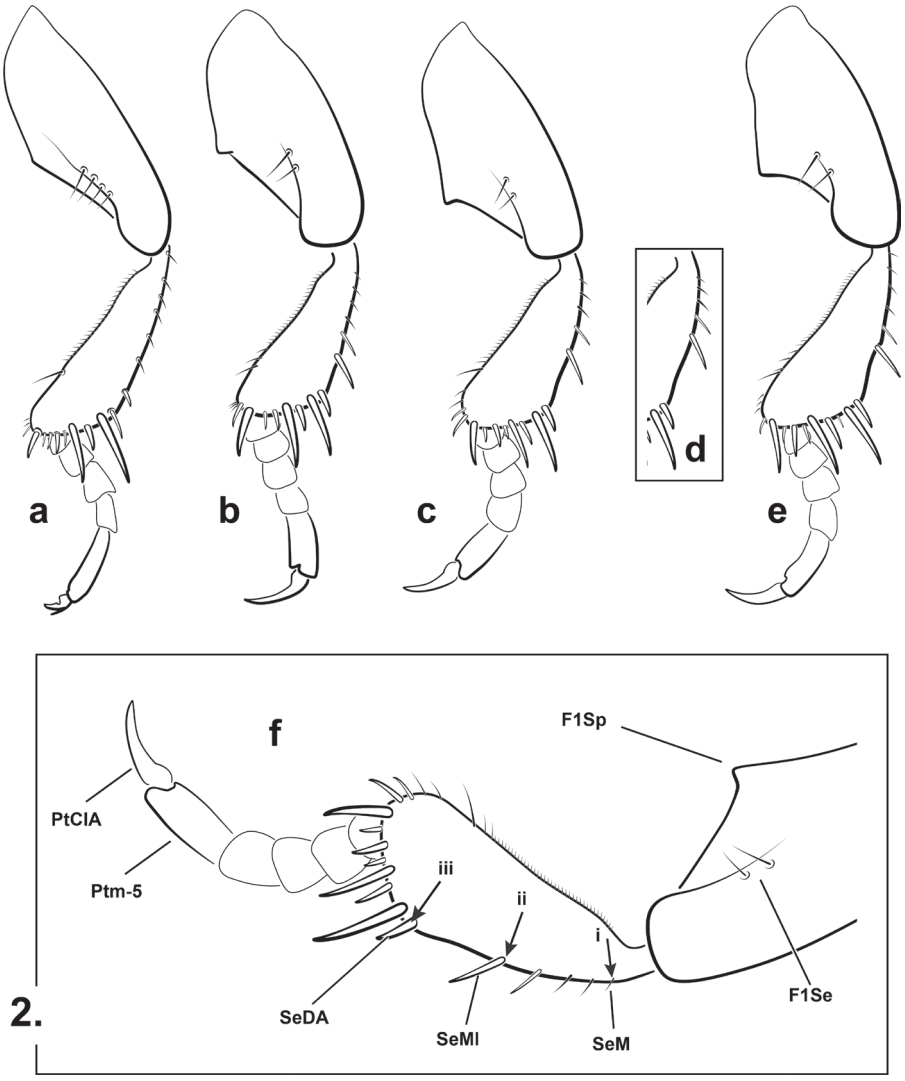

Figure 2. Representative prolegs of *Notomicrus* species groups (left proleg, anterior aspect) **a** *josiahi* group (*N. josiahi*) **b** *nanulus* group (*N. nanulus*) **c** *meizon* group (*Notomicrus* sp.) **d** *meizon* group, alternative setal spacing of dorsal (outer) protibial margin (*Notomicrus* sp.) **e** *traili* group (*N.* cf. *traili*) **f** detail of structures of importance. F1Se = setae of anteroventral margin of profemur; F1Sp = protuberance of posteroventral margin of profemur; PtCA = anterior protarsal claw; Ptm-5 = protarsomere V; SeDA = first robust seta of dorsoapical angle; SeMl = robust seta at mid-length of anterodorsal margin of protibia; SeM = First seta of anterodorsal margin of protibia; arrows indicate points for relative lengths (see key): i = anteroapical angle, ii = robust seta at mid-length, iii = first seta of marginal row.

width of the head (HW) and interocular distance (EW). Measurements are taken from dorsal aspect, approximately at posterolateral margins of the eyes. Interocular distance is taken from the narrowest point between the eyes. The larger the eyes relative to

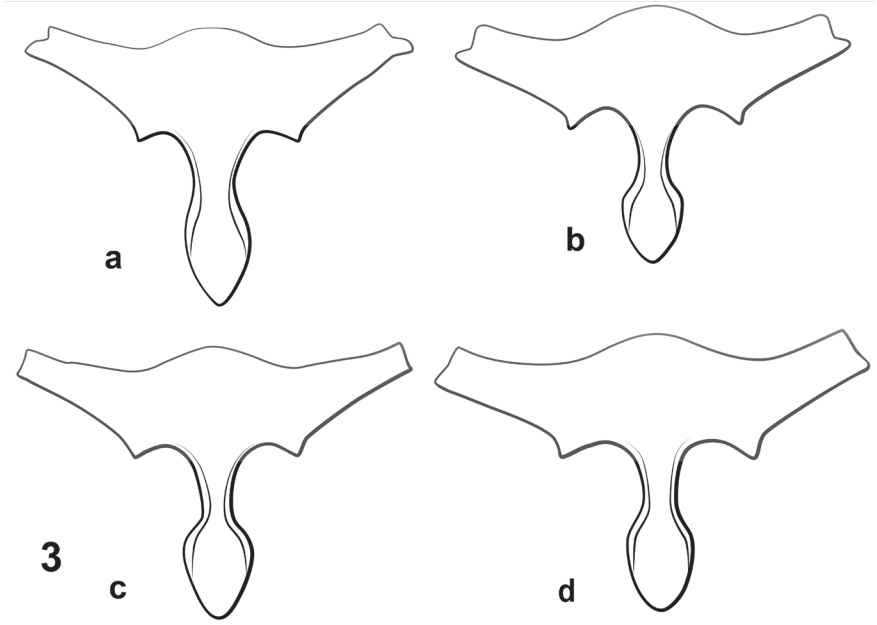

Figure 3. Representative prosterna of *Notomicrus* species groups **a** *N. josiahi* group (*N. josiahi*) **b** *N. nanulus* group (*N. nanulus*) **c** *N. meizon* group (*N.* sp. nr. *malkini*) **d** *N. traili* group (*N.* cf. *traili*).

the head capsule, the larger the ratio HW/EW, for example, *N. josiahi* HW/EW = 2.35–2.53, *N. petrareptans* Baca & Short, 2018 HW/EW = 1.65–1.73.

Prosternal process. The shape of the prosternal process was observed to be variable among some species and species groups of *Notomicrus* (Fig. 3). In particular, the shape of the apex and degree of constriction between the procoxae can be diagnostic in combination with other characters. For example, being acutely angled as in *N. josiahi* (Fig. 3a) or more rounded or blunt, as in *N. nanulus* (Fig. 3b).

Tarsal claws. The pro- and mesotarsal claws of males of *Notomicrus* show significant interspecific variation in size and shape. Following Young (1978), the shape of the claws, as well as the relative sizes of the anterior claws and posterior claws can be helpful in diagnosing species. Here we describe and illustrate the claws in lateral view (Figs 8, 9). The finer details of the claws' shape may be difficult to view without the use of a compound microscope. It should be noted that slide mounting the claws can variably alter the appearance compared to the *in situ* appearance under a stereomicroscope, this in part being due to their asymmetrical shape or the claws being slightly splayed on dried specimens. Characters of the tarsal claws are best used in combination with other characters.

Aedeagus. The aedeagus is especially helpful for diagnosing species. The median lobe should be observed from several angles as it tends to be asymmetric and an oblique orientation can give the appearance of a different shape. Despite relative reliability, the aedeagus is still best used in combination with other characters for identification. Many species, even those across species groups, can present very similar

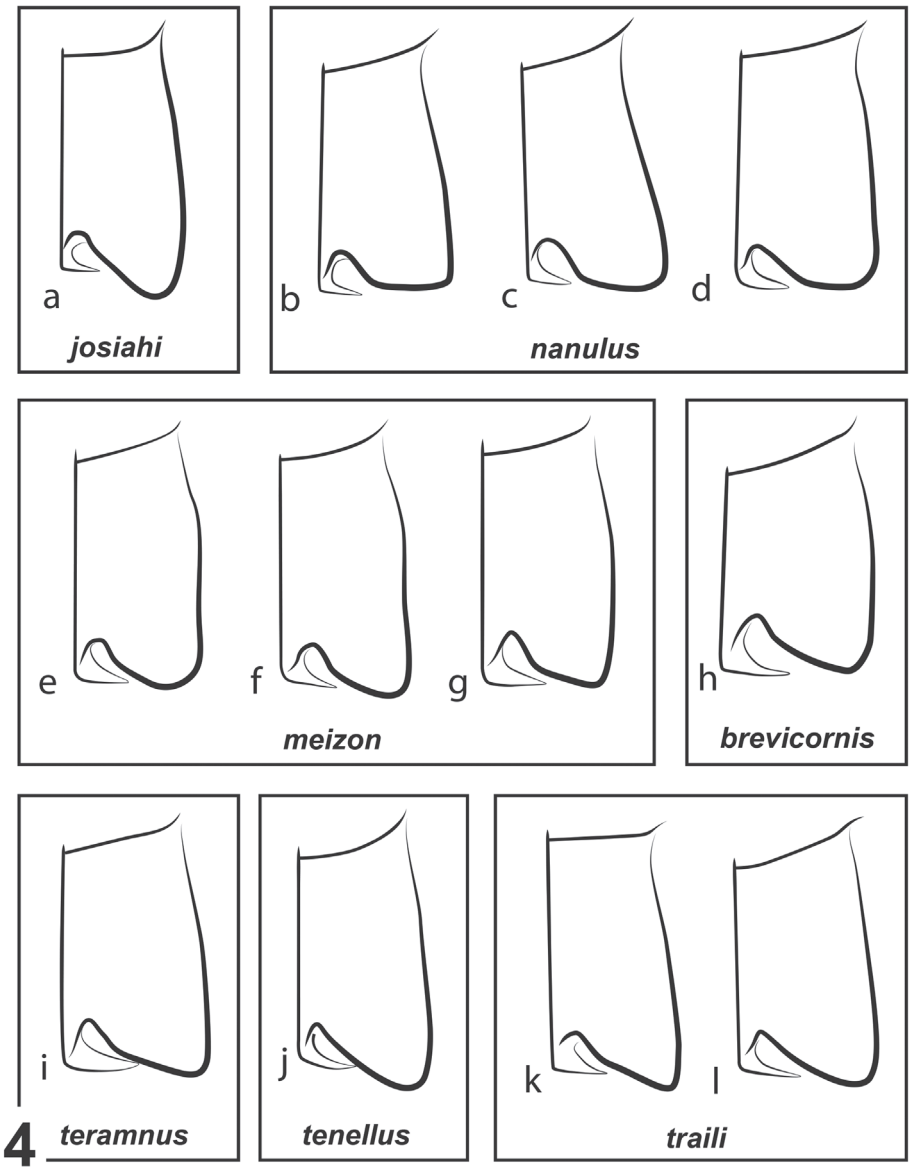

Figure 4. Representative noterid platforms of *Notomicrus* species groups (left side, ventral aspect). Names in boxes indicate species groups or species **a** *N. josiahi* **b** *N. nanulus* **c** *N. sharpi* **d** *N.* sp. (nr. *chailliei*) **e** *N.* sp. nr. *meizon* **f** *N. meizon* (paratype) **g** *N.* sp. nr. *malkini* **h** *N. brevicornis* (female syntype) **i** *N. teramnus* (female paratype) **j** *N. tenellus* (Indonesia) **k** *N. sabrouxi* (female paratype, sketched from Manuel (2015:518) **l** *N. petrareptans*.

aedeagi. For example, the aedeagus of *N. interstinctus* sp. nov. (Fig. 7) converges very closely on members of the *traili* group. Additionally, the males of some species are unknown, suggesting these lineages may only comprise females, for example, *N. femineus* Manuel, 2015.

Taxonomy

Genus *Notomicrus* Sharp, 1882

Type species. *N. brevicornis* Sharp, 1882. Designation by Guignot 1946: 115.

Diagnosis. (1) Eyes present; (2) metacoxae and metaventrite fused, suture indistinct laterad of noterid platform; (3) noterid platform not extending anteriorly on to metaventrite; (4) protibia with loose rows of spines and setae, lacking large spur at apex and tight comb of small spines on distolateral margin and not expanded distally beyond protarsal insertion; (5) partial fusion of metafurca and metacoxae, not forming complete ring; (6) mid-gular apodeme absent (Beutel and Roughley 1987; Miller 2009); (7) female laterotergite short, posteriorly extending beyond base of gonocoxae (Miller 2009).

Remarks. As noted by Miller (2009) and others (Manuel 2015 and citations therein), the characters that define *Notomicrus* are primarily plesiomorphic with the exception of the fusion of the metacoxae and metaventrite. *Speonoterus* Spangler is also defined by the above character combination, except absence of eyes. Spangler (1996) also noted that the distance from the anterior terminus of the noterid platform (metacoxal lamellae) to the mesocoxal cavities is shorter in *Speonoterus*, less than the width of the mesocoxal cavities, whereas in *Notomicrus*, this distance is greater than the width of the mesocoxal cavities (See Spangler 1996; Manuel 2015). Notomicrine species are all notably small (ca. 1.0–1.8 mm). Characters listed above without specific citation have been more common in use for defining *Notomicrus* (e.g. Sharp 1882; Young 1978; Buetel and Roughley 1987); see Miller (2009) and Manuel (2015) for details.

Key to species groups and insertae sedis species of *Notomicrus* Sharp

This key is intended to be used as a first step in identifying New World species of *Notomicrus*. Identification of *Notomicrus* species can prove difficult for non-specialists, especially without additional species in hand for comparisons. Diagnoses of the species groups of *Notomicrus* also reflect this difficulty.

1 Size small, TL = 1.3 mm. Elytral punctation almost entirely indistinct, except discal row and submargin of elytral suture with distinct punctures, with very fine scattered setose punctures near lateral margins; elytral surface with microreticulation consisting of round, isodiametric cells, somewhat scale-like in appearance. Head appendages short, antennomeres VI–X wider than long; apical palpomeres distinctly bifurcate with enlarged sensory fields. Aedeagus as in Fig. 2 of Guimarães and Ferreira-Jr (2019); median lobe with large base and very large processes and hooks. Male pro- and mesotarsal claws short, anterior protarsal claw expanded at base. Known only from high elevation hygropetric habitats in Minas Gerais, Brazil ..... ***N. teramnus***

– Size variable, ca. 1.2–1.9 mm. Elytral punctation and microsculpture variable. Antennomeres usually longer than wide; apical palpomeres variable. Median lobe

of aedeagus without conspicuous hooks or large processes (e.g. Figs 6, 7). Male pro- and mesotarsal claws variable. Habitat preference variable **2**

2 Dorsal (outer) margin of protibia without notable robust seta at or near mid-length (Fig. 2a). Eyes large relative to head capsule (Fig. 5), HW/EW ≥ 2.0. Elytra with notable contrasting dark and light colors (Fig. 5a, c). Profemur with > 3 distinct closely spaced setae on anteroventral margin (Fig. 2a); posteroventral margin of male profemur lacking notable protuberance, only weakly angled near mid-length (Fig. 2a); male protarsal claws very small, distinctly shorter than half the length of protarsomere V, anterior protarsal claw bifurcate, branching dorsally (Figs 8, 9)..... ***josiahi* group**

– Dorsal margin of protibia with a robust seta at or near mid-length (often two in females), at least as long as most dorsal seta on dorsoapical angle (Fig. 2b–f). Eyes smaller, HW/HW < 2.0. Elytra with or without contrasting colors. Profemur with < 3 closely-spaced setae on anteroventral margin; posteroventral margin of male profemur with notable protuberance or acute angle at ca. mid-length; male protarsal claws variable, anterior claw length almost always at least half the length of protarsomere V, almost always larger than female claws, sometimes bifurcate..... **3**

3 Noterid platform with angles of posterior lobes squared or rounded (Fig. 4b–e).... **4**

– Noterid platform with angles posterior lobes acutely angled (as in Fig. 4a, f–l) **5**

4 Elytral surface impunctate to weakly punctate, punctures usually inconspicuous and sporadic under normal magnification, except for discal series; microreticulation variably impressed, consisting of small, round, isodiametric cells, giving the appearance of small scales. Body form variable, but usually oblong, less attenuated posteriorly (Fig. 1a–c). Elytral color uniform, brown, sometimes shiny, not iridescent or only weakly so..... ***nanulus* group**

– Punctation distinctly present and often dense on posterior half of elytra, punctures finely to moderately impressed, bearing short setae, often extending on to anterior half of elytra; microreticulation variably impressed, consisting of fine mesh-like reticulation. Body form variable, but more elongate and attenuated posteriorly (Fig. 1g–i). Color variable, but elytra of mature specimens of most species with darker triangular area medially at base (Fig. 1g, i); in most species, dorsal surface very shiny and iridescent ..... ***meizon* group (in part)**

5 Color uniformly brown. Elytral surface with microreticulation variably impressed, consisting of small, round, isodiametric cells, giving the appearance of fine scales, somewhat shiny, but never iridescent; punctation variable. Males with anterior protarsal claw bifurcate or branched (as in Fig. 8a)..... **6**

– Color variable, uniform or bicolorous. Elytral surface with microreticulation variably impressed, consisting of fine mesh-like reticulation, sometimes iridescent. Males with protarsal claws never bifurcated or branched **7**

6 Body form oblong, rounded posteriorly (as in Fig. 1l or similar to *nanulus* group, for example, Fig. 1d). Elytral surface weakly punctate. Median lobe in lateral view as in Fig. 12b. New World ..... ***N. brevicornis* Sharp, 1882**

– Body form ovoid, more elongate, more attenuated posteriorly (as in Fig. J). Elytral surface weakly to moderately punctate. Median lobe different. Indomalaya and Oceania..... ***tenellus* group**

7 Protibia with robust seta of dorsal margin distinctly distad of half-length of outer margin, approximately at 2/3 margin length (Fig. 2e), distance between robust seta and dorsoapical angle distinctly shorter than distance between robust seta and first seta from protibial insertion. Dorsal coloration uniformly brown or bicolorous (Fig. 1d–f), with pronotum distinctly lighter than head and elytra. Elytral surface matte to somewhat shiny and iridescent ..... ***traili* group**

– Protibia with robust seta of dorsal margin approximately at half-length of outer margin, distance between robust seta and dorsoapical angle subequal to distance between robust seta and protibial insertion (Fig. 2d). Color variable, but elytra of mature specimens of most species with darker triangle medially at base (Fig. 1g, i). Most species with elytral surface very shiny, iridescent .... ***meizon* group (in part)**

Description of species groups

1. *N. josiahi* species group

Diagnosis. The *josiahi* group is diagnosed by the following combination of characters. Dorsal (outer) margin of protibia without notable robust seta at or near mid-length (Fig. 2a). Body form elongate, strongly, but regularly attenuated posteriorly. Eyes large relative to head capsule. Elytra with notable contrasting dark and light colors (Figs 5, 6); shiny and iridescent; microsculpture very fine. Prosternal process narrow (Fig. 3a). Protibiae elongate, with penultimate dorsal seta only slightly longer than others on dorsal margin (Fig. 2a); males with profemur lacking notable protuberance on posteroventral margin (Fig. 2a), only weakly angulate at mid-length; protarsal claws very small, distinctly less than half the length of protarsomere V (Figs 2a, 8, 9), not distinctly larger than female claws, anterior protarsal claw bifurcate, with small dorsal spur (Figs 8, 9). The large eyes, elytral color pattern and coloration and characters of the protibiae, make this species group easily distinguishable from others. There are only two species known.

Notomicrus josiahi Miller, 2013

Figs 2a, 3a, 4a, 5a, b, 6, 8

Notomicrus josiahi Miller, 2013: 244; Holotype: MIZA

Type locality. Venezuela, Amazonas State, Communidad Caño Gato, Rio Sipapo, 4°58.838'N, 67°44.341'W.

Material examined. *Paratypes*: "VENEZUELA: Amazonas State/ 4°58.845'N, 67°44.341'W, 100 m/ Communidad Caño Gato on Rio/ Sipapo; sandy stream; 7.i.2006; AS-06-016; leg. A.E.Z. Short" [White label, typed print] (1 female ex. SEMC); "VENEZUELA: Amazonas State/ 4°58.845'N, 67°44.341'W, 100 m/ Communidad Caño Gato on Rio/ Sipapo; 16.i.2009; leg. Short,/ Miller, Camacho, Joly, &

Garcia/ VZ09-0116-01X; along stream" [White label, typed print] (1 male, 2 females ex. SEMC) All paratypes with white barcode label with the following numbers and "KUNHM-ENT": "SM0843570" "SM0831496" "SM0842848" "SM0843672"; all paratypes with "PARATYPE/ *Notomicrus josiahi*/ Miller, 2013" [Blue label with black border, typed print].

Other material. Venezuela: Amazonas State, 4°58.845'N, 67°44.341'W, 100 m, Communidad Caño Gato on Rio Sipapo; 16.i.2009; leg. Short, Miller, Camacho, Joly, & Garcia/ VZ09-0116-01X; along stream (64 males and females ex. SEMC).

Measurements. TL = 1.46–1.69 mm (mean = 1.59 mm, SD. = 0.058, males = 1.46–1.69 mm, male mean = 1.58, SD. = 0.069, females = 1.55–1.68 mm, female mean = 1.62, SD. = 0.036); TLPn = 1.33–1.53 mm (mean = 1.44, SD. = 0.045, males = 1.33–1.49 mm, females = 1.43–1.53 mm); GW = 0.68–0.78 mm (mean = 0.74 mm, St. Dev. = 0.025, males = 0.68–0.78 mm, females = 0.72–0.78 mm); HW = 0.40–0.45 mm (mean = 0.42 mm, SD. = 0.014, males = 0.40–0.43 mm, females = 0.42–0.45 mm); EW = 0.16–0.19 mm (mean = 0.175 mm, SD. = 0.01, males = 0.16–0.17 mm, females = 0.17–0.19 mm); TL/GW = 1.99–2.31 (mean = 2.16; SD = 0.070; males = 1.99–2.31, females = 2.13–2.22); HW/EW = 2.21–2.53 (mean = 2.39, SD = 0.083, males = 2.41–2.53, females = 2.21–2.44).

Diagnosis. *Notomicrus josiahi* can be diagnosed by the following combination of characters: (1) Size large TL = 1.46–1.69 mm; (2) elytron with strongly darkened region in anterior 1/3rd, contrasting against brownish-yellow of rest of elytron (Fig. 5a); (3) Eyes very large relative to head capsule (HW/EW = 2.21–2.53; males 2.41–2.53, females 2.21–2.37); (4) aedeagus as in Fig. 6, median lobe expanded on right side in dorsal or ventral aspect, weakly attenuated to apex from mid-length in lateral aspect, with apex curved dorsolaterally to the left, left lateral lobe with dense tuft of setae at apex, few setae along dorsal margin and sparse tuft near base; right lateral lobe with small tuft of setae at apex; (5) pro- and mesotarsal claws as in Fig. 8, anterior protarsal claw strongly bent, bifurcate, with slender spur originating on dorsal margin where curved (Fig. 8a), ventral margin strongly expanded ventrally near base.

Re-description. Males. Body elongate-oval, attenuated posteriorly (Fig. 5a), TL/GW = 1.99–2.31 lateral outline of elytra and pronotum continuous in dorsal aspect; regularly curved to head, posteriorly evenly attenuated to elytral apex from point of greatest width; widest point just posterior to humeral angles of elytra, as in Fig. 5a.

Color. Head, pronotum, venter and legs yellow; elytron dark brown to black in basal 1/3, darkened region extending posteriorly along elytral suture and contrasting against brownish-yellow color of posterior 2/3 of elytron (Fig. 5a); elytron with surface weakly iridescent. Venter and legs uniformly yellow (Fig. 5b).

Structures. Eyes very large relative to head capsule (HW/EW = 2.35–2.53); antennae with length greater than greatest width of head. Prosternal process narrow, not strongly constricted between procoxae, with apex attenuated (Fig. 3a). Noterid platform with lateral margins subparallel (weakly convergent in posterior 2/3, convergent in anterior 1/3 (Fig. 4a); posterior lobes acute, angled, acutely rounded at apex. Profemur with loose comb of 3–5 stiff setae on anteroventral margin (Fig. 2a), posteroventral margin weakly angled at mid-length (Fig. 2a). Protibia elongate, dorsal and ventral

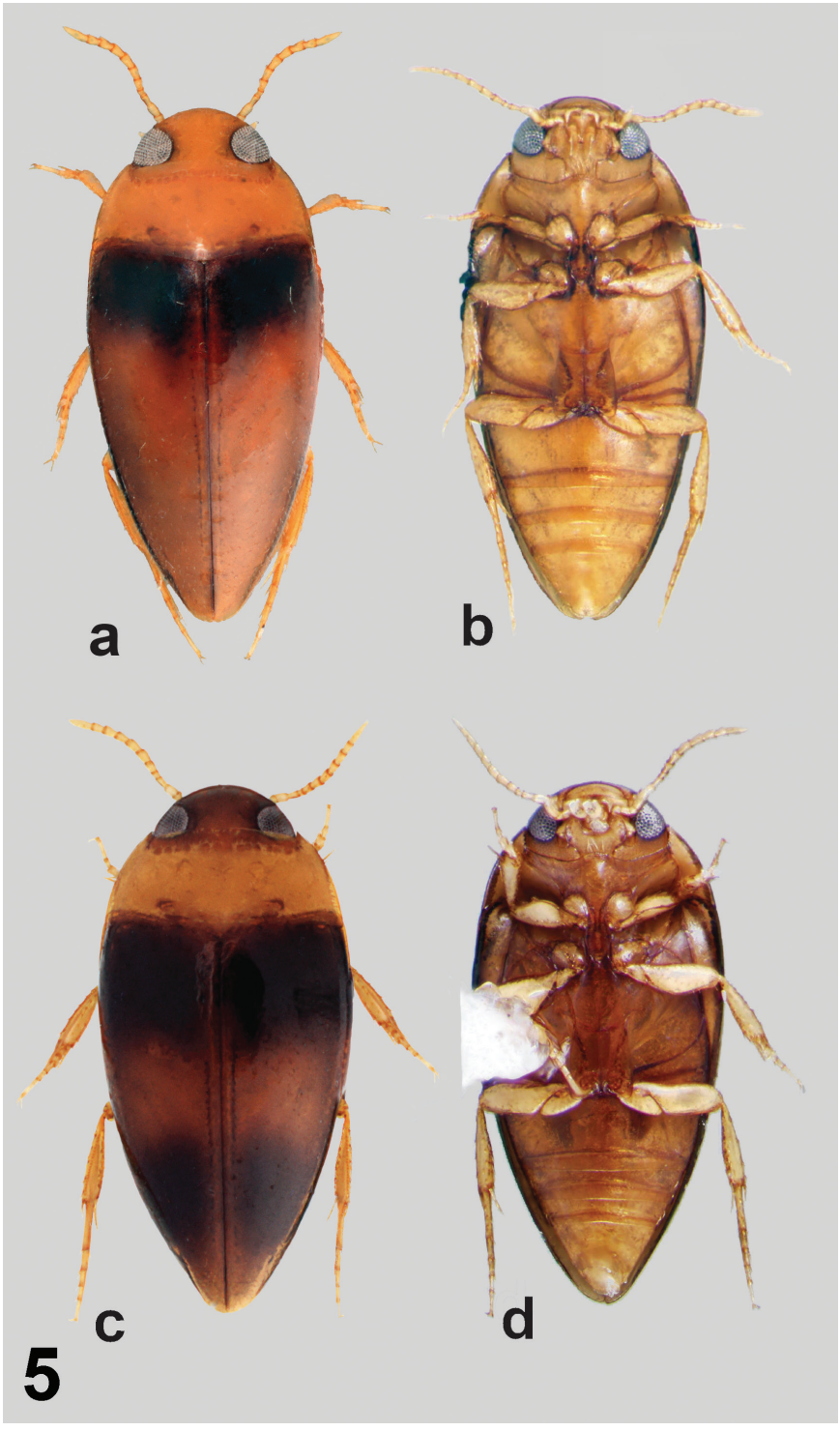

Figure 5. *Notomicrus josiahi* species group, dorsal and ventral habitus **a, b** *Notomicrus josiahi* Miller, 2013 (paratype) **c, d** *Notomicrus interstinctus* sp. nov. (paratype).

margins weakly divergent distally in anterior aspect (Fig. 2a), anterodorsal margin with row of 6–7 stout setae, without distinctly larger seta near mid-length. Protarsi with adhesive discs on ventral surface of protarsomeres II and III, lacking disc on ventral surface of protarsomere I; protarsal claws as in Fig. 8a, b, subequal in length, small, length ca. 1/3 that of protarsomere V, anterior claw distinctly bifurcate in distal half, expanded basally, very sharply curved, posterior claw slender, weakly expanded basally, moderately curved. Mesotarsi with adhesive discs on ventral surface of protarsomere II only, lacking disc on ventral surface of protarsomere I; mesotarsal claws as in Fig. 8c, d, subequal in length, small, length slightly greater than that of protarsal claws, slender, weakly expanded at base and weakly curved.

Sculpture. Dorsal surface of head with microsculpture very weakly impressed, microreticulation very fine, meshes mostly indistinct; micropunctation nearly indistinct. Pronotum with microsculpture similar to that of head, microreticulation fine; with scattered punctation near base and lateral margin, lateral punctures moderately dense, some with very fine setae. Elytron with microsculpture weakly impressed, microreticulation very fine, nearly indistinct; with punctation sparse in anterior half, with fine punctures along lateral margin and along discal row, with very few to no punctures between discal row and elytral suture, punctate in posterior half, punctures fine, many with very fine setae; discal row composed of fine and irregularly scattered punctures, denser posteriorly, lateral row similar to discal row but more sparse; micropunctation present, evenly scattered. Noterid platform and metaventrite surface with microsculpture weakly to moderately impressed, very fine, meshes of microreticulation nearly indistinct, cells transversely elongated.

Aedeagus. Aedeagus as in Fig. 6. Median lobe in lateral aspect gradually curved from base to apex, dorsal and ventral margins subparallel, converging at apex; apex acute, sharply curved, in ventral aspect subapically expanded and curved to left (Fig. 4a–c). Left lateral lobe in lateral aspect elongate, curved dorsally, with dense tuft of setae at apex (Fig. 6d). Right lateral lobe in lateral aspect oval; apex rounded with small tuft of setae in apical cleft (Fig. 6e).

Females. As males, except eyes slightly smaller than in males (HW/EW females = 2.21–2.39); profemur with posteroventral margin smooth, lacking weak angle at mid-length; pro and mesotarsomeres unmodified, slender, lacking adhesive discs; pro and mesotarsal claws unmodified, claws of respective tarsi subequal in length, slender, weakly curved.

Variation. As this species is known from only a single series, it is difficult to assess the degree of intraspecific variation. However, some variation was observed in the relative lightness or darkness in coloration of the individuals, with some brighter in color, more yellow, and others darker in color, more brownish yellow. The darkened region of the elytra also varied somewhat, occupying 1/4 to greater than 1/3 of the basal region of the elytron.

Differential diagnosis. *Notomicrus josiahi* is among the most easily distinguished species of *Notomicrus* by the combination of the large eyes, color pattern, shape of male protarsal claws and of male aedeagus. Superficially, *N. josiahi* is similar to some species of the *N. meizon* group in color, wherein *N. meizon* Guimarães & Ferreira-Jr,

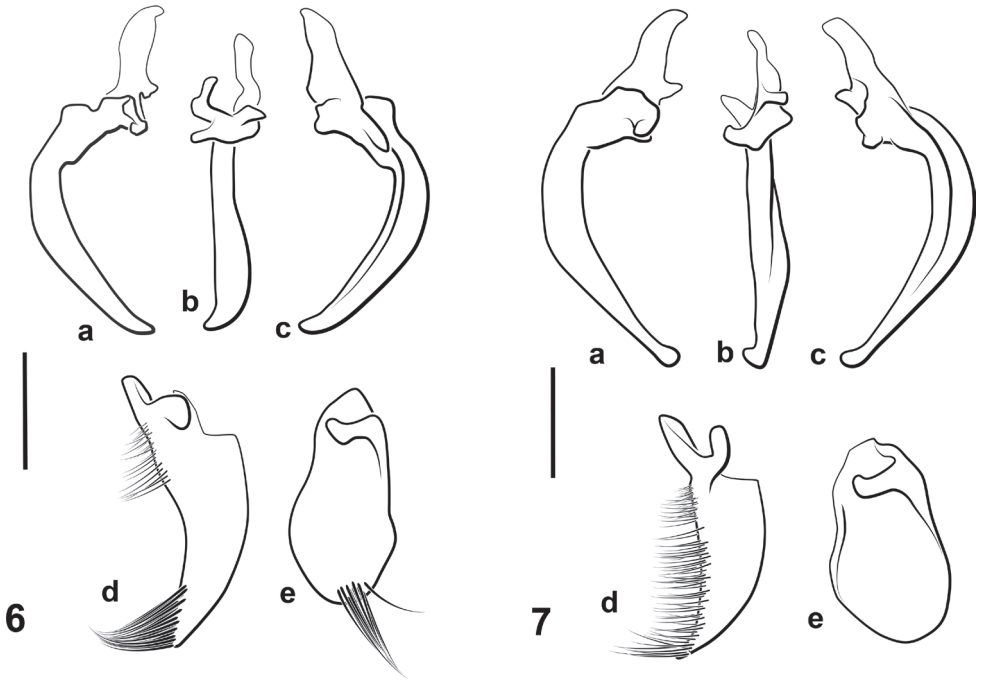

Figures 6, 7. Aedeagi of *josiahi* species group **6** *N. josiahi* **7** *Notomicrus interstinctus* sp. nov. **a** median lobe, left lateral aspect **b** median lobe, dorsal aspect **c** median lobe, right lateral aspect **d** left lateral lobe, medial surface/aspect **e** right lateral lobe, medial surface/aspect. Scale bars: 100 μm

2019, *N. malkini* Young, 1978 and other undescribed species are also darkened at the base of the elytra. However, in *N. josiahi*, this darkened area is better defined with the posterior border less oblique, thus expanding more completely over the humeral angles of the elytron. More distinctly, *N. josiahi* differs from these and other species by the much larger eyes and bifurcate protarsal claws (in males), which to date, has only been observed in *N. interstinctus*, *N. brevicornis* and the *tenellus* group. Among all other species of *Notomicrus*, the aedeagus of *N. josiahi* is distinct, with the right lateral lobe rounded and bearing a small tuft of setae at apex, rather than without setae, as in all other neotropical species.

Distribution. Known only from Venezuela (Fig. 10).

Ecology. This species has been collected from only a single locality, from the margins of a small, sandy stream (Fig. 11a).

***Notomicrus interstinctus* sp. nov.**
http://zoobank.org/9098C43C-66D4-4245-8F3F-5A4F7FB62549
Figs 5c, d, 7, 9

Type locality. Brazil: Amapá, Calcoene, 2.50019, -50.97712.

Material examined. *Holotype*, male: "BRAZIL: Amapá: Calcoene/ 2.50019°, -50.97712°; 5 m/ Colcoene (1 km W) on BR-156/ 22.vii.2018; leg. Short; Marshy/ savannah; BR18-0722-01A" [White label, typed print] "HOLOTYPE/ *Notomicrus*/ *interstinctus*/ Baca & Short, 2020" [Red label, black border, typed print] (ex.INPA). ***Paratypes*:** Same data as holotype, except with "PARATYPE/ *Notomicrus*/ *interstinctus*/ Baca & Short, 2021" [Blue label, black borders, typed print] (4 males, 5 females exs. SEMC, INPA); Brazil: Amazonas, Manacapuru Municipality, -3.23037, -60.64269, 35 m, 9.vi.2017, leg. Benetti, margin of large marsh/river, lots of vegetation; BR17-0609-01A; with "PARATYPE/ *Notomicrus*/ *interstinctus*/ Baca & Short, 2021" [Blue label, black borders, typed print] (3 males, 6 females exs. SEMC, INPA).

Measurements. TL = 1.50–1.63 (Holotype = 1.50 mm, mean = 1.56 mm, SD. = 0.045, males 1.50–1.63 mm, females 1.50–1.63 mm); TLPn = 1.38–1.48 (Holotype = 1.40 mm, mean = 1.42 mm, SD = 0.039, males = 1.40–1.45 mm, females = 1.38–1.48 mm); GW = 0.72–0.80 mm (Holotype = 0.72 mm, mean = 0.75 mm, SD. = 0.027, males = 0.72 mm–0.76 mm, females = 0.73–0.80 mm; HW = 0.41–0.45 mm (Holotype = 0.41 mm, mean = 0.43 mm, SD. = 0.013, males = 0.41–0.42 mm, females = 0.42–0.45 mm); EW = 0.18–0.22 mm (Holotype = 0.18 mm, mean = 0.20 mm, SD. = 0.013, males = 0.18–0.19 mm, females = 0.19–0.22 mm), TL/GW = 1.99–2.26 (Holotype = 2.08, mean = 2.07, SD. = 0.074, males = 2.06–2.26, females = 1.98–2.11); HW/EW = 2.04–2.33 (Holotype = 2.28, mean = 2.19, SD. = 0.088, males = 2.16–2.33, females = 2.04–2.26)

Diagnosis. *Notomicrus interstinctus* can be diagnosed by the following combination of characters: (1) Size large TL = 1.53–1.63 mm; (2) elytron dark with contrasting yellow band at mid-length, apices yellow (Fig. 5c, d); (3) eyes very large relative to head capsule (HW/EW = 2.04–2.33; Fig. 5c); (4) aedeagus as in Fig. 7; median lobe not broadly expanded on right side in dorsal aspect, attenuated to apex in lateral aspect, with small, round apical club oriented laterally to left; left lateral lobe with row of setae along entire dorsal margin, only somewhat denser at apex; right lateral lobe glabrous, without small tuft of setae at apex; (5) protarsal claws as in Fig. 9a, b; anterior protarsal claw strongly bent, bifurcate, branching at mid-length, ventral margin somewhat expanded ventrally near base.

Description. *Holotype*. As described for *N. josiahi*, except the following. Size large, TL = 1.53 mm. Body very broad, elongate-oval, strongly attenuated posteriorly, TL/GW = 2.08; lateral outline of elytron evenly and gradually curved to apex from point of greatest width, as in Fig. 5c, d.

***Color*.** Dorsal surface of head brown, lighter near clypeus; pronotum yellow; elytron dark, nearly black in anterior and posterior thirds, with lighter contrasting brownish-yellow transverse band near mid-length of elytron, elytral apex also lighter, brownish-yellow; elytron with surface moderately iridescent. Ventral surface of head and prosternum light brownish-yellow; rest of venter yellowish-brown; legs yellow.

***Structures*.** Eyes large relative to head capsule (HW/EW = 2.28). Posterior lobes of noterid platform with angles acute, apices rounded (as in Figs 3a, 5d). Pro- and mesotarsal claws as in Fig. 9.

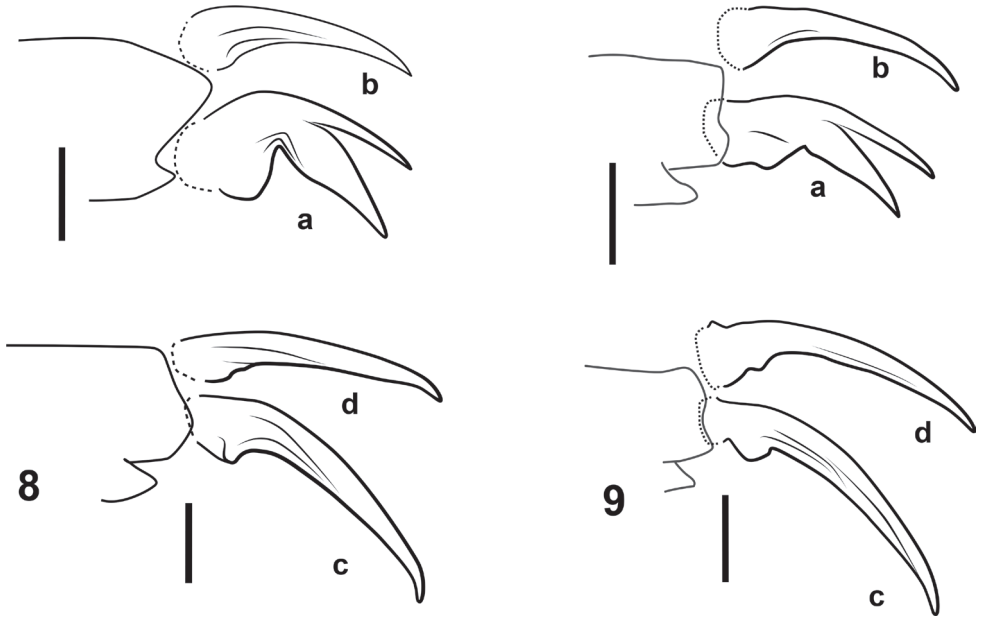

Figures 8, 9. Pro- and mesotarsal claws of *josiahi* species group **8** *N. josiahi* **9** *N. interstinctus* sp. nov. **a** anterior protarsal claw **b** posterior protarsal claw **c** anterior mesotarsal claw **d** posterior mesotarsal claw. All anterior aspect. Scale bars: 25 μm.

Sculpture. Elytron with punctation as described in *N. josiahi*, but denser overall and less restricted to posterior half, with punctures along lateral margin and puncture rows more widely distributed and denser.

Aedeagus. Aedeagus as in Fig. 7. Median lobe in lateral aspect, strongly curved at base, distally weakly curved, nearly straight; dorsal and ventral margins subparallel to mid-length, then attenuated to apex; apex with small club, sharply bent dorsally and left; left lateral lobe in lateral aspect, elongate, dorsal margin curved with dense row of fine setae (Fig. 7d). Right lateral lobe in lateral aspect oblong, rounded distally.

Females. As males, except eyes slightly smaller (HW/EW = 2.04–2.16); profemur with posteroventral margin smooth, lacking weak angle at mid-length; pro- and mesotarsomeres unmodified, slender, lacking adhesive discs; pro- and mesotarsal claws unmodified, claws of respective tarsi subequal in length, slender, weakly curved.

Variation. The most notable variation was in size and color, with some specimens darker overall than others, with the yellow bands sometimes smaller.

Differential diagnosis. *Notomicrus interstinctus* is easily distinguished by the combination of large eyes and elytral color pattern, darkened in anterior and posterior thirds with a yellow transverse band. This color pattern is unique among known species of *Notomicrus*. This species is also unusual in that it is one of the few known species (along with *N. brevicornis*, *N. josiahi* and members of the *tenellus* group), with males that present bifurcated anterior protarsal claws. The aedeagus, color pattern and more subtly the denser punctation, easily differentiates this species from *N. josiahi*. The ae-

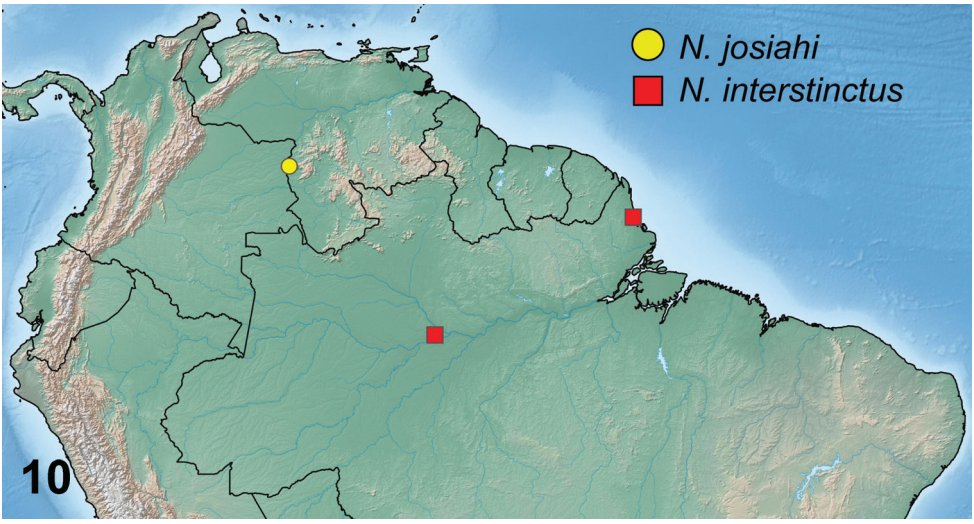

Figure 10. Distribution map of *josiahi* group species.

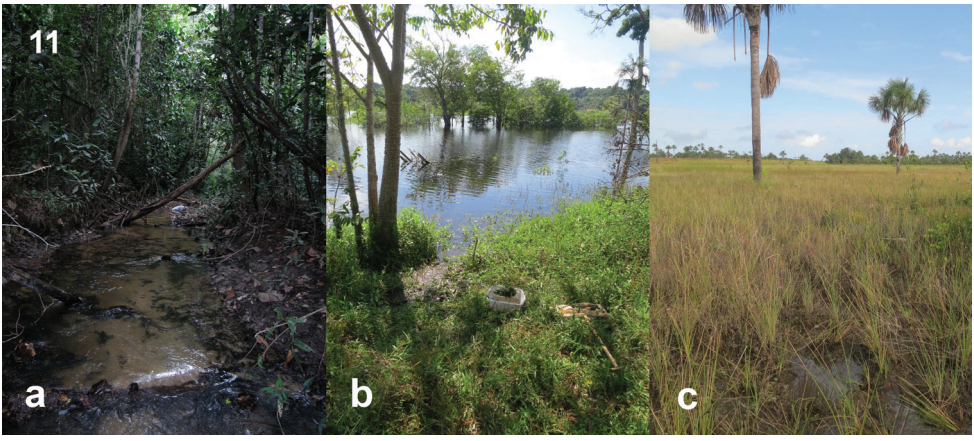

Figure 11. Habitats of *N. josiahi* group species **a** Type locality of *N. josiahi*, Venezuela: Amazonas (collection code VZ09-0116-01A); Localities of *N. interstinctus* **b** Brazil, Amazonas (collection code BR17-0609-01A) **c** type locality, Brazil, Amapá (collection code BR18-0722-01A).

deagus of *N. interstinctus* is similar to that of the *N. traili* group with the median lobe attenuated and the apex enlarged and bent in a left-dorsal direction, but other external characters, such as the color pattern, tarsal claws and large eyes, readily distinguish this species from the *traili* group. The elytral punctuation is somewhat similar to that of some members of the *N. meizon* group, being somewhat densely punctate posteriorly, with punctures fine, but the aforementioned combination of characters will differentiate *N. interstinctus* from these species as well.

Etymology. *Notomicrus interstinctus* sp. nov. derives its name from the Latin adjective *interstinctus*, meaning checkered or variegated. This refers to the color pattern of the elytra of this species. It is treated as an adjective in the nominative singular.

Distribution. Known from northern Brazil, Amazonas and Amapá states (Fig. 10).

Ecology. The species seems to be a generalist in terms of habitat, but seems to prefer vegetated environments. It was collected from a very shallow open marshy area (Fig. 11c) in the Brazilian state of Amapá and the vegetated margins of a river in Amazonas (Fig. 11b).

Taxonomic comments. *Notomicrus interstinctus* appears very similar to specimens misidentified as *N. traili* Sharp, 1882 by Guimarães and Ferreira-Jr (2019). This was due to the similarities of the size, punctation and shape of the aedeagus. The records from this work would potentially add to the distribution above, as most appear to be from the same regions of the Amazon Basin as the Amazonas specimens. Verification will be needed to confirm these individual records and these are not formally attributed to *N. interstinctus* here. Observations of the lone female syntype of *N. traili* (NHM) indicate that the species is as described by Young (1978), with males attributable to *N. traili*, appearing as in Fig. 2, with the head and elytra brown, without a pattern.

2. *Notomicrus nanulus* species group

Diagnosis. Members of this species group are most easily identified by their (1) monotone brown elytral color (Fig. 1a–c); (2) rounded, oval body shape; (3) rounded posterior lobes of the noterid platform (Fig. 4b–d); and (4) by their coarser microsculpture, consisting of isodiametric cells, appearing scale-like, rather than as a finer mesh of transversally elongated cells. This latter character is best viewed in light reflecting off the elytra. Even in species with finer variants of the cell-like microsculpture (e.g. *N. sharpi*), there is no iridescence. Punctation is largely indistinct, except for the discal series and sometimes sporadic punctures posteriorly.

Members of the *N. nanulus* group present a combination of characters that are variably shared with *N. brevicornis*, *N. teramnus* and the members *N. tenellus* group. This pattern, in tandem with our phylogenetic understanding, for example, *tenellus* group being sister to all other *Notomicrus* (Baca and Short 2020), suggest that *N. nanulus* species are united by a combination of characters that are plesiomorphic at some level within the genus. All share similar microsculpture consisting of isodiametric cells, often appearing scale-like to some degree. However, the *N. nanulus* group is distinguished from the *N. tenellus* group by the more rounded body outline (Fig. 1a–c, j) and from the *N. tenellus* group and *N brevicornis* by the shape of the noterid platform, with the *nanulus* group presenting posterior lobes that are rounded or squared (Fig. 4b–d). The rounded/squared lobes of the noterid platform character distinguish the *nanulus* group from *N. teramnus* (Fig. 4i) also, but more subtly. The *nanulus* group also typically presents a noterid platform with more longitudinally-elongated proportions than *N. brevicornis* (Fig. 4h). Males of the *N. nanulus* group present unbifurcated anterior protarsal claws, unlike *N. brevicornis* and the *N. tenellus* group. The aedeagi of known males of the *N. nanulus* group are easily distinguished; see Young (1978) and Manuel (2015).

Composition. *N. chailliei* Manuel, 2015; *N. femineus* Manuel, 2015; *N. huttoni* Young, 1978; *N. nanulus* (LeConte, 1863); *N. sharpi* Balfour-Browne, 1939.

Identification resources. Young (1978); Manuel (2015).

Remarks. Future work on this group may prove difficult as many species are collected with high ratios of females to males. An example was *N. femineus* Manuel, 2015, in which extensive collecting yielded only females, raising the possibility of parthenogenetic reproduction. Personal observations indicate that multiple undescribed species are represented by females only. We note that females of this group can be especially difficult to distinguish and are often misidentified as *N. brevicornis* (see comments on *N. brevicornis*, below). *Notomicrus teramnus* is a potential member of this species group based on color, shape and microsculpture, but is treated separately in the key, pending further investigation (see *insertae sedis* species below).

3. *Notomicrus meizon* species group

Diagnosis. Non-teneral specimens of this group tend to have the following combination of characters: (1) triangular pigmented area medially on the base of the elytra (Fig. 1g–i), similar to *N. josiahi*, but not as prominent and not always discernible in some populations or in teneral specimens; (2) dense, fine punctures bearing short setae on the posterior half of the elytra and sometimes extending far anteriorly (not as coarse as in members of the *traili* group); (3) microreticulation variably impressed, consisting of fine mesh-like reticulation; often iridescent; (4) posterior lobes of noterid platform with squared or rounded angles (Fig. 4e); if posterior angles of noterid platform more acute (Fig. 4f, g), protibia presents robust seta of outer margin approximately at half-length of outer margin, distance between robust seta and dorsoapical angle subequal to distance between robust seta and first seta from protibial insertion (Fig. 2d).

Composition. *N. malkini* Young, 1978; *N. meizon* Guimarães & Ferreira-Jr, 2019.

Identification resources. Young (1978); Guimarães and Ferreira-Jr (2019).

Remarks. The *meizon* group is sometimes difficult to discern from the *traili* group, as the differences amongst diagnostic characters can be subtle. The darkened basal area of the elytra in the *meizon* group is helpful, but investigators may find great difficulty in diagnosing teneral members of this group, which often lack the pigmented triangular area on the elytra. It is important to note that this darkened area is truly pigmented, not just darker in appearance due to the folding of the wings under the elytra as often happens in lighter colored species (as in Fig. 1f, j, k). Fortunately, males of most individual species of the *meizon* group are easy to identify by their aedeagi in combination with other characters, such as tarsal claws. The male median lobes of the *meizon* group species are usually (but not always) very irregularly shaped (for example, see Young 1978 and Guimarães and Ferreira-Jr 2019). The aedeagus of most species of the *traili* group appear similar to Fig. 8, with a small club at apex, often hooked to the left (see Young 1978; Manuel 2015; Baca and Short 2018). Additionally, males of *meizon* spe-

cies often present notable unequal lengths between the anterior and posterior protarsal claws. These are usually subequal in length in the *traili* group.

4. *Notomicrus traili* species group

Diagnosis. Non-teneral specimens of this group tend to have the following combination of characters: (1) lacking triangular pigmented area on the medial base of the elytra (Fig. 1d–f), lacking maculae; elytra with uniform shades of tan or brown; (2) irregular setose punctures in posterior half of elytral surface with density variable, increasingly coarse if extending on to anterior half of elytron; (3) microreticulation variably impressed, consisting of fine mesh-like reticulation; matte to shiny; elytral surface sometimes somewhat iridescent; (4) posterior lobes of noterid platform with angles acute (Fig. 4k, l); (5) protibia as in Fig. 2e, with robust seta of outer margin at ca. 2/3 length of margin, distance between robust seta and dorsoapical angle distinctly less than distance between robust seta and first seta from protibial insertion.

Composition. *N. gracilipes* Sharp, 1882; *N. petrareptans* Baca & Short, 2018; *N. reticulatus* Sharp, 1882; *N. sabrouxi* Manuel, 2015; *N. traili* Sharp, 1882.

Identification resources. Young (1978); Manuel (2015); Baca and Short (2018).

Remarks. Species of the *traili* group are difficult to discern and constitute a widespread species complex (see Baca and Short 2020). Personal observations coupled with the phylogenetic reconstructions of Baca and Short (2020) show that the diagnostic power of the dorsal punctation (see Young 1978) is unreliable, with multiple clades within the complex sharing similar patterns of punctation; for example, the pattern of punctation attributed to *N. gracilipes* by Young (1978) arises in multiple places within the complex. The group will require careful taxonomic investigation. The members of the *traili* group can be difficult to distinguish from those of the *meizon* group, but mature members lack a pigmented triangular area at the base of the elytra and most males of the *traili* group have similarly-shaped median lobes of the aedeagus, distinct from the *meizon* group. See notes in remarks of *meizon* group above.

5. *Insertae sedis* species

These species present characters combinations not found in other species groups. Both by presented character combination and even general *gestalt*, these are difficult to place with certainty. Molecular sequence data were unavailable for these species in the phylogenetic reconstruction of Baca and Short (2020). In particular, the species listed here both exhibit body shape, color, microsculpture and sparse punctation that would place them in the *N. nanulus* species group. However, in comparison with the *N. tenellus* species group, the sister to all New World taxa, several of these characters appear plesiomorphic in *Notomicrus*, making it difficult to discern their likely relatives from morphology alone.

***N. brevicornis* Sharp, 1882**
Figs 1k, 12

Material examined. *Syntypes*: Male specimen on small rectangular card, "♂" is drawn around genitalia and other parts, prosternal process flanks the specimen. "Boa Sorta Nov./ Sahlberg 1850" [small rectangular label, handwritten], "Sharp Coll/ 1905-313" [small rectangular label, typed], "Notomicrus/ brevicornis Ind. typ./ D.S." [small rectangular label, handwritten] "SYN/ TYPE" [small circular label with blue border, printed] (ex. NHM); female specimen on rectangular card, "S. America/ Brazil." [small rectangular label with blue line across, typed], "Sharp Coll/ 1905-313." Small rectangular label, typed], "Boa Sorta Nov./ Sahlberg 1850" [small rectangular label, handwritten], "Type 470/ Notomicrus/ brevicornis/ Boa Sorta" [rectangular label, handwritten], "SYN/ TYPE" [small circular label with blue border, printed], "TYPE" [small circular label with red border, printed], (ex. NHM); female specimen disarticulated on large card, "S. America/ Brazil." [small rectangular label with blue line across, typed], "Boa Sorta Nov./ Sahlberg 1850" [small rectangular label, handwritten], "Notomicrus/ brevicornis, Sharp./ Co-type." [rectangular label, handwritten], "SYN/ TYPE" [small circular label with blue border, printed], (ex. NHM); female specimen on small rectangular card, "Co-/ type" [small circular label with yellow border, printed], "S. America/ Brazil." [small rectangular label with blue line across, typed], "Sharp Coll/ 1905-313." Small rectangular label, typed], "Notomicrus/ brevicornis, Sharp./ Co-type." [rectangular label, handwritten] "SYN/ TYPE" [small circular label with blue border, printed] (ex. NHM). Note: this latter specimen also with small label "Not brevicornis/ maybe gracilipes?/ Manuel det. 2016". See notes below.

Remarks. *Notomicrus brevicornis* would otherwise appear to be a member of the *nanulus* group by the aforementioned characters. However, it differs by the more acute posterior angles of the noterid platform, a character shared with members of the *tenellus*, *josiahi* and *traili* groups. The male syntype presents a bifurcate anterior protarsal claw (as in fig. 8A), a character shared by the *josiahi* and *tenellus* species groups. With the Old World and New World taxa being reciprocally monophyletic (Baca and Short 2020) and the plesiomorphic appearance of these characters, we would speculate that this species is likely to be sister to one of the New World species groups.

Based on observation of the single male of the syntype series, it is suspected that Young (1978) based his description, key and illustration of the aedeagus of *N. brevicornis* on the male of a different species. First, the illustration in Young (1978) of the aedeagus of *N. brevicornis* does not match that observed in the syntype. Second, Young (1978: 288–289) describes *N. brevicornis* as being sexually dimorphic in elytral punctation, with males being more punctate than females. However, as noted by Sharp (1882: 261), there is very little dimorphism observed between males and females of the syntype series beyond characters of the tarsi. The punctation and sculpture are very weakly dimorphic, both sexes being almost entirely impunctate, except for the weak discal rows and a few scattered punctures near the elytral apex. The punctation is slightly less impressed in females, with discal rows slightly less prominent. The relative difference of

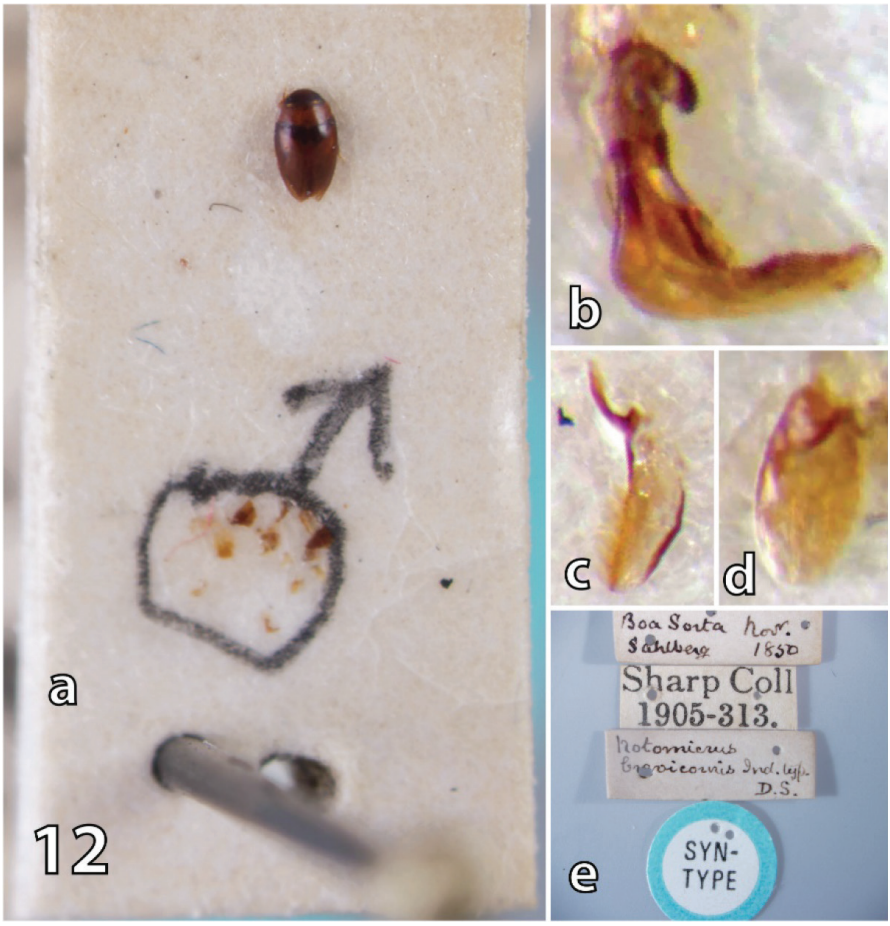

Figure 12. Card mount, aedeagus and labels of male syntype of *N. brevicornis* **a** *Notomicrus brevicornis* card mount, dorsal **b** median lobe lateral aspect **c** left lateral lobe, medial aspect **d** right lateral lobe **e** syntype labels.

punctation between the male and female syntypes of this species is so slight that splitting them up in the key as did Young (1978: 288, couplet 7) seems largely unnecessary, wherein the couplet describing females of *N. brevicornis* also closely describes the male syntype (Young 1978: 288). The specimens of the UMMZ, observed by Young, were not observed for this study, but the stated differences by Young (1978) and the grouping of males of *N. brevicornis* with *N. malkini* in Young's (1978: 288) key call the identity of the depicted male in Young (1978) into question. Further adding to this suspicion is the fact that some male specimens attributable to *N. malkini* or other undescribed species of the *meizon* group in the FSCA were identified as *N. brevicornis* by Young (date of determination not recorded). For aiding in identification, we have included images of the male syntype, labels and aedeagus (Figs 1k, 12). One specimen of the syntype series appears to be of a different species than the others; likely it is a member of the *traili* species group. See last listed specimen and note in the examined syntype material above.

Personal observations show that many members of the *N. nanulus* group are misidentified as *N. brevicornis* in collections. This is no doubt due to the superficial similarities of *N. brevicornis* to members of the *nanulus* group and scarcity of males in the *nanulus* group. With that, there are likely inaccuracies in literature with respect to records and distributions.

N. teramnus Guimarães & Ferreira-Jr, 2019

Remarks. *Notomicrus teramnus* would also appear a member of the *nanulus* group, given the above-mentioned characters. An argument could be made that this is the case as it only appears to differ in the shape of the posterior lobes of the noterid platform being more angular than most species in the *nanulus* group. This species otherwise appears to lack characters that would unite it with other species groups, though this will require examination and/or phylogenetic investigation. We abstain from placing it as member of the *nanulus* group as *N. teramnus* is known only from a high elevation hygropetric habitat, which may present confounding morphological specialization. Aedeagal morphology is not here considered to be indicative of a particular placement, but the very unusual morphology of the aedeagus of *N. teramnus* (see Guimarães and Ferreira-Jr 2019) further raises questions of placement.

Acknowledgements

We are grateful for the assistance and support of many colleagues during fieldwork in Brazil, including Neusa Hamada (INPA) and Cesar Benetti (INPA). We would also like to extend a warm thanks to our colleagues M. Manuel, M. Toledo and B. Guimarães for helpful comments, specimens and information over the course of this ongoing project and a special thanks to the reviewers of the manuscript for their consideration and constructive comments. This study was supported in part by US National Science Foundation grant DEB-1453452 to AEZS and US National Science Foundation NSF GRF #0064451 to SMB. Fieldwork in Brazil was partly funded by a Fulbright fellowship to AEZS and conducted under SISBIO license 59961-1.

References

Baca SM, Short AEZ (2018) *Notomicrus petrareptans* sp. n., a new seep-dwelling species of Noteridae from Suriname (Coleoptera: Adephaga). Zootaxa 4388(2): 182–190. https://doi.org/10.11646/zootaxa.4388.2.2

Baca SM, Short AEZ (2020) Molecular phylogeny of the notomicrine water beetles (Coleoptera: Noteridae) reveals signatures of Gondwanan vicariance and ecological plasticity. Insect Systematics and Diversity 4(6): 1–4. https://doi.org/10.1093/isd/ixaa015

Baca SM, Toussaint EFA, Miller KB, Short AEZ (2017) Molecular phylogeny of the aquatic beetle family Noteridae (Coleoptera: Adephaga) with an emphasis on partitioning strategies. Molecular Phylogenetics and Evolution 107: 282–292. https://doi.org/10.1016/j.ympev.2016.10.016

Balfour-Browne J (1939) A contribution to the study of the Dytiscidae. – I. (Coleoptera, Adephaga). The Annals and Magazine of Natural History (11) 3: 97–114. https://doi.org/10.1080/00222933908526903

Belkaceme T (1991) Skelet und muskulatur des kopfes und thorax von *Noterus laevis* Sturm.ein beitrag zur morphologie und phylogenie der Noteridae (Coleoptera: Adephaga). Stuttgarter Beiträge zur Naturkunde A 462: 1–94.

Beutel RG, Roughley RE (1987) On the systematic position of the genus *Notomicrus* Sharp (Hydradephaga, Coleoptera). Canadian Journal of Zoology 65(8): 1898–1905. https://doi.org/10.1139/z87-290

Clark H (1863) Descriptions of new East-Asiatic species of Haliplidae and Hydroporidae. T. Roy. Entomological Society of London (3) 1: 417–428. https://doi.org/10.1111/j.1365-2311.1862.tb01288.x

Fauvel A (1903) Faune analytique des coléoptères de la Nouvelle-Calédonie. Revue d'Entomologie 22: 203–379.

Guimarães BA, Ferreira-Jr N (2019) Two new species and new records of *Notomicrus* Sharp, 1882 (Coleoptera: Noteridae) from Brazil. Zootaxa 4629(2): 263–270. https://doi.org/10.11646/zootaxa.4629.2.8

LeConte JL (1863) New species of North American Coleoptera. Part 1. Smithsonian Miscellaneous Collections 6(167): 1–92.

Manuel M (2015) The genus *Notomicrus* in Guadeloupe, with description of three new species (Coleoptera: Noteridae). Zootaxa 4018(4): 506–534. https://doi.org/10.11646/zootaxa.4018.4.2

Miller KB (2009) On the systematics of Noteridae (Coleoptera: Adephaga: Hydradephaga): phylogeny, description of a new tribe, genus and species, and survey of female genital morphology. Systematics and Biodiversity 7: 191–214. https://doi.org/10.1017/S1477200008002946

Miller KB (2013) Notomicrus josiahi, a new species of Noteridae (Coleoptera) from Venezuela. Zootaxa 3609(2): 243–247. https://doi.org/10.11646/zootaxa.3609.2.11

Miller KB, Nilsson AN (2003) Homology and terminology: Communicating information about rotated structures in water beetles. Latissimus 17: 1–4.

Nilsson AN (2011) A World Catalogue of the family Noteridae, or the Burrowing water beetles (Coleoptera: Adephaga). Version 16.VIII.2011, 54 pp. http://www2.emg.umu.se/projects/biginst/andersn/WCN/WCN_20110816.pdf [accessed 1 June 2017]

Sharp D (1882) On aquatic carnivorous Coleoptera or Dytiscidae. Scientific Transactions of the Royal Dublin Society 2: 179–1003. https://www.biodiversitylibrary.org/page/10137421

Toledo M (2010) Noteridae: Review of the species occurring east of the Wallace line (Coleoptera). In: Jäch MA, Balke M (Eds) Water Beetles of New Caledonia (part 1): monographs of Coleoptera (Vo. 3). Zoologische-Botanische Gesellshaft, Vienna, 195–236.

Young FN (1978) The New World species of the water-beetle genus Notomicrus (Noteridae). Systematic Entomology 3(3): 285–293. https://doi.org/10.1111/j.1365-3113.1978.tb00121.x